U.S. DEPARTMENT OF COMMERCE

WEATHER BUREAU

TECHNICAL PAPER NO. 42

Generalized Estimates of Probable Maximum Precipitation and Rainfall-Frequency Data for Puerto Rico and Virgin Islands

for Areas to 400 Square Miles, Durations to 24 Hours, and Return Periods from 1 to 100 Years

U.S. DEPARTMENT OF COMMERCE
LUTHER H. HODGES, *Secretary*
WEATHER BUREAU
F. W. REICHELDERFER, *Chief*

TECHNICAL PAPER NO. 42

DATA HAVE BEEN ENTERED

Generalized Estimates of Probable Maximum Precipitation and Rainfall-Frequency Data for Puerto Rico and Virgin Islands

for Areas to 400 Square Miles, Durations to 24 Hours, and Return Periods from 1 to 100 Years

Prepared by

Cooperative Studies Section
Hydrologic Services Division
U.S. Weather Bureau

for

Engineering Division
Soil Conservation Service
U.S. Department of Agriculture

WASHINGTON, D.C.
1961

For sale by the Superintendent of Documents, U.S. Government Printing Office, Washington 25, D.C. - Price 50 cents

CONTENTS

LIST OF ILLUSTRATIONS

Generalized Estimates of Probable Maximum Precipitation and Rainfall-Frequency Data for Puerto Rico and Virgin Islands

for Areas to 400 Square Miles, Durations to 24 Hours, and Return Periods from 1 to 100 Years

INTRODUCTION

Assignment. The Soil Conservation Service's need for rainfall data for hydrologic design purposes in connection with its Watershed Protection and Flood Prevention Program (authorization: P.L. 566 83d Congress, and as amended) led to its cooperating with the Weather Bureau in deriving the required information.

Scope. This report presents rainfall data for various hydrologic design problems involving areas up to 400 sq. mi. and rainfall durations up to 24 hr. Included in the report are generalized estimates of (1) probable maximum precipitation (PMP) from cloudbursts and from hurricanes, and (2) rainfall-intensity-frequency data for return periods from 1 to 100 yr.

Accuracy of results. The generalized estimates of the upper limits of rainfall intensities presented herein are as accurate as available data and current meteorological and statistical procedures permit. The accuracy of the rainfall-intensity-frequency data for the 1- to 100-yr. return periods is chiefly dependent on precipitation-network density and length of record. As time passes more data will become available through increases in length of records and probably in density of station networks. Also, knowledge of hurricane structure is rapidly being extended by airplane and radar observations. It is therefore only logical to expect that more reliable estimates than those presented herein will be possible in the near future, say 10 years from now, with the greatest increase in reliability very likely to be reflected in the estimates of the upper limits of rainfall intensity.

Acknowledgments. The project was under the supervision of J. L. H. Paulhus, Chief of the Cooperative Studies Section of the Hydrologic Services Division, W. E. Hiatt, Chief. D. M. Hershfield directed the statistical phases of the study. L. L. Weiss conducted the tests and applications of the hurricane model used in the meteorological phases. W. E. Miller and N. S. Foat supervised the collection and processing of basic data. R. L. Higgs, Meteorologist in Charge, Weather Bureau Airport Station, San Juan, and David Smedley, Territorial Climatologist, Weather Bureau Office, San Juan, provided some very useful unpublished rainfall data for this report. Drafting was supervised by C. W. Gardner. Coordination with the Soil Conservation Service was maintained through H. O. Ogrosky, Chief, Hydrology Branch, Engineering Division.

Chapter 1

TROPICAL STORMS OF PUERTO RICO AND VIRGIN ISLANDS

1.1 Introduction

1.1.1 The first step in any derivation of probable maximum precipitation estimates is the study of the meteorology of the problem area. The meteorological situations associated with maximum observed rainfall rates are naturally of primary interest and are usually studied most intensively. In the case of Puerto Rico and the Virgin Islands, it was quickly determined that probable maximum precipitation for durations of about 6 hr. and longer and for areas greater than about 50 sq. mi. would most likely be associated with hurricanes. Data on tropical storms affecting those islands were therefore thoroughly investigated.

1.2 Maximum observed rainfalls

1.2.1 Figures 1–1 and 1–2 show the estimated, or adjusted, maximum observed 24-hr. rainfalls for Puerto Rico and Virgin Islands, respectively. The amount shown for San Juan, which is the only station having a recording-gage record exceeding 20 yr., is the only unadjusted value shown. All other amounts were adjusted upward to approximate the maximum value for any consecutive 24-hr. period from the maximum observational-day amounts measured in the non-recording gages.

1.2.2 The basic data for figures 1–1 and 1–2 were compiled from the Weather Bureau's *Climatological Data* for the West Indies. A tabulation by Quinonés [1] was an additional source of data for figure 1–1. One of three types of adjustment was used in approximating the true maximum 24-hr. rainfalls from the basic observational-day maxima. The adjustment most commonly used consisted of adding to the maximum observational-day value one-half of the higher of the amounts for the adjoining days; i.e., the preceding or following day. Comparative tests made in various regions in the United States indicate that, on the average, this procedure yields satisfactory approximations of the true 24-hr. maxima.

1.2.3 Another adjustment used consisted of multiplying the maximum observational-day amount by 1.13. This procedure is also a result of statistical studies of precipitation data for various regions of the United States and yields generally reliable results when applied to rainfall-frequency data. When applied to individual amounts, however, the factor might yield appreciably erroneous estimates, which may nevertheless be more nearly correct than estimates based on the assumption that the observational-day maxima are also true 24-hr. maxima. The 1.13 factor was used only when precipitation amounts for days adjoining the date of maximum precipitation were not available. A few of the amounts shown on figure 1–1 were adjusted by this method.

1.2.4 The third adjustment was used to estimate true maximum 24-hr. rainfalls for several stations which all had acquired their maximum observational-day amounts from the same storm, the disastrous *San Felipe* hurricane of September 13, 1928. The amounts for these stations were adjusted by applying the ratio of the true 24-hr. maximum to the observational-day value derived from the San Juan recording-gage record.

1.2.5 Maximum rainfall amounts for durations under 24 hr. are also of interest. Unfortunately, the only station with an adequate recording-gage record is San Juan, P.R. Its maximum intensities for the 51-yr. period 1900–1950 are given in table 1–1. None

TABLE 1–1.—*Maximum rainfall intensities at San Juan, P.R., 1900–1950*

Duration (hr.)	1	2	3	6
Rainfall (in.)	3.5	4.9	5.6	6.2

TABLE 1–2.—*Maximum observed rainfall intensities in Puerto Rico*

Station	Duration	Rainfall (in.)
Jauca	45 min	4.3
Toro Negro Plant No. 2	4 hr	10.1
Naguabo	12 hr	18.2

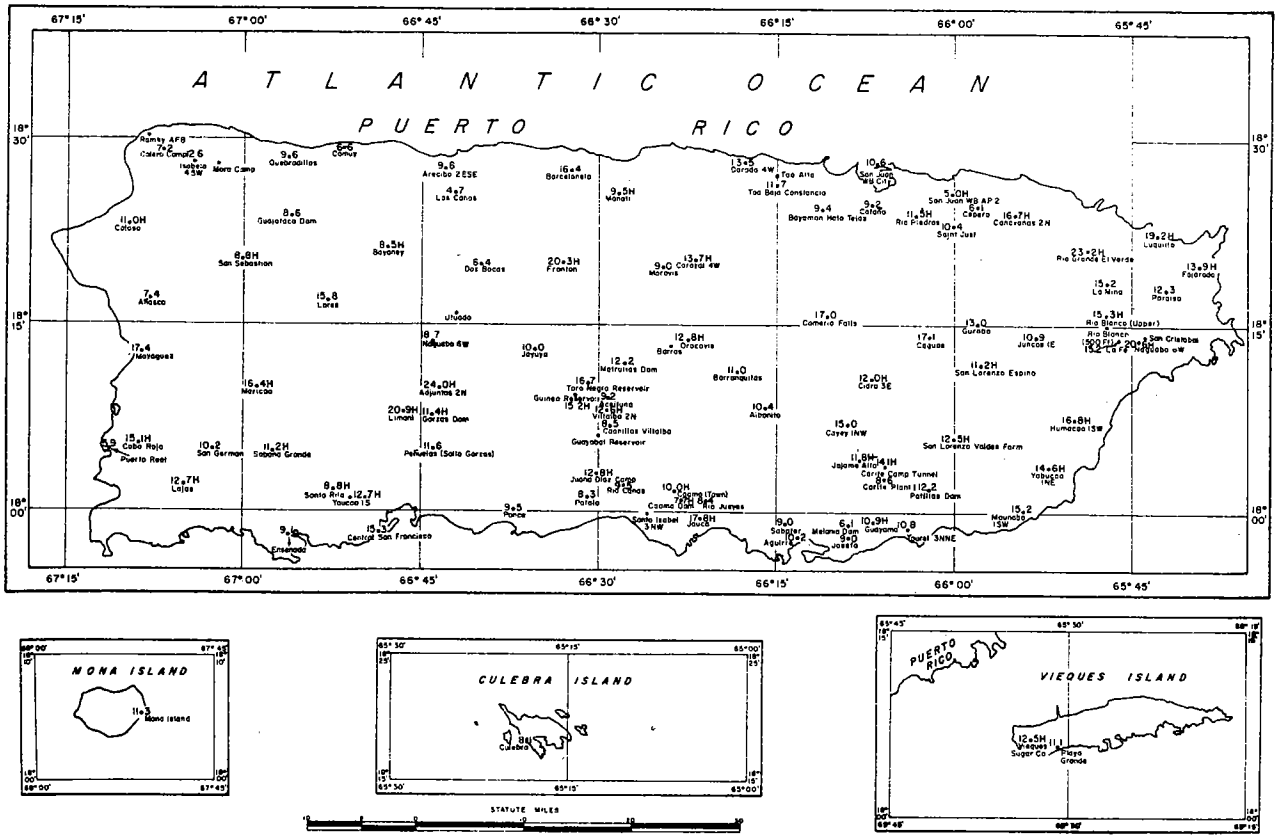

FIGURE 1–1.—Adjusted maximum observed 24-hr. rainfalls (in.) for Puerto Rico. The letter "H" indicates that the rainfall was associated with a hurricane

of these record intensities was associated with a tropical storm. San Juan's record rainfalls have been exceeded at other stations in Puerto Rico. Quinones [1] listed the maxima of table 1–2. Of these maxima, only the 12-hr. amount was associated with a tropical storm, one of hurricane intensity.

1.2.6 Comparison of maximum rainfalls observed in a problem region with those observed throughout the world is always interesting. Table 1–3 lists the world's maximum observed rainfalls. It also includes some near-maximum values that are associated with hurricanes, or typhoons, or observed in the Tropics. When the data of table 1–3 are plotted on logarithmic paper as in figure 1–3, they delineate the enveloping straight line

$$R = 15.3\, D^{0.486} \qquad (1.1)$$

where R is the rainfall in inches and D is the duration in hours. This enveloping line indicates maximum rainfalls two to three times the maxima observed in Puerto Rico and the Virgin Islands (tables 1–1 and 1–2 and figs. 1–1 and 1–2). Equation (1.1) is often given in the modified form,

$$R = 15\sqrt{D} \qquad (1.2)$$

which yields acceptable rainfall values for the range of duration usually of interest in hydrologic design.

1.3 Meteorological situations associated with maximum observed 24-hr. rainfalls

1.3.1 The maximum observed 24-hr. amounts identified with the letter "H" in figures 1–1 and 1–2 resulted from hurricanes. Practically all maxima so identified were associated with one or the other of two very violent hurricanes: *San Ciriaco* of August 7–8, 1899, and *San Felipe II* of September 13, 1928. Both hurricanes followed approximately the same path across Puerto Rico, entering near the southeastern corner and leaving near the northwestern corner. Most of the maxima are associated with the 1928 hurricane. This fact does not necessarily mean that the 1928 hurricane was a more efficient rain

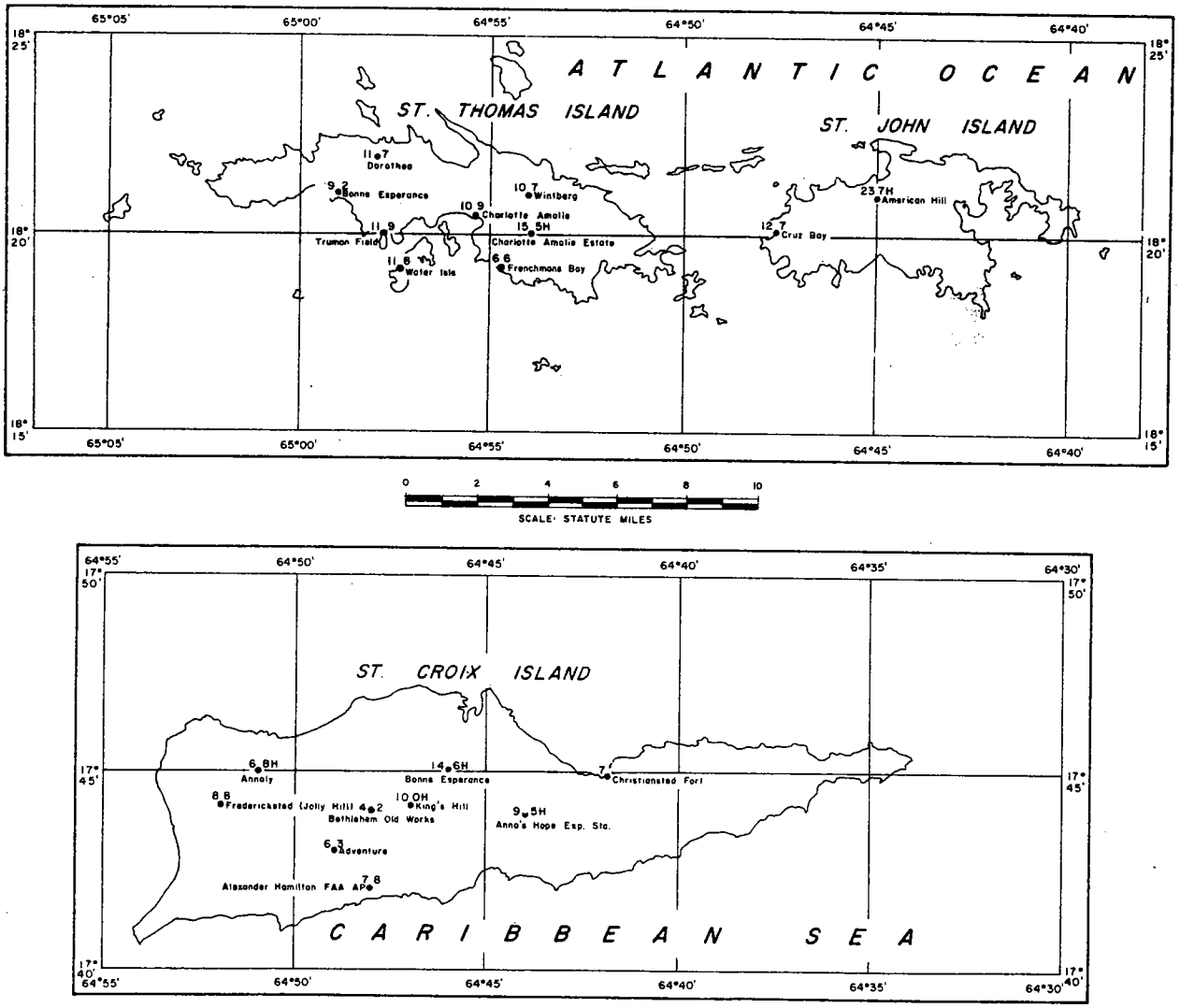

FIGURE 1–2.—Adjusted maximum observed 24-hr. rainfalls (in.) for Virgin Islands. The letter "H" indicates that the rainfall was associated with a hurricane

producer than that of 1899. The raingage network was increased appreciably during the period 1899–1928, and the larger number of gages in 1928 is very likely the reason for more maxima being recorded in that storm.

1.3.2 The non-hurricane maxima were associated with either the passage of a cold front or its attendant trough sweeping across the area from the northwest or with an inverted pressure trough, or easterly wave, moving slowly westward or remaining almost stationary. Figures 1–1 and 1–2 show numerous maxima apparently identified with one or the other of these two situations. Many stations reporting such maxima, however, have relatively short records during which they have not experienced the full effect of an intense hurricane. Some stations with longer records also have never experienced the heaviest rainfalls of a hurricane because they are fairly well sheltered by orographic barriers from the worst effects of hurricanes traveling their usual paths. It should also be kept in mind that the raingage catch in a hurricane is likely to be too low because of the gage effect on the wind [2]. The deficiency might be considerable in the case of hurricane winds. Taking all these factors into consideration, it appears reasonable to expect that the maximum 24-hr. rainfalls from records ex-

TABLE 1–3.—*World's maximum and near-maximum observed point rainfalls*

Duration	Depth (in.)	Location	Date
1 min	1.23	Unionville, Md	July 4, 1956.
5 min	2 48	Portobelo, Panama	Nov 29, 1911.
8 min	4.96	Fussen, Bavaria	May 25, 1920.
15 min	7.80	Plumb Point, Jamaica	May 12, 1916
20 min	8.10	Curtea-de-Arges, Romania	July 7, 1889.
42 min	12.00	Holt, Mo	June 22, 1947.
2 hr. 10 min	19.00	Rockport, W. Va	July 18, 1889.
2 hr. 45 min	22.00	D'Hanis, Tex	May 31, 1935.
4 hr	23.00	Basseterre, St. Kitts	Jan. 12, 1880.
4 hr. 30 min	30.8+	Smethport, Pa	July 18, 1942.
12 hr	30.50	Kadena AFB, Okinawa	Sept. 8, 1956.
18 hr	38 00	do	Sept. 8, 1956.
24 hr	45.99	Baguio, Philippine Islands	July 14–15, 1911.
39 hr	62.39	do	July 14–16, 1911.
2 days	65.79	Funkiko, Formosa	July 18–20, 1913.
2 days 15 hr	79.12	Baguio, Philippine Islands	July 14–17, 1911.
3 days	81.54	Funkiko, Formosa	July 18–20, 1913.
4 days	101 84	Cherrapunji, India	June 12–15, 1876.
5 days	114 50	Silver Hill Plantation, Jamaica	Nov 5–9, 1909.
5 days	[1] 150.	Cherrapunji, India	Aug. —, 1841
6 days	122.50	Silver Hill Plantation, Jamaica	Nov. 5–9, 1909.
7 days	131.15	Cherrapunji, India	June 24–30, 1931
8 days	135 05	do	June 24–July 1, 1931.
15 days	188.88	do	June 24–July 8, 1931.
31 days	366 14	do	July 1861
2 mo	502 63	do	June–July 1861.
3 mo	644.44	do	May–July 1861.
4 mo	737 70	do	Apr.–July 1861.
5 mo	803 62	do	Apr.–Aug. 1861
6 mo	884 03	do	Apr.–Sept. 1861.
11 mo	905.12	do	Jan.–Nov. 1861.
1 yr	1,041 78	do	Aug. 1860–July 1861.
2 yr	1,605.05	do	1860–61

[1] Questionable because of rounded value and missing dates.

tending over several hundred years would all be associated with hurricanes.

1.3.3 The maximum amounts for durations under 12 hr. at San Juan and other stations listed in tables 1–1 and 1–2 were found to be associated with situations of the type discussed in paragraph 1.3.2, perhaps augmented by thunderstorm activity. The magnitudes of these maxima are so low that they should be exceeded easily by an intense slow-moving hurricane with an optimum path.

1.3.4 Of the maximum rainfall amounts listed in table 1–3 and plotted in figure 1–3 for durations of 24 hr. and less, only the Kadena AFB, Okinawa, and Baguio, Philippine Islands, amounts for 12, 18, and 24 hr. can be classified as hurricane rainfalls. Amounts for durations under 6 hr. are from localized cloudbursts. The Plumb Point, Jamaica, amount of 7.8 in. in 15 min. is of special interest because Jamaica has a climate very similar to that of the problem area and because the Plumb Point record value is one of the control points for the shorter durations on the enveloping line of figure 1–3. Here is the report on this observation from the official *Jamaica Meteorological Observations* for May 1916:

> At 3 p.m. on the 12th there was a tremendous downpour or "cloudburst" at the Plumb Point Lighthouse. Mr. Plummer [the observer] writes that an outbuilding was torn from its foundation and smashed to pieces, that trees were thrown down and that the main building and especially the lighthouse rocked on their bases. It was confined to quite a small area and was plainly seen from Kingston. At the time of the occurrence there was only about 0.20 inch in the rain gauge; the cloudburst lasted only 15 minutes; but at the end of that time the gauge which holds 8 inches had overflowed. The cloudburst was followed by a small whirlwind.

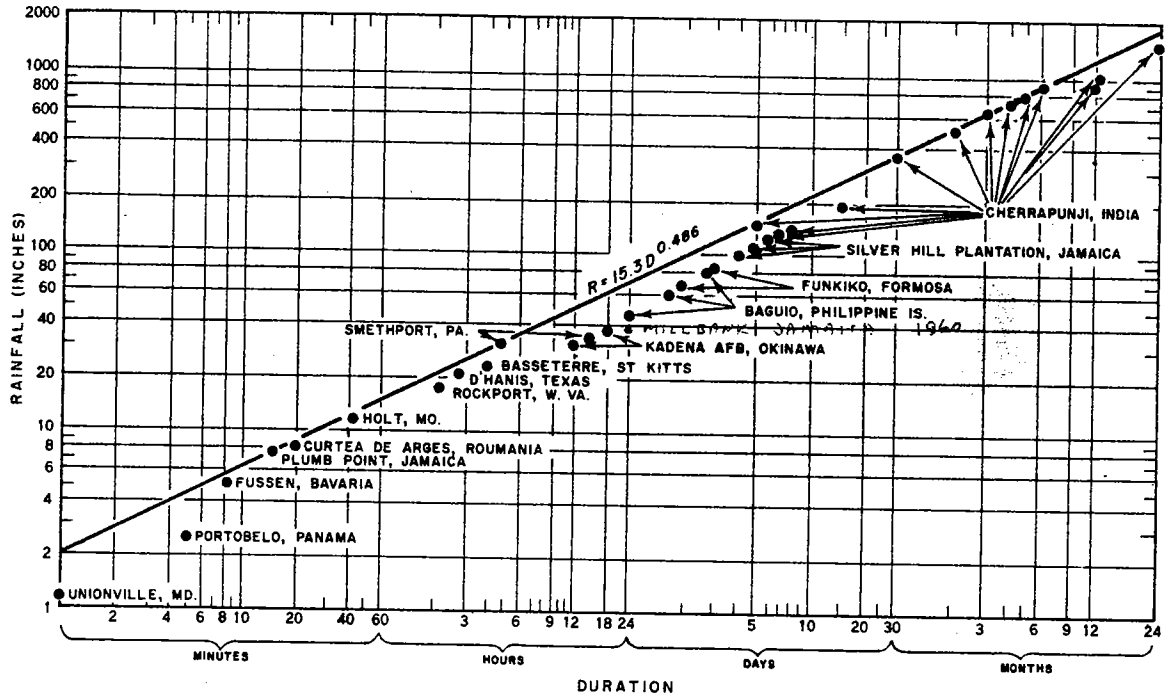

FIGURE 1–3.—World's maximum observed rainfalls.

In view of the above report it appears that the Plumb Point cloudburst was very likely associated with a waterspout, or overwater tornado. Waterspouts are relatively common over tropical and subtropical waters but they break up, or dissipate, very rapidly upon passing inland. They would almost certainly dissipate completely before reaching a location suitable for a dam site; hence their rainfalls may be neglected for the purpose of this report.

1.3.5 The other controlling values on the curve of figure 1–3 for durations under 6 hr. are all from local cloudbursts of extraordinary intensity occurring during the May–July season. The stations reporting these controlling values are all inland stations in the middle latitudes, where precipitation networks are generally densest. However, meteorological conditions favorable for cloudbursts of the magnitude indicated by figure 1–3 may be more likely in such localities than in a maritime tropical region like the problem area. In the late spring or summer, when such cloudbursts are observed, an inland soil surface may reach relatively high daytime temperatures which tend to steepen the lapse rate in the air layer in contact with the ground. Also, in middle latitudes the contrasts in temperature and moisture content of air masses brought into contact with each other are much greater than in the Tropics. In the absence of data to the contrary, the possibility of cloudbursts of world's record magnitude occurring in the problem area appears somewhat doubtful. It should not be inferred that cloudbursts cannot occur in tropical maritime climates. Two outstanding cases are shown on figure 1–3. One is the 5-min. 2.48-in. rainfall observed at Portobelo, Panama, and the other is the 4-hr. 23-in. rainfall reported for Basseterre, St. Kitts. Both these amounts plot well below those controlling the envelope curve.

1.3.6 The 12- and 18-hr. amounts (30.5 and 38.0 in., respectively) shown on figure 1–3 for Kadena AFB, Okinawa, were definitely associated with typhoon *Emma*, which passed off the southern tip of Okinawa on September 8, 1956 [3]. These amounts were measured in a standard 8-in. raingage read at 6-hr. intervals; hence, the true maxima may well have been higher than the measured amounts shown. Similarly, the 24-hr. 45.99-in. value shown for Baguio, Phillippines, also associated with a typhoon [4], is an observational-day measurement (noon, July 14 to noon, July 15, 1911) and not a true 24-hr. maximum. The 2- and 3-day maxima at Funkiko, Formosa, were also associated with a tropical storm. The Jamaica maxima for 5 and 6 days resulted from

an easterly wave (par. 1.3.2). All maxima for Cherrapunji, India, resulted from the strong orographic lifting of the monsoons from the Bay of Bengal.

1.4 Tropical storms of Puerto Rico and Virgin Islands.

1.4.1 A *tropical storm* is a more or less circular area of low atmospheric pressure originating over the tropical oceans and having sustained winds (counterclockwise in the Northern Hemisphere) of 32 to 72 m.p.h. If the sustained wind speeds exceed 72 m.p.h., the storm is called a *hurricane*. (This classification is relatively new but little change has been made in the limits since the classification was first suggested in the late 19th century.) Tropical storms have diameters ranging from about 60 to 1,000 mi. The center, or eye, of a severe tropical storm or hurricane is a roughly circular area of light winds and fair weather, and its diameter may range from about 4 to 40 mi.

1.4.2 Puerto Rico and the Virgin Islands lie in a region where tropical storms are relatively common. Because of the small size of these islands and the relatively small diameter of many of the tropical storms, the islands are not disastrously affected by such storms as often as one might expect. Table 1–4 lists the tropical storms whose centers have passed within two latitude degrees (about 140 mi.) of any of these islands during the period 1515–1959. The listing for the period 1515–1885 is based on the work of Tannehill [5] and for 1886–1958, on Weather Bureau *Technical Paper No. 36* [6]. The list may not be complete, however, because of the probable irregularity and poor quality of meteorological reports prior to about 1890. Wherever possible, the tropical storms of table 1–4 are identified as tropical storms or hurricanes (par 1.4.1). The classification refers only to the intensity at the time the storms were in the vicinity of the Virgin Islands or Puerto Rico. Many storms identified as of tropical storm intensity developed hurricane intensity after leaving the vicinity of the islands. It is possible that in the listing for the years prior to the late 19th century, when classification of hurricanes was standardized, some storms identified as hurricanes could have been merely severe tropical storms.

TABLE 1–4.—*Tropical storms passing within two latitude degrees of Puerto Rico and Virgin Islands in the period 1515–1959*

Date	Remarks
1515, July	Exact date unknown. Caused death of many Indians in Puerto Rico.
1526, Oct. 4	Great damage in Puerto Rico.
1527, Oct. 4	Affected Puerto Rico.
1530, July 26, Aug. 23 and 31.	These three storms within 6 weeks blew down half the houses in San Juan, P.R., and unroofed the remainder. Many cattle drowned.
1537, July and Aug.	Three hurricanes within 2 months in Puerto Rico; exact dates unknown. Many slaves and cattle drowned.
1568, Aug. 24	Affected Puerto Rico.
1575, Sept. 21	Severe hurricane, known as *San Mateo I* in Puerto Rico.
1615, Sept. 12	Severest hurricane to affect Puerto Rico in 40 yr. (This suggests that other tropical storms may have occurred between 1575 and 1615.)
1738, Sept. 12	Affected Puerto Rico.
1740, —	Affected Puerto Rico; exact date unknown but probably occurred in August.
1751, Aug. 18	Affected Puerto Rico.
1767, Aug. 7	Plantations destroyed and livestock drowned in Puerto Rico.
1772, Aug. 28	Affected Puerto Rico.
1772, Sept. —	Affected Puerto Rico; exact date unknown.
1780, June 3	Great destruction of property in Puerto Rico, especially crops.
1780, Oct. 14	Probably the most terrible hurricane of record up to this date and known as *The Great Hurricane*. Passed off southwestern corner of Puerto Rico moving in SE to NW direction.
1785, Sept. 25	A furious hurricane that passed over Puerto Rico.
1788, Aug. 16	Seriously affected Puerto Rico.
1804, Sept. 21	This great hurricane, known as *San Mateo II*, long remained in the memory of the Puerto Ricans.
1807, Aug. 17–19	Severe hurricane from the east lasted 50 hr. in Puerto Rico.
1812, July 23 and Aug. 21	Seriously affected Puerto Rico.
1813, July 23	Do
1814, July 22–23	Do
1816, —	A hurricane of extraordinary violence in Puerto Rico; exact date unknown.
1818, Sept. 22	Seriously affected Puerto Rico.
1819, Sept. 22	Very destructive in Virgin Islands and severe in Puerto Rico.
1825, July 26–27	A very violent hurricane, known as *Santa Ana*, which was very destructive in Puerto Rico.
1827, Aug. 18–19	Very destructive hurricane crossed Puerto Rico in SE to NW direction.
1827, Aug. 28	Affected Virgin Islands severely, especially St. Thomas Island.
1830, Aug. 11–12	Severely affected St. Thomas Island.
1835, Aug. 13	Crossed Puerto Rico in ESE to WNW direction.
1837, July 31	Severely affected St. Thomas Island.
1837, Aug. 2–3	A violent hurricane, known as *Los Angeles*, struck St. Thomas Island and skirted northeastern coast of Puerto Rico in ESE to WNW direction.
1840, Sept. 16	Severely affected Puerto Rico.
1846, Sept. 12–13	Passed by northeastern corner of Puerto Rico in a SE to NW direction.
1851, Aug. 18–19	A violent hurricane, known as *Santa Elena* skirted south coast and crossed southwestern corner of Puerto Rico in ESE to WNW direction.
1852, Sept.	Affected Puerto Rico; exact date unknown.
1867, Oct. 29	The most violent hurricane experienced in many parts of Puerto Rico and known as *San Narcisco*. Accounts indicate it was a storm of small diameter and rapid movement. Also affected St. Thomas Island where 1,000 lives were lost.

TABLE 1-4.—*Tropical storms passing within two latitude degrees of Puerto Rico and Virgin Islands in the period 1515–1959*—Continued

Date	Remarks
1876, Sept 13	A hurricane of great violence, known as *San Felipe I*, struck St. Thomas Island and skirted south coast of Puerto Rico.
1889, Sept. 3	Severe hurricane destructive in St. Thomas Island and passing east of it in SE to NW direction.
1891, Aug. 19–20	Hurricane crossed eastern Puerto Rico in SE to NW direction.
1891, Oct 2–4	Tropical storm skirted south coast of Puerto Rico in E to W direction.
1893, Aug. 16–17	Hurricane crossed Puerto Rico in ESE to WNW direction.
1896, Aug 31–Sept. 1	Hurricane crossed southwestern corner of Puerto Rico in SE to NW direction.
1898, Sept. 21–22	Tropical storm crossed northeastern Puerto Rico in ESE to WNW direction.
1899, Aug 7–8	Disastrous hurricane, known as *San Ciriaco*, crossed Puerto Rico in ESE to WNW direction.
1899, Aug. 30–31	Hurricane crossed southwestern corner of Puerto Rico in ESE to WNW direction.
1900, Aug 30–Sept 1	Tropical storm skirted south coast of Puerto Rico in E to W direction
1900, Oct 24–26	Tropical storm crossed southwestern corner of Puerto Rico in SE to NW direction
1901, July 6–8	Hurricane crossed southwestern Puerto Rico in SE to NW direction
1901, Sept. 11–13	Tropical storm skirted north coast of Puerto Rico in SE to NW direction
1901, Oct 8–10	Tropical storm crossed northeastern corner of Puerto Rico in SE to NW direction
1903, July 19–20	Tropical storm crossed Puerto Rico in ESE to WNW direction
1908, Sept 9–10	Hurricane passed off north coast of Puerto Rico in E to W direction
1908, Sept 26–27	Tropical storm passed off south coast of Puerto Rico in E to W direction.
1909, Nov 12–13	Tropical storm passed off northwestern corner of Puerto Rico in WSW to ENE direction
1910, Aug 24–25	Tropical storm passed off south coast of Puerto Rico in E to W direction.
1910, Sept 6–7	Hurricane skirted south coast of Puerto Rico in E to W direction
1915, Aug 10–12	Hurricane skirted south coasts of St. Croix Island and Puerto Rico in E to W direction
1916, July 12–14	Tropical storm passed through Virgin Islands in SE to NW direction
1916, Aug 21–22	Hurricane passed through Virgin Islands and across Puerto Rico in E to W direction. Destructive winds in Puerto Rico extended over an area only 50 mi wide
1917, Sept 21–22	Hurricane passed about 1° lat south of Puerto Rico in E to W direction
1918, Sept 10–11	Tropical storm passed about 1° lat. south of Puerto Rico in ESE to WNW direction
1919, Sept 3	Tropical storm passed between Hispaniola and Puerto Rico in SE to NW direction
1922, Sept 16	Hurricane passed just northeast of Virgin Islands in ESE to WNW direction
1924, Aug 18	Tropical storm passed through Virgin Islands in SE to NW direction
1924, Aug 28	Hurricane passed less than 2° lat northeast of Virgin Islands in SE to NW direction.
1926, July 23–24	Hurricane just tipped southwestern corner of Puerto Rico in ESE to WNW direction
1928, Sept 13	Most destructive hurricane in many years, known as *San Felipe II*, passed through Virgin Islands and across Puerto Rico in ESE to WNW direction
1930, Sept 2–3	Hurricane passed just off southwestern corner of Puerto Rico in ESE to WNW direction
1931, Aug. 17	Tropical storm crossed Puerto Rico in SE to NW direction.
1931, Sept. 10–11	Violent hurricane, known as *San Nicolas*, passed through Virgin Islands and skirted north coast of Puerto Rico in E to W direction causing destruction along a strip 10 to 12 mi. wide
1932, Sept 26–27	Destructive hurricane, known as *San Ciprian*, passed through Virgin Islands and across Puerto Rico in E to W direction.
1933, July 14–15	Tropical storm passed within 1° lat. south of Puerto Rico in E to W direction.
1933, July 25–26	Tropical storm passed just northeast of Virgin Islands in ESE to WNW direction.
1933, Sept. 27–28	Tropical storm passed within 1° lat. south of Puerto Rico in E to W direction.
1934, Aug. 21–22	Tropical storm passed with 2° lat. south of Puerto Rico in E to W direction.
1934, Sept 18	Tropical storm passed within 2° lat. northeast of Virgin Islands in SE to NW direction.
1937, Aug. 24–25	Tropical storm passed within 2° lat. northeast of Virgin Islands in ESE to WNW direction.
1938, Aug. 8	Tropical storm passed through Virgin Islands and skirted north coast of Puerto Rico in E to W direction.
1939, Aug. 7	Tropical storm apparently developed about 1° lat. northeast of St. Thomas Island and moved northwestward
1940, Aug. 5	Tropical storm passed just north of St. Thomas Island in ESE to WNW direction.
1942, Nov 4	Tropical storm apparently developed just off southeastern Puerto Rico and crossed northeastern part of island in ESE to WNW direction
1943, Aug. 13–14	Tropical storm passed just northeast of St. Thomas Island in ESE to WNW direction.
1943, Oct 14	Hurricane passed between Hispaniola and Puerto Rico in S to N direction
1944, July 12–13	Tropical storm apparently developed just off northwest corner of Puerto Rico and moved northwestward.
1945, Aug 3	Tropical storm passed within 1° lat. of southwestern corner of Puerto Rico in ESE to WNW direction.
1945, Sept. 12–13	Hurricane passed within 2° lat north of Virgin Islands and Puerto Rico in ESE to WNW direction
1947, Oct. 16–17	Tropical storm passed just northeast of St. Thomas Island in SE to NW direction
1949, Sept 2–3	Tropical storm developed between Puerto Rico and the Virgin Islands and moved northwestward, reaching hurricane intensity and changing course to northward after passing 20° N. lat on the 3d.
1950, Aug 23	Tropical storm tipped southwest corner of Puerto Rico in ESE to WNW direction
1953, Sept 14	Tropical storm *Edna* passed within 1° lat northeast of Virgin Islands in SE to NW direction
1954, Aug 30–31	Tropical storm *Dolly* formed just off northwestern corner of Puerto Rico and moved off in NNW direction
1955, Jan 3	Hurricane *Alice* passed within 1° lat southeast of St. Croix Island in ENE to WSW direction.
1955, Sept 11–12	Tropical storm *Hilda* passed within 1° lat. north of St. Thomas Island in ESE to WNW direction, reaching hurricane intensity on 12th
1956, Aug 11–12	Hurricane *Betsy* crossed Puerto Rico in SE to NW direction.
1957, Sept 13–14	Tropical storm *Gerda* passed about 1° lat from southwestern corner of Puerto Rico in ESE to WNW direction.

Chapter 2

THE HURRICANE MODEL

2.1 Introduction

2.1.1 The information contained in chapter 1 suggests that the PMP, at least for durations of 6 to 24 hr., would probably occur in connection with a hurricane. Ordinarily, the procedure for estimating PMP consists of maximizing depth-area-duration data obtained by analysis of hurricane rainfalls. This procedure cannot be used for estimating PMP in the problem region for two reasons. First, there are no readily available depth-area-duration data for hurricanes in the region and, second, the rugged orography of the region makes it unreasonable to transpose such data already analyzed for hurricane rainfalls on the Gulf and Atlantic Coasts of the United States. In this study a hurricane model was postulated, tested on observed hurricane rainfalls, and then used to derive estimates of probable maximum hurricane rainfalls. This chapter discusses the model selected, its tests, the manner of its application to obtain PMP estimates, and the results.

2.2 The convergence component of the model

2.2.1 The model selected for computing rainfall resulting from convergence alone was based on the results of fairly recent hurricane research conducted without any consideration whatever of the possible use of the results for estimating PMP. The wind pattern used is the one presented by Graham and Nunn (p. 45 [7]). This particular wind pattern (fig. 2–1), based on envelopment of meteorological events of record with a few extremes excepted, is intended to represent the wind field 30 ft. above the sea surface for a large-radius hurricane with a central pressure of 26.74 in. (906 mb.) and moving about 12 m.p.h. just off the east coast of southern Florida.

2.2.2 The similarity of the climates of southern Florida, Puerto Rico, Virgin Islands, and their surrounding waters suggests that the wind field of figure 2–1 is applicable to the problem area. There are very few accurate measurements of central pressure in hurricanes. The lowest reported [5] for hurricanes over the Caribbean Sea and Gulf of Mexico are listed in table 2–1. Lower central pressures have been reported in other regions. Consequently, while the central pressure of 26.74 in. for which the wind field of figure 2–1 was developed is a rare phenomenon, the wind field is considered conservative, i.e., not extremely rare, for the purpose of estimating PMP for the problem area.

TABLE 2–1.—*Lowest central pressures observed in hurricanes of the Caribbean Sea and Gulf of Mexico*

Place	Date	Sea level pressure	
		(in.)	(mb.)
Florida Keys	Sept. 2, 1935	26.35	892
Morne Rouge, Martinique	Aug. 18–19, 1891	26.85	909
Havana, Cuba	Oct. 10–11, 1846	27.06	916
Guayama, P.R.	Sept. 13, 1928	27.65	936

2.2.3 The vertical structure of the hurricane model was based on the results of studies by Riehl [8] and Miller [9]. The height of the inflow, or convergence, layer (fig. 2–2) was assumed to be equivalent to a pressure difference of 100 mb. (For the range in elevation involved in this study, a pressure difference of 100 mb. represents a height change of 1 km., or 3,300 ft.) This assumption was based on two reasons. Riehl obtained some realistic rainfall values from computations based on the rate of moisture inflow in the bottom 100-mb. layer. Later studies by Miller indicated no inflow above the 1-km. level within at least 100 mi. of the hurricane center. Some recent radar observations tend to confirm Miller's computations. Moreover, the studies of both investigators indicated little outflow except above the 6-km. (20,000-ft.) level (fig. 2–3). Consequently, the hurricane model of figure 2–2 was assumed to have no inflow or outflow, i.e., no convergence or divergence, between the 1- and 6-km. levels. Thus, the moist air is brought into the bottom 1-km. layer of the model by the radial component, v_r, of the wind. This convergence of flow into the bottom layer produces an

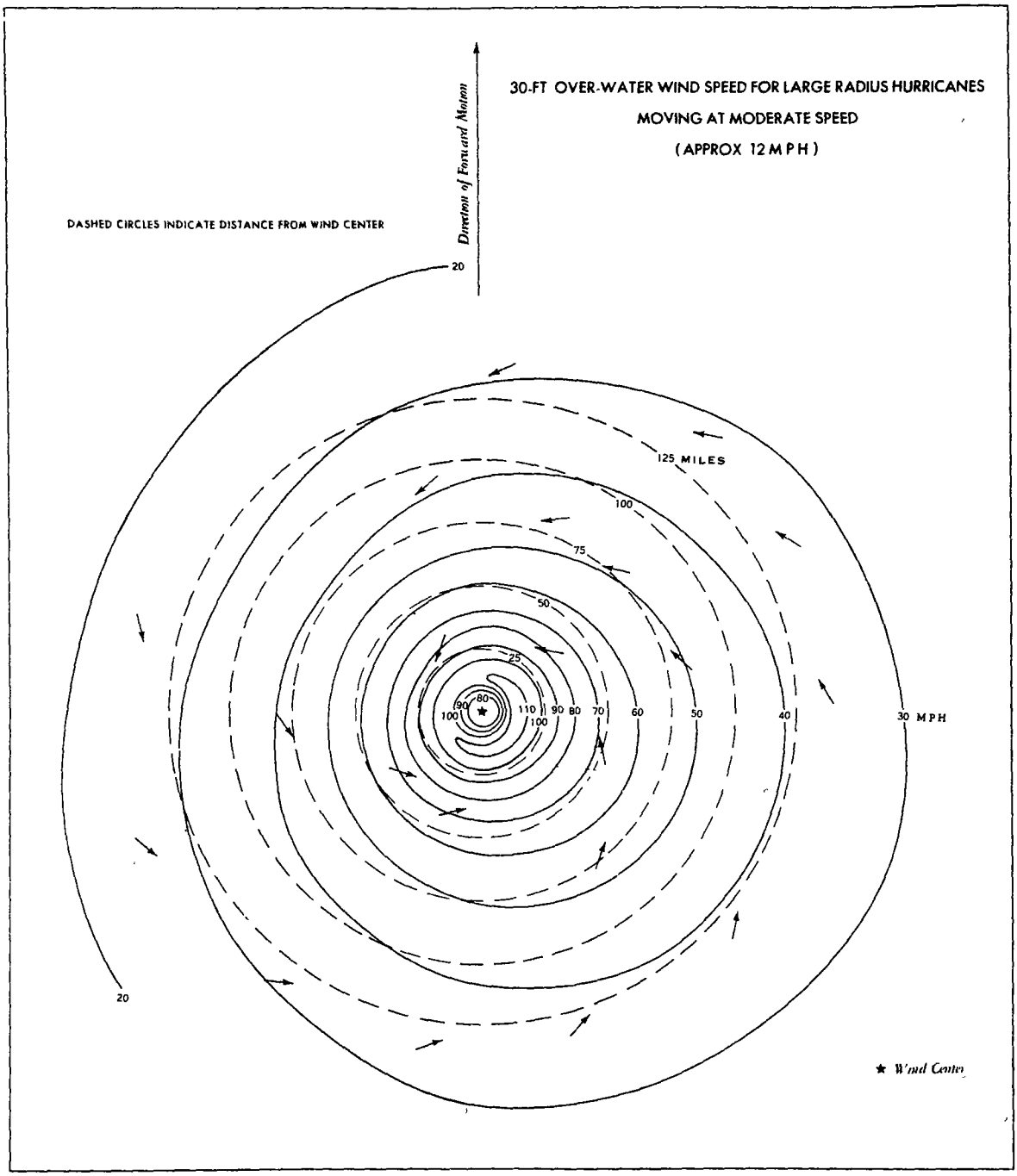

FIGURE 2–1.—Hurricane model surface wind field.

upward component, v_z, which provides the lifting required to cool the air and effect condensation and precipitation of its moisture. The outflow, or divergence, above the 6-km. layer carries condensation moisture and rainfall out of the model. The amount of moisture above the 6-km. level, however, is less than 10 percent of that below. This loss was neglected in using the model for computing rainfall and may be considered as a maximizing factor.

2.2.4 Of paramount importance in the use of the above model is the rate of moisture inflow, which is a function of the radial, or inflow, wind speed and the

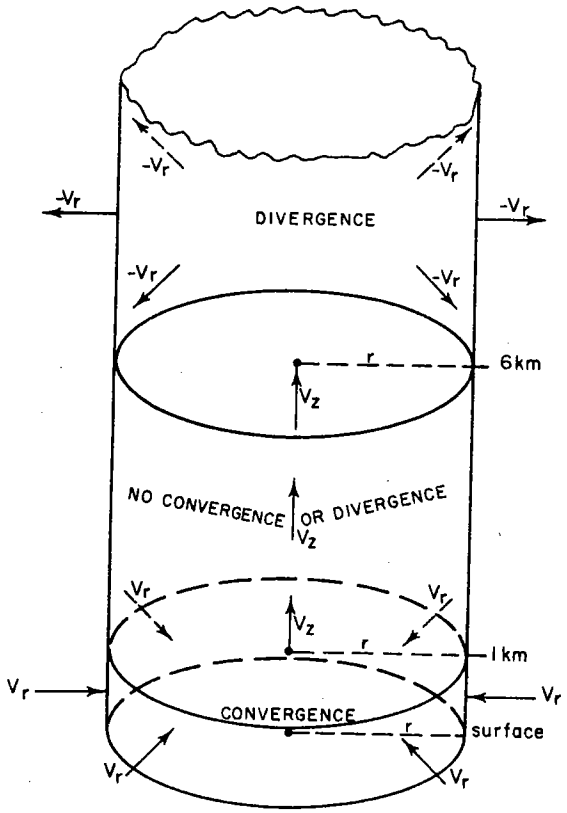

FIGURE 2–2.—Vertical distribution of convergence and divergence in hurricane model.

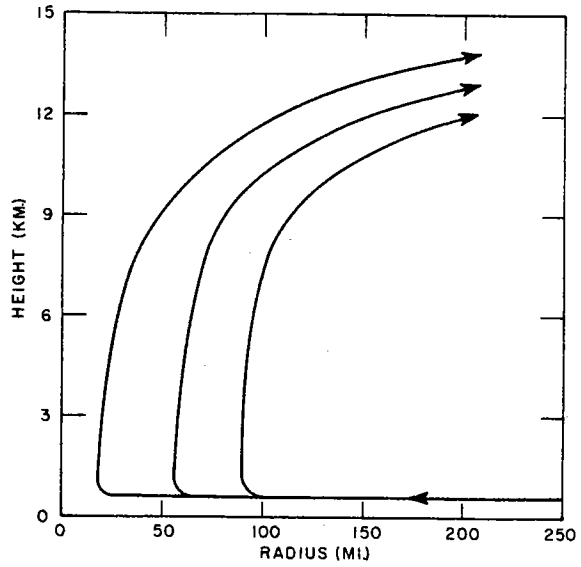

FIGURE 2–3.—Vertical circulation in hurricane model (after Riehl)

water vapor content of the inflowing air. The radial components of the wind are easily computed from the wind field of figure 2–1, the wind speeds being indicated by the isovels and the direction by the arrows. All arrows make an angle of 25° with tangents at point of arrowhead to circles (or cylindrical surfaces) centered about wind center. In other words, the winds would be entering the cylindrical surface of the bottom 1-km. layer of the model at an angle of 25° with the tangent to the surface at point of entry.

2.2.5 The wind field of figure 2–1 was originally intended to represent conditions 30 ft. above the surface of the sea (par. 2.2.1). The wind speeds would be expected to increase with height in the hurricane model because of the lesser effects of surface friction. The tangential angles would be expected to decrease for the same reason. The higher speeds and smaller tangential angles have opposite effects on the radial, or inflow, component of the wind, the higher speeds tending to produce an increase and the smaller angles, a decrease. Data on the variation of inflow with height within that bottom layer are apparently unavailable. Also unknown are the changes in inflow rates that would result from applying the wind field of figure 2–1 over a land surface. The larger frictional effects of the land surface would undoubtedly act to reduce wind speeds and increase tangential angles, but the results on inflow rates cannot be evaluated until additional data become available. It was for these reasons that the wind field depicted in figure 2–1 was assumed to apply over land and to be unchanged with height within the 1-km. inflow layer of the hurricane model.

2.2.6 As indicated in paragraph 2.2.4, the water vapor content of the air is the second important factor governing moisture-inflow rates. The water vapor content of the air is, of course, limited by the air temperature, i.e., the vapor pressure cannot exceed the saturation vapor pressure, which is a function of temperature. Near-saturation conditions are known to prevail within the hurricane except within the eye. Consequently, the assumption that saturated air would be flowing into the hurricane model to be used in estimating PMP is logical.

2.2.7 It is generally accepted [10] that the surface air temperature within a hurricane tends to remain relatively constant. Examination of a few thermograph traces associated with hurricanes indicates, however, that the temperature tends to fall as the hurricane approaches, but does level off within the hurricane proper. A typical example is shown on page 16 of Tannehill's *Hurricanes* [5], which presents the

thermograph trace for San Juan, P.R., during the passage of the great *San Felipe II* hurricane of September 13, 1928. The hurricane center passed about 30 mi. south of San Juan. The thermograph trace shows a surface air temperature of about 85°F. at noon on September 12, when the wind speed was 20 to 30 m.p.h. This temperature is only a few degrees warmer than the mean sea surface temperature for that time of year. By about 9 a.m. on September 13, when the wind speed reached hurricane force, the air temperature had dropped from 85°F. to 75° or 76°F., and fluctuated between 72° and 76°F. long after the hurricane winds had subsided.

2.2.8 During the initial temperature fall described in the preceding paragraph the wind direction remained in the NE quadrant, so the lowering of temperature cannot be ascribed to advection of air from another source. Furthermore, the greatest rate of fall occurred while the atmospheric pressure was falling only about 0.2 in. (7 mb.), a pressure change that could not possibly explain a temperature drop of about 10 F.° as resulting from adiabatic expansion. A partial explanation of the initial fall and relative stability in surface air temperature associated with a hurricane may lie in the rain itself. The rain has its source in the higher and colder levels, and its fall through the warmer lower layers is bound to produce cooling through conduction, entrainment, and evaporation.

2.2.9 The purpose of the study of temperatures associated with hurricanes was to determine a reasonable upper limit of temperature that could be used to estimate a practical evaluation of the upper limit of water vapor to be used in the hurricane model. Examination of several temperature traces recorded in hurricanes [11, 12] indicated little departure from a mean temperature of 75°F. Study of these temperature traces and of synoptic charts for several other hurricanes led to the decision to use 75° F. as the surface air temperature of the hurricane model. Following the standard practice in deriving estimates of PMP, the air in the model was assumed to be saturated and the temperature lapse rate, or variation with height, to be pseudoadiabatic.

2.3 Computation of convergence rainfall

2.3.1 The convergence rainfall is the rainfall that the hurricane would produce over the ocean or flat land surface; i.e., without orographic influences. The computation of convergence rainfall was conducted in the manner suggested by Riehl [8]. The inflow of moisture through the vertical cylindrical surface of the inflow layer (fig. 2–2) with radius, r, is equal to the circumference, $2\pi r$, multiplied by the mean specific humidity, $\bar{q}$, of the inflow and the mass flux of moist air, $\bar{v}_r \Delta p/g$, where Δp is the pressure difference between the bottom and top of the inflow layer and g is gravity. The moisture inflow is thus $2\pi r \bar{q} \bar{v}_r \Delta p/g$. If the inflowing air is assumed to be initially saturated and the moisture to be precipitated as soon as condensed, and if the loss of outflowing moisture above the 6-km. level is neglected, the moisture inflow must be equal to πr^2, the horizontal cross-sectional area of the cylindrical model, multiplied by R, the rainfall per unit time and area, or

$$R = \frac{2v_r}{r} \cdot \bar{q} \cdot \frac{\Delta p}{g} \tag{2.1}$$

2.3.2 In the computations of rainfall discussed in this report the mean mixing ratio $\bar{w}$ was used instead of $\bar{q}$ in equation (2.1) because values of the former are more readily available and the quantitative difference between the two is insignificant for the conditions pertinent to the study described herein. The mixing ratio is the ratio of the mass of water vapor to the mass of dry air, or

$$w = \frac{0.622e}{p-e} \tag{2.2}$$

where e is the vapor pressure and p is the atmospheric pressure. In applying the hurricane model to compute rainfall, the saturation vapor pressure, e_s, based on the model's inflow-layer temperature (par. 2.2.9) was used for e. The pressure, p, presented a somewhat more complicated problem since the pressure gradient is extremely steep near a hurricane center. Examination of the wind field of figure 2–1 suggested that the maximum convergence and/or orographic rainfall might be realized when the center of the hurricane depicted by the model passed within 15 mi. (the radius of maximum winds) to the left of the spot for which rainfall was being computed. A previous study [13] of hurricane pressure profiles indicated that a pressure of 27.92 in. (945 mb.) 15 mi. from the center of the model was reasonable. At 40 mi. from the center, roughly the outer limit of hurricane winds (fig. 2–1), the pressure would be about 28.93 in. (980 mb.). The assumption of a fixed pressure (to simplify rainfall computations) within the range 945 to 980 mb. could not result in an error of more than 4 percent in the computed rainfall values. It was suspected that the computed rainfalls might be at a maximum for a point less than 15 mi. from the path

TABLE 2–2.—*Convergence rainfall rates computed with equation (2.3) for various distances from hurricane center*

r (mi.)	$\bar{v}_r$ (m.p.s.)	R_1 (in./hr.)	R_2 (in./hr.)
5	0	0	
			9.25
10	20.8	6.92	
			2.36
20	21.0	3.50	
			.73
30	17.7	1.96	
			.39
40	15.0	1.25	
			.21
50	13.1	.87	
			.13
60	11.5	.64	
			.10
70	10.6	.50	
			.07
80	9.8	.40	
			.05
90	9.0	.33	
			.03
100	8.3	.28	
			.01
110	7.9	.24	
120	7.3	.20	

NOTE:—R_1 is the average rainfall intensity within the circle of indicated radius. R_2 is the average rainfall intensity within the area between two adjoining concentric circles of indicated radii. The hurricane eye, an area of no rain, is assumed to have a radius of 5 mi.

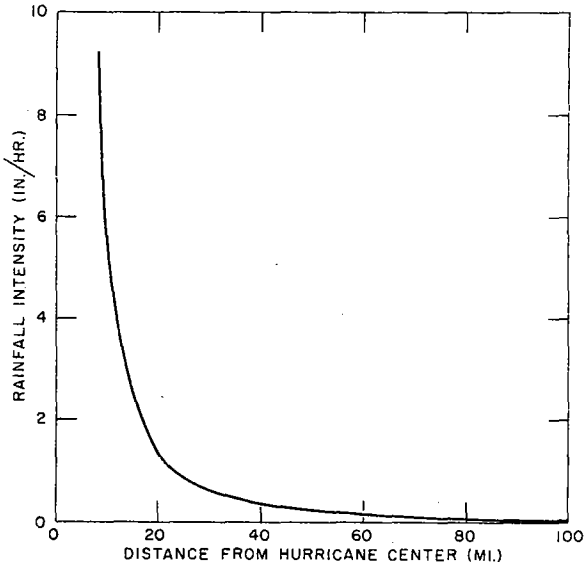

FIGURE 2–4.—Variation of computed convergence rainfall intensity with distance from center of model hurricane.

of the hurricane center so a fixed pressure of 950 mb. would result in less error than one nearer the midpoint of the 945 to 980-mb. range. (As it later developed, this value of 950 mb. was a fortunate choice since tests indicated that 8 mi. from the center, where the pressure would be 922 mb., was the critical distance.) Thus it was that 950 mb., approximately the halfway point between 922 and 980 mb., was selected as the pressure at the base of the hurricane model when used at sea level.

2.3.3 In order to simplify the computations of convergence rainfall with the hurricane model of figure 2–2, which has an inflow-layer thickness equivalent to 100 mb., equation (2.1) was modified to

$$R=\frac{0.18\bar{v}_r\bar{w}}{r} \tag{2.3}$$

where R is the rainfall intensity in in./hr., $\bar{v}_r$ is the mean radial inflow wind component in m.p.s., $\bar{w}$ is the mean mixing ratio in gm./kg., and r is the radius in mi. The average mixing ratio, $\bar{w}$, for the model's inflow layer with base at 950 mb., top at 850 mb., and pseudoadiabatic saturated air with a base temperature of 75°F. is 18.5 gm./kg. This model yielded the rainfall amounts of table 2–2. Plotting of the R_2 values of table 2–2 at the radii delineating the circles that would divide each ring, or "washer," into two equal areas yields the curve of figure 2–4.

2.4 The orographic component of the model

2.4.1 As the hurricane moves across mountainous regions, the upward motion of the air resulting from convergence will be supplemented by orographic lifting whenever the wind has an onslope component. The rate of lifting is determined by the magnitude of the onslope component and the degree of slope. Once the upward wind component is known, the rainfall intensity can be computed as suggested by Showalter [14] if the air is saturated and has a pseudoadiabatic lapse rate, which are assumed conditions of the hurricane model. Showalter's equation is

$$R=\frac{v_z\rho_0(w_0-w_1)}{7} \tag{2.4}$$

where R is the rainfall intensity in in./hr., v_z is the vertical wind speed in m.p.s. at the base of the air column, ρ_0 is the air density in gm./m.^{3} at the base of the air column, and w_0 and w_1 are the mixing ratios in gm./gm. at the base and top, respectively, of the air column.

2.4.2 The determination of the height of the air column to be lifted orographically presented a fairly difficult problem. Studies [15, 16] suggest that a 3,000-ft. mountain barrier in the path of a strong

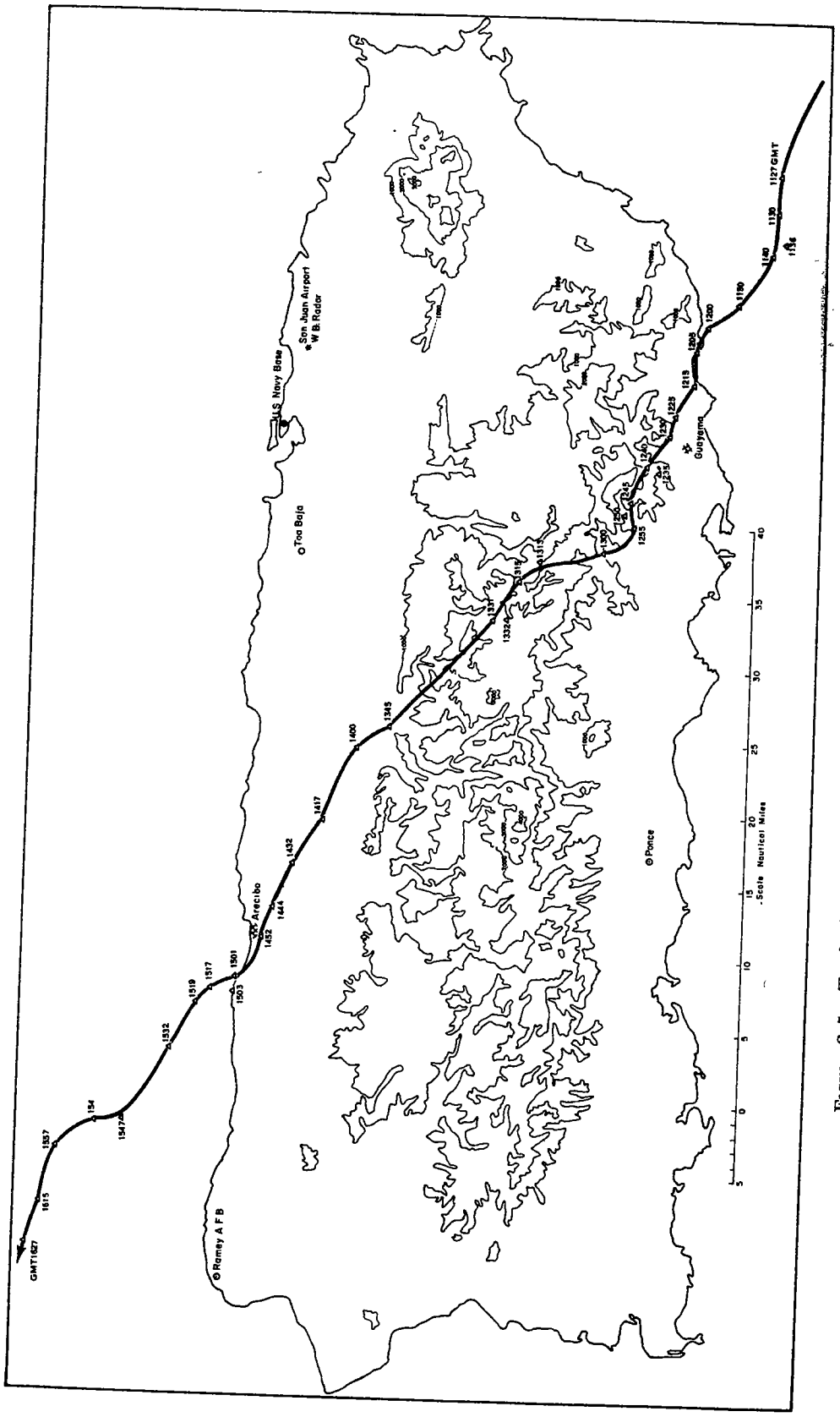

FIGURE 2–5.—Track of hurricane *Betsy* across Puerto Rico, August 12, 1956 (after Colón)

wind should certainly produce an upward wind component that would persist above the 6-km. level. All known studies, however, are based on the assumption of irrotational flow. What happens when a wind field like that of figure 2–1 meets a mountain barrier is another problem entirely. Radar observations suggest that the path of a hurricane tends to be disturbed by orographic influences. For example, the track of hurricane *Betsy* (fig. 2–5), which crossed Puerto Rico on August 12, 1956, shows an erratic, unsteady, and wavering movement as long as some part of the hurricane was being affected by the orography of the island. Other effects were also noted [17]. The eye appeared to be sharply tilted toward the northwest while over the island, i.e., the upper part was ahead of the surface position, perhaps mainly because of excessive surface friction. Moreover, the shape of the eye was apparently distorted, appearing to be almost square at one time.

2.4.3 In view of the above evidence, it is reasonable to expect that the idealized hurricane model depicted by figures 2–1 and 2–2 would be appreciably distorted by orographic influences. The effect of these distortions cannot be evaluated, which means that the lifting effect of the onslope wind also cannot be evaluated. It was necessary, however, that the convergence and orographic effects be combined in some manner so as to yield reasonable rainfall values, the degree of reasonableness to be determined by comparison with observed hurricane rainfalls. The first trial was based on the assumption that the hurricane model (figs. 2–1 and 2–2) would be unchanged except that the base would be at the elevation of the point for which the rainfall was to be computed. The inflow layer was to remain 1 km. in depth; i.e., a difference of 100 mb. between bottom and top.

2.4.4 The orographic rainfall produced by the lifting effect of onslope winds was assumed to be equivalent to the moisture that would be condensed from the saturated air in the 1-km. inflow layer under steady state conditions. This assumption does not invalidate the earlier statement (par. 2.4.2) that the orographic lifting effect may be observed well above the 1-km. inflow layer. The lifting effect of an onslope wind at a point on a windward slope acts both to decrease and to increase rainfall at the point. It acts to decrease rainfall by keeping aloft the smaller raindrops that would fall to the ground at the point in question if the upward wind component due entirely to meteorological effects were not augmented by the orographic component. It acts to increase rainfall by augmenting the upward wind component, hence the cooling and condensation rates of the atmospheric water vapor. Furthermore, it should be kept in mind that the orographic lifting directly above a point on a mountain slope acts on only a small part of the rainfall measured at that point. Practically all rainfall formed above the point is carried downwind. For example, assuming a 75-m.p.h. wind with an upward component of 20 f.p.s., even the largest raindrops, which have a terminal velocity of about 30 f.p.s., would be carried horizontally over 5 mi. while falling $\frac{1}{2}$ mi. Smaller drops or drops falling greater distances would, of course, be carried horizontally much farther. Hence, most of the rainfall falling at the point is formed upwind where the orographic lifting effect may be much different from that above the point. This is especially true in the case of hurricanes because their almost circular wind fields with relatively small radii result in rapid variation of wind speed and direction, hence of onslope and upward wind components, with distance from a point. Current meteorological knowledge is inadequate to permit an evaluation of the above factors for the reliable computation of orographic rainfall at a point. The assumption that the orographic component of hurricane rainfall could be approximated by considering only the orographic lifting effect on the water vapor in the 1-km. inflow layer is therefore in effect a postulation of a computational rather than a physical model that had to be tested to determine its reasonableness.

2.4.5 Now, the vertical component of the wind, v_z, is:

$$v_z = v_f \tan\alpha \tag{2.5}$$

where v_f, is the onslope, or forward, horizontal component of the wind perpendicular to the orientation of the orographic barrier for whose slope the rainfall is being computed, and α is the angle of inclination of the terrain with the horizontal. The air density, in gm./m.^{3}, as used in equation (2.4), can be computed [14] by

$$\rho_0 = \frac{348.4 p_0}{T_0} \tag{2.6}$$

where p_0 and T_0 are, respectively, the atmospheric pressure, in mb., and air temperature, on the Kelvin scale, at the base of the air column, or model. The base pressure and temperature of the hurricane model having been determined to be 950 mb. and 75°F. (297°K.), ρ_0 may be computed readily. Moreover, since the pressure difference between the base and

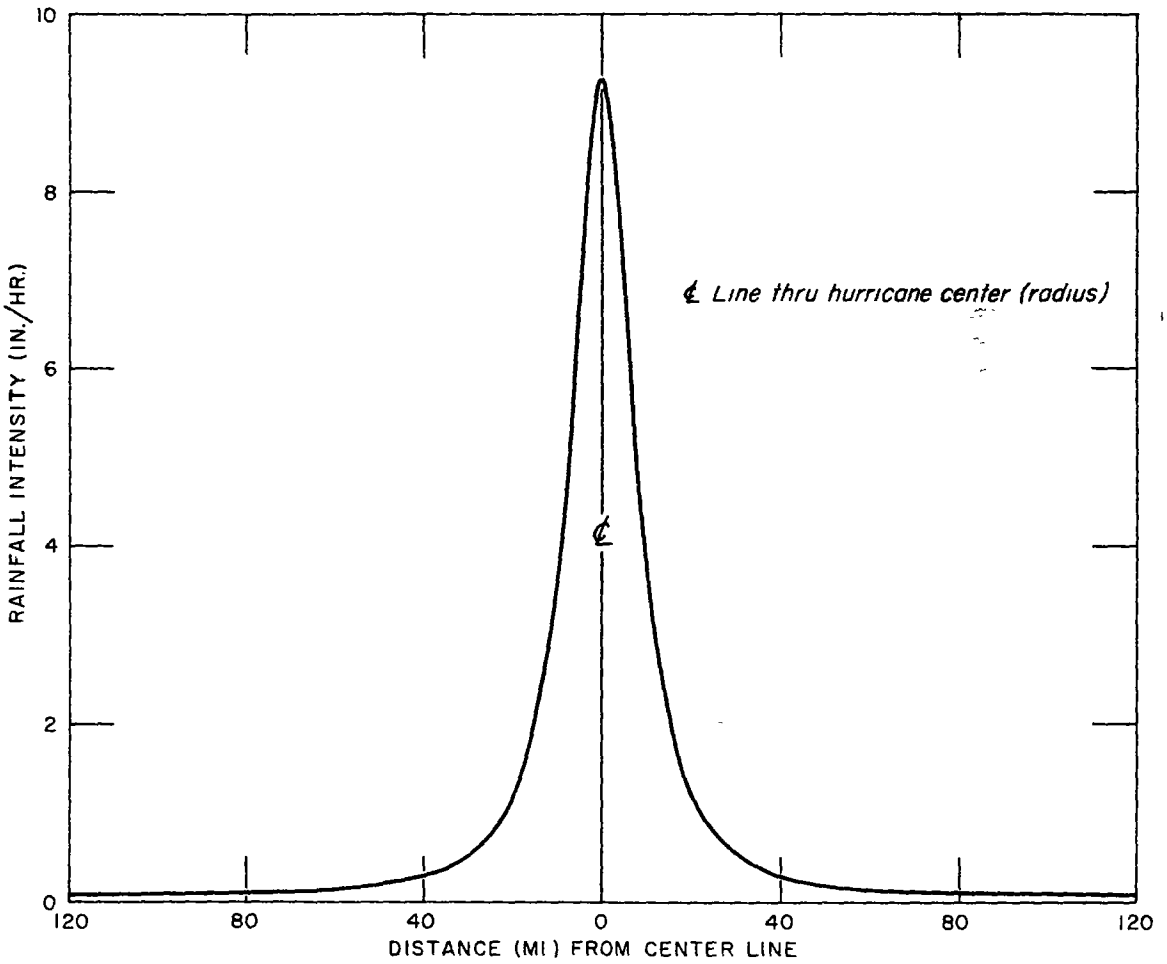

FIGURE 2–6 —Variation of computed convergence rainfall intensity with distance along a line 8 mi. from model hurricane center and perpendicular to a radius (center line).

top of the model was taken as 100 mb., the difference between the mixing ratios, $w_0 - w_1$, can also be readily evaluated. This difference is 0.00255 gm./gm. Introduction of these values and equation (2.5) into equation (2.4) produced the following relation:

$$R = 0.41 v_f \tan\alpha \qquad (2.7)$$

2.5 Computation of orographic rainfall

2.5.1 Values of $\tan\alpha$ were obtained directly from topographic maps by dividing elevation differences between contours by the horizontal distance between them. Values of the onslope wind speed, v_f, were determined from the wind field of figure 2–1. The wind speeds are greater to the right of the direction of motion of the hurricane. Consequently, higher, hence more critical, values of v_f will be found to the right of the hurricane center. Values of v_f, which is the wind component parallel to and in the direction of the hurricane movement, were computed along lines 8, 10, 15, 20, and 40 mi. to the right of the storm path. The v_f values along the 15-mi. line, which passes through the area of maximum wind speeds (fig. 2–1), turned out to be the most critical. However, the convergence rainfall intensities (fig. 2–6) were so much greater along the 8-mi. line than along the 15, that when combined with the orographic, they more than compensated for the lower orographic intensities along the 8-mi. line. The 8-mi. line thus turned out to be the most critical distance from the storm path insofar as rainfall intensities are concerned. The variation of v_f with distance along this line is shown in figure 2–7.

2.5.2 The profile of v_f having been established, the computation of rainfall intensities for various slopes by means of equation (2.7) was an easy matter.

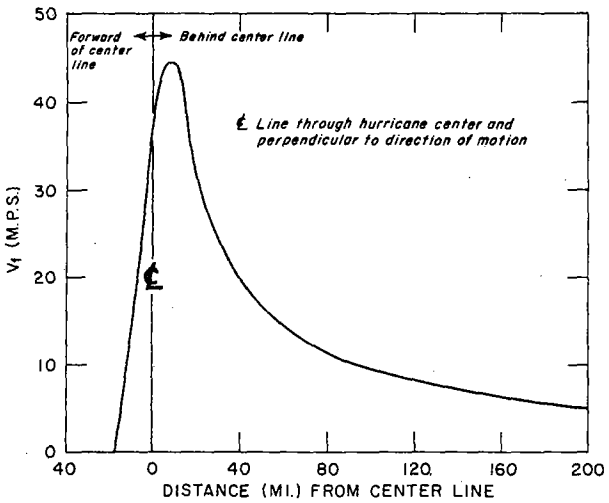

FIGURE 2–7.—Variation of computed forward, or onslope, horizontal wind component (v_f) along a line 8 mi. to right of model hurricane center and parallel to the direction of motion of the center.

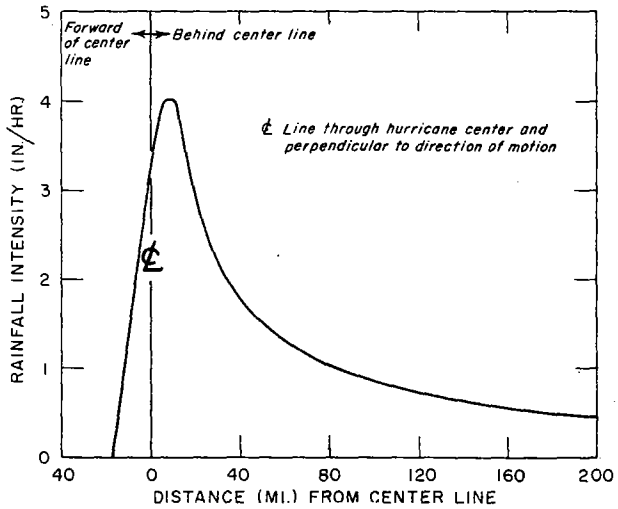

FIGURE 2–8.—Profile of orographic rainfall intensity computed from the v_f-profile of figure 2–7 for a slope of 1/4 at an elevation of 1 km., m.s.l.

The profile of rainfall intensities for the 8-mi. line as determined from the v_f profile of figure 2–7 and a slope of 1/4 (the maximum measured for Puerto Rico) at an elevation of 1 km is shown in figure 2–8. Several other rainfall-intensity profiles were constructed for various lesser values of slope.

2.6 Combining convergence and orographic rainfall

2.6.1 The convergence and orographic components of rainfall were combined by simply adding the profiles of rainfall intensity. The temperature and moisture characteristics of the hurricane model had to be adjusted for the different altitudes to which the model had to be applied. It developed that a simple adjustment factor applied to the convergence component of the rainfall intensity computed for sea level would yield the proper intensity for a particular altitude. The adjustment factors for various altitudes (table 2–3) were based, of course, on the variation with altitude of the mean mixing ratio, $\bar{w}$, in the 1-km. inflow layer with base at various altitudes, pseudoadiabatic saturated conditions being assumed.

TABLE 2–3.—*Reduction factors (in percent) for adjusting sea level convergence and orographic rainfall intensities to higher altitudes*

Altitude (m.)	sea level	100	300	500	700	1,000
Altitude (ft.)	sea level	328	984	1,640	2,297	3,281
Convergence rainfall	100	99	96	93	90	86
Orographic rainfall	100	99	97	95	93	91

2.6.2 The variation with altitude of the orographic component of precipitation was handled in the same manner as that for the convergence component. In other words, the orographic component was computed for a fixed elevation (sea level, or 950 mb.), and reduction factors were used to adjust that component for other elevations. The reduction factors used are different from those for convergence rainfall because the variables differ. Instead of $\bar{w}$ (eq. 2.3), the variables are now $w_0 - w_1$ and p_0, T_0 (eqs. 2.4 and 2.6). The difference between mixing ratios for the base and top of the 1-km. inflow layer, i.e., $w_0 - w_1$, or Δw, is practically constant for the range of elevation required. In other words, the value of Δw can be taken as 0.00255 no matter whether the model is at sea level or at 1,000 m. The fraction p_0/T_0 of equation (2.6) is thus the variable term which determines the reduction factors in the last line of table 2–3.

2.6.3 The combining of convergence and orographic components of rainfall intensities was accomplished by first constructing the profiles of each and then adding. The procedure is illustrated in figure 2–9.

2.7 Tests of model

2.7.1 Various tests of the hurricane model were made to determine if the rainfall amounts it yielded were reasonable. The first test consisted of using the

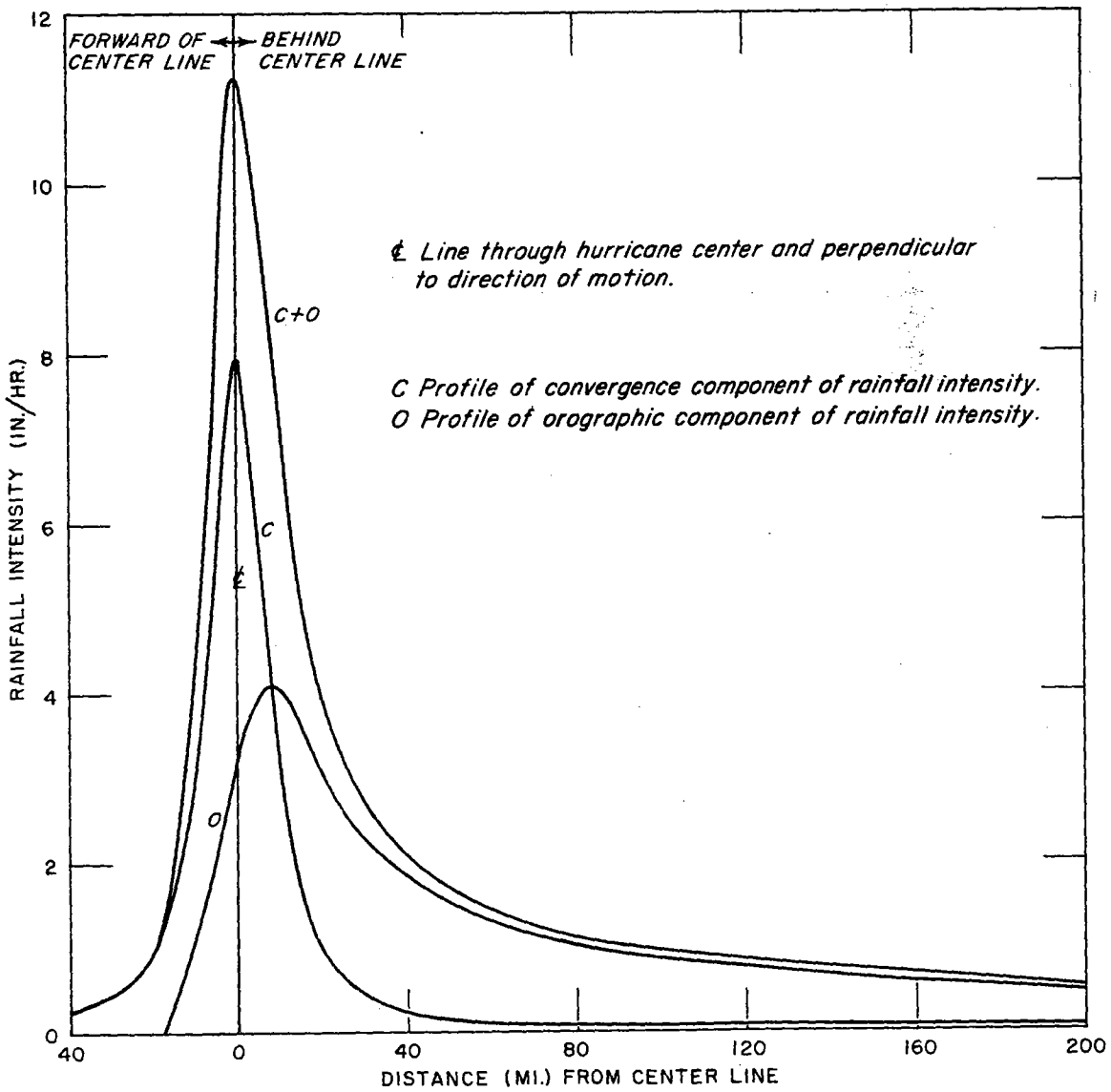

FIGURE 2-9.—Combination of convergence and orographic rainfall intensity profiles for a slope of 1/4 at an elevation of 1 km., m.s.l. Resultant profile is for a line 8 mi. to right of model hurricane center and parallel to the direction of motion of the center.

convergence element of the model in trying to duplicate measured hurricane rainfall amounts. This particular test was restricted to hurricane rainfalls measured at stations near sea level where orographic effects, if any, would be negligible. The data required for such a test are the station wind and rainfall and the path and speed of the hurricane center. It is not often that all these data are available.

2.7.2 Hurricane *Betsy's* invasion of Puerto Rico on August 12, 1956, provided a good opportunity for a test. The associated wind and rainfall data had been summarized by Colón [11], and the path and speed of the hurricane had been well fixed by radar observations [17]. *Betsy* crossed the southeastern coast of the island moving at about 21 m.p.h. in a northwestward direction, the eye passing within 20 mi. southwest of San Juan. The maximum wind speed at San Juan was only about 75 m.p.h. The wind speed 20 mi. to the right of the center of the hurricane model (fig. 2-1) is about 106 m.p.h. This difference in wind speeds may have been because of *Betsy's* lesser intensity and smaller radius of maximum wind

speeds. Radar observations showed the eye as having a radius of only 3 mi., and the lowest pressure reported in Puerto Rico was 28.88 in. (978 mb.) at Ramey Field, less than 15 mi. from the path of the hurricane center. Regardless of the reason for the difference in wind speeds, the method of computation of convergence rainfall by means of the model makes adjustment of the results by the ratio of the wind speeds reasonable. Moving the model at *Betsy's* speed, the maximum 6- and 24-hr. rainfalls for a point 20 mi. to the right of the path are found to be 2.8 and 4.5 in., respectively. The maximum rainfalls observed at San Juan for these durations were 2.26 and 3.19 in. Reduction of the computed amounts by the ratio of observed to model wind speeds (75/106) yields 2.0 and 3.2 in. These adjusted amounts are in good agreement with the observed.

2.7.3 Hurricane *Easy*, September 1950, which took a tortuous path northward along the Florida west coast before looping and crossing the central part of the peninsula, provided sufficient, though incomplete, data for a test of the model. This hurricane, while making a double loop just off Florida's west coast, produced the maximum rainfalls of record for the United States for durations of 12 to 72 hr. over areas from 10 to 2,000 sq. mi. These record rainfalls were at Yankeetown, Fla., during the period September 3–6, 1950. Unfortunately, lack of wind observations at Yankeetown precluded adjustment of the hurricane model. Maximum winds of 125 m.p.h. were reported [18] for the storm, however, suggesting that *Easy* and the model hurricane are of comparable intensities. Duplicating *Easy's* path and speed with the hurricane model, the 6-, 12-, 18-, and 24-hr. rainfall amounts for Yankeetown were computed to be 25.8, 33.2, 37.2, and 39.4 in., respectively. Except for the 6-hr. amount these computed values are in good agreement with the observed, i.e., 16.0, 28.6, 36.3, and 38.7 in.

2.7.4 The typhoon that produced the world's record 24-hr. rainfall of 45.99 in. at Baguio, Philippine Islands, on September 14–15, 1911, presented a wonderful opportunity for an individual test of the orographic component of the model (sec. 2.4). The typhoon center was at no time nearer than about 120 mi. from Baguio, so convergence rainfall could be neglected (fig. 2–4). Moreover, there was a very good hourly record of rainfall and wind speed and direction available [4]. The elevation of Baguio is 4,500 ft., and the windward (WSW) slope was determined to be 1/4. The rainfall was computed by means of equation (2.7) and adjusted by a factor of 0.86 for the elevation of Baguio. The observed and computed data are presented in table 2–4. The observed and computed 24-hr. rainfall amounts are in remarkably good agreement. The hourly amounts show considerable differences in some cases but that is to be expected because of the limitations of the computational method used. Some of the differences can be explained. The observed 1-hr. amount of 3.55 in. between 4 and 5 p.m. on the 14th, when the wind speed was only 32 m.p.h. and the computed rainfall only 1.2 in., resulted from a thunderstorm. The comparison on a 6-hourly basis is much better, the observed being 7.67, 12.02, 13.65, and 12.65 in. as against the computed 6.4, 11.0, 12.9, and 15.8 in., respectively. The deficiency of the computed rainfall amount for the first 6-hr. period is explained by the thunderstorm that occurred in that period. The excess in the last 6-hr. period may actually be a deficiency in the observed rainfall resulting from the higher wind speeds (hence greater gage error) in that period.

2.7.5 The *San Felipe* hurricane, which crossed Puerto Rico in an ESE to WNW direction on September 13, 1928, provided the one opportunity for a test, albeit a rough one, of the convergence—oro-

TABLE 2–4.—*Observed and computed meteorological data at Baguio, Philippine Islands., for typhoon of Sept. 14–15, 1911*

Date	Time	Observed average wind direction and speed (m.p.h.)	Hourly rainfall (in.)	
			observed	computed
Sept. 14	noon–1	W 23	0.10	0.9
	1–2	W 21	.33	0.8
	2–3	W 32	.70	1.2
	3–4	W 31	1.61	1.2
	4–5	W 32	3.55	1.2
	5–6	WSW 28	1.38	1.1
	6–7	WSW 37	2.62	1.4
	7–8	WSW 57	2.40	2.2
	8–9	WSW 49	2.04	1.9
	9–10	WSW 48	1.56	1.9
	10–11	SW 50	1.63	1.9
	11–mid	SW 44	1.77	1.7
Sept. 15	mid.–1	WSW 45	1.40	1.8
	1–2	SW 47	1.70	1.8
	2–3	SW 58	2.50	2.2
	3–4	SW 55	2.75	2.2
	4–5	WSW 65	2.85	2.5
	5–6	WSW 62	2.45	2.4
	6–7	WSW 65	1.78	2.5
	7–8	WSW 68	2.12	2.6
	8–9	SW 61	2.40	2.4
	9–10	WSW 63	2.45	2.5
	10–11	WSW 71	2.23	2.8
	11–12	SW 77	1.67	3.0
Total			45.99	46.1

graphic model in the problem area. This unusually destructive hurricane produced many of the maximum rainfalls of record shown on figure 1–1. The rainfall observed at Adjuntas was selected for the test because it is the maximum 24-hr. amount of record in Puerto Rico and because Adjuntas is one of the highest stations having a long rainfall record. The station is at an elevation of about 1,700 ft. on the northern slope of the Guaybana Mountains. The average slope at the station site is roughly 1/8. Adjuntas was about 10 mi. to the left to the path of the hurricane center, which was moving at about 13 m.p.h. [12]. The lowest central pressure recorded in Puerto Rico was 27.65 in. (936 mb.) at Guayama, which suggests a weaker intensity than that of the model hurricane. *San Felipe*, however, is known as one of the most intense storms to have invaded Puerto Rico, so it can by no means be considered a weak hurricane. Three factors hampered the test of the hurricane model: (1) lack of wind data for Adjuntas, (2) the necessity for estimating the true maximum 24-hr. rainfall from observational-day amounts, and (3) the station's location to the left of the hurricane path instead of to the right, for which rainfall-intensity profiles had been computed (sec. 2.5). In the test, possible differences in wind speed were neglected. The total-storm rainfall at Adjuntas was 29.60 in. distributed into two observational days. The estimate of true maximum 24-hr. rainfall based on the maximum observational-day amount plus one-half the higher amount of the two adjoining days yields 24 in. The winds on the left side of the hurricane model 10 mi. from the center are about 5 percent less than those on the right side at the same distance (fig. 2–1). Moving the model at 13 m.p.h. along the storm path and reducing the computed 24-hr. rainfall it yields for Adjuntas by 5 percent results in a value of 25.8 in., which agrees very well with the estimated maximum observed amount.

2.7.6 The tests described above could hardly be classified as rigid. They suggest, nevertheless, that the postulated model should yield reasonable results, at least for some hurricane situations. It was decided therefore to use the model to derive tentative estimates of PMP, which would be accepted as final if they appeared reasonable. Chapter 3 discusses the various factors involved in the use of the model to derive PMP estimates, their modification on the basis of statistics of extreme values, the results, and their appraisal.

Chapter 3

PROBABLE MAXIMUM PRECIPITATION

3.1 Estimation

3.1.1 The rainfall-intensity profiles of figures 2–6, 2–8, and 2–9 suggest that a point would receive its maximum precipitation for any duration if it were located at the optimum site for maximum intensity and the hurricane were standing still. It should be kept in mind, however, that the model wind field of figure 2–1 is for a moving hurricane, presumably one moving at about 12 m.p.h. Consequently, it would be improper to apply the selected model to a standing hurricane. Moreover, the record of hurricanes in the problem region offers very little support to the assumption that a hurricane could sit still for, say, 24 hr. In the remarks for the hurricane of August 17–19, 1807, in table 1-4, there is the entry, "Severe hurricane from the east lasted 50 hr. in Puerto Rico." The remark certainly suggests that the hurricane was stationary or nearly so for a period of at least 24 hr., i.e., if hurricane wind speeds were then classified as at present. However, since there was no such classification then existent, and since the wind speeds were undoubtedly estimated instead of measured and the observation made by non-meteorologists, it would be folly to put much weight on the remark. About all that one can conclude from the remark is that there probably was a hurricane and that high winds, not necessarily of hurricane force, persisted for 50 hr.

3.1.2 Examination of tropical storm tracks in the problem region indicates their slowest speed to be about 5 m.p.h. (table 3–1). This speed was therefore accepted as that which would produce the probable maximum precipitation. Hence, the PMP was derived by assuming that the various rainfall-intensity profiles were moving over a particular point of given elevation and slope at 5 m.p.h. Thus, for example, the PMP for a point at sea level and practically no slope would be obtained by moving the convergence rainfall-intensity profile of figure 2–6 at 5 m.p.h. This operation was actually performed by first taking the average intensity for the interval from $2\frac{1}{2}$ mi. ahead of the center line to $2\frac{1}{2}$ mi. behind (5 mi. in 1 hr.) for the maximum 1-hr. rainfall. Successive intervals would then be $2\frac{1}{2}$ to $7\frac{1}{2}$ mi., $7\frac{1}{2}$ to $12\frac{1}{2}$ mi., etc., both ahead of and behind the center line. The results are given in table 3–2 in the chronological order in which the 24 1-hr. increments of rainfall would be observed at a point as the hurricane center passed 8 mi. away. While the rainfall-intensity profile of figure 2–6 is symmetrical about the center line, the tabulation of 1-hr. rainfall increments of table 3–2 is not because of the even number of increments. Summation of the rainfall increments of table 3–2 to obtain PMP for 1, 3, 6, 12, and 24 hr. yields 8.8, 21.8, 31.0, 37.1, and 40.1 in., respectively.

3.1.3 PMP including an orographic component was estimated in the manner just described except that the composite profile, like that of figure 2–9, for a particular slope and elevation was used. The profile of figure 2–9, for example, yields the PMP for a point at an elevation of 1,000 m. (3,300 ft.) on a slope of 0.25 and located 8 mi. to the right of the path of the center of the model hurricane moving at 5 m.p.h. The hourly increments of the 24-hr. PMP for such a

TABLE 3–1.—*Distribution of hurricanes by speed of movement in the area 15° to 20° N. and 60° to 70° W. during the period 1886–1958*

Average speed for 24-hr. period (m.p.h.)	Hurricanes (number of occurrences)
<6	0
6–8	3
8–10	7
10–12	11
12–14	17
14–16	12
16–18	8
18–20	4
20–22	1
22–24	2
24–26	1
>26	0

Average speed: 13 m.p.h.

TABLE 3-2.—*Probable maximum 24-hr. convergence precipitation (in.), by hourly increments, for a point at sea level and 8 mi. from the path of the model hurricane center moving at 5 m.p.h.*

Hour	Rain	Hour	Rain	Hour	Rain
1	0.1	9	1.1	17	1.1
2	.1	10	2.0	18	.7
3	.2	11	3.6	19	.5
4	.2	12	6.5	20	.4
5	.3	13	8.8	21	.3
6	.4	14	6.5	22	.2
7	.5	15	3.6	23	.2
8	.7	16	2.0	24	.1

TABLE 3-3.—*Probable maximum 24-hr. precipitation (in.), by hourly increments, for a point at 1,000 m. elevation on a slope of 0.25 and located 8 mi. to the right of the model hurricane center moving at 5 m.p.h.*

Hour	Rain	Hour	Rain	Hour	Rain
1	1.0	9	3.9	17	1.4
2	2.0	10	3.1	18	1.3
3	4.2	11	2.6	19	1.2
4	8.5	12	2.3	20	1.2
5	10.9	13	2.0	21	1.1
6	9.0	14	1.8	22	1.1
7	6.5	15	1.6	23	1.0
8	5.1	16	1.5	24	.9

point are tabulated in chronological order in table 3-3. Summation of the rainfall increments of table 3-3 to obtain PMP for 1, 3, 6, 12, and 24 hr. yields 10.9, 28.4, 44.2, 60.1, and 75.2 in., respectively.

3.1.4 The PMP amounts yielded by the model were compared to the amounts indicated by the enveloping curve of the world's maximum observed rainfalls (par. 1.2.6) to determine whether the former were compatible with these worldwide extremes. The enveloping values for 1, 3, 6, 12, and 24 hr., as determined by equation 1.1, are 15.3, 26.1, 36.6, 51.2, and 71.7 in., respectively. These values exceed some of the PMP values of paragraphs 3.1.2 and 3.1.3. Recalling that all controlling values of the world's maxima for durations up to 6 hr. were associated with thunderstorms or cloudbursts (pars. 1.3.4 and 1.3.5), it is not surprising that they exceed some hurricane PMP values computed by the model. Thunderstorms within hurricanes are not unusual, but the high winds preclude the concentration of the rainfall within a small area. It is also possible that meteorological situations associated with hurricanes are not favorable for the type of severe localized storm responsible for cloudbursts. If only probable maximum hurricane rainfall intensities are considered, the values obtained from the model appear reasonable. Consequently, two sets of limiting values of maximum rainfall rates for durations up to about 6 hr. are indicated, one for cloudbursts and one for hurricanes. However, in view of (1) the doubt expressed in paragraph 1.3.5 as to the possibility of cloudbursts of world-record magnitude occurring in the problem region and (2) the very small probability that a cloudburst of such magnitude would occur over a particular problem watershed, it was decided to consider only PMP from hurricanes as being more practical from the viewpoint of hydrologic design. The PMP maps and pertinent data presented in the remainder of this chapter refer to PMP from hurricanes. The designer wishing to consider cloudburst PMP will find the necessary information in Appendix A.

3.1.5 In determining PMP for hurricanes, a knowledge of the various directions in which hurricanes could cross the problem area was required. The only guide in such a matter is the record of hurricane paths. Study of several hundred hurricane tracks [5, 6] disclosed that practically all of the hurricanes disastrous to the problem area approached from directions between east and southeast. However, figure 3-1, showing unusual hurricane tracks in and adjacent to the problem area, suggests that hurricanes affecting the problem area might approach from almost any direction.

3.1.6 The degree of orographic slope at various elevations exposed to a hurricane approaching from the most critical direction was then determined by measurement from a large-scale (1:240,000) topographic map. The PMP for various durations for the indicated slope were then determined as described in paragraph 3.1.2. The map of 24-hr. PMP for Puerto Rico thus determined is presented in figure 3-2.

3.1.7 The method for estimating PMP just described is relatively crude. The lack of procedures for evaluating the accuracy of the estimates thus derived makes it advisable to determine their reasonableness by comparison with estimates derived by a different approach and to modify them if it appears necessary. An index to PMP may be obtained on the basis of statistics [19]. The statistical approach is premised on the assumption that valuable information on extreme values is contained in the rainfall record of each station. An exploration of the thou-

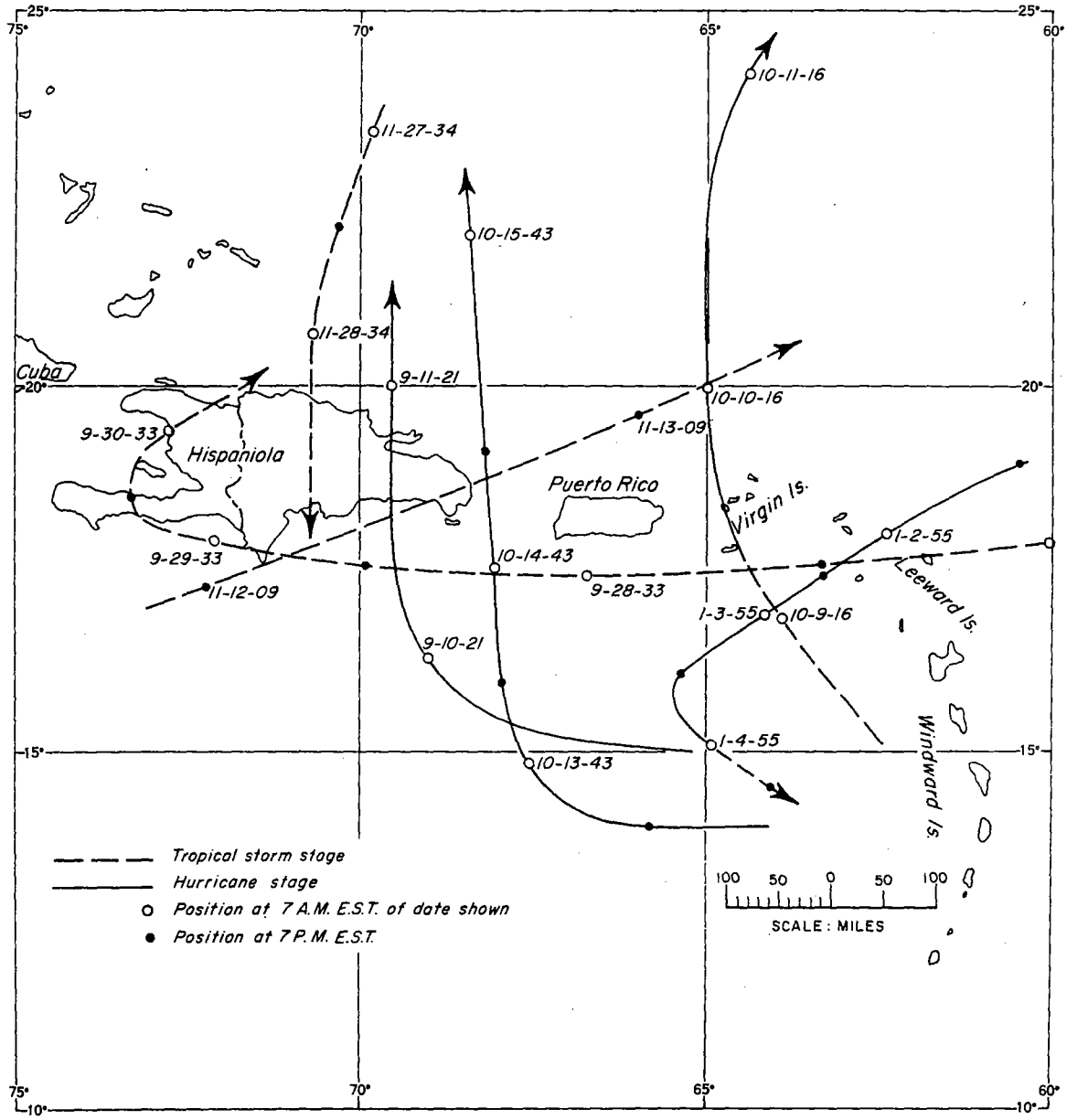

FIGURE 3-1.—Selected tropical storm tracks showing various directions of approach to Puerto Rico and Virgin Islands.

sands of station-years of data now available should provide an enveloping statistic that can be used as an index to PMP.

3.1.8 The frequency factor, K, is the number of standard deviations, s_N, that must be added to the mean of the annual maxima for a particular duration, $\bar{x}$, to obtain a rainfall value, $\bar{x}_M$, of a particular magnitude, or

$$x_M = \bar{x} + Ks_N \qquad (3.1)$$

where s_N is the standard deviation of a sample of size N. Analysis of over 100,000 station-years of rainfall data from 2,600 stations in various widely scattered countries has never yet revealed any value of K higher than 15. Of all data analyzed, the highest value of K ever obtained was 14.4 for an Icelandic station. A value of 15 therefore appears to be a reasonable upper limit of the frequency factor K. Table 3-4 shows the distribution of the K value for 89 Puerto Rican stations having 10 or more years of

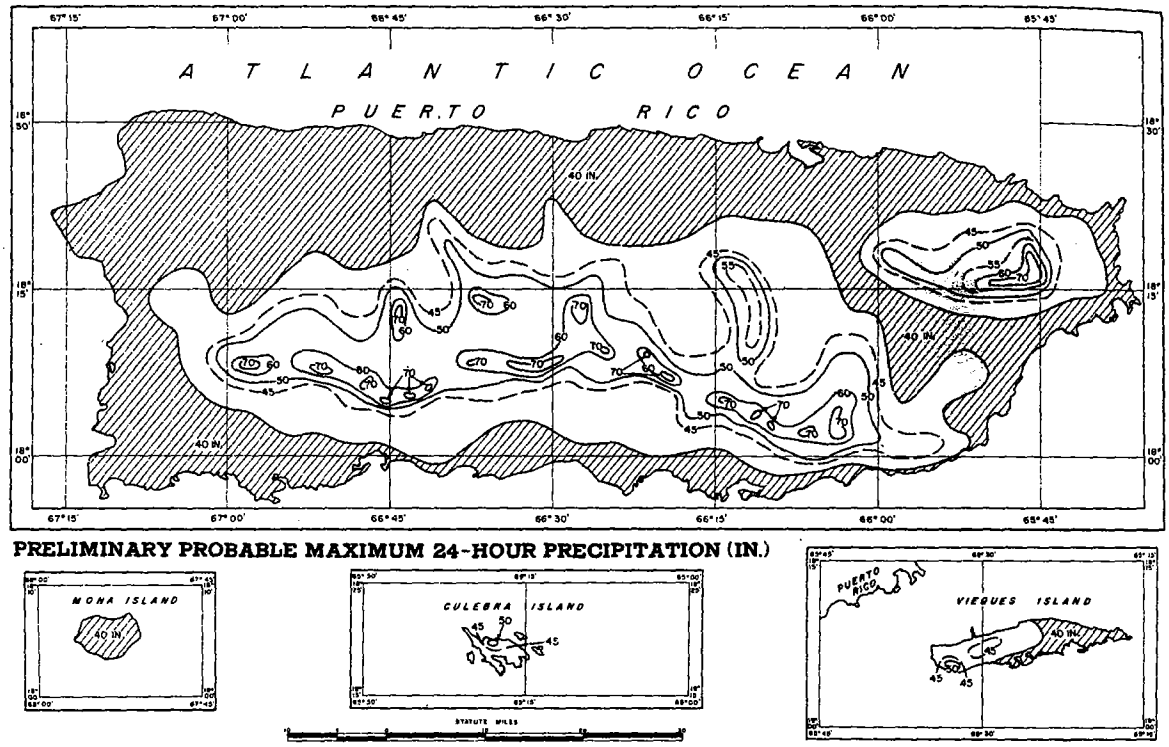

FIGURE 3-2.—Preliminary estimate of probable maximum 24-hr. point precipitation based on application of hurricane model of chapter 2 moving from permissible directions at 5 m.p.h.

record. The highest value of K was less than 9. Obviously, the use of $K=15$ represents a substantial increase of the computed x_M over the observed. The use of an overall value of K as applicable to various regions presumes randomness or absence of geographic variation. While there is reason to suspect that there may be some geographical variation, the relatively biased samplings provided by the current gage networks (e.g., relatively small number of long-record stations above 5,000 ft.) makes it practically impossible to evaluate geographical variation reliably. Tests made so far indicate no appreciable geographical variation, and the assumption that there is none is considered justifiable for the present.

TABLE 3-4.—*Distribution of frequency factor K computed from records of 24-hr. rainfalls for 89 Puerto Rican stations*

K	Freq.	K	Freq.
1.0-1.9	3	5.0-5.9	11
2.0-2.9	17	6.0-6.9	3
3.0-3.9	34	7.0-7.9	1
4.0-4.9	19	8.0-8.9	1

3.1.9 The use of the statistical approach as a guide to PMP consisted of first computing the mean, $\bar{x}$, and the standard deviation, s_N, adjusted for outliers and sample size, of the annual series for all stations having at least 10 years of record. Maps of $\bar{x}$ and s_N (figs. 3-3 and 3-4) were then analyzed. A grid was superimposed on these two maps, and values of $\bar{x}$ and s_N for each grid point were tabulated. Substituting these data for corresponding grid points into equation (3.1) with a K value of 15 yielded x_M for each grid point used in constructing the map of figure 3-5.

3.1.10 The differences between the upper limits of Puerto Rican rainfall depicted by figure 3-2 and those depicted by figure 3-5 are fairly large in places but still within the limits of accuracy that may be expected from PMP estimates derived by either approach. The differences exist in large part because of differences in basic considerations involved in the two approaches. For example, the meteorological approach considered the possibility of a hurricane crossing Puerto Rico from north to south because a few hurricanes have been observed traveling south-

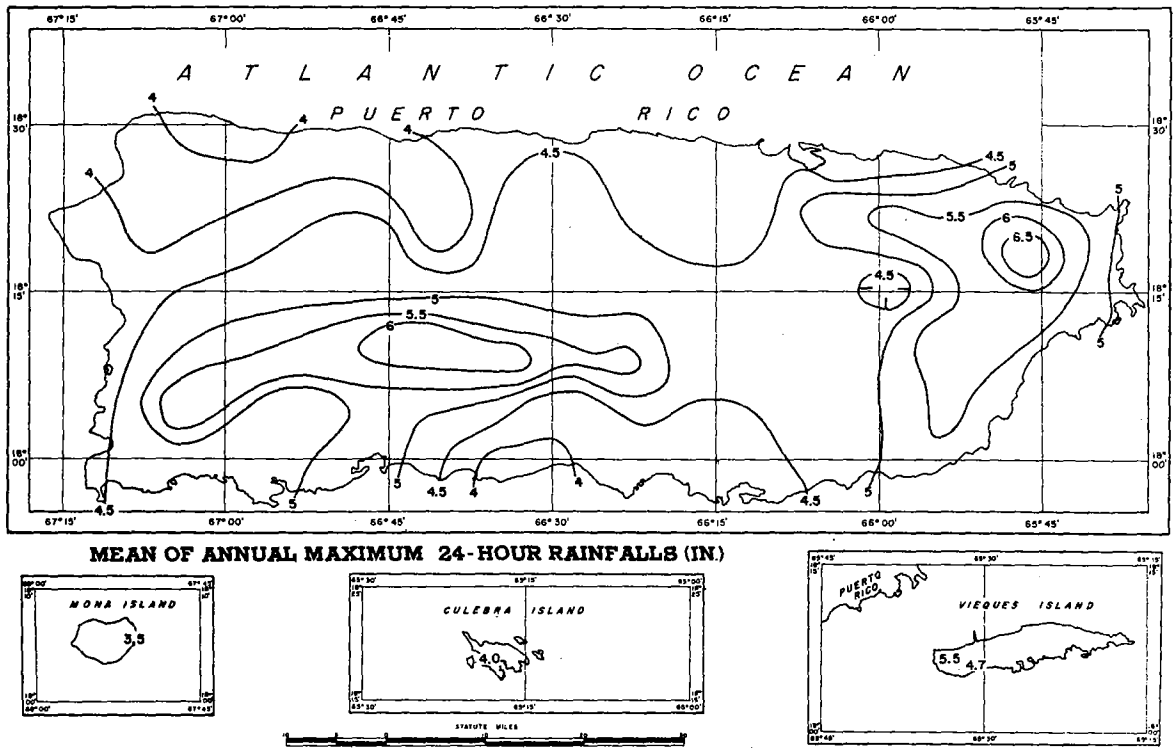

FIGURE 3–3.—Mean ($\bar{x}$) of annual series of 24-hr. point precipitation.

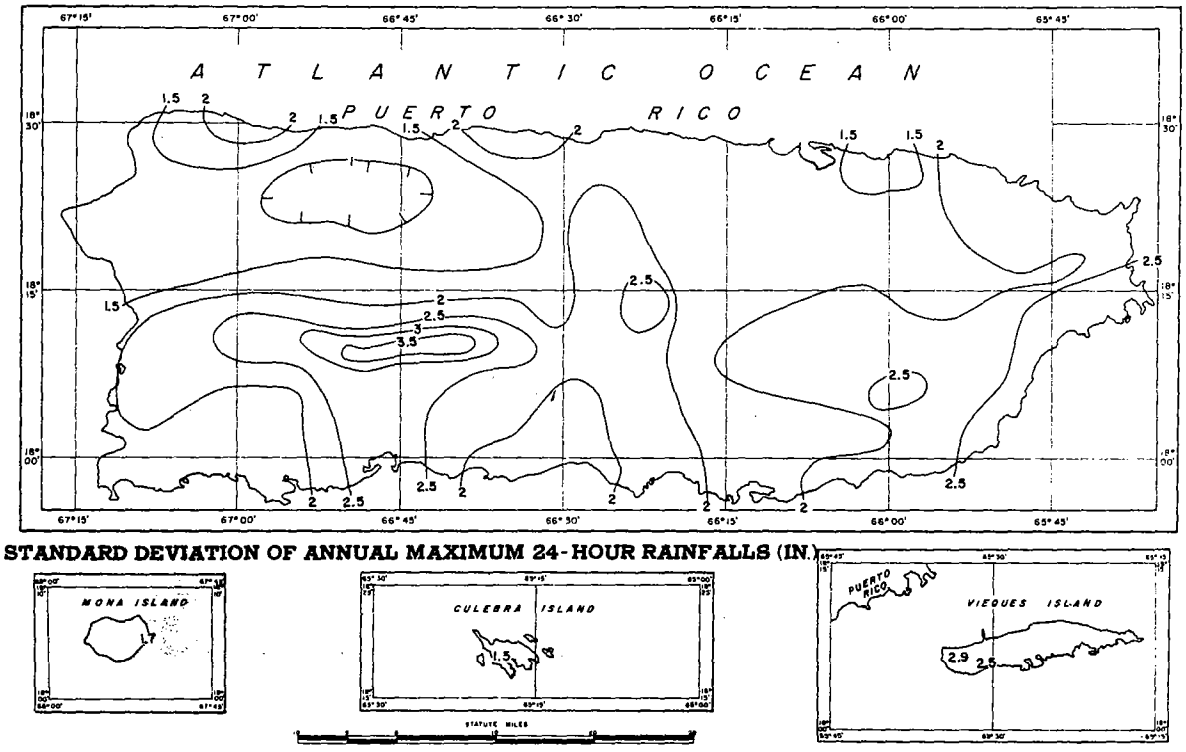

FIGURE 3–4.—Adjusted standard deviation (s_N) of annual series of 24-hr. point precipitation.

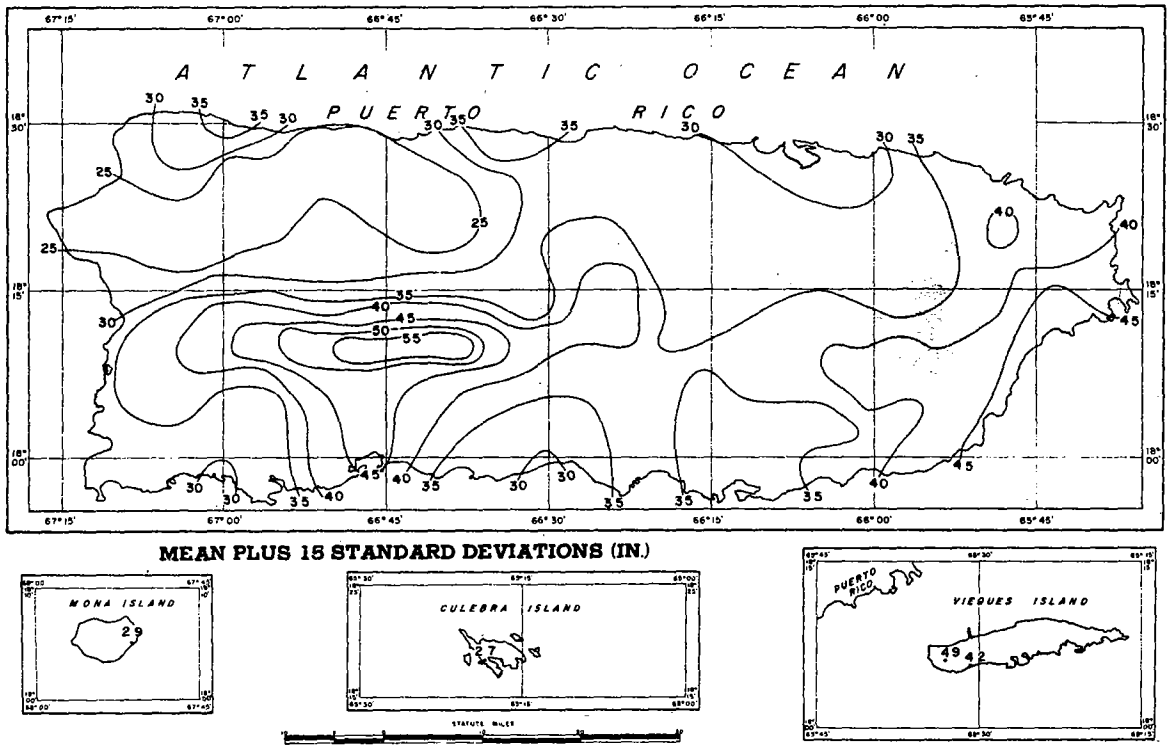

FIGURE 3-5.—Preliminary estimate of probable maximum 24-hr. point precipitation based on the equation $x_M = \bar{x} + 15s_N$.

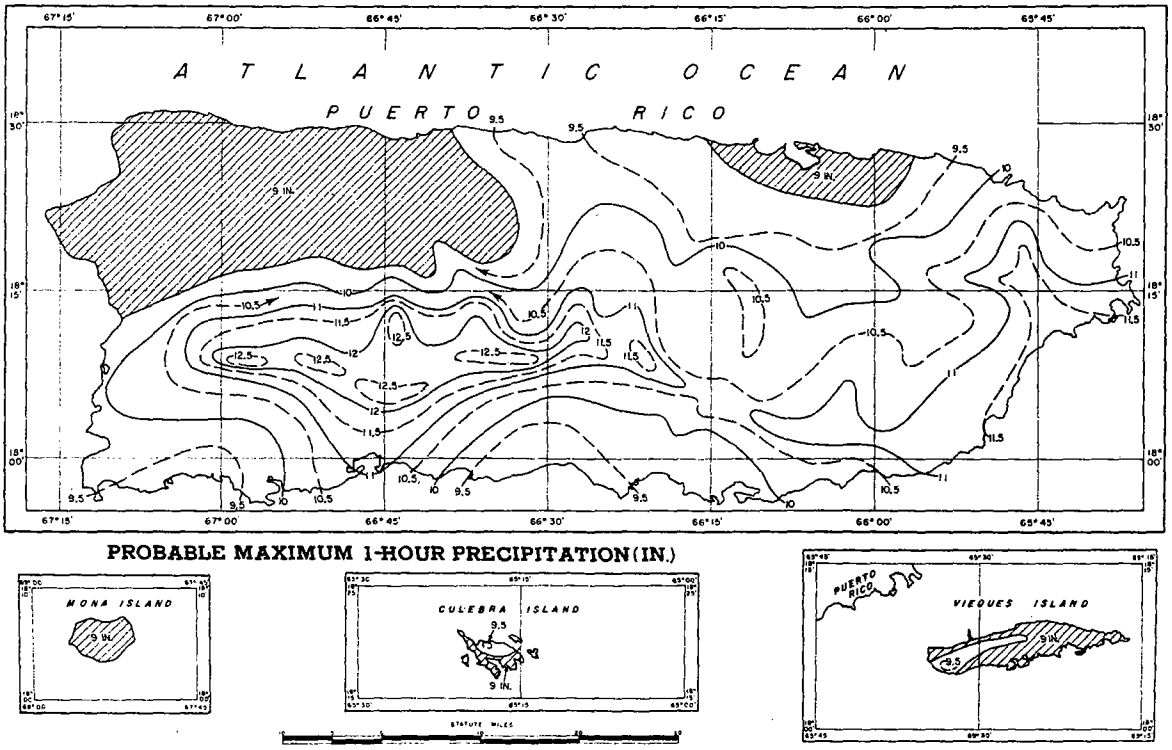

FIGURE 3-6.—Probable maximum 1-hr. point precipitation (in.) for Puerto Rico.

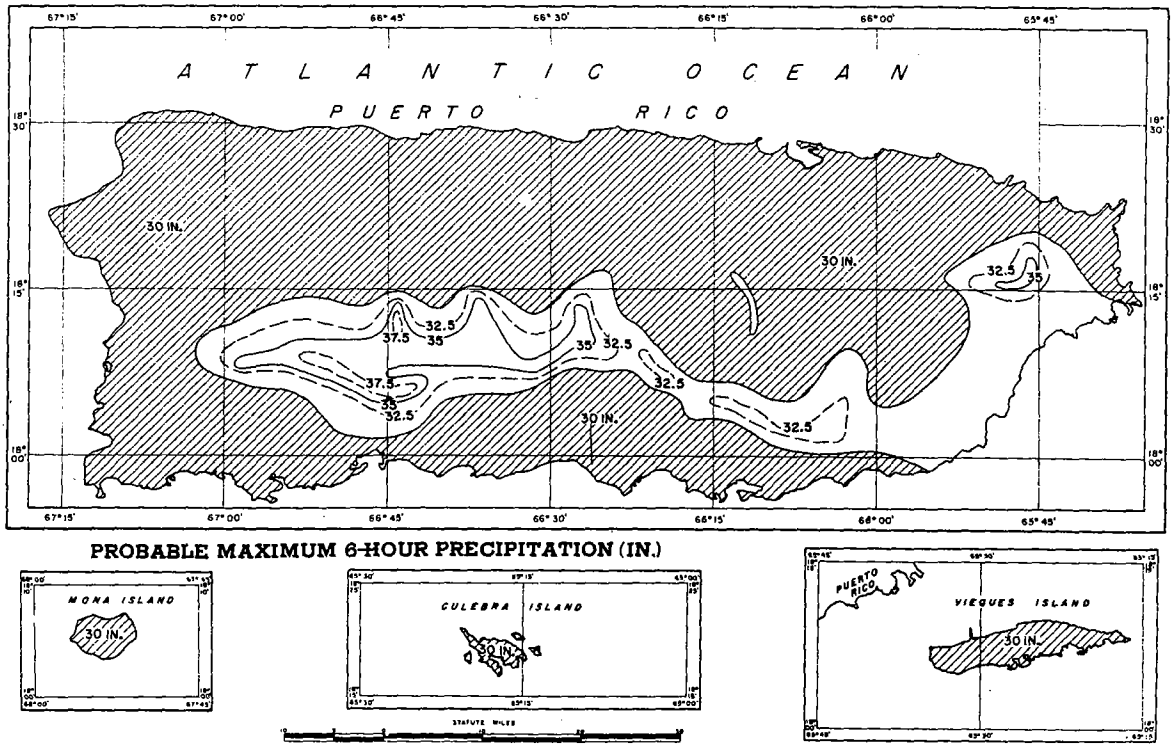

FIGURE 3–7.—Probable maximum 6-hr. point precipitation (in.) for Puerto Rico.

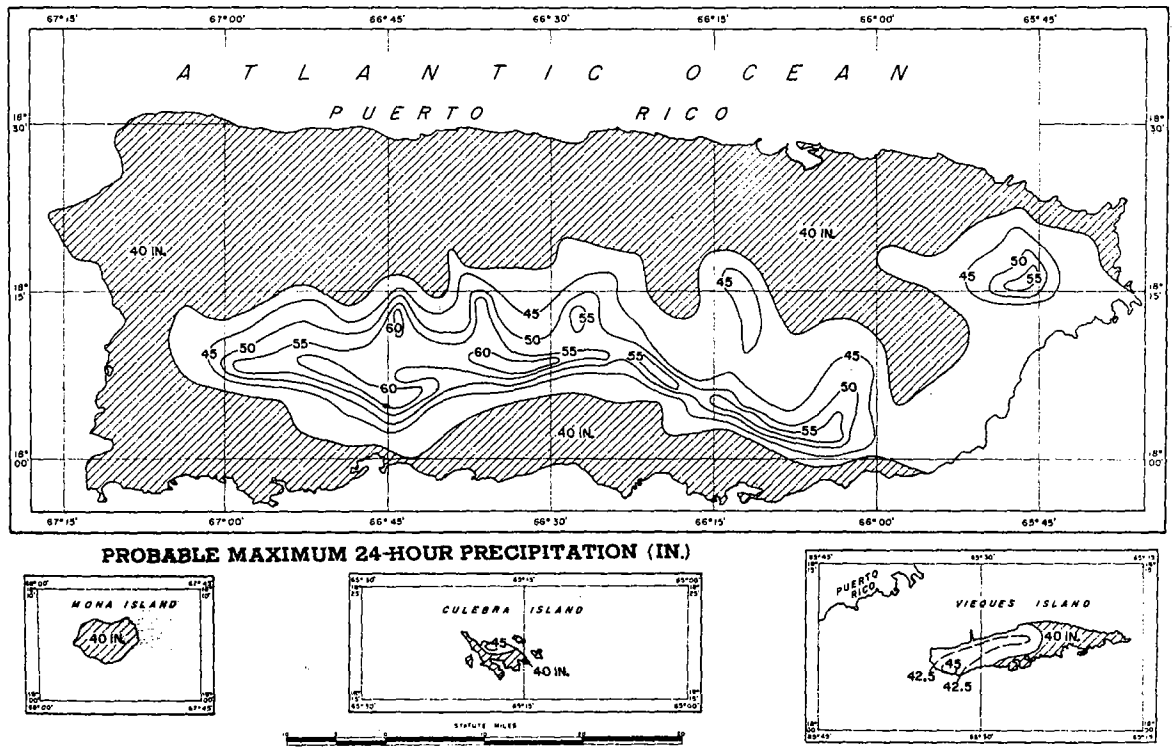

FIGURE 3–8.—Probable maximum 24-hr. point precipitation (in.) for Puerto Rico.

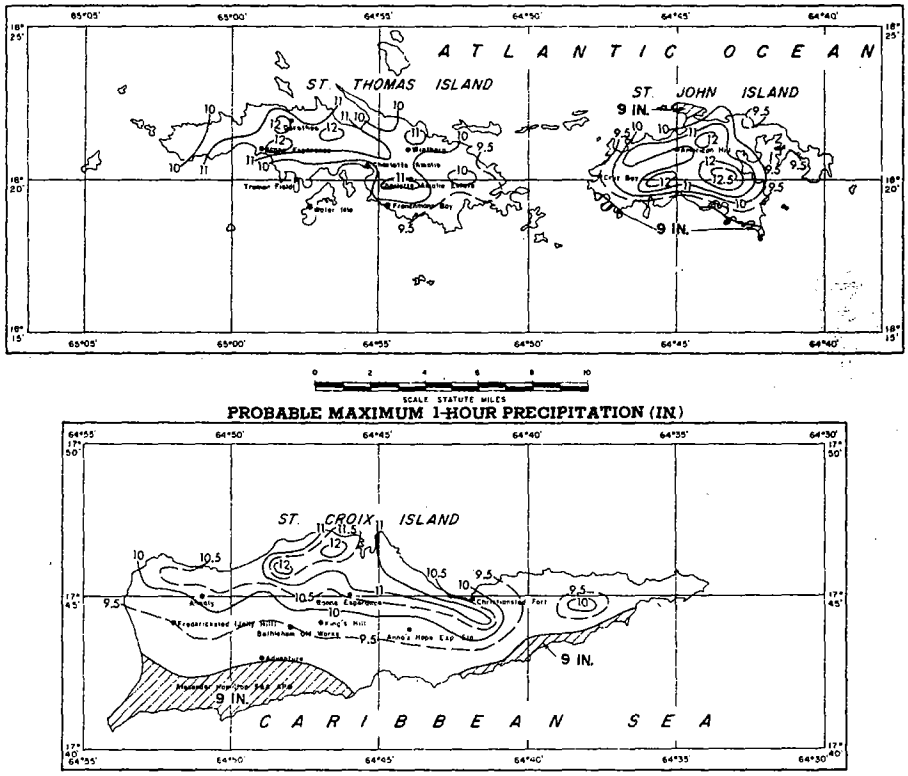

FIGURE 3-9.—Probable maximum 1-hr. point precipitation (in.) for Virgin Islands

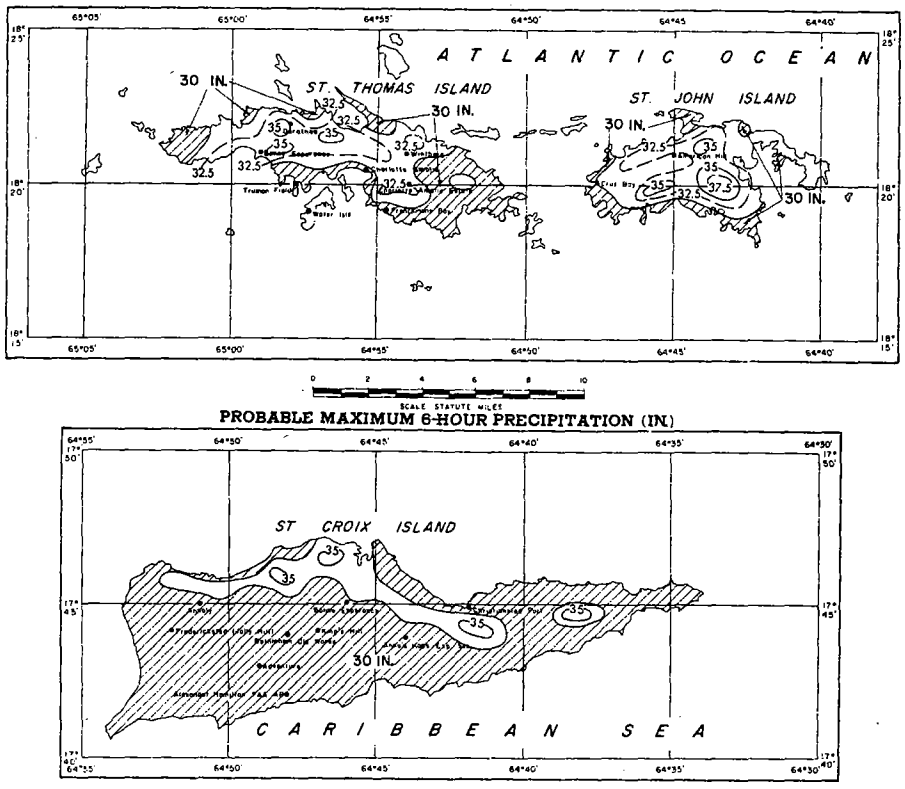

FIGURE 3-10.—Probable maximum 6-hr. point precipitation (in.) for Virgin Islands.

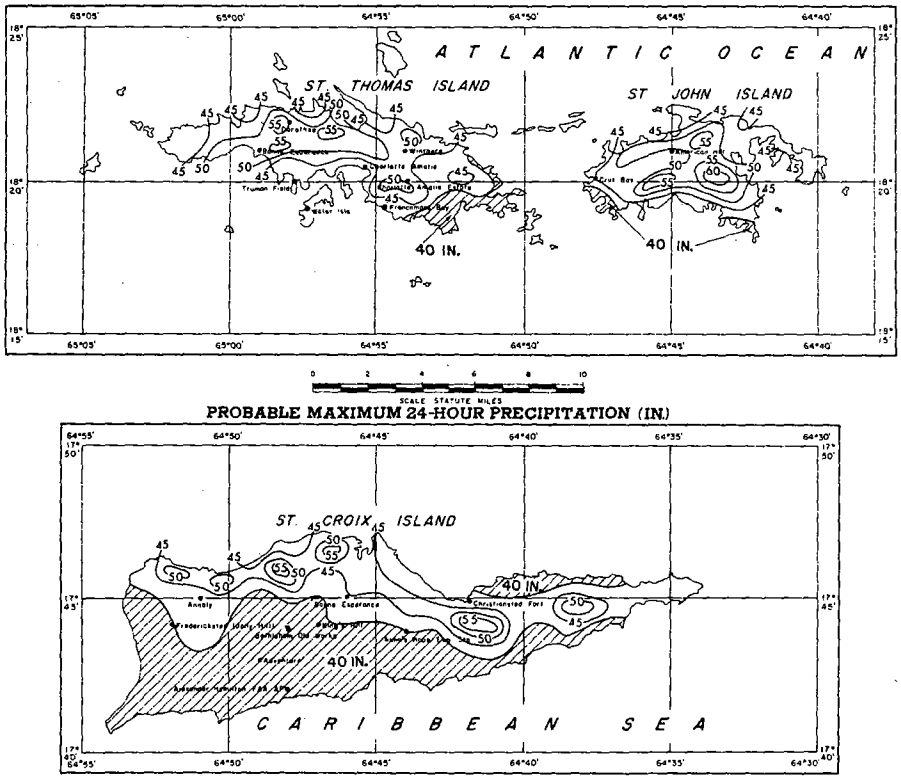

FIGURE 3-11.—Probable maximum 24-hr. point precipitation (in.) for Virgin Islands.

ward both east and west of the island although none has ever been known to cross the island in that direction. The statistical approach on the other hand, being based on actual records, does not reflect this possibility. After weighing the advantages and shortcomings of the two approaches, it was decided that a composite map constructed by averaging the values of figures 3–2 and 3–5 might well provide the most acceptable PMP estimates possible at this stage of meteorological and statistical knowledge. This composite map is shown in figure 3–8. The shaded area representing the 40-in. PMP in the coastal regions is the only place where a straight average of figures 3–2 and 3–5 was not used. The meteorological approach had yielded 40 in. for the coastal areas and because hurricane *Easy* (par. 2.7.3) had produced 38.7 in. in 24 hr. at Yankeetown, Fla., in September 1950, it was considered advisable to maintain the 40-in. value for PMP.

3.1.11 The 1-hr. and 6-hr. point PMP maps of figures 3–6 and 3–7 were obtained in almost the same manner just described for the 24-hr. PMP. The only differences occurred in the statistical approach to PMP. The fact that only San Juan had a long recording-gage record necessitated the use of relationships of precipitation for these durations to 24-hr. precipitation as determined from records in southeastern United States.

3.1.12 Similar procedures were used to estimate PMP for the Virgin Islands. Their 1-, 6-, and 24-hr. PMP are presented in figures 3–9, 3–10, and 3–11, respectively.

3.2 Depth-duration relations

3.2.1 Figure 3–12 shows a generalized duration-interpolation relationship for determining precipitation amounts for durations from 1 to 24 hr. when values for 1, 6, and 24 hr. are known.

EXAMPLE: Determine hourly increments of 9-hr PMP for a point at 18°05′ N., 66°45′ W. Figures 3–6, 3–7, and 3–8 yield 1-, 6-, and 24-hr. PMP values of 12.5, 36, and 60 in., respectively. Plot the 1- and 6-hr. values on their respective duration lines on the left diagram of figure 3–12 and draw a straight line between the two plotted points. Construct a similar line for the 6- and 24-hr. PMP plotted on the right diagram. The nine PMP values for durations from 1 to 9 hr. as read to the nearest 0.5 in. from the lines drawn on the two diagrams are: 12.5, 20.5, 25.5, 29.5, 33.0, 36.0, 38.5, 40.5, and 43.0 in. The hourly increments

are: 12.5, 8.0, 5.0, 4.0, 3.5, 3.0, 2.5, 2.0, and 2.5 in. The last hourly increment is 2.5 in., and the next to last is 2.0 in. The last increment should be the smallest. The discrepancy results from reading the values to the nearest 0.5 in. In order to smooth out such inconsistencies, it is recommended that the PMP values be plotted against duration and that a smooth depth-duration curve be constructed so as to provide minimum envelopment. New PMP values are read from this curve, and hourly increments computed therefrom. If the enveloping curve has been drawn properly, the hourly increments will show a gradual decrease.

3.2.2 The empirical relationship of figure 3–12 was derived from annual series data as described in Weather Bureau *Technical Papers* No. 28 [20] and No. 29 [21]. While there may be regional variation in this type of relation as applied to PMP, it has not been possible to evaluate it. For the purpose of generalizing, the diagrams of figure 3–12 are believed to be as good as any yet devised for application to PMP.

3.2.3 It is ordinarily pertinent to distinguish between the 6-hr. PMP and the maximum 6-hr. increment that would be associated with, say, a 24-hr. PMP. This applies, of course, to other durations. In many regions the 6-hr. and 24-hr. PMP might be limited to different seasons. This problem does not arise in this study because all PMP estimates of figures 3–6 through 3–11 would supposedly be associated with hurricanes, and the PMP for any short duration might well occur in connection with the 24-hr. PMP. Of course, if the hydrologist wishes to use the cloudburst PMP estimates discussed in Appendix A, he should consider the fact that cloudbursts of that magnitude have never been observed within the area of, and during the period of, the maximum 24-hr. rainfall of a major hurricane.

3.3 Depth-area relations

3.3.1 Examination of the depth-area-duration data [22] for several hurricanes indicated a relationship not appreciably different from the depth-area curves presented in Weather Bureau *Technical Paper* No. 38 [23] except for durations under 6 hr. Hurricane rainfall appears to be somewhat more evenly distributed with respect to time, and the 1- and 3-hr. curves were lowered slightly. Also, all curves were adjusted to show percentages in terms of the maximum station value instead of 10 sq. mi. (fig. 3–13). The original curves were expressed in terms of percentage of the 10-sq.-mi. value because the relative sparseness of the gage-network density, hence relative crudeness of depth-area-duration analyses, makes it generally difficult, if not impossible, to assign a definite representative area for the gage. In other words, it is usually impossible to determine whether the rainfall caught in a gage is representative of that over an area of 0.1, 1, or 10 sq. mi. In most cases where bucket surveys of a storm have not been made, it is common practice to assume that the maximum gage measurement for a particular storm is representative for 10 sq. mi. In general, this assumption is still justified. In the present study, however, it was advisable to consider the rainfall computed by means of the hurricane model as applicable to a point rather than to 10 sq. mi. The reason for this departure from common practice is that if the model were used to compute rainfall for a 10-sq.-mi. area instead of for a point, the resulting amounts would be somewhat less.

3.4 Chronological distribution

3.4.1 While hurricane rainfall intensities at a point tend to gradually increase as the center approaches and to decrease as the hurricane recedes, there is no corresponding order within the period of maximum 24-hr. rainfall. It is, of course, problematic whether the rainfall outside of the 24-hr. maximum rainfall period can be properly classified as hurricane rainfall. Hurricane winds are seldom experienced at a point for as long as 24 hr. In the absence of any observed definite, typical chronological order within the maximum 24-hr. period, it is suggested that the distribution indicated by the intensity profiles provided by the hurricane model be used. The distribution would range from that depicted in figure 2–6 for non-orographic hurricane rainfall to that shown in figure 2–8 for the greatest orographic effect. Table 3–5 shows the suggested chronological order of hourly hurricane PMP increments for various values of 24-hr. point PMP.

3.5 Appraisal

3.5.1 There is only one way in which the accuracy of PMP estimates can be definitely established and that is in the negative sense only. In other words, if a PMP estimate is exceeded by an observed rainfall, the estimate is undeniably too low. If it is equalled by an observed rainfall, the estimate may be adequate but there is a greater probability that it is too low. It is also possible that a PMP estimate may be excessive, i.e., it is beyond the limits of

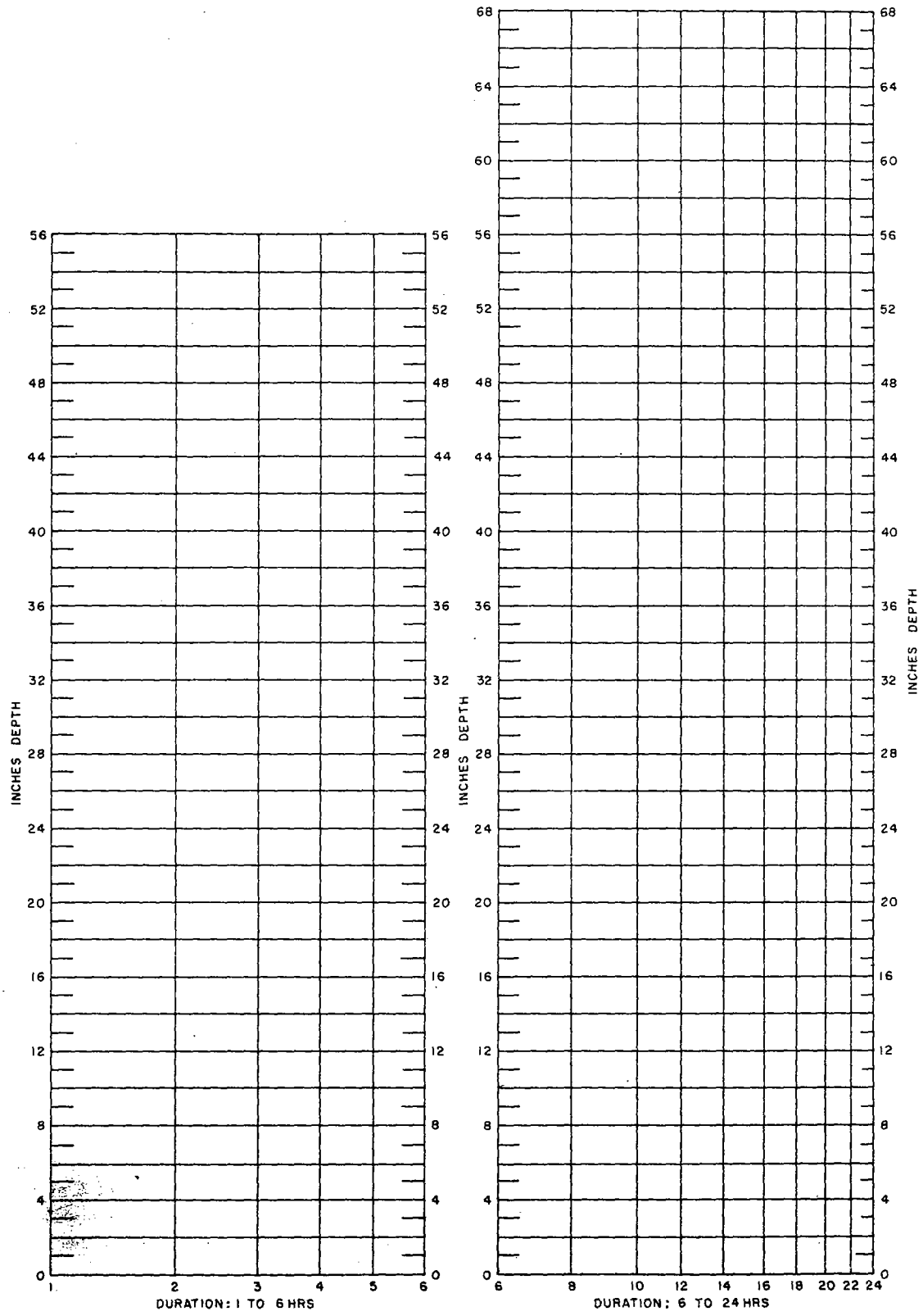

FIGURE 3–12.—Depth-duration diagrams for hurricane PMP (See par. 3.2.1 for example of use).

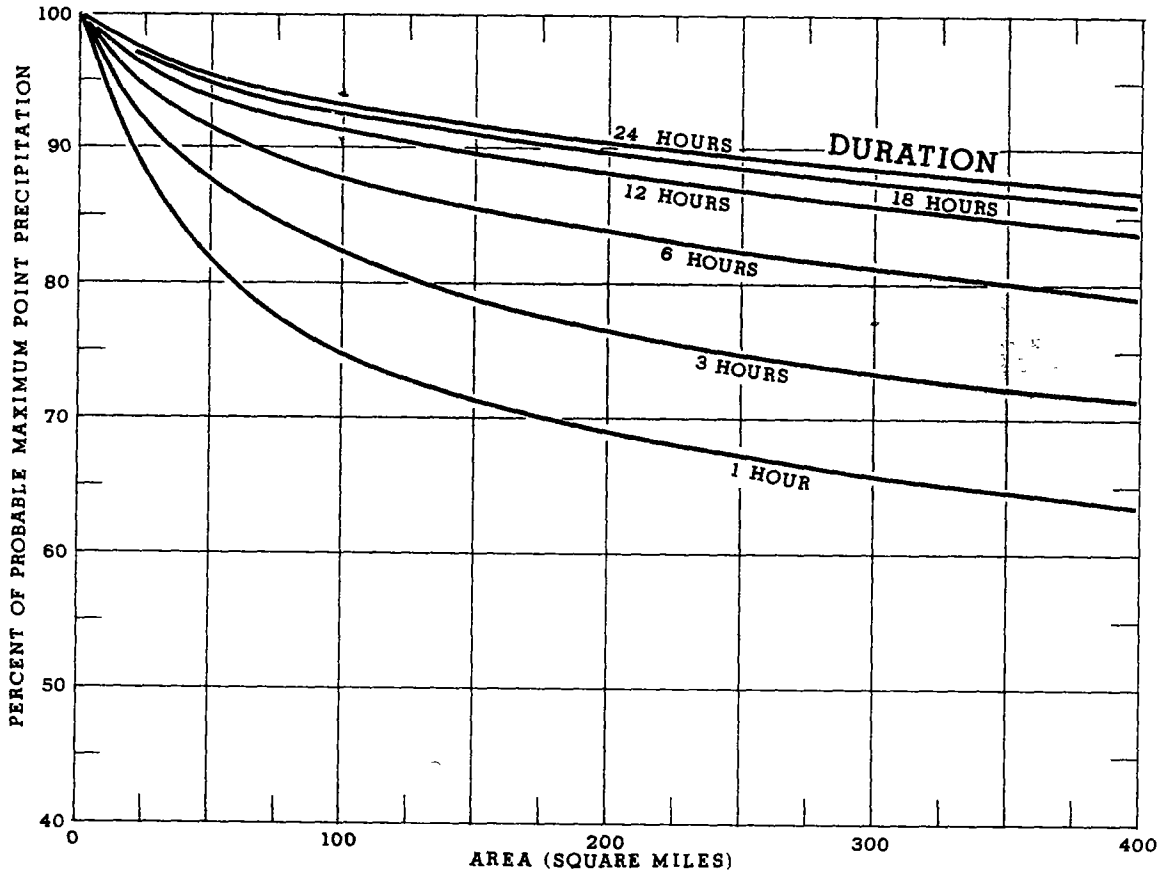

FIGURE 3–13 —Depth-area curves for hurricane PMP for use with figures 3–6 to 3–11.

EXAMPLE: Determine the hourly increments of 9-hr. PMP for a 50-sq. mi. watershed centered at 18°05′ N., 66°45′ W.

The 1-, 6- and 24-hr. point PMP for that location are found to be 12.5, 36, and 60 in., respectively. The depth-duration diagrams of figure 3-12 indicate 3- and 12-hr. PMP values of 25.5 and 47.5 in , respectively. Figure 3–13 indicates 50-sq. mi. reduction factors of 82, 87. 92. and 94 percent for the 1-, 3-, 6- and 12-hr. durations, respectively. Application of these factors to the point PMP for the corresponding durations yields 10.2, 22.2. 33.1, and 44.6 in. for the 1-, 3-, 6-, and 12-hr. 50-sq. mi. PMP, respectively. These amounts are then plotted against duration, and a curve is drawn through the points Values of PMP for every duration up to 9 hr are obtained from this curve and are used to compute the required hourly increments.

meteorological possibility. These limits are what PMP evaluation procedures attempt to establish, of course, but the required data and procedures are only barely adequate to provide approximate solutions to the problems involved.

3.5.2 The considerations that figured in the postulation and use of the hurricane model of chapter 2 provide a rough appraisal. First, the model was tested against observed rainfalls (sec. 2.7) with an acceptable degree of success. Two of the test cases involved hurricane rainfalls of world record magnitude: the Yankeetown, Fla., storm of September 3–6, 1950 (par. 2.7.3) and the Baguio, Philippine Islands, storm of July 14–15, 1911 (par. 2.7.4). Thus, it appears that the model when subjected to conditions of speed of movement, distance from the point in question, etc., similar to those of observed severe hurricanes satisfactorily approximates their rainfalls.

3.5.3 The assigned problem, of course, was to estimate PMP for Puerto Rico and Virgin Islands. The only appreciable maximizing factor applied to the hurricane model was the use of 5 m.p.h. as the speed of movement. In the relatively short period for which good observations have been available, severe hurricanes invading the problem area have been found to have an average speed of 12–13 m.p.h. However, there have been several instances of hurricanes in the general area moving at the slower speed.

TABLE 3-5.—*Suggested order of hourly rainfall increments for hurricane PMP (Numbers indicate rank of increment, 1 being the greatest).*

24-hr PMP (in.)			
40	45	50	55–65
24	23	22	20
23	18	15	13
21	14	12	9
19	10	8	5
17	7	5	3
15	5	3	1
13	2	1	2
11	1	2	4
9	3	4	6
7	4	6	7
5	6	7	8
3	8	9	10
1	9	10	11
2	11	11	12
4	12	13	14
6	13	14	15
8	15	16	16
10	16	17	17
12	17	18	18
14	19	19	19
16	20	20	21
18	21	21	22
20	22	23	23
22	24	24	24

EXAMPLE Hourly increments for 6-hr. PMP when the 24-hr. PMP is 55 in. would be ranked in the following order: 5, 3, 1, 2, 4, 6. In other words, the largest increment would be in the third hour, and the smallest, in the sixth hour.

EXAMPLE Hourly increments for 9-hr. PMP when the 24-hour PMP is 45 in. would be ranked in the following order: 7, 5, 2, 1, 3, 4, 6, 8, 9. The largest increment is in the fourth hour and the smallest in the ninth hour.

Also a maximizing factor was the use of a wind pattern based on the higher speeds without modification. The magnitude of this maximizing factor is not appreciable. The failure to correct for the unprecipitated moisture escaping from the top of the model (par. 2.2.3) should be a maximizing factor. However, the fact that this loss was neglected in satisfactorily approximating some of the observed hurricane rainfalls suggests that it may be a compensating factor for some unknown deficiency in the model.

3.5.4 The effectiveness of the statistical guides utilized is severely limited by the quality and quantity of the basic precipitation data available. An additional 20 years of record and an adequate network of favorably located recording gages would have done much to increase the reliability of the statistical approach. Also, the possibility of geographic variation in the frequency factor K casts some doubt on the acceptability of a maximum value of 15.

3.5.5 In spite of the shortcomings of the procedures used in estimating PMP, the results appear reasonable. The estimates given in figures 3–6 through 3–11 are unquestionably much greater than the maximum observed rainfalls (figs. 1–1 and 1–2). This does not indicate that the estimates are excessive. Rainfall measurements tend to be appreciably deficient in the case of hurricanes because of the large wind error. Moreover, the record of rainfall observations is very short compared to the period of history of hurricanes. Also to be considered is that the heaviest rainfall in a hurricane is limited to a relatively small size of area, and there is not much chance that a gage would sample the heaviest intensities. It is not astonishing, therefore, that the PMP estimates may appear to be excessive. Comparison with the values indicated by the envelope of the world's maximum rainfalls (fig. 1–3) suggests, however, that the magnitudes of the estimates are realistic.

Chapter 4

RAINFALL-FREQUENCY DATA

4.1 Basic data

4.1.1 *Station data.* Table 4–1 groups number of daily precipitation stations by length of record. A total of 102 Puerto Rican stations which take precipitation observations once daily were used in the frequency analysis. The only recording-gage stations with usable records were San Juan, Las Ochenta SCS #3, and Las Mesas #2. San Juan has a long record but the last two stations had but 7 yr. and 6 yr., respectively. A total of 17 nonrecording stations were available for the Virgin Islands. Stations with records longer than 19 yr. were used to define the frequency relationships, whereas the shorter records were used to define the 2-yr. regional pattern.

4.1.2 *Time increments.* Analysis of hundreds of years of precipitation data has produced reliable empirical factors for converting observational-day and clock-hour data into maximum 24- and 1-hr. rainfalls. The factor 1.13 was used throughout to convert observational-day (or clock-hour) rainfall to maximum 24-hr. (or 1-hr.) rainfall.

TABLE 4–1.—*Daily precipitation stations grouped by length of record*

Length of record (years)	Number of stations	Length of record (years)	Number of stations
5–9	15	35–39	10
10–14	8	40–44	6
15–19	14	45–49	12
20–24	5	50–54	10
25–29	16	55–59	12
30–34	11		
			119

4.2 Frequency analysis

4.2.1 *Two types of data series.* The *partial-duration series*, which includes all high values even though several may have occurred in the same year, was required for this study. However, the processing of partial-duration data is very laborious. Furthermore, there is no theoretical basis for extrapolating these data beyond the length of record. For these reasons an alternate procedure was used. The annual maximum event was collected for each year to form the *annual series*. After analysis for frequency, the annual series statistics were converted to partial-duration statistics for corresponding return periods, and the rainfall-frequency maps presented in this report thus, in effect, represent the results of a partial-duration analysis. Table 4–2, based on a sample of 50 widely scattered stations in the United States, gives the empirical factors for converting the partial-duration series to the annual series for return periods up to 10 yr. The two types of data series show no appreciable differences for return periods greater than 10 yr.

TABLE 4–2.—*Empirical factors for converting partial-duration series to annual series*

Return period	Conversion factor
2-yr	0.88
5-yr	.96
10-yr	.99

EXAMPLE: What are the 2-, 5-, and 10-yr. 24-hr. annual series values for the point at 18°15′ N., 66°45′ W.? From the maps of figures 4–50, 4–51, and 4–52, the partial-duration values are estimated to be 5.4, 7.2, and 8.3 in., respectively. Multiplying by the above factors, the annual series values are 4.8, 6.9, and 8.2 in.

4.2.2 *Duration-interpolation diagram.* The generalized depth-duration relation presented in figure 4–1 provides a means for computing rainfall depth for any duration between 1 and 24 hr. if the 1- and 24-hr. amounts for a particular return period are given. The generalization was obtained empirically from data for 200 U.S. Weather Bureau first-order stations, and is the same relation shown in "Rainfall-Frequency Atlas of the United States" [24]. Rainfall values for durations between 1 and 24 hr. are obtained by plotting the 1- and 24-hr. values for the same return period on the corresponding duration lines and laying a straightedge between the two points. Intersections of the straightedge and inter-

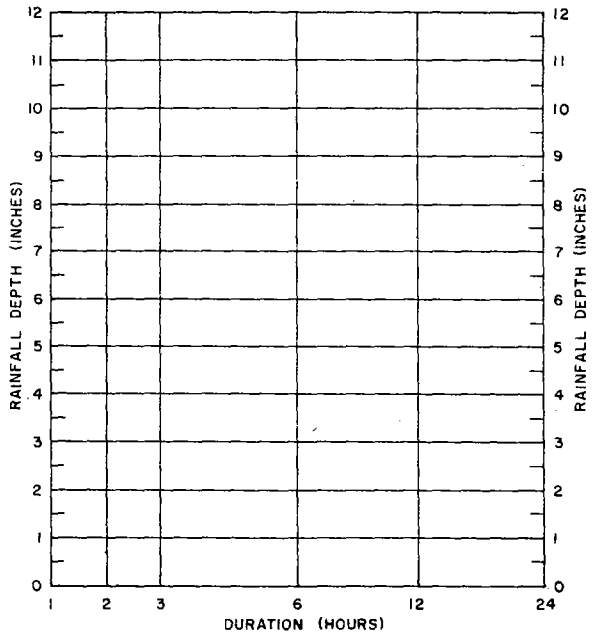

FIGURE 4–1.—Duration-interpolation diagram.

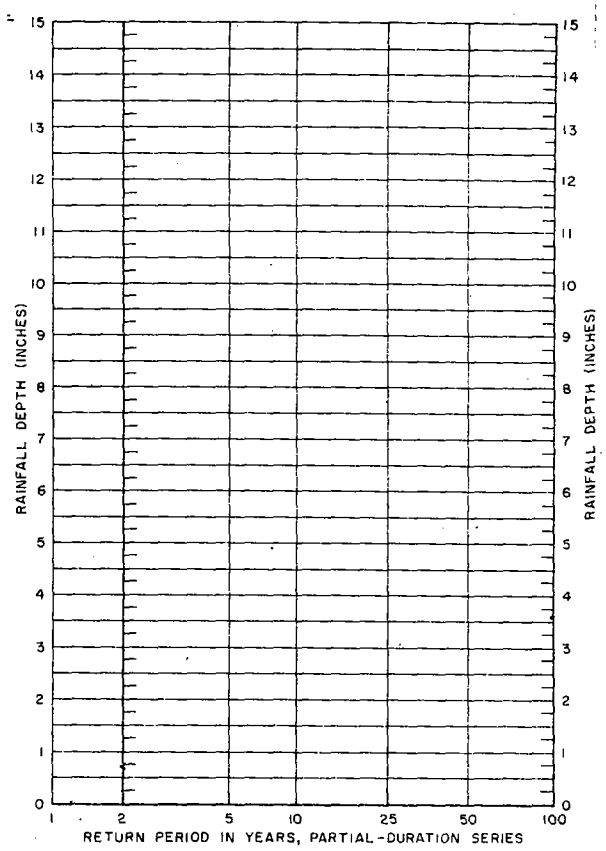

FIGURE 4–2.—Return-period-interpolation diagram.

mediate duration lines yield corresponding rainfall values. Tests with recording-gage data showed that the depth-duration diagram yielded reasonable values. The 30-min. rainfall values for a particular return period were obtained by multiplying the 1-hr. rainfall for that return period by 0.79.

4.2.3 *Return-period-interpolation diagram.* The return-period diagram of figure 4–2 is based on data from 200 Weather Bureau first-order stations and is identical to the diagram used in [24]. The spacing of the ordinates is partly empirical and partly theoretical. From 1 to 10 yr. it is entirely empirical, being based on free-hand curves drawn through plots of partial-duration series data. The spacing for return periods of 20 yr. and longer was based on the Gumbel procedure [25] for analyzing annual series data. The transition was smoothed subjectively between the 10- and 20-yr. return periods. If values between 2 and 100 yr. are read from the return-period diagram, then converted to annual series values and plotted on either Gumbel or log-normal probability paper, the points will very nearly define a straight line. The application of the Gumbel extreme-value procedure, which is supported by theory, is also supported by experience [26].

4.2.4 *Tests for secular trend.* The use of short-record data introduces the question of possible secular trend and biased sample. Routine tests with data from records of equal length but for different periods showed no trend. The use of short-record data thus appears justified.

4.3 Tropical versus nontropical storms

4.3.1 *Definition.* The term *tropical storm* (sec. 1.4) as used in this chapter refers to a cyclone of tropical Atlantic or Caribbean origin. Only those storms whose tracks are given in Weather Bureau *Technical Paper* No. 36 [6] have been considered in the analysis described later in this chapter. In most cases of annual maximum rainfall investigated, there was no difficulty in determining whether or not the rainfall was associated with a tropical storm. Occasionally, however, it was difficult to establish whether a storm was tropical or nontropical. In some cases there was some question as to the characteristics of the storm as, for example, when a tropical storm becomes extratropical. In other cases, the rainfall occurred between storms of different origin. The rainfalls in all those cases were classified as being of the type that appeared to provide the predominating influence in producing the rainfall.

4.3.2 *Distribution of San Juan's annual maximum 24-hr. rainfalls.* The distribution by storm type of the annual maximum 24-hr. amounts for San Juan is shown in table 4–3. The distinctive characteristic of San Juan's record is the relatively small number of annual maxima associated with tropical storms—only 7 out of 58. Moreover, the two largest amounts are not among these seven. The largest nontropical rainfall is about 50 percent larger than the largest tropical storm. A similar analysis for stations in the Unites States that experience tropical storms shows similar results. It is not unusual, however, for closely spaced stations to show entirely dissimilar results with regard to storm type.

4.3.3 *Distribution of 24-hr. rainfall by storm type and return period.* Although tropical storms are relatively infrequent, they produce a large proportion of the annual maximum 24-hr. rainfall amounts. A total of 1,646 24-hr. annual maximum amounts from 33 stations were investigated. About 15 percent of this total were found to be associated with tropical storms. A breakdown of all 1,646 amounts by storm type and magnitude on the return-period scale is given in table 4–3.

4.3.4 Table 4–3 could have been extended to include all storm rainfall instead of just annual maxima. Had this been done, less than 1 percent of all rainy days would have been found to be associated with tropical storms. Nevertheless, tropical storms account for 15 percent of the annual 24-hr. maxima, and half of the amounts equaling or exceeding the 100-yr. value. An analysis based on 48 Weather Bureau stations in the United States [27] which experiences tropical storms yielded similar results (see values in parentheses, table 4–3).

TABLE 4–3.—*Distribution of annual maximum 24-hr. rainfall amounts by storm type and return period for 33 Puerto Rican stations. Comparative values for 48 United States stations are shown in parentheses.*

Return period (yr.)	Cumulative probability (percent)		
	Tropical storm	Nontropical storm	Total
<2	15.4 (18.2)	84.6 (81.8)	100.0
2	10.9 (12.8)	34.9 (34.5)	45.8
5	6.2 (6.9)	11.1 (10.6)	17.3
10	3.8 (4.2)	4.8 (4.7)	8.6
25	2.0 (1.9)	2.0 (1.6)	4.0
50	.9 (1.0)	1.3 (.7)	2.2
100	.5 (.5)	.5 (.5)	1.0

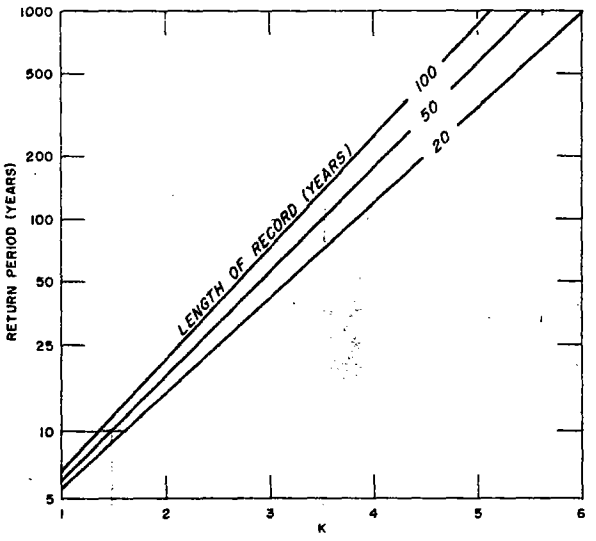

FIGURE 4–3.—Relation between K and return period for 20-, 50-, and 100-yr. records (after Gumbel).

4.4 Isopluvial maps

4.4.1 *$\bar{x}$ and s_N 24-hr. maps.* Because of the large amount of 24 hr. data available and the relatively small standard error associated with the arithmetic mean of the annual maximum rainfalls (annual series), $\bar{x}$, the $\bar{x}$ 24-hr. map was constructed first. ($\bar{x}$ is approximately equal to the 2.3-yr. return period.) A preliminary standard deviation map was also prepared. The reliability of the latter map was increased by adjusting its values on the basis of a smoothed coefficient-of-variation map. The adjustments were made only on the standard deviation map because this statistic is sensitive to anomalous events whereas the mean is affected only slightly. Also, the standard deviation values had been adjusted when required to a common 50-yr. record standard. Table 4–4 lists the empirical adjustment factors determined from 200 24-hr. precipitation stations in the United States.

4.4.2 *2-yr. and 100-yr. 24-hr. maps (figs. 4–50, 4–99, and 4–55, 4–104).* The values indicated on the 2-yr. map are for the partial-duration series and are approximately 7 percent greater than those on the $\bar{x}$ map. The smoothed 100-yr. map is based on a combination of values from the $\bar{x}$ and s_N maps. The mean plus 3.5

TABLE 4–4.—*Factors for adjusting standard deviation to 50-yr. record*

Length of record (yr.)	10	20	30	40
Factor for increasing standard deviation	1.29	1.08	1.04	1.02

standard deviations, as illustrated in the diagram of figure 4–3 based on the Gumbel procedure, was used to obtain the 100-yr. values.

4.4.3 *Estimating the 1-hr. statistics.* The lack of recording-gage data necessitated the synthesis of an hourly rainfall regime based on stations in the United States. The selection of the stations used was based on similarity of climatic factors such as hurricanes, thunderstorms, temperature and dewpoint. The stations used and the manner in which the required statistics on hourly rainfall were obtained are shown in table 4–5.

4.4.4 *Basic 1-hr. maps* ($\bar{x}$, s_N, *2- and 100-yr.*). An average 2-yr. 1- to 24-hr. ratio of 45 percent (table 4–5) was applied to both the 2-yr. 24-hr. and $\bar{x}$ 24-hr. maps to determine the corresponding 1-hr. maps. Both the 2-yr. and $\bar{x}$ values are measures of the central tendency of the extreme value distribution. However, the fact that the coefficients of variation ($s_N/\bar{x}$) are generally less for the 1-hr. than for the 24-hr. value at the same station (table 4–5) indicates that the 24-hr. amounts increase with return period at a faster rate than do the 1-hr. amounts. In order to adjust for this difference, the factor 32/43, as determined from table 4–5, was applied to the 24-hr. coefficient-of-variation (c_v) map. The $\bar{x}$ and c_v maps were then used to prepare a standard deviation map. The 100-yr. map was constructed by adding the mean to 3.5 times the standard deviation ($\bar{x}+3.5s_N$).

TABLE 4–5.—*Data used for developing hourly rainfall regime.*

Station	Ratio: 2-yr. 1-hr. / 2-yr. 24-hr.	Coefficient of variation.	
		1-hr.	24-hr.
San Juan P.R.	0.45	0.35	0.46
Galveston, Tex.	.42	.39	.45
San Antonio, Tex.	.47	.37	.47
New Orleans, La.	.39	.29	.49
Shreveport, La.	.45	.30	.40
Birmingham, Ala.	.40	.28	.36
Mobile, Ala.	.40	.25	.33
Jacksonville, Fla.	.48	.28	.40
Key West, Fla.	.41	.39	.52
Pensacola, Fla.	.39	.33	.37
Tampa, Fla.	.54	.30	.36
Savannah, Ga.	.55	.26	.51
Charleston, S.C.	.49	.32	.44
Hatteras, N.C.	.41	.34	.49
Wilmington, N.C.	.41	.32	.33
Total	6.66	4.77	6.38
Mean ($\bar{x}$)	.44	.32	.43

4.4.5 *Additional isopluvial maps.* The 2-yr. 1-hr., 2-yr. 24-hr., 100-yr. 1-hr., and 100-yr. 24-hr. maps were than used in conjunction with the duration and return-period relations of figures 4–1 and 4–2 to obtain 38 isopluvial maps for intermediate durations and return periods. The computations were made by a digital computer. Values were computed for and plotted on the grid of figure 4–4, and the isopluvials were then drawn with reference to these grid values. The seven 30-min. maps were developed from the relationship 0.79 times the values on the 1-hr. maps for corresponding return periods. The 98 rainfall-frequency maps (49 for Puerto Rico and 49 for the Virgin Islands) are presented at the end of this chapter (figs. 4–7 to 4–55 and 4–56 to 4–104, respectively).

4.5 Depth-area relationships

4.5.1 There are two basic types of depth-area relationships: (1) storm-centered relations, and (2) geographically fixed relations. The depth-area curves of figure 3–13 are storm centered, i.e., they were developed from rainfall data in storm centers. The frequency-derived, geographically fixed, depth-area curves of figure 4–5 are based on different parts of different storms instead of on the highest amounts surrounding the storm centers. Since the area is geographically fixed, its precipitation stations measure rainfall sometimes near the storm center, sometimes on the outer edges, and sometimes in between the two. The averaging process results in the geographically fixed curves being flatter than storm-centered curves. This is understandable considering that such curves are steeper near the centers of storms. Each type of curve is appropriate for its respective application—the storm-centered for PMP and the geographically fixed for frequency data.

4.5.2 The depth-area curves of figure 4–5 are based on data from 20 dense raingage networks and are identical with those of Weather Bureau *Technical Paper* No. 29 series [21]. The ordinates of the 24-hr. curve, for example, are conveniently expressed as ratios (in percent) whose numerator is the average of the 2-yr. 24-hr. point values in the area.

4.6 Seasonal variation

4.6.1 The frequency analysis discussed followed the conventional procedures of using only the annual maxima (annual series) or n-maximum events for n years of record (partial-duration series). Obviously, some months contribute more events to these series

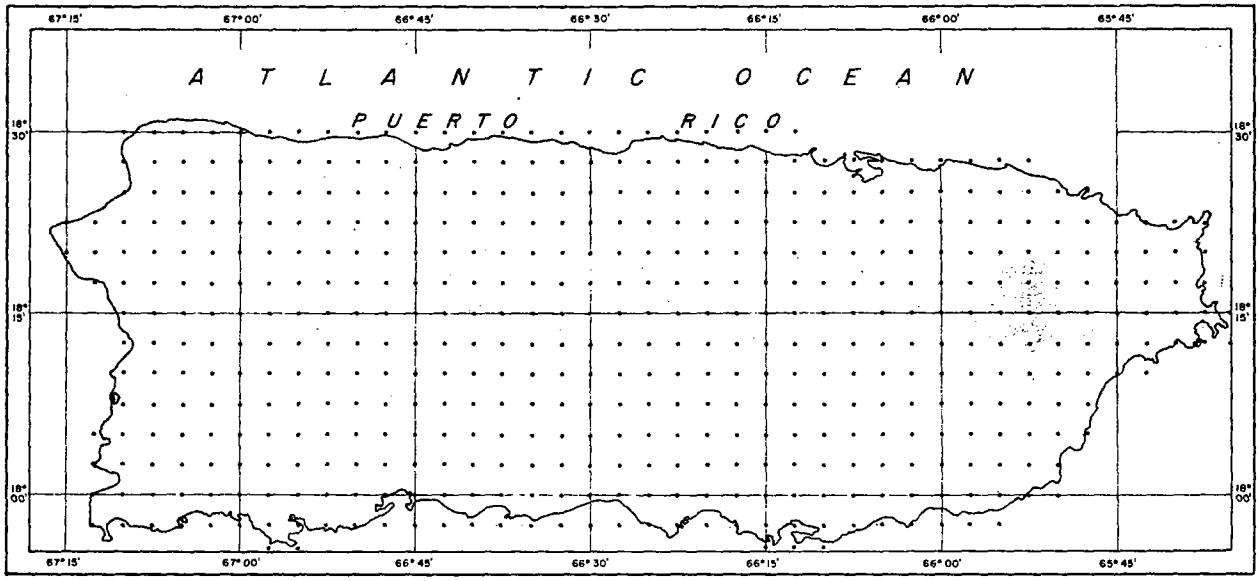

FIGURE 4–4.—Grid showing points for which rainfall-frequency data were computed in construction of maps showing precipitation values for durations between 1 and 24 hr. and return periods between 2 and 100 yr.

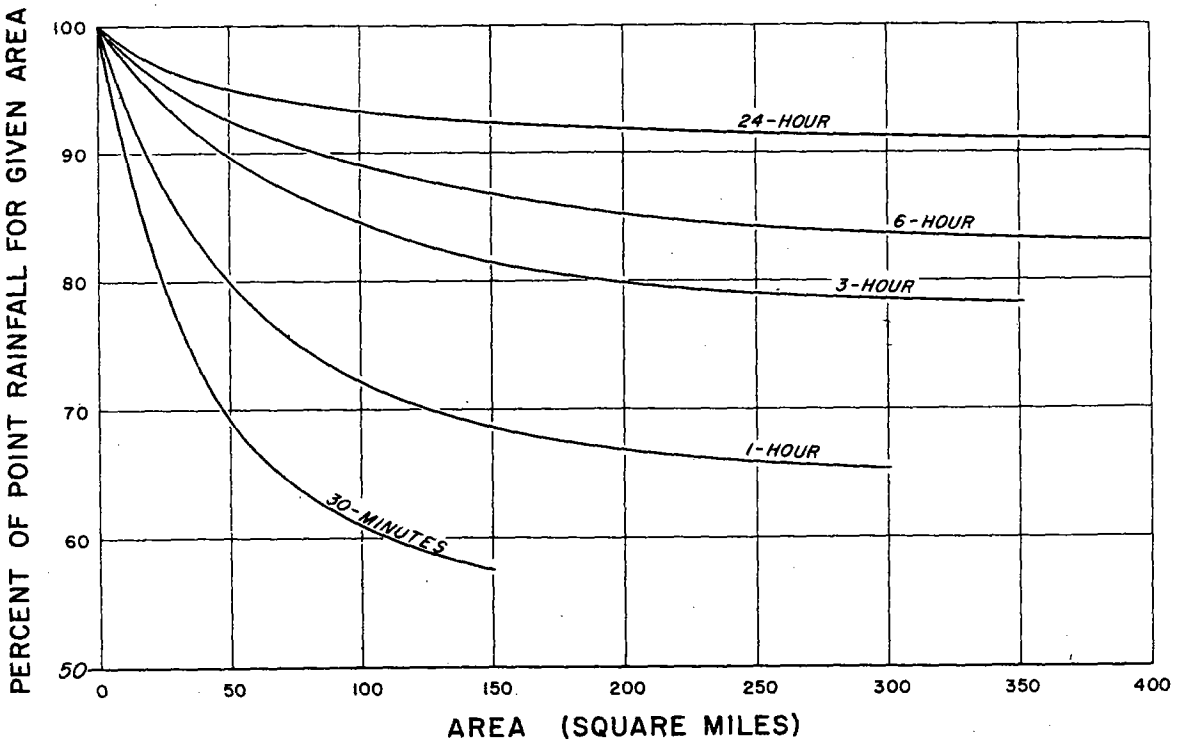

FIGURE 4–5.—Depth-area curves for rainfall-frequency data for use with figures 4–7 to 4–104.

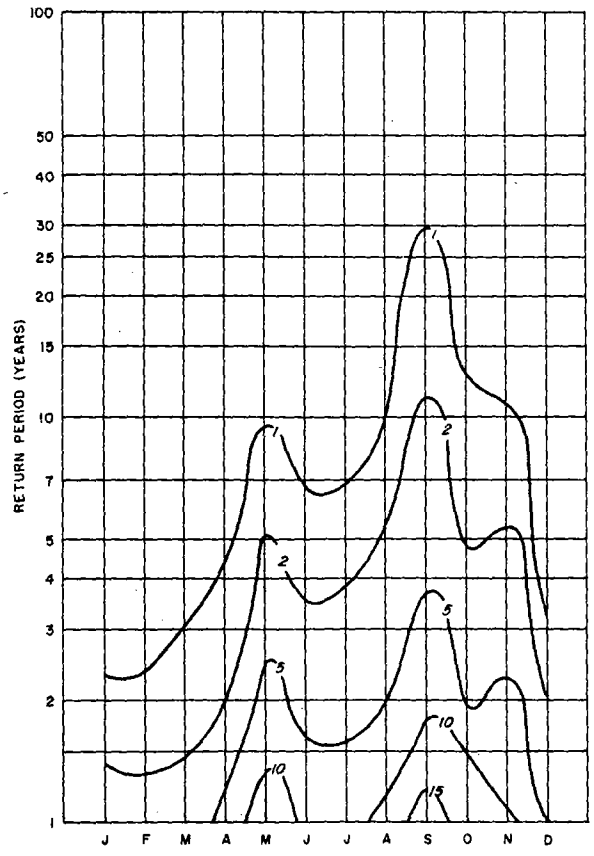

FIGURE 4–6.—Monthly distribution (in percent) of 24-hr rainfalls for various return periods.

Example: Determine the probability of occurrence of a 5-yr, 24-hr. rainfall for the months May through August.

From figure 4–6, the probabilities for each month are interpolated to be 2, 1.5, 1.5, and 2 percent, respectively. In other words, the probability of occurrence of a 5-yr, 24-hr. rainfall in May of any year is 2 percent; for June, 1.5 percent; etc.

than do other months, and some months may not contribute at all. As a matter of interest the annual maximum 24-hr. data were analyzed to determine their monthly distribution. The diagram of figure 4–6 was developed from 24-hr. rainfall data for San Juan and from 40 nonrecording-gage stations, all in Puerto Rico. All stations had at least 40 yr. of data, providing a total of 2,016 station-years of data. All 24-hr. events which made up the partial-duration series for the 41 stations were classified according to month of occurrence and return period. After the data for each station were summarized, the frequencies were computed for each month by determining the ratio (in percent) of the number of occurrences of amounts equal to or greater than the value for a particular return period to the total number of occurrences (years of record). Cases of non-occurrence as well as occurrence of rainfall events were considered in order to arrive at numerical probabilities. The probabilities were then plotted as a function of return period and season and smoothed isopleths fitted to the probabilities. The September peak of figure 4–6, as expected, coincides with the month that experiences the greatest number of tropical storms. In fact, one out of every two 24-hr. annual maxima associated with tropical storms occurs in September.

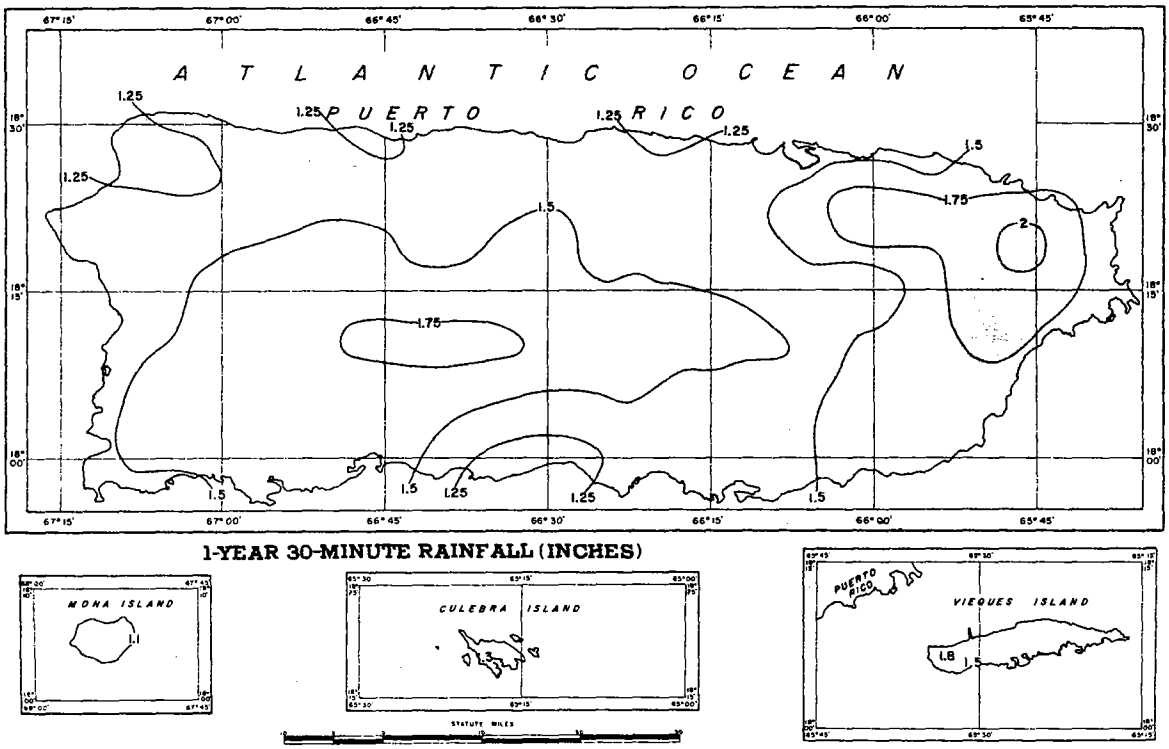

FIGURE 4–7.—1-yr. 30-min. rainfall for Puerto Rico (in.).

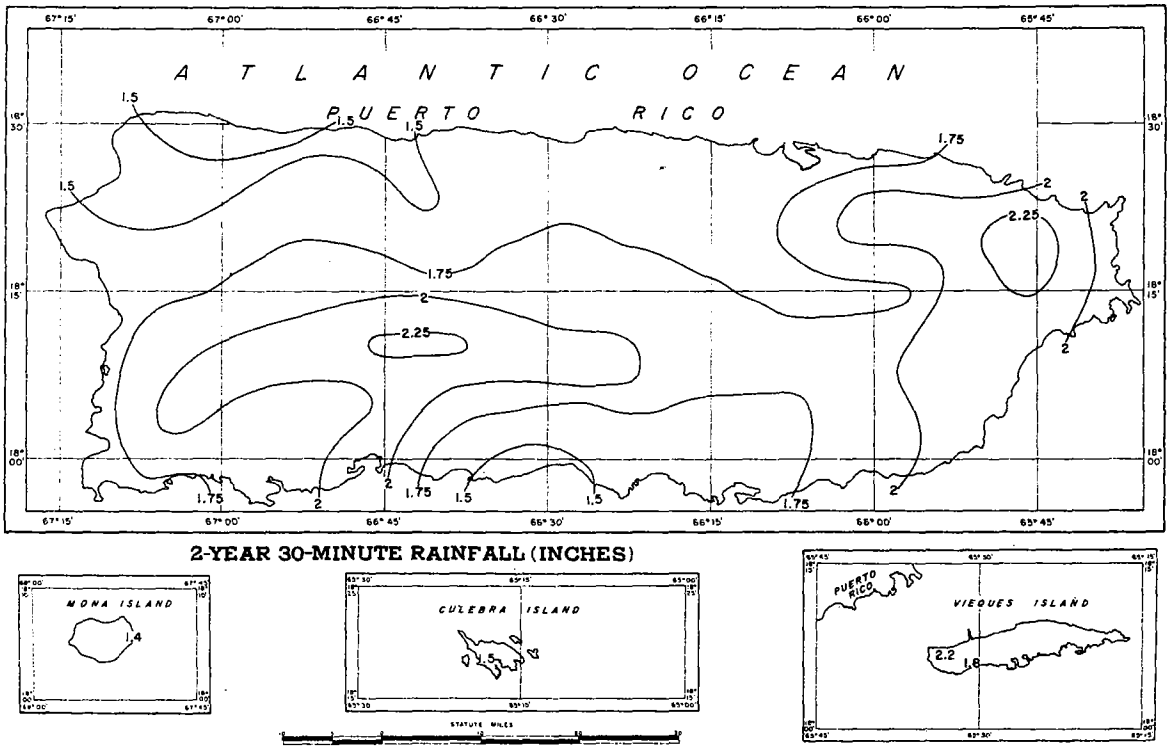

FIGURE 4–8.—2-yr. 30 min. rainfall for Puerto Rico (in.).

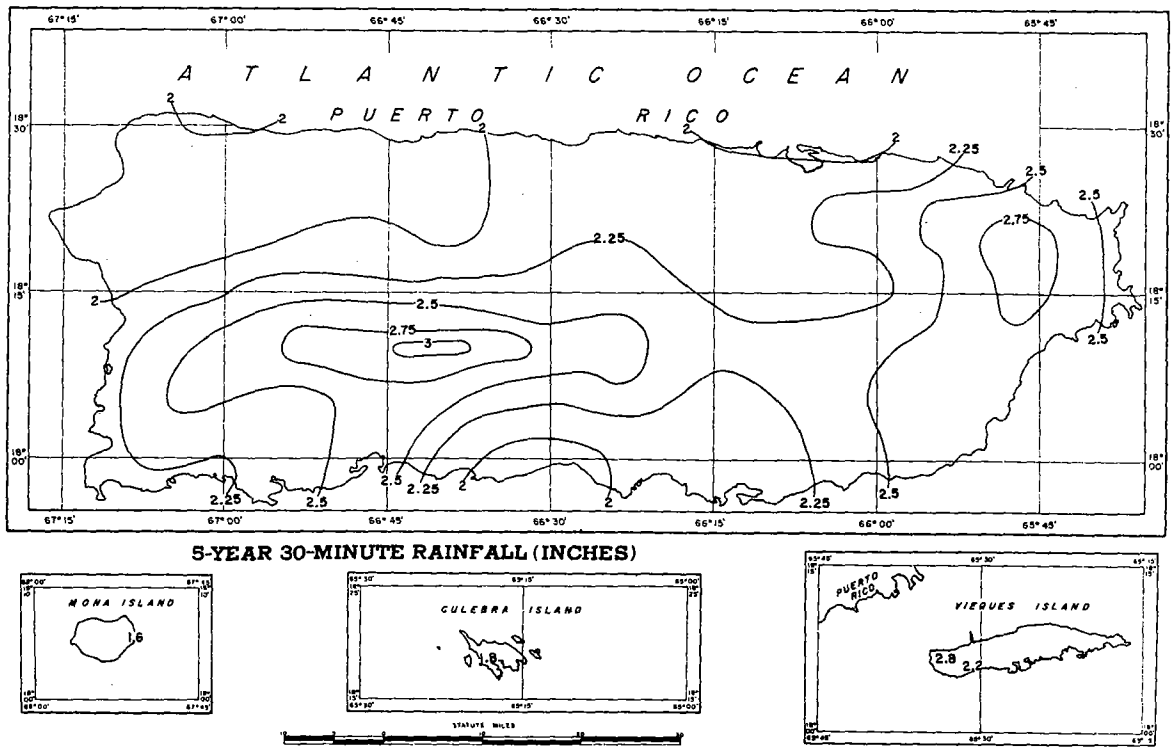

FIGURE 4–9.—5-yr. 30-min rainfall for Puerto Rico (in.).

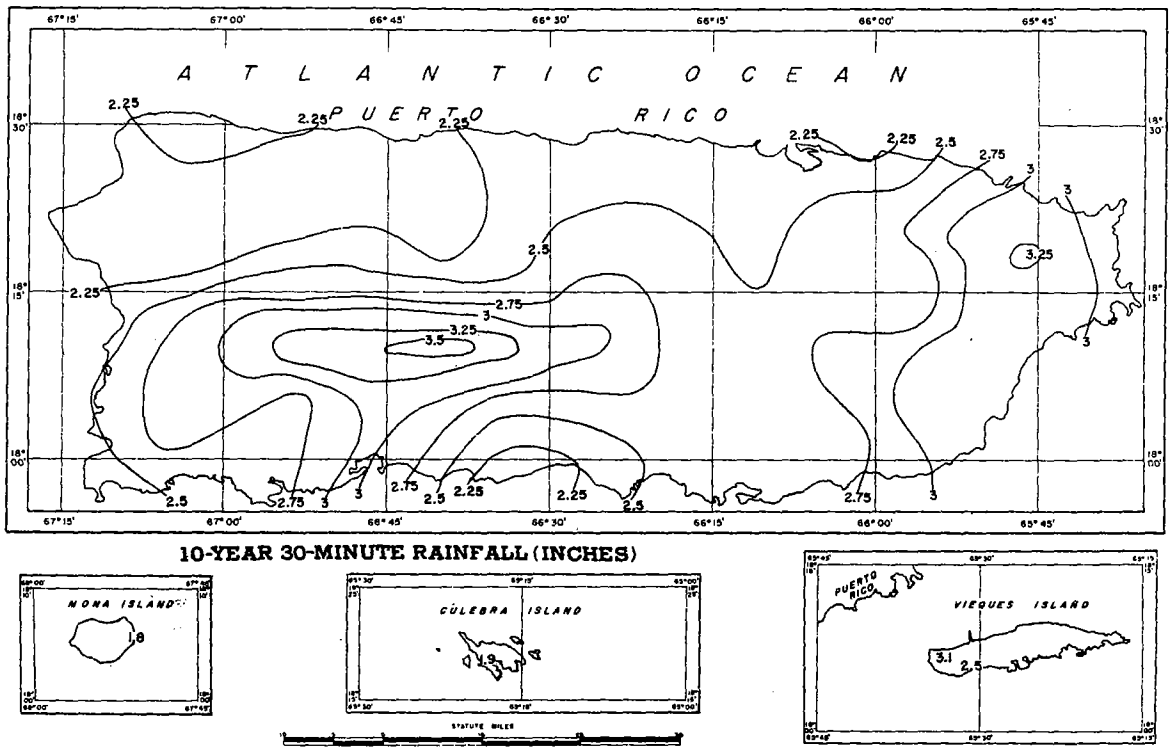

FIGURE 4–10.—10-yr. 30-min. rainfall for Puerto Rico (in.).

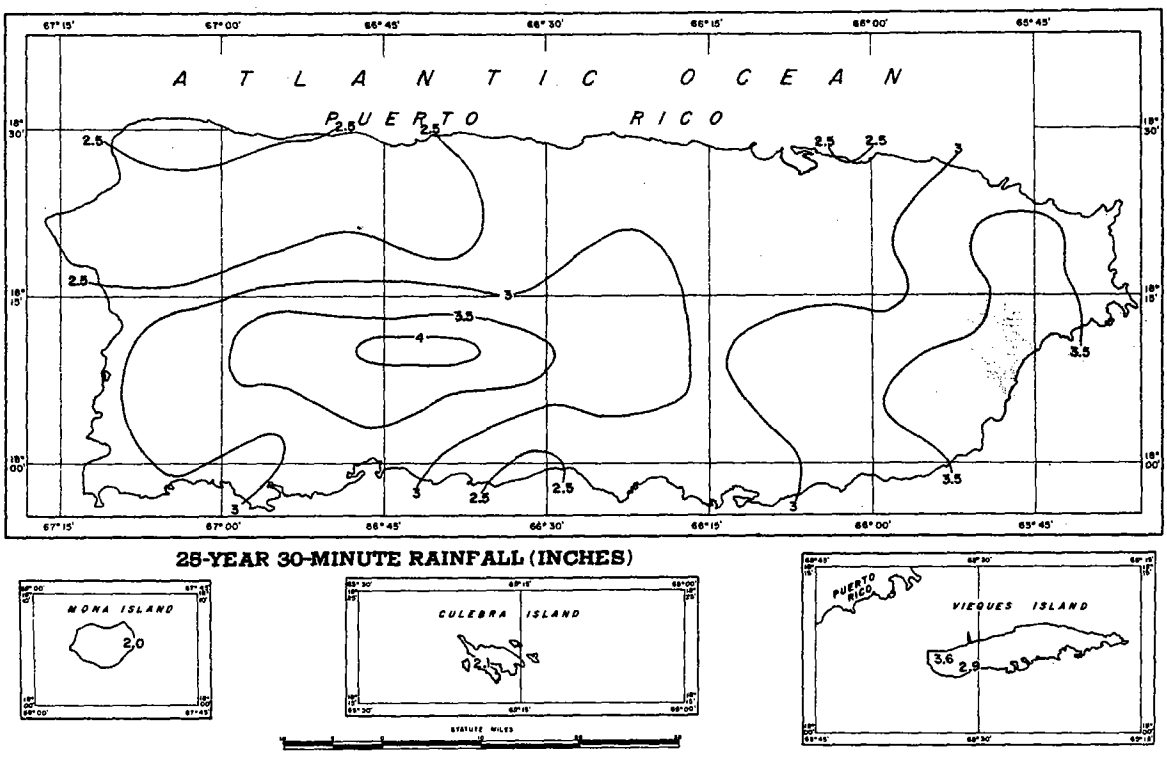

FIGURE 4–11.—25-yr. 30-min. rainfall for Puerto Rico (in.).

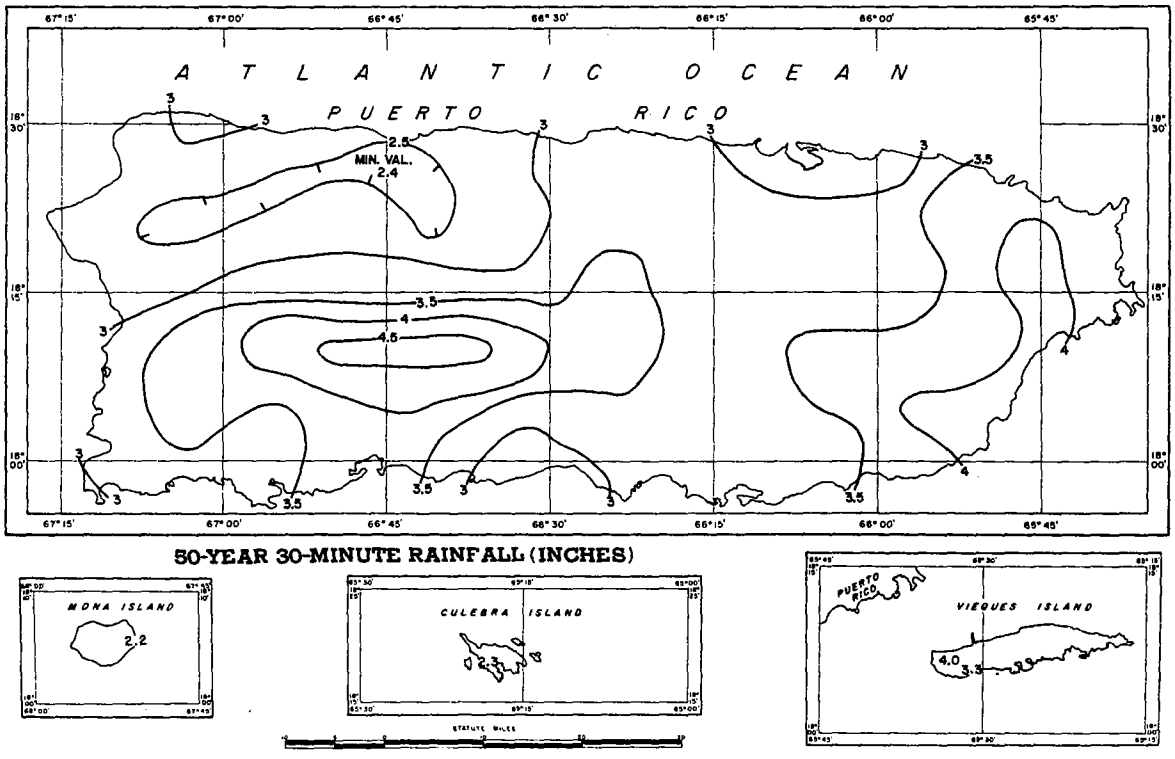

FIGURE 4–12.—50-yr. 30 min. rainfall for Puerto Rico (in.).

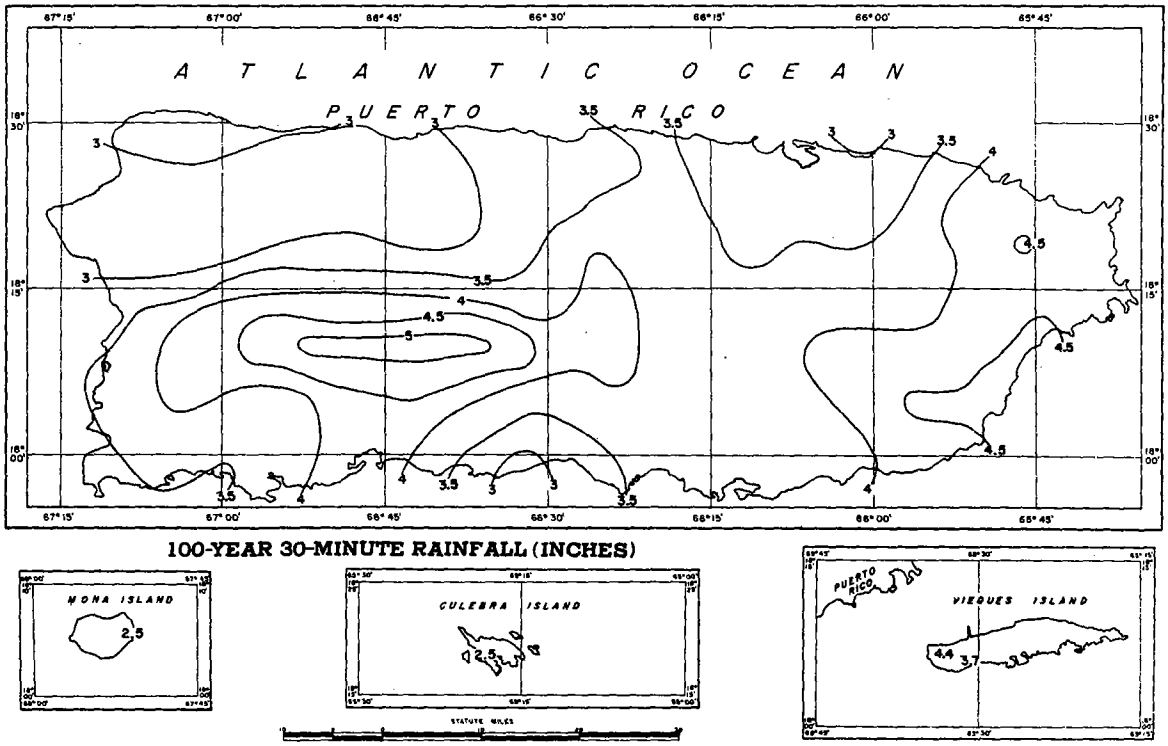

FIGURE 4–13.—100-yr. 30-min. rainfall for Puerto Rico (in.).

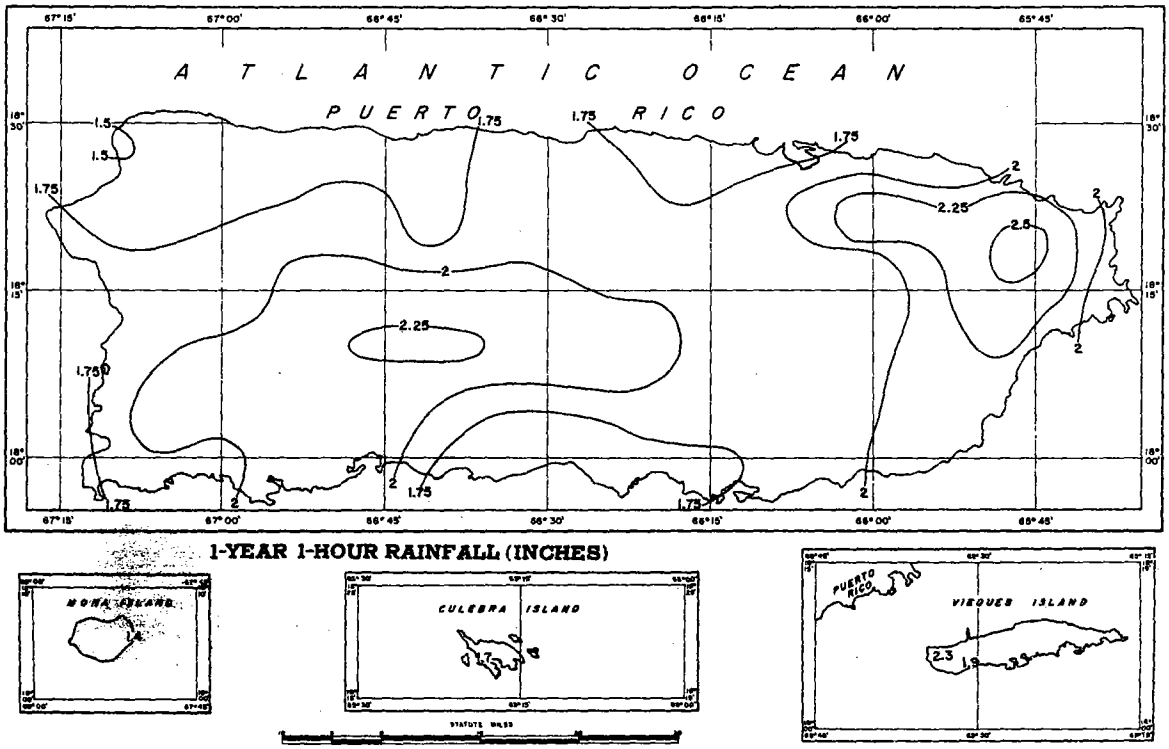

FIGURE 4–14.—1-yr. 1-hr. rainfall for Puerto Rico (in.).

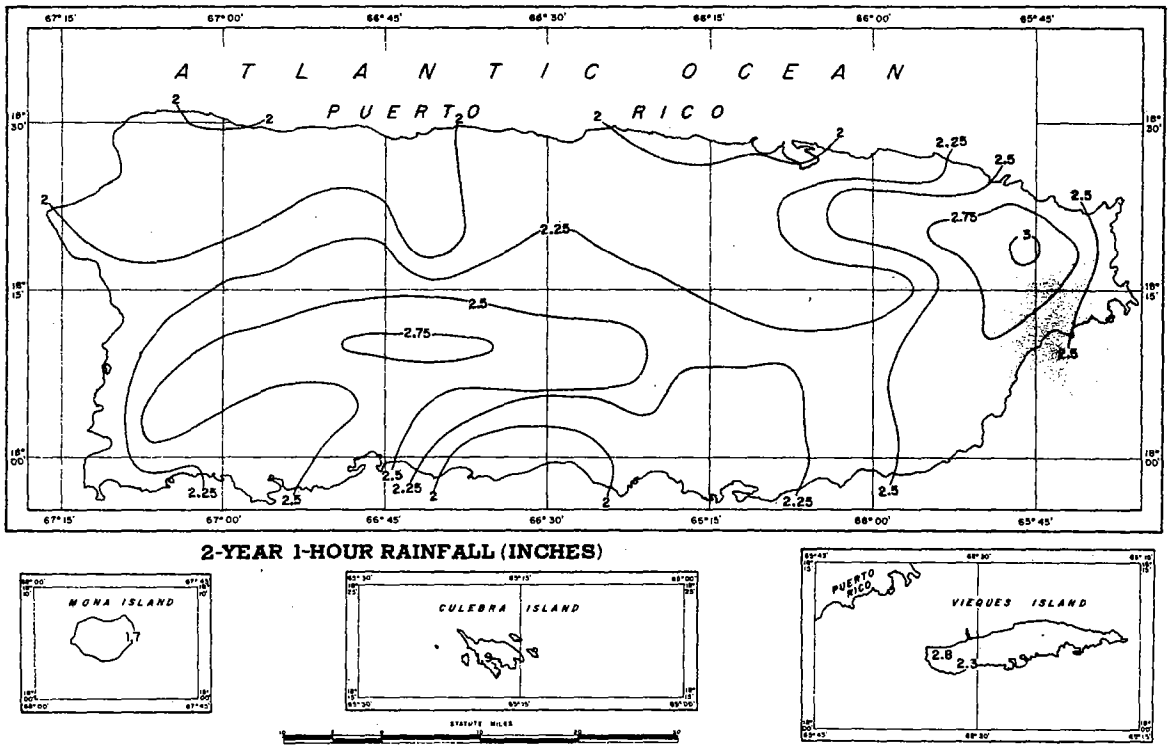

FIGURE 4–15.—2-yr. 1-hr. rainfall for Puerto Rico (in.).

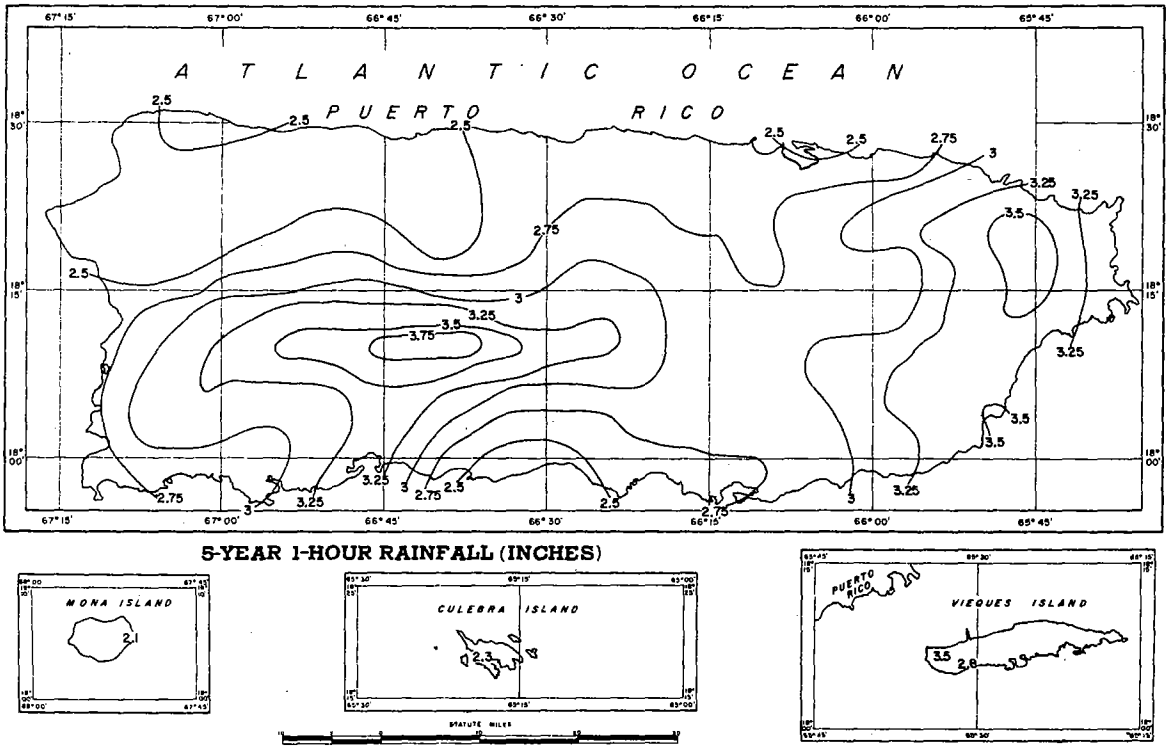

FIGURE 4–16.—5-yr. 1-hr. rainfall for Puerto Rico (in.).

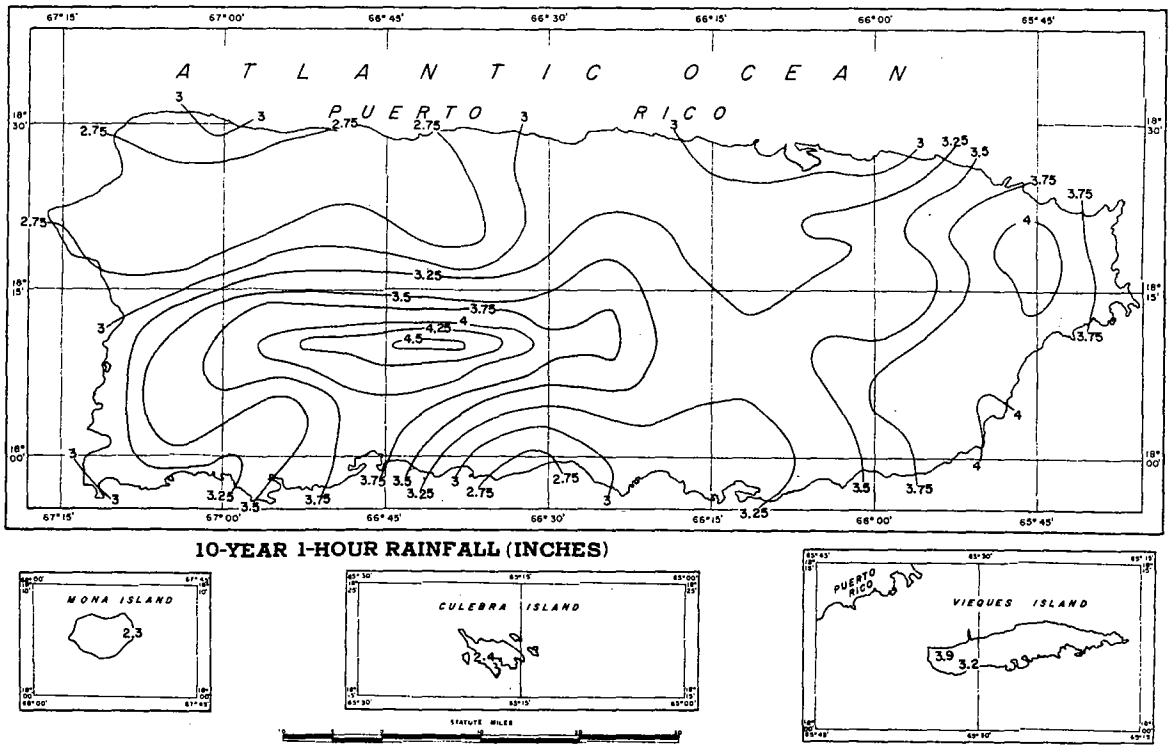

FIGURE 4–17.—10-yr. 1-hr. rainfall for Puerto Rico (in.).

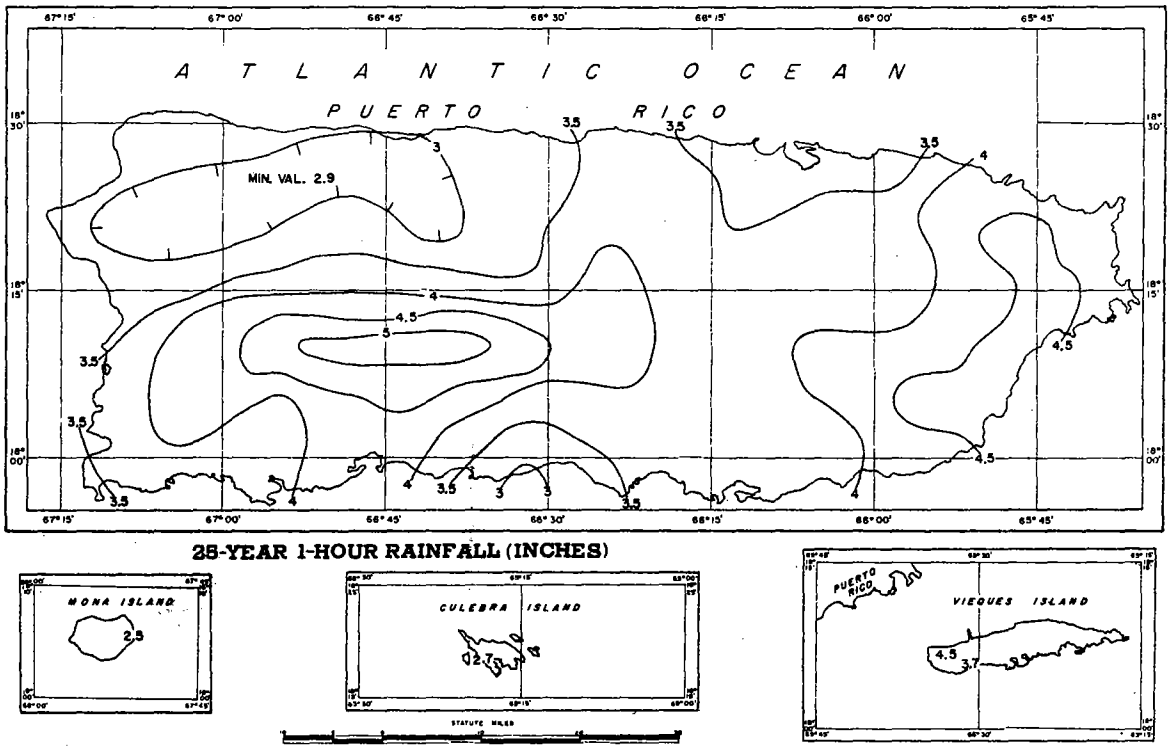

FIGURE 4–18.—25-yr. 1-hr. rainfall for Puerto Rico (in.).

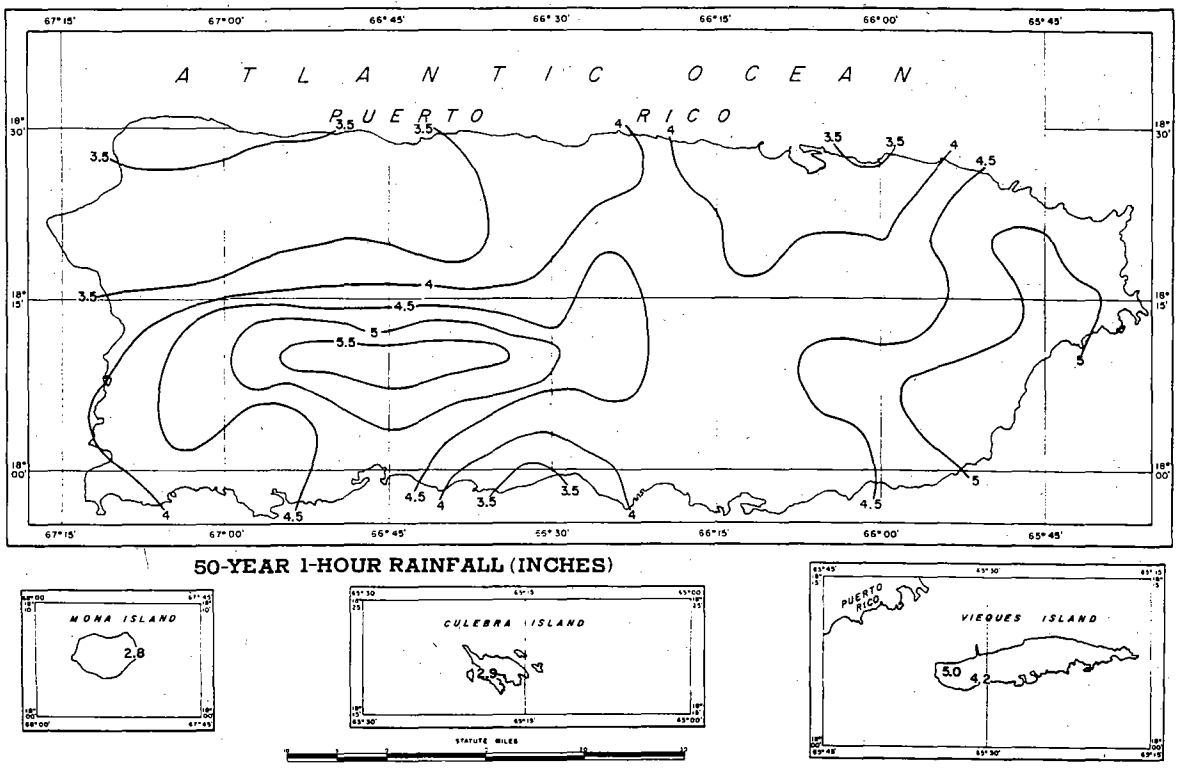

FIGURE 4–19.—50-yr. 1-hr. rainfall for Puerto Rico (in.)

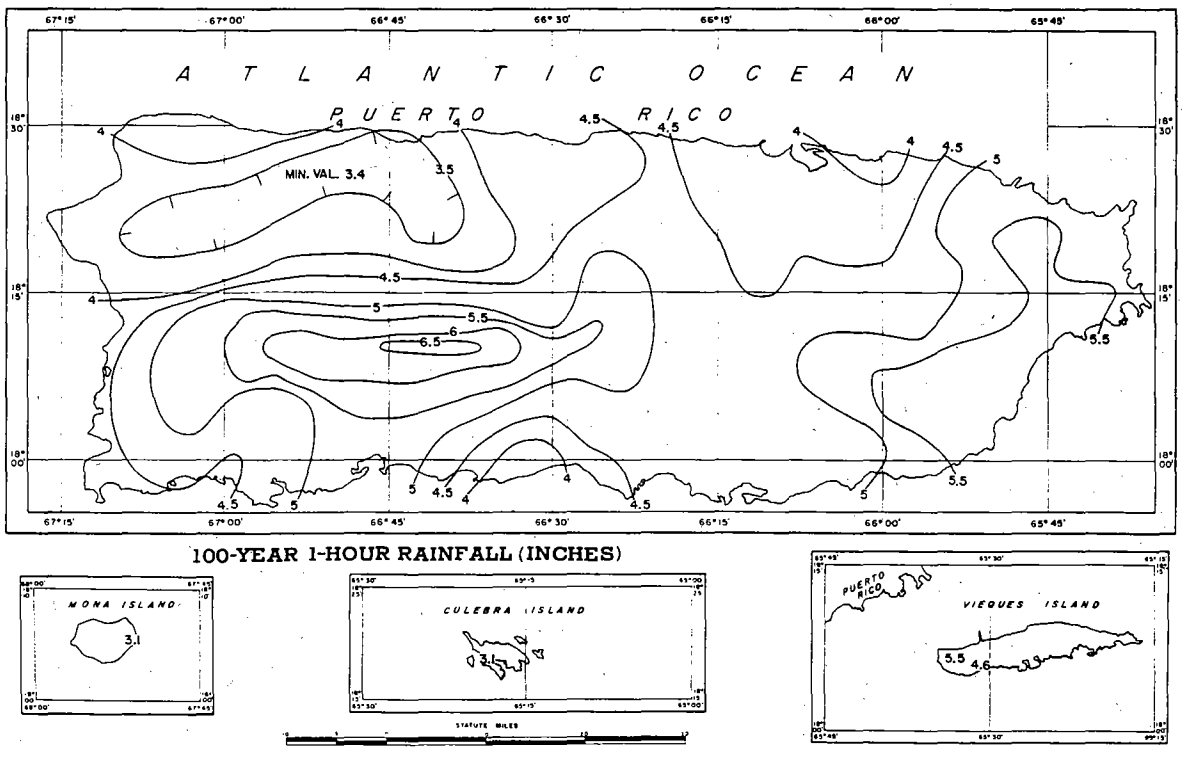

FIGURE 4–20.—100-yr. 1-hr. rainfall for Puerto Rico (in.).

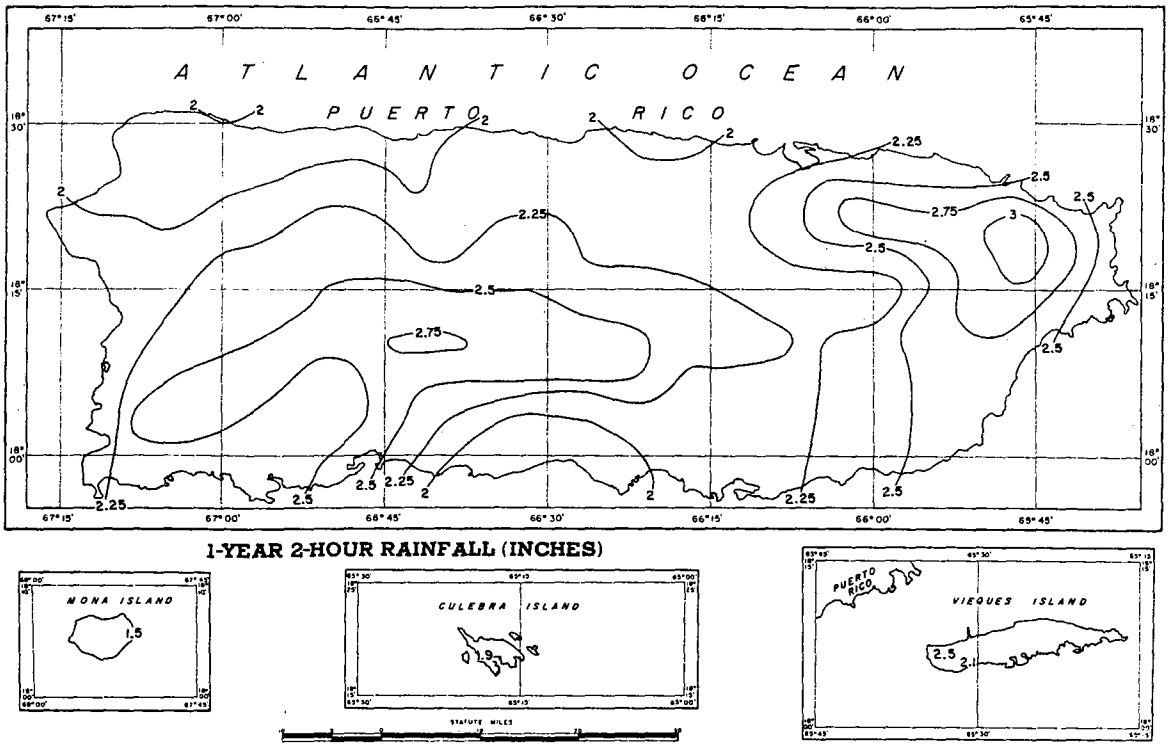

FIGURE 4–21.—1-yr. 2-hr. rainfall for Puerto Rico (in.).

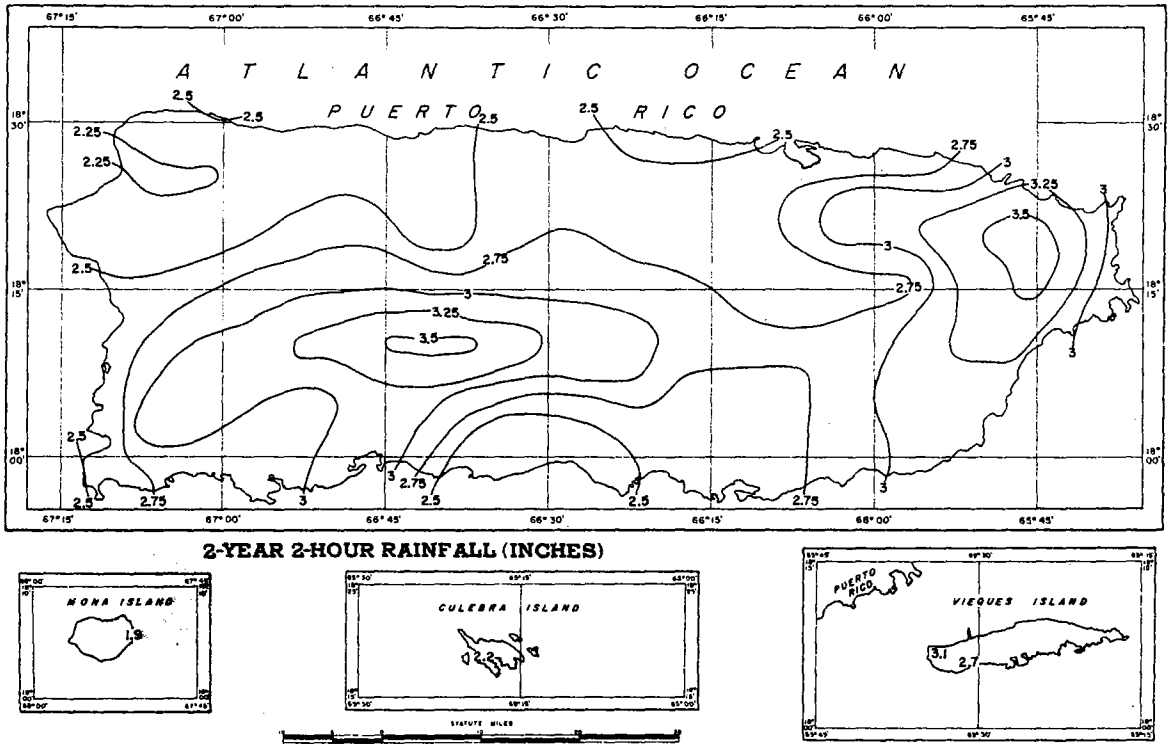

FIGURE 4–22.—2-yr. 2-hr. rainfall for Puerto Rico (in.).

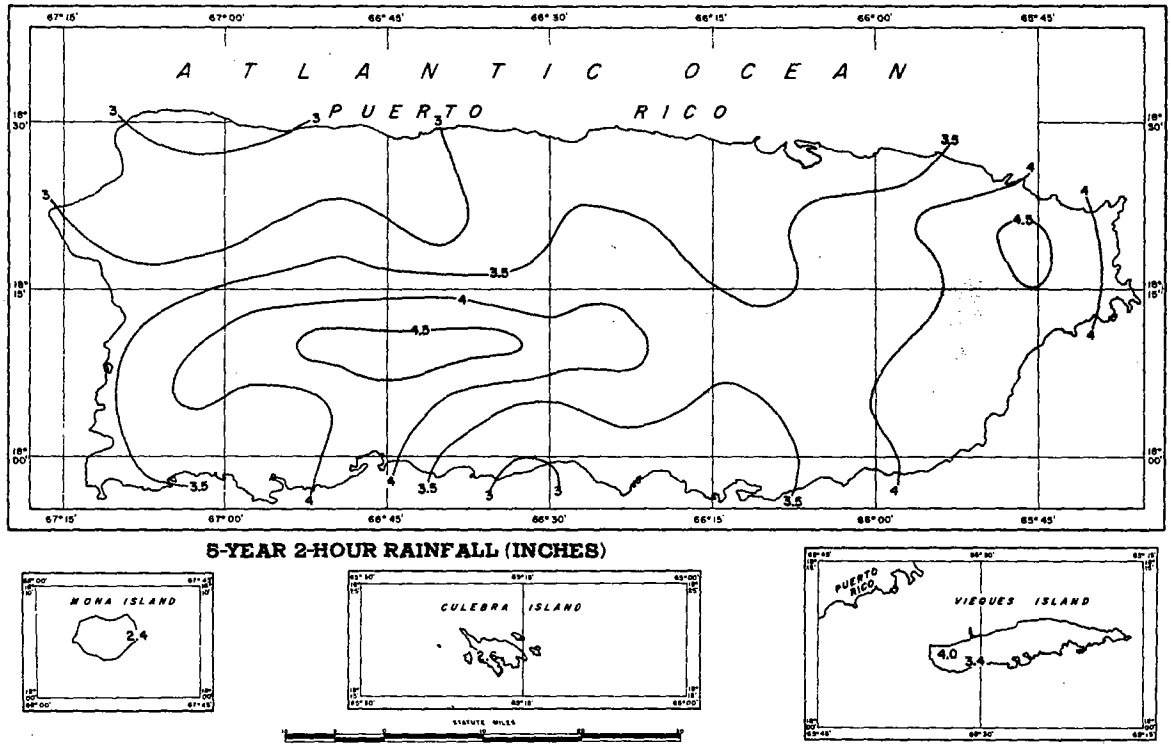

FIGURE 4–23.—5-yr. 2-hr. rainfall for Puerto Rico (in.).

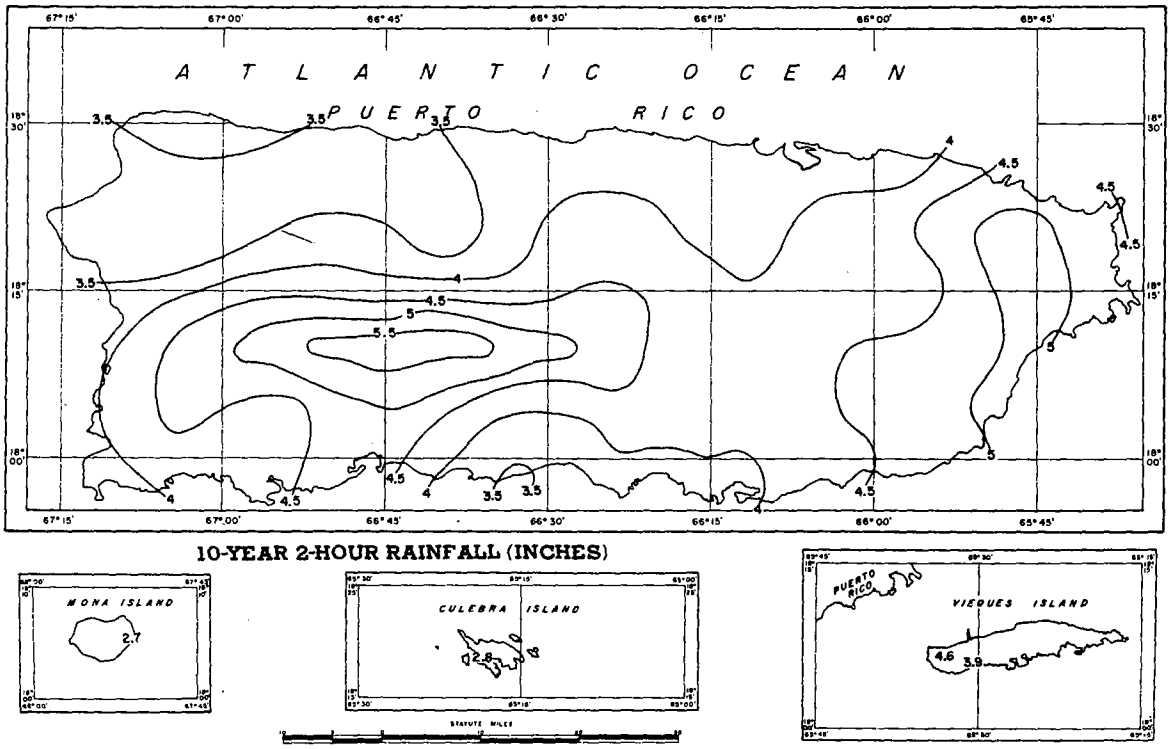

FIGURE 4–24.—10-yr. 2-hr. rainfall for Puerto Rico (in.).

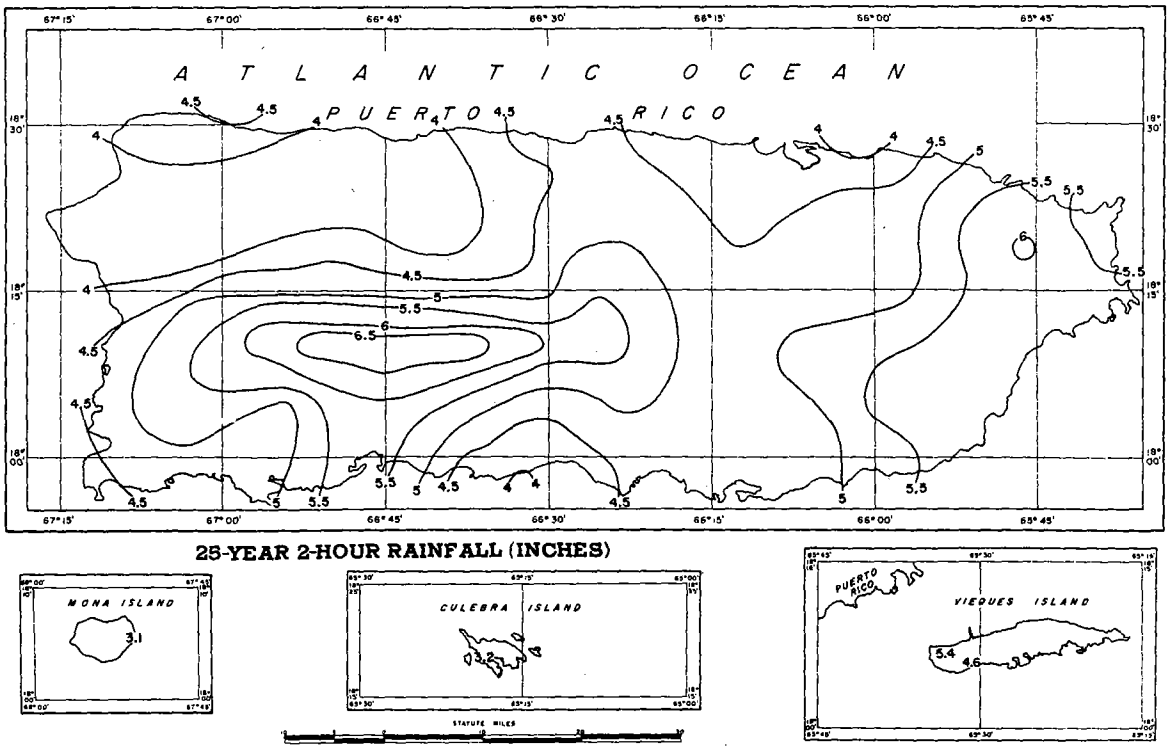

FIGURE 4–25.—25-yr. 2-hr. rainfall for Puerto Rico (in.).

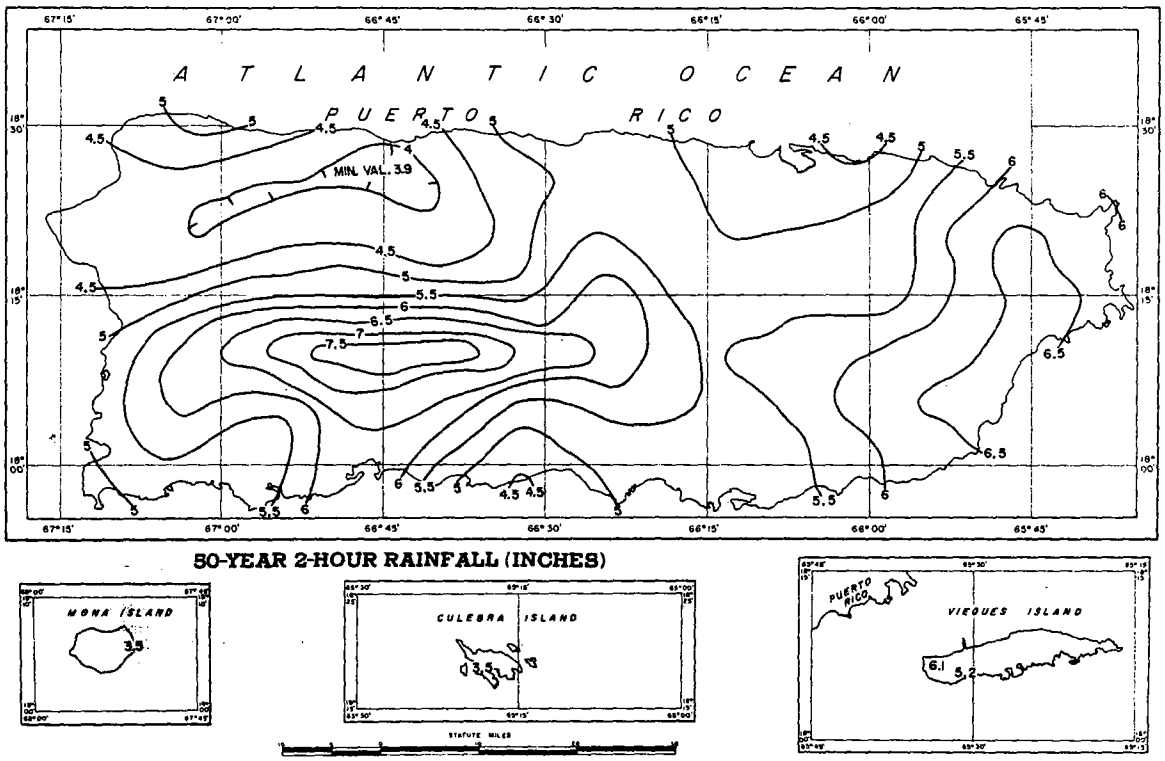

FIGURE 4–26.—50-yr. 2-hr. rainfall for Puerto Rico (in.).

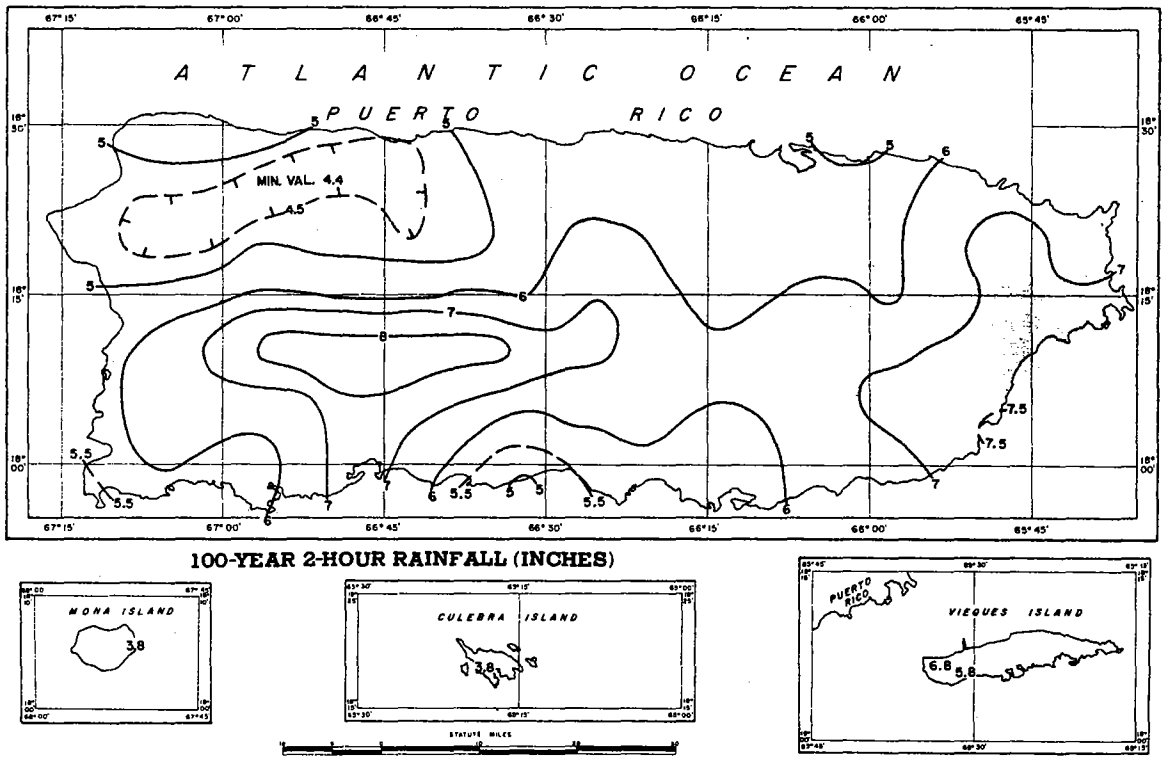

FIGURE 4–27.—100-yr. 2-hr. rainfall for Puerto Rico (in.).

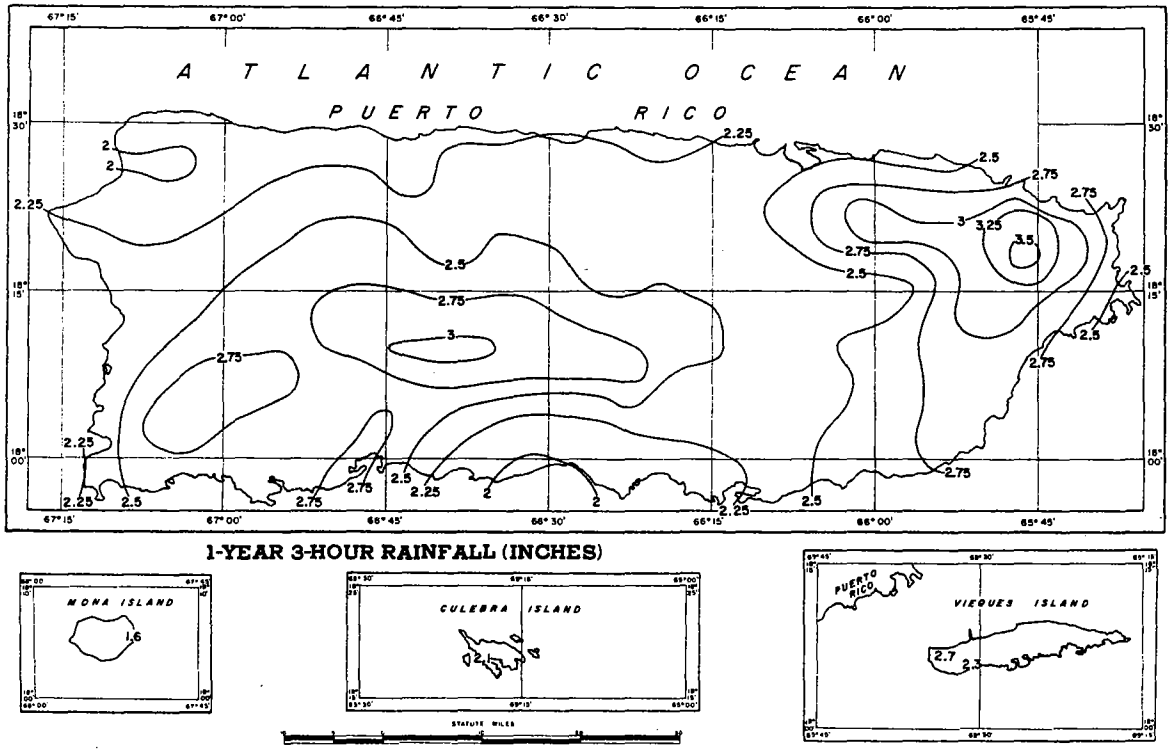

FIGURE 4–28.—1-yr. 3-hr. rainfall for Puerto Rico (in.).

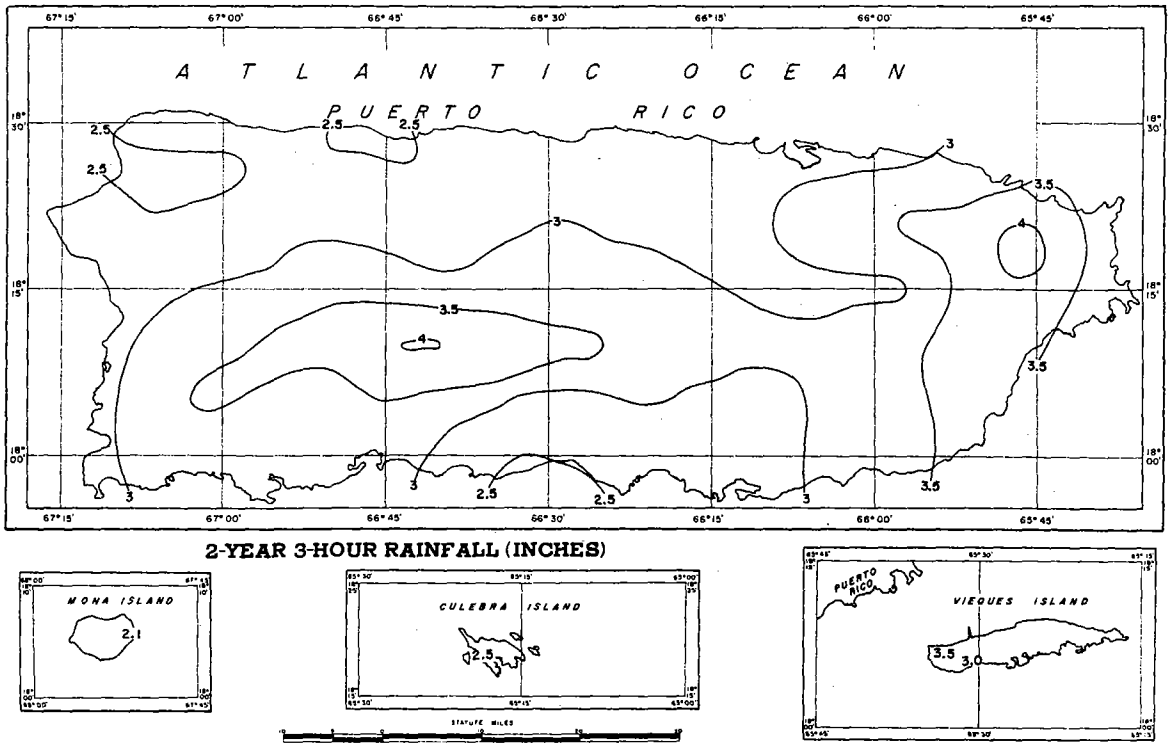

FIGURE 4–29.—2-yr. 3-hr. rainfall for Puerto Rico (in.).

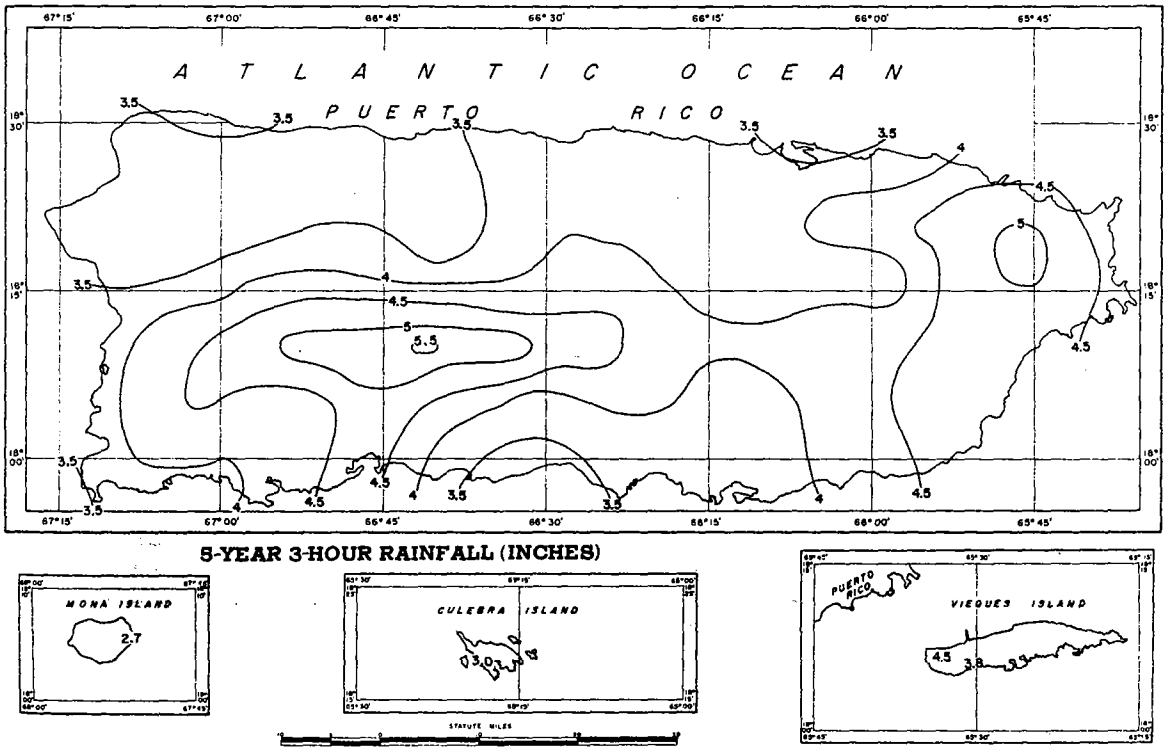

FIGURE 4–30.—5-yr. 3-hr. rainfall for Puerto Rico (in.).

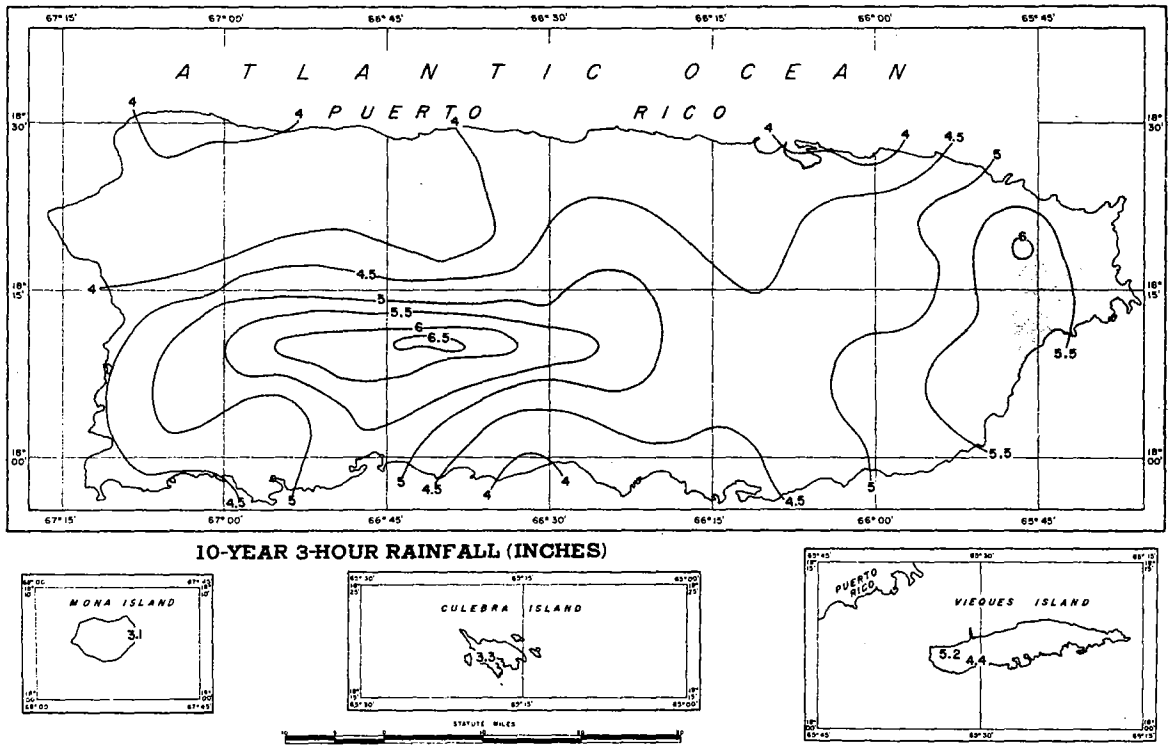

FIGURE 4-31.—10-yr. 3-hr. rainfall for Puerto Rico (in.).

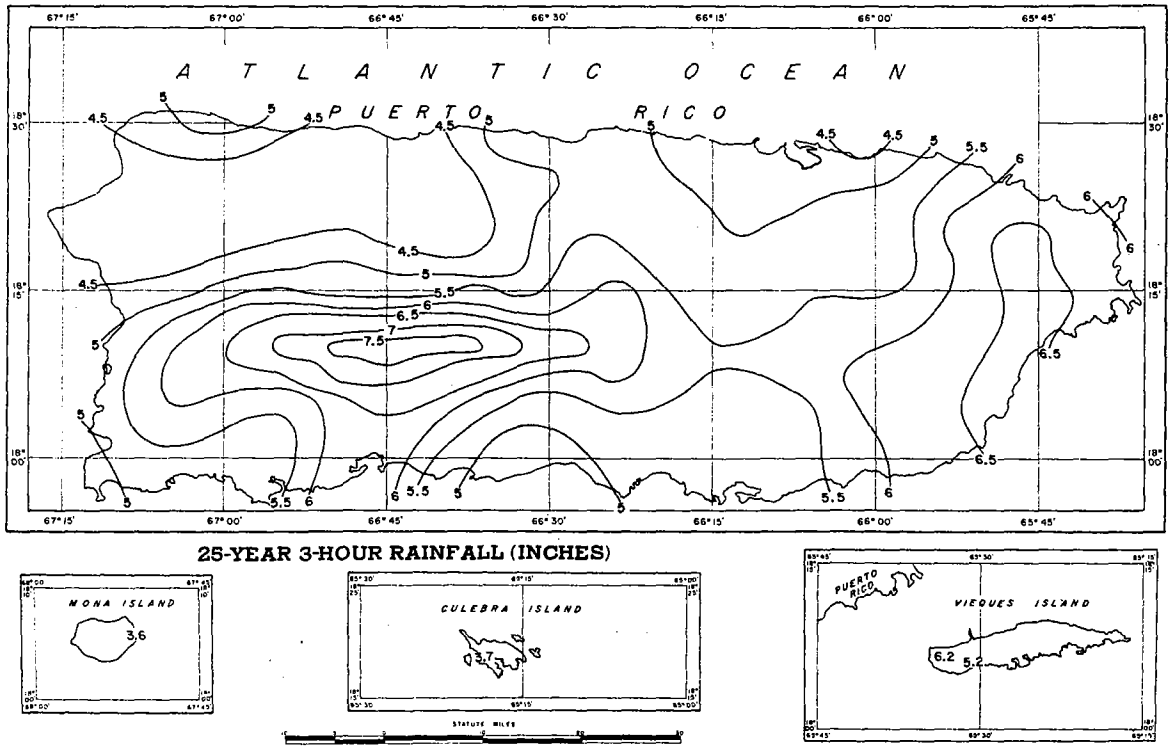

FIGURE 4-32.—25-yr. 3-hr. rainfall for Puerto Rico (in.).

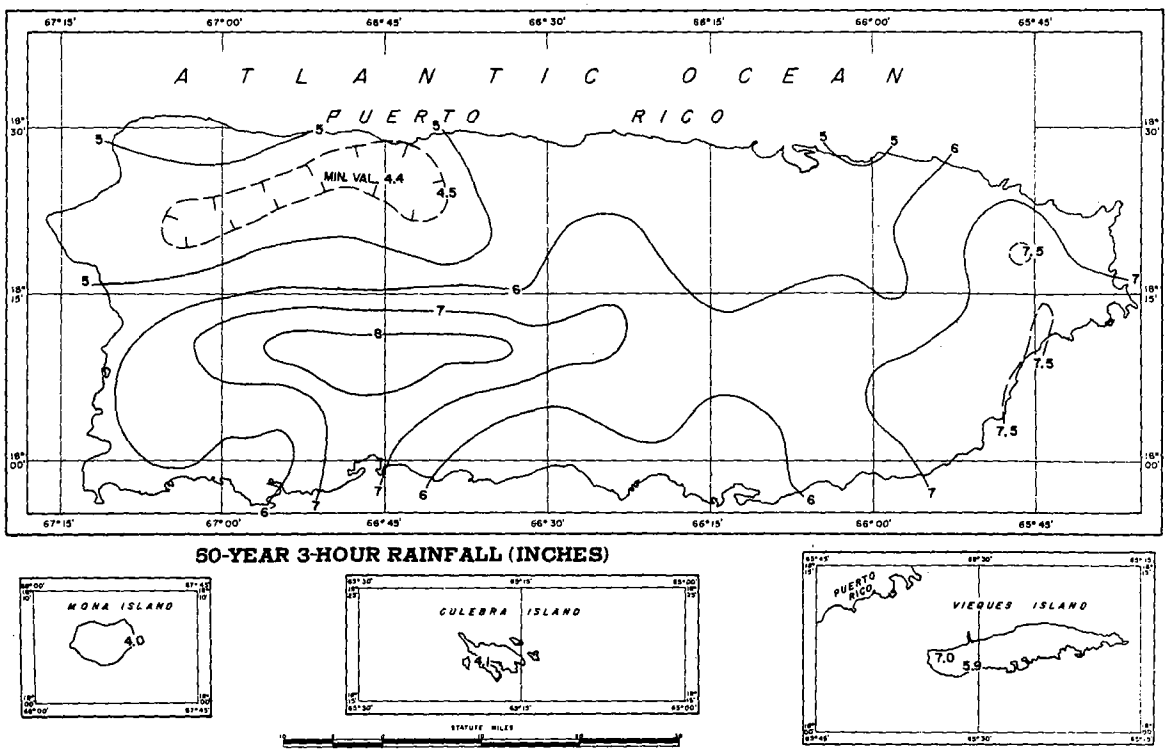

FIGURE 4–33.—50-yr. 3-hr. rainfall for Puerto Rico (in.).

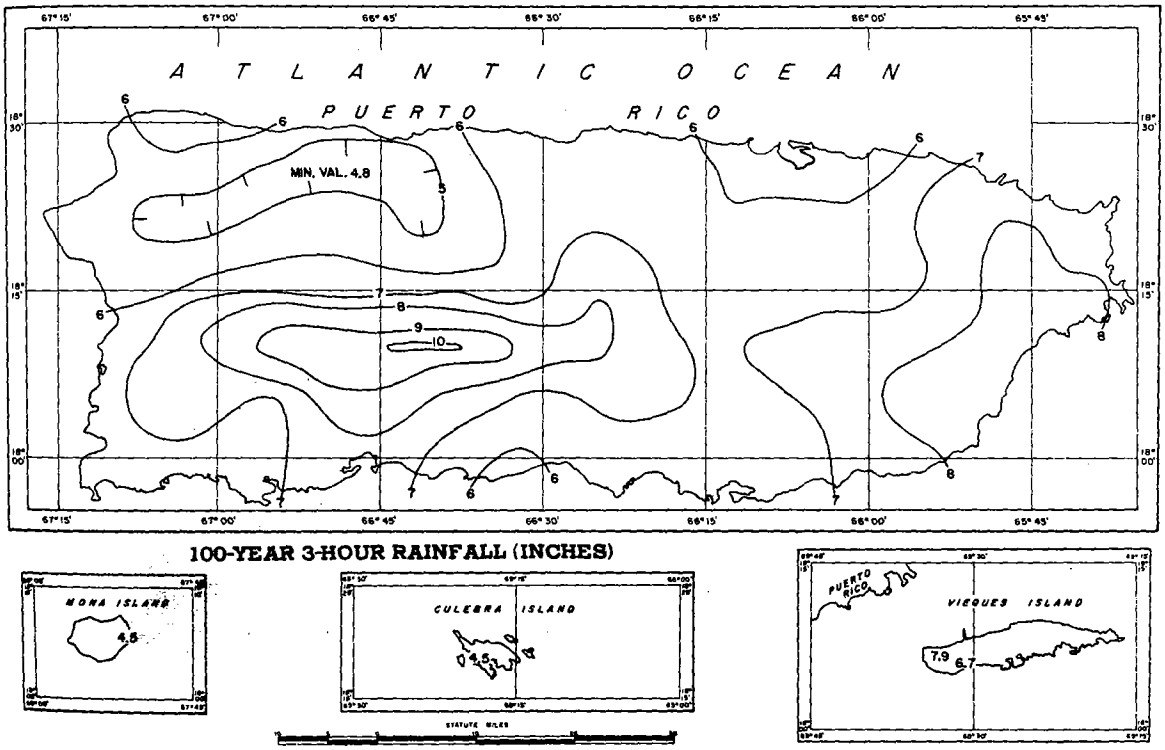

FIGURE 4–34.—100-yr. 3-hr. rainfall for Puerto Rico (in.).

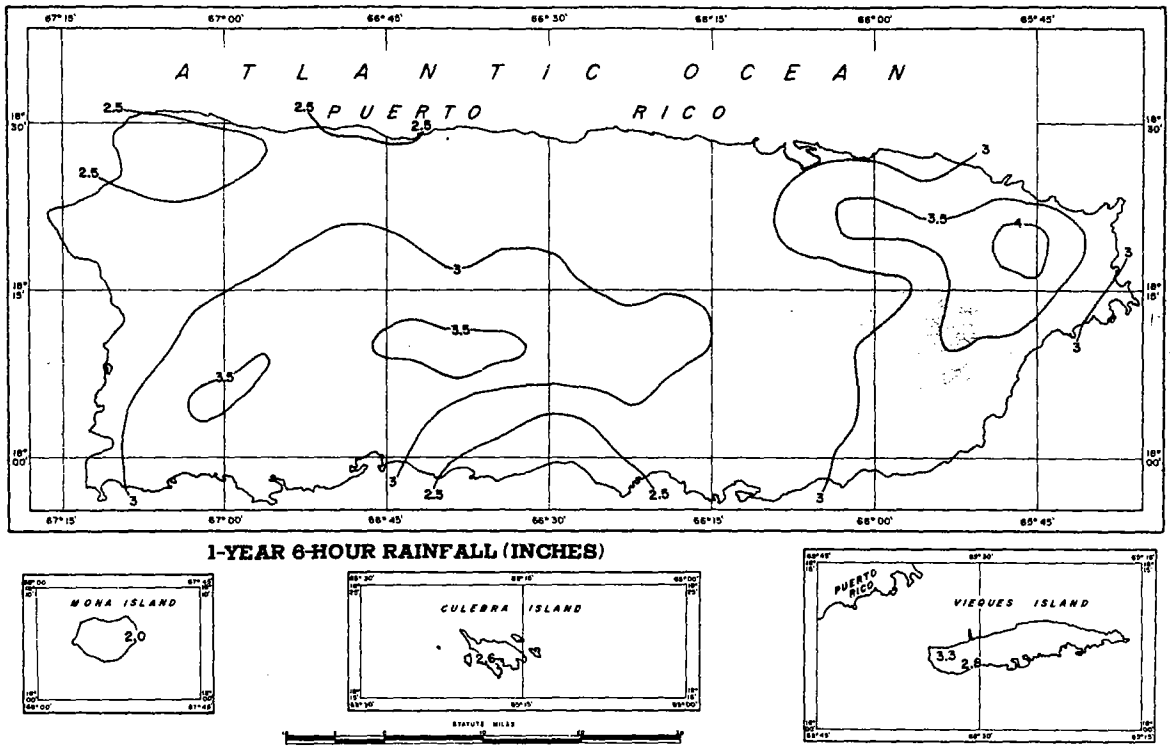

FIGURE 4–35.—1-yr. 6-hr. rainfall for Puerto Rico (in.).

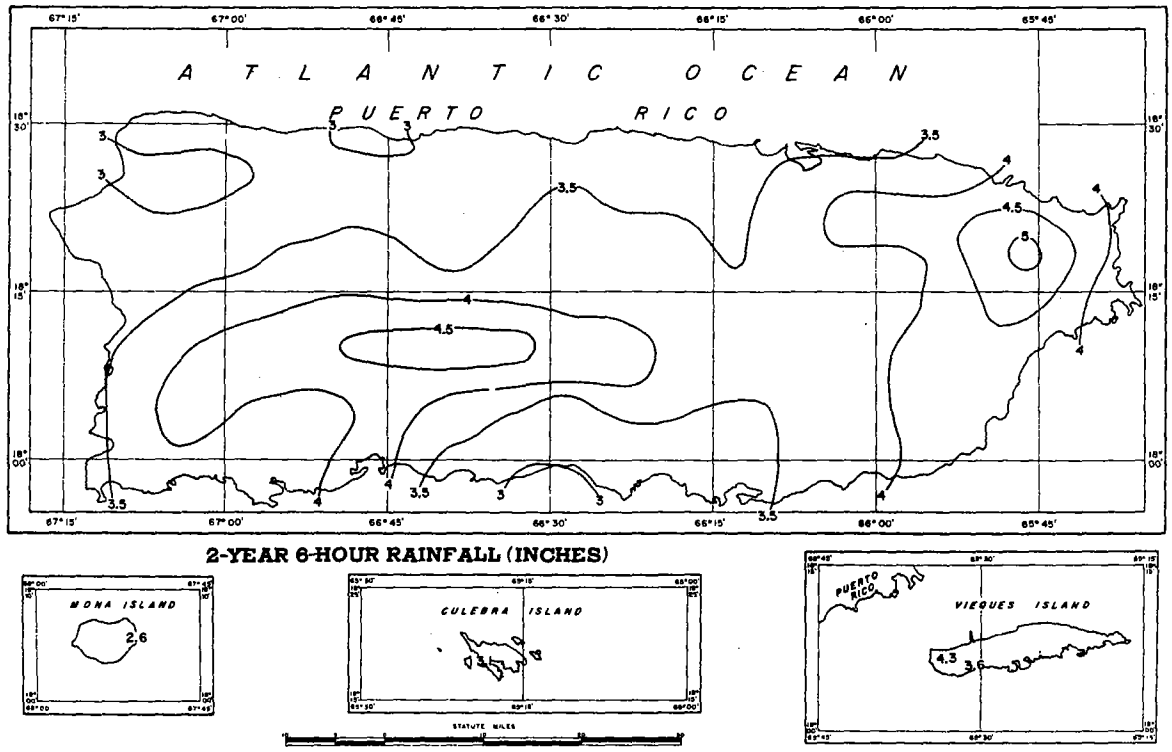

FIGURE 4–36.—2-yr. 6-hr. rainfall for Puerto Rico (in.).

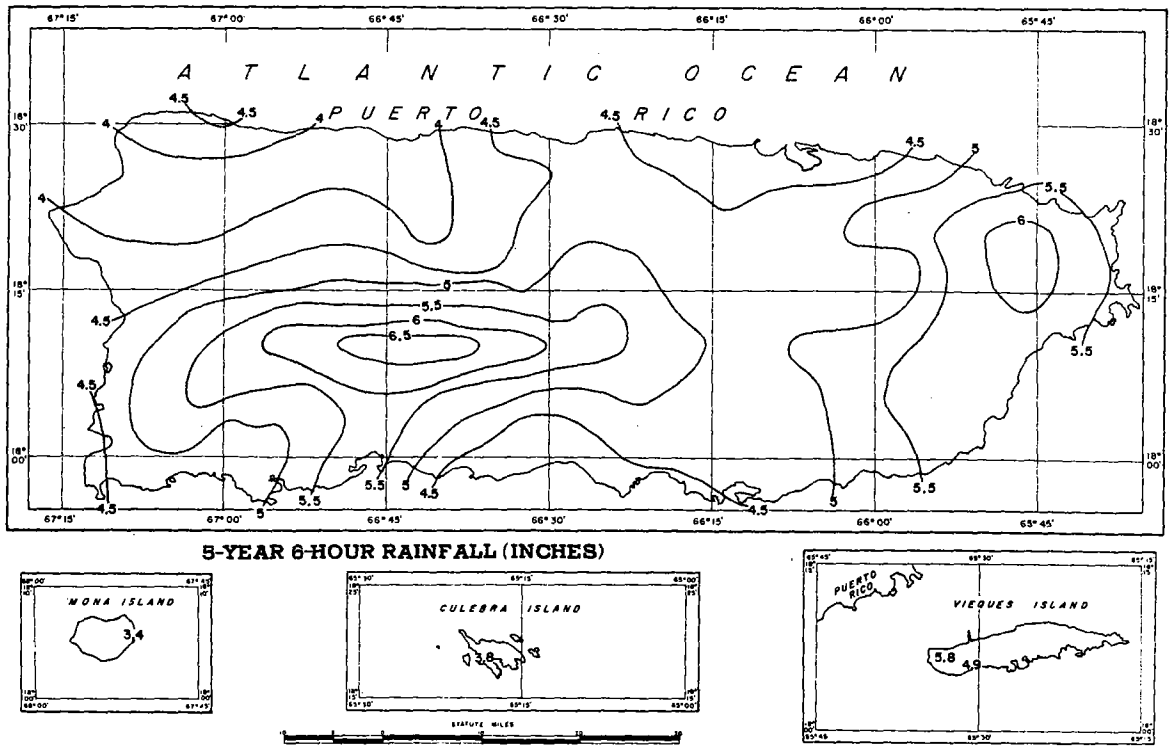

FIGURE 4–37.—5-yr. 6-hr. rainfall for Puerto Rico (in.).

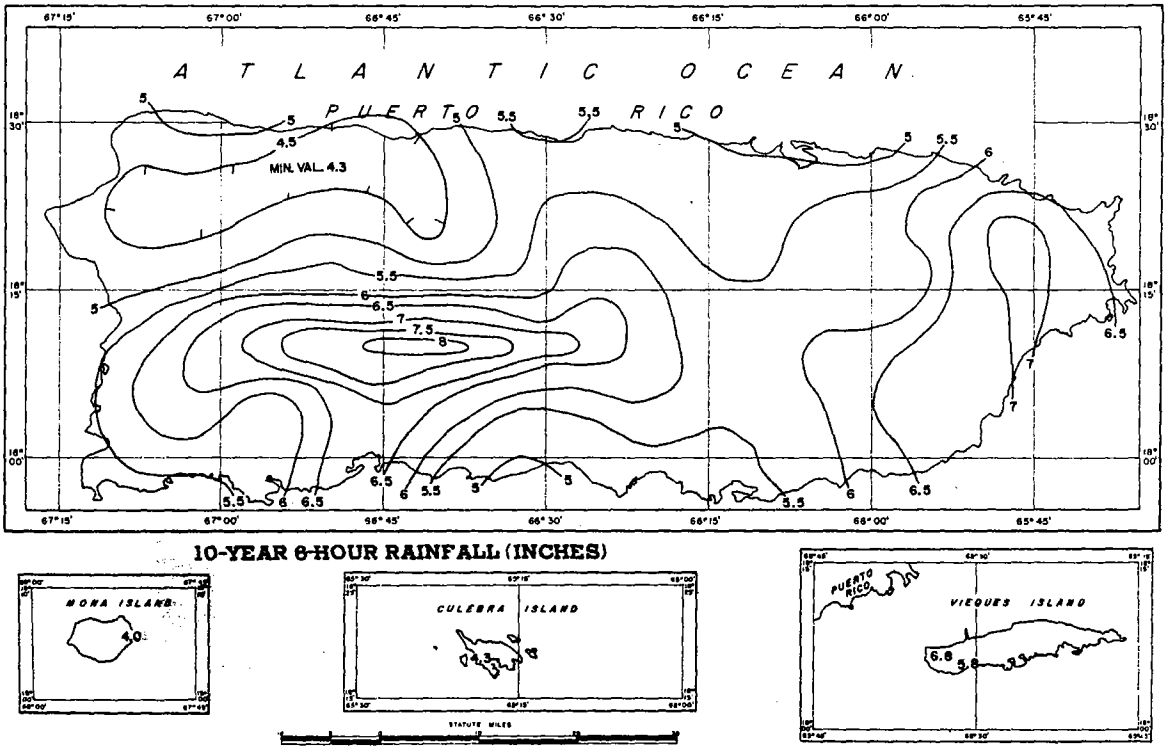

FIGURE 4–38.—10-yr. 6-hr. rainfall for Puerto Rico (in.).

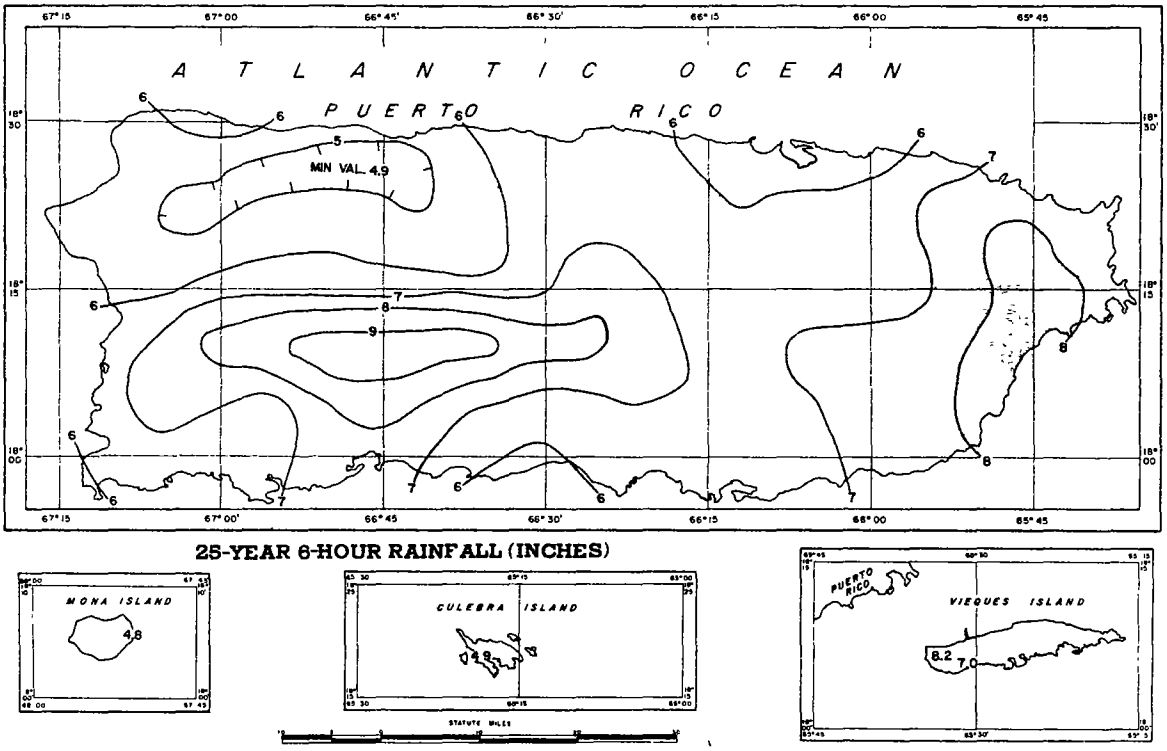

FIGURE 4-39.—25-yr. 6-hr. rainfall for Puerto Rico (in.).

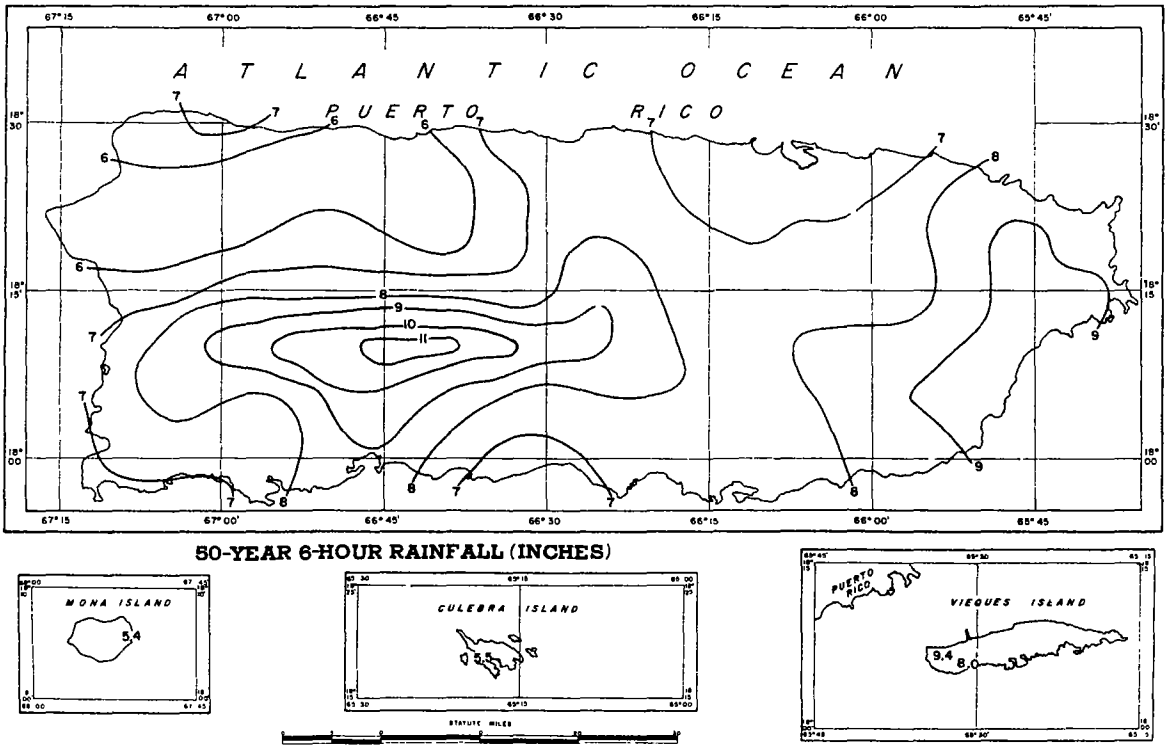

FIGURE 4-40.—50-yr 6-hr rainfall for Puerto Rico (in.).

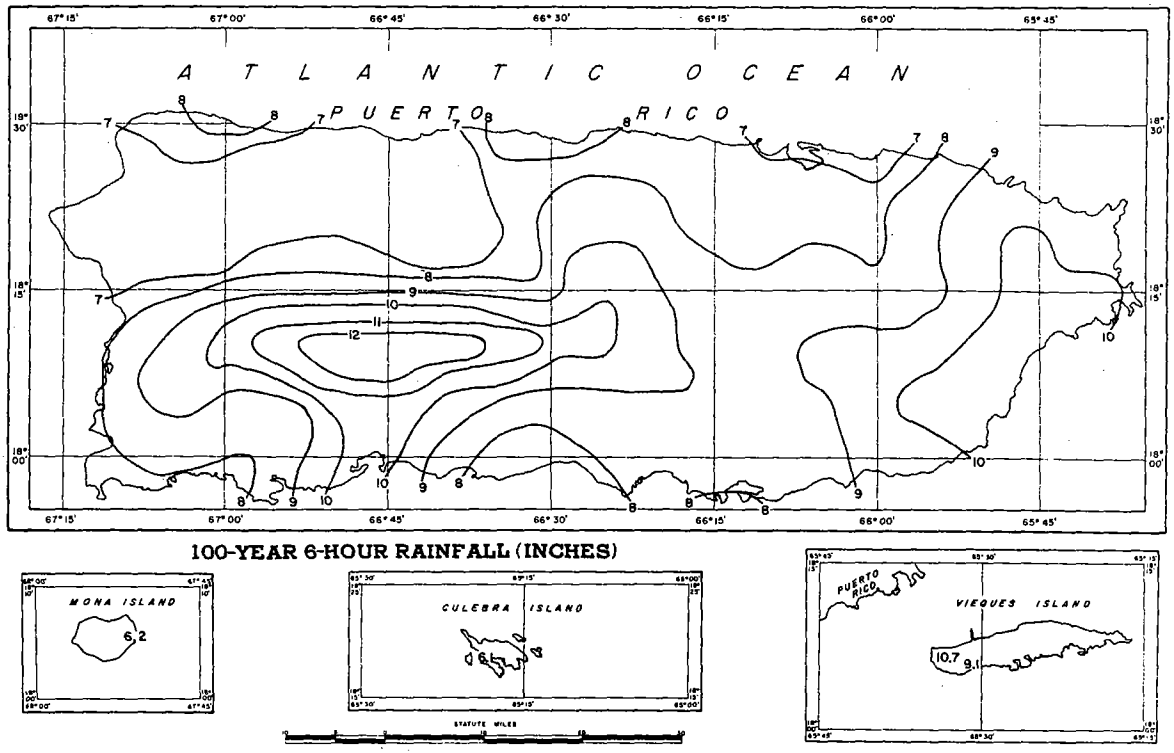

FIGURE 4–41.—100-yr. 6-hr. rainfall for Puerto Rico (in.).

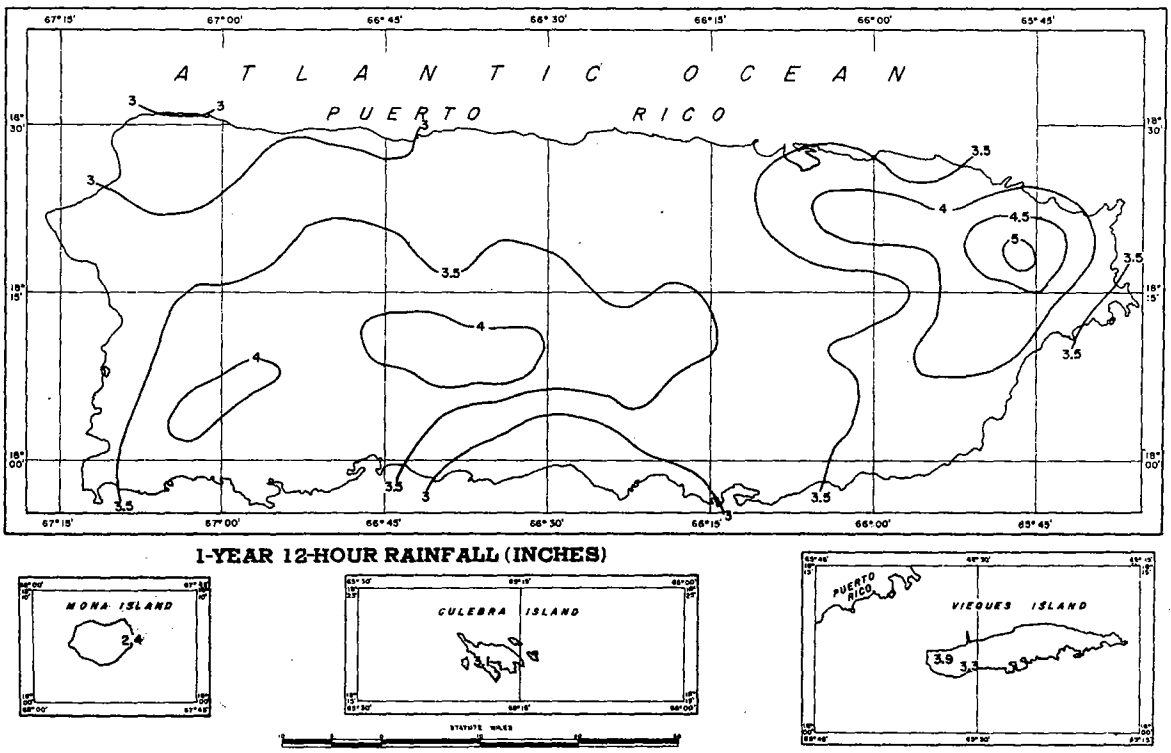

FIGURE 4–42.—1-yr. 12-hr. rainfall for Puerto Rico (in.)

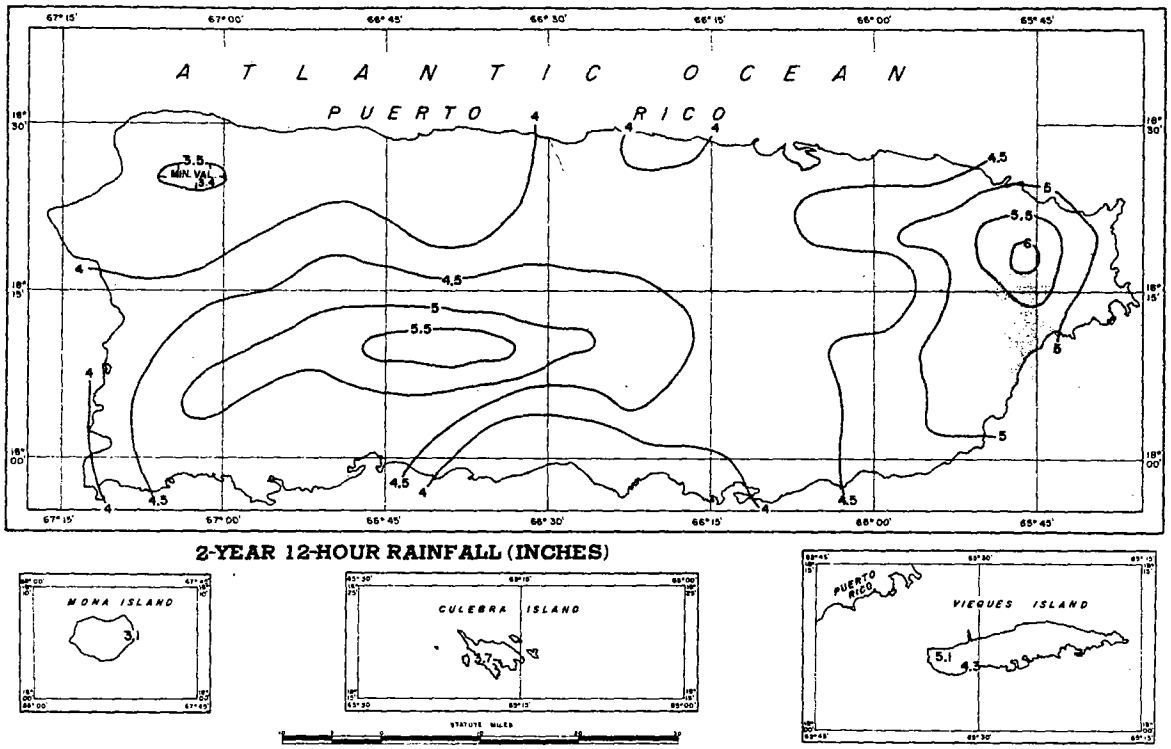

FIGURE 4-43.—2-yr. 12-hr. rainfall for Puerto Rico (in.).

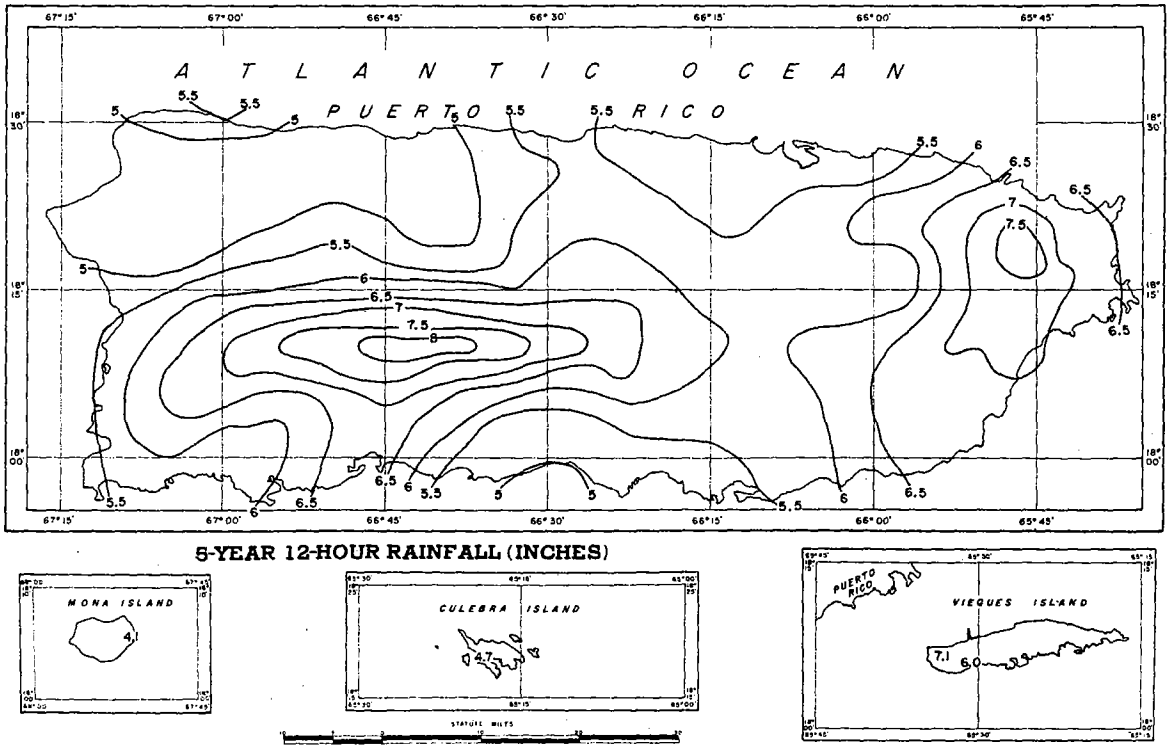

FIGURE 4-44.—5-yr. 12-hr. rainfall for Puerto Rico (in.).

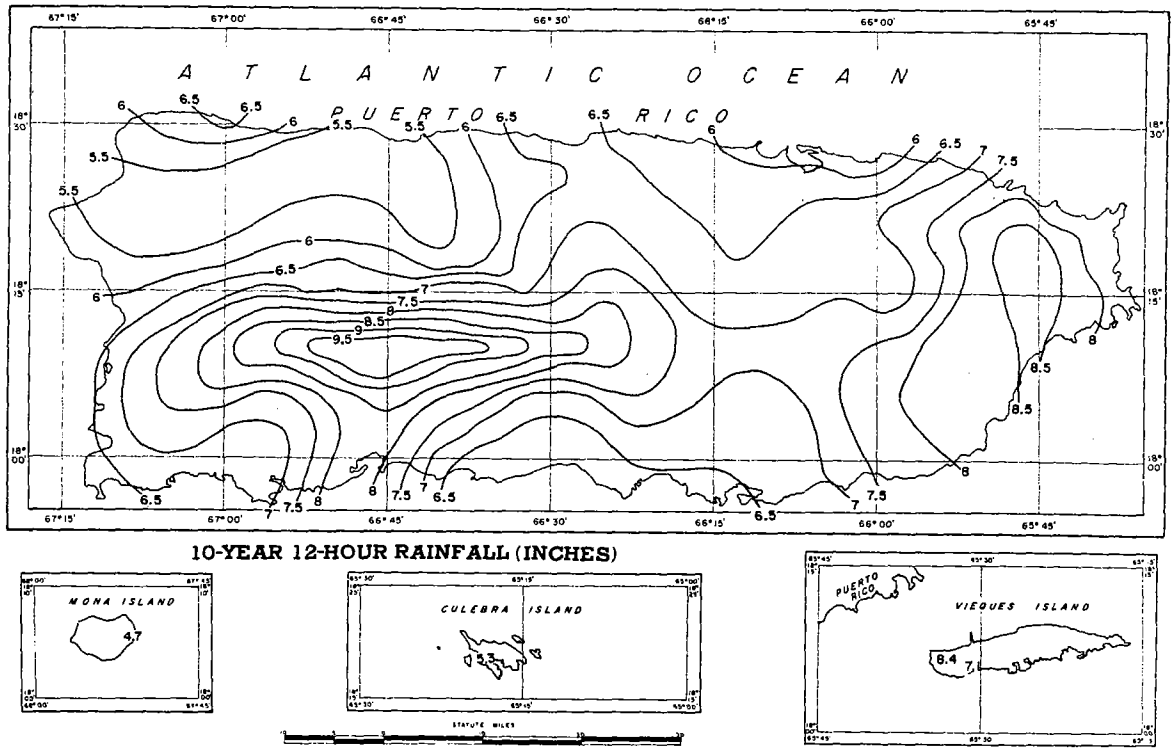

FIGURE 4–45.—10-yr. 12-hr. rainfall for Puerto Rico (in.).

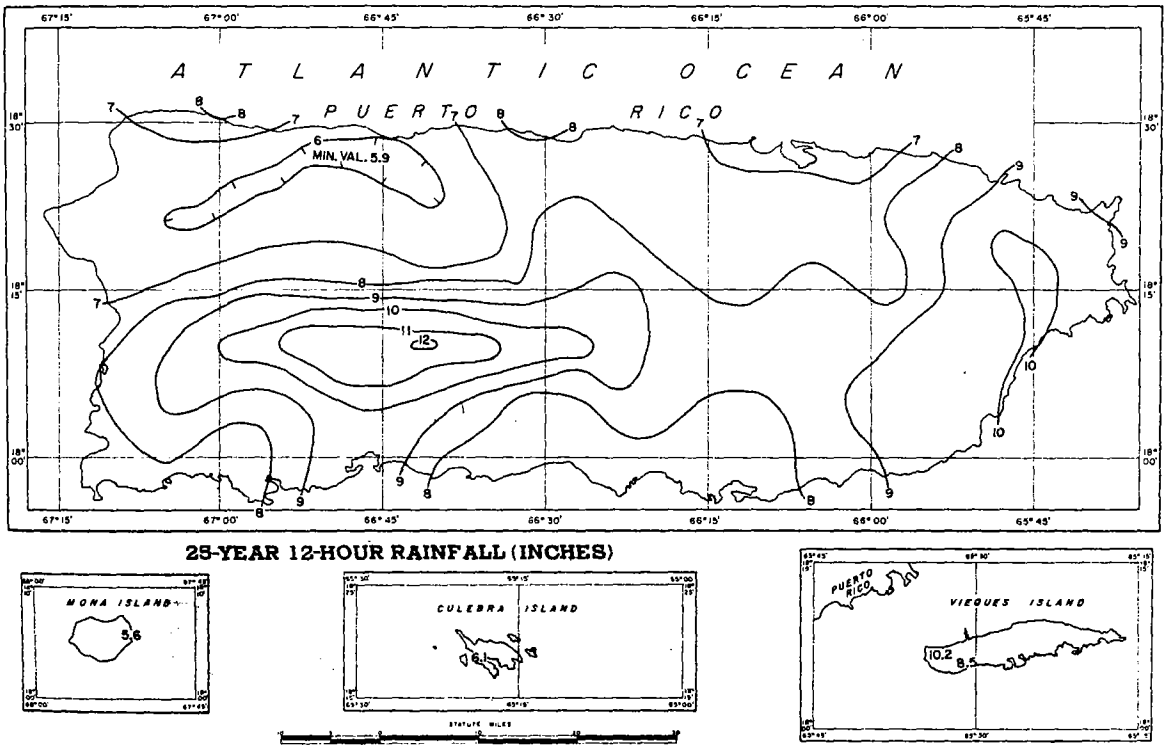

FIGURE 4–46.—25-yr. 12-hr. rainfall for Puerto Rico (in.).

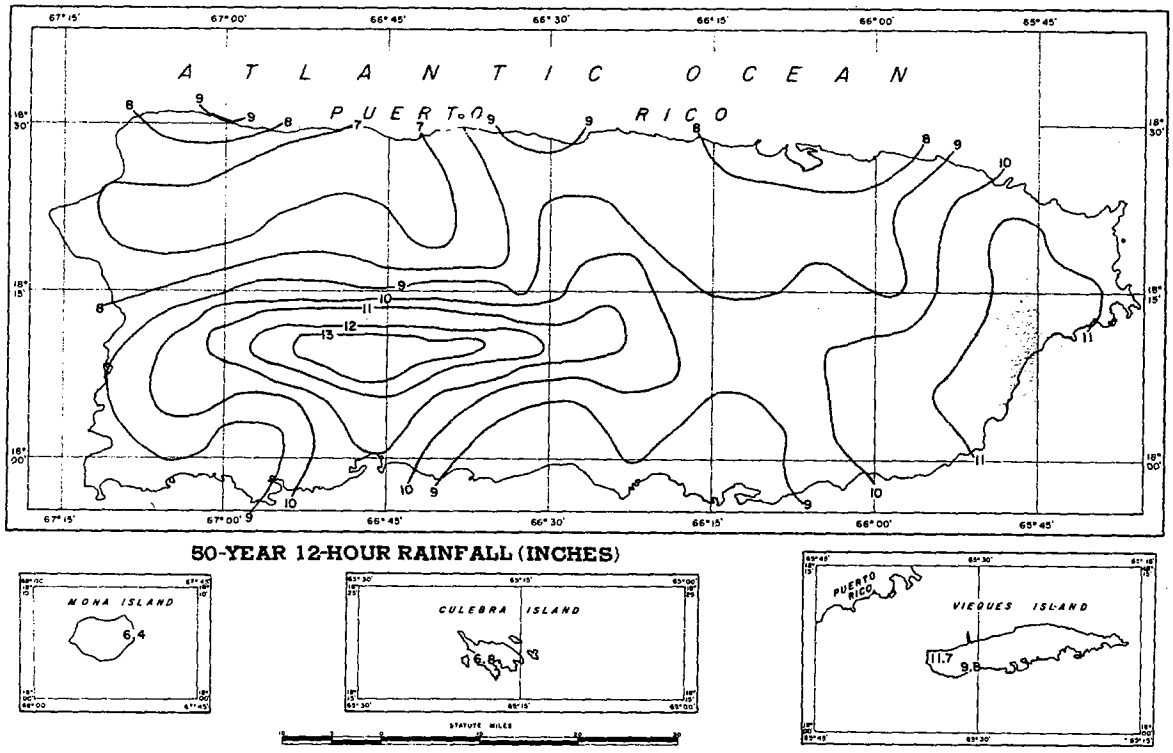

FIGURE 4–47.—50-yr. 12-hr. rainfall for Puerto Rico (in.).

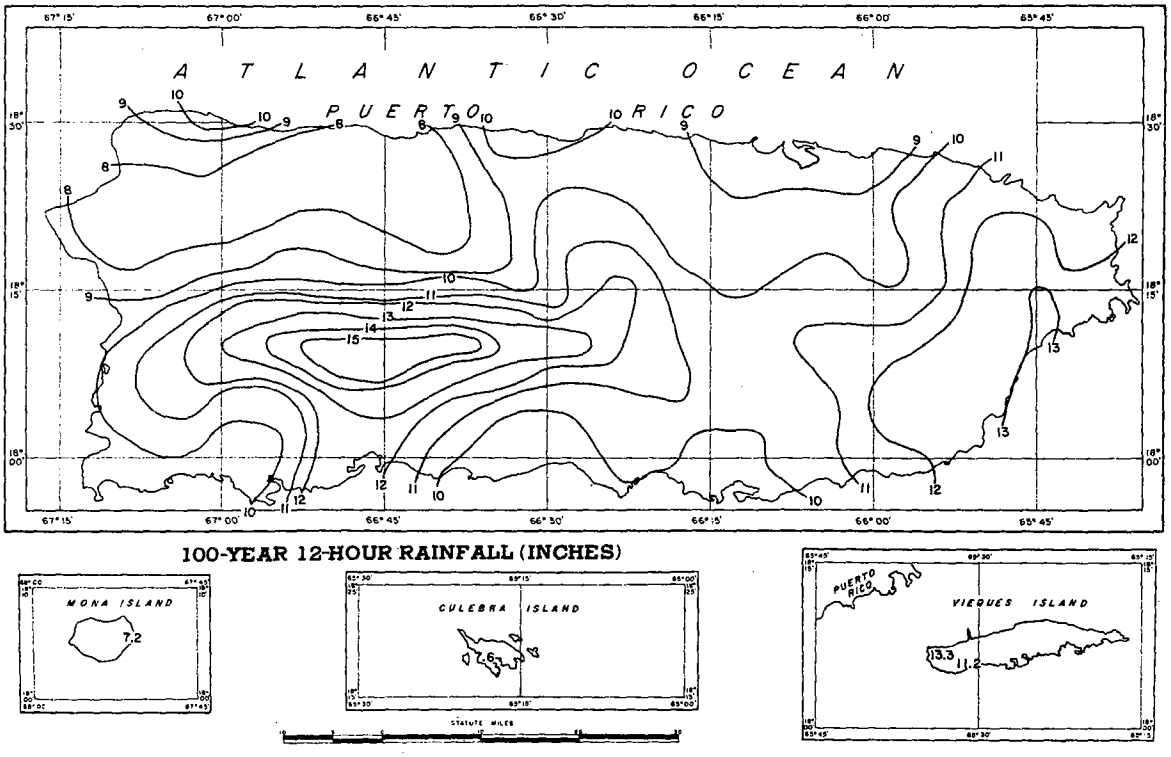

FIGURE 4–48.—100-yr. 12-hr. rainfall for Puerto Rico (in.).

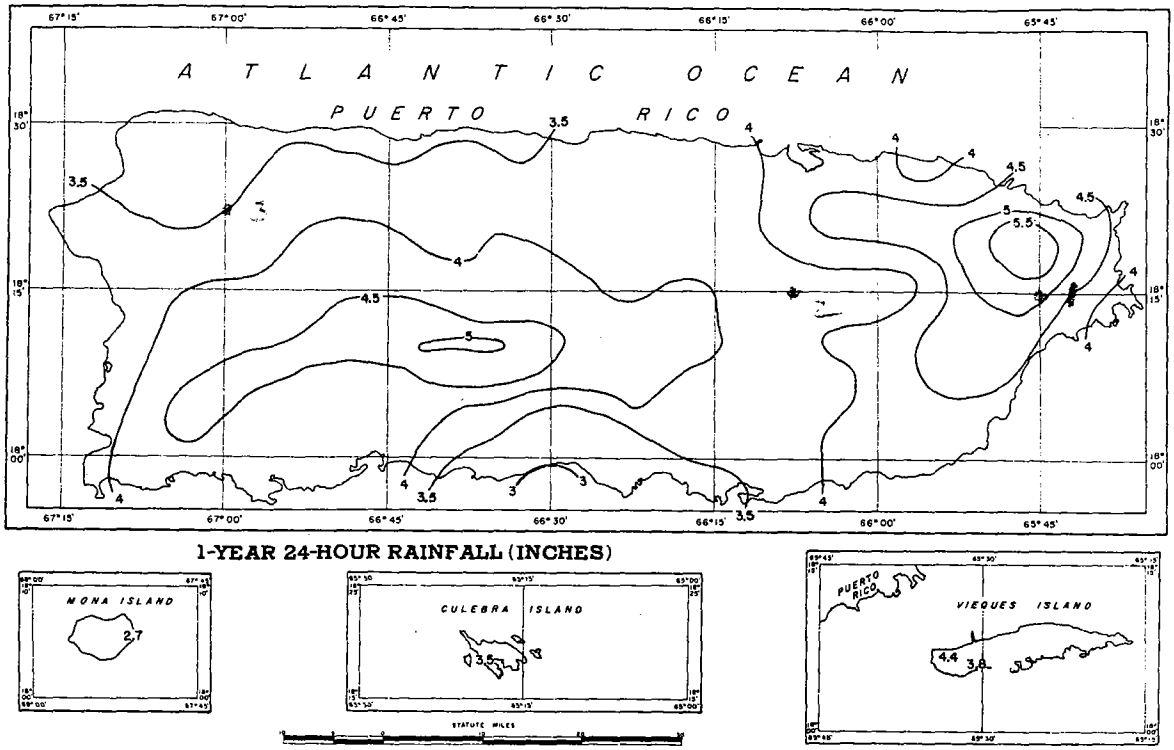

FIGURE 4–49.—1-yr. 24-hr. rainfall for Puerto Rico (in.).

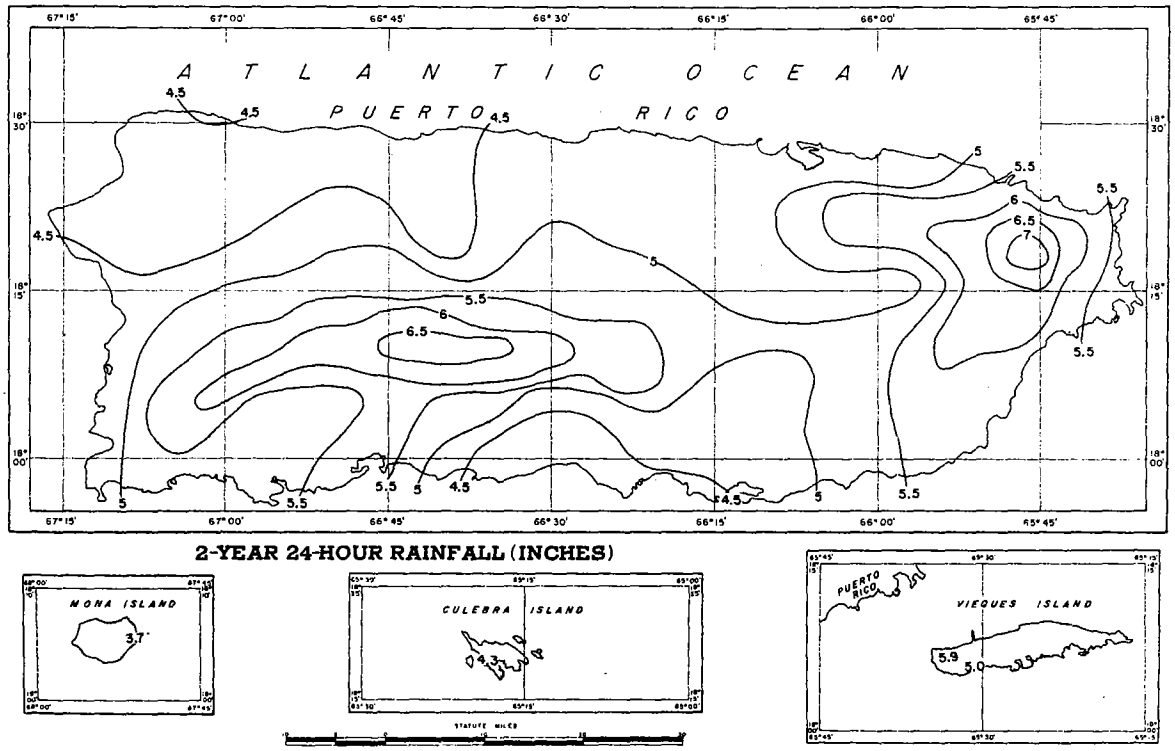

FIGURE 4–50.—2-yr. 24-hr. rainfall for Puerto Rico (in.).

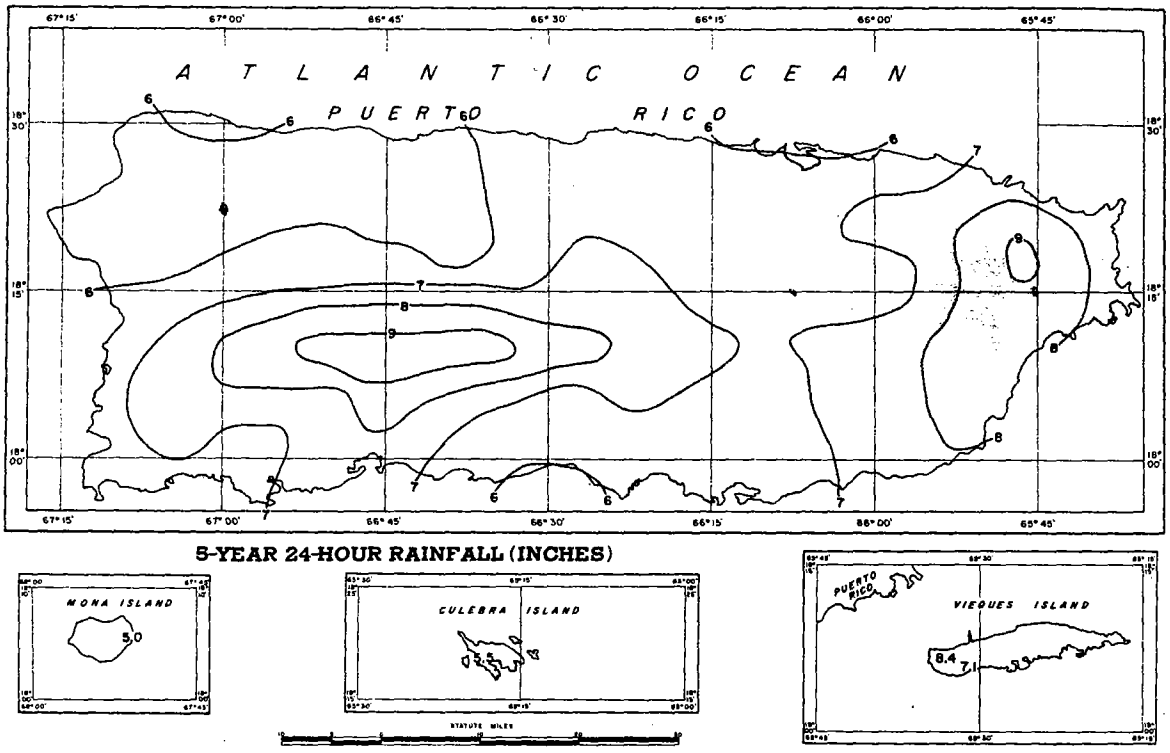

FIGURE 4–51.—5-yr. 24-hr. rainfall for Puerto Rico (in.).

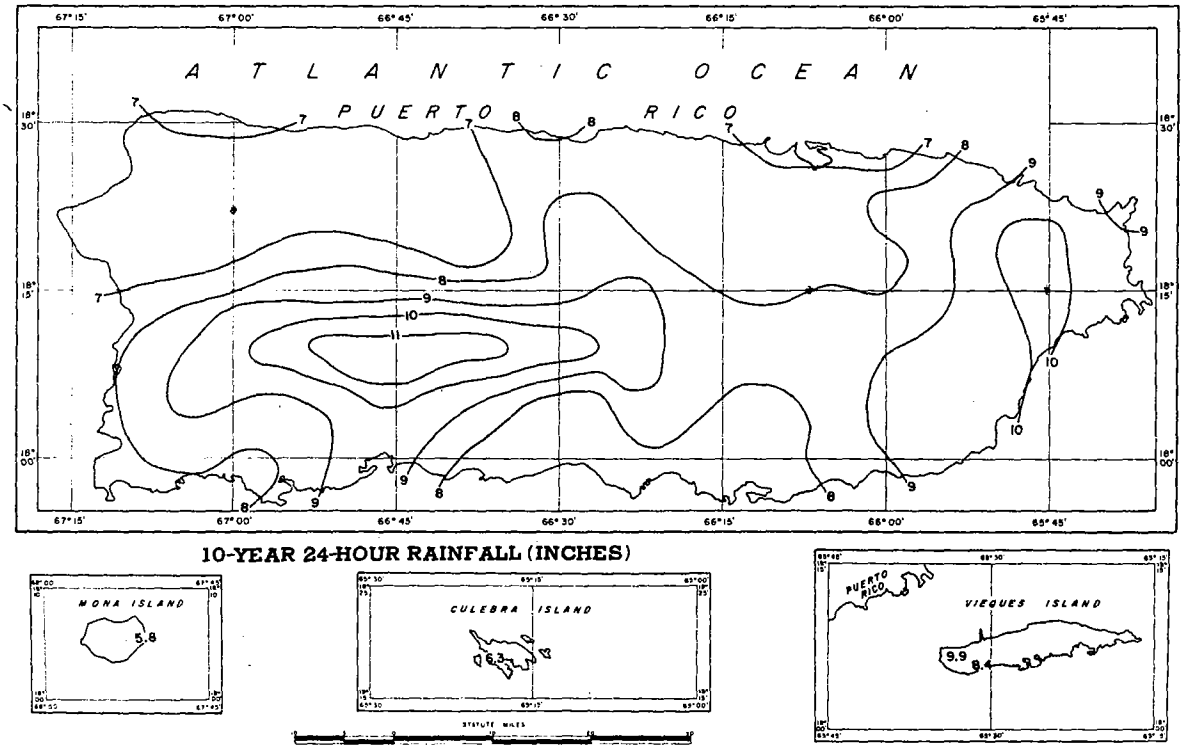

FIGURE 4–52.—10-yr. 24-hr. rainfall for Puerto Rico (in.).

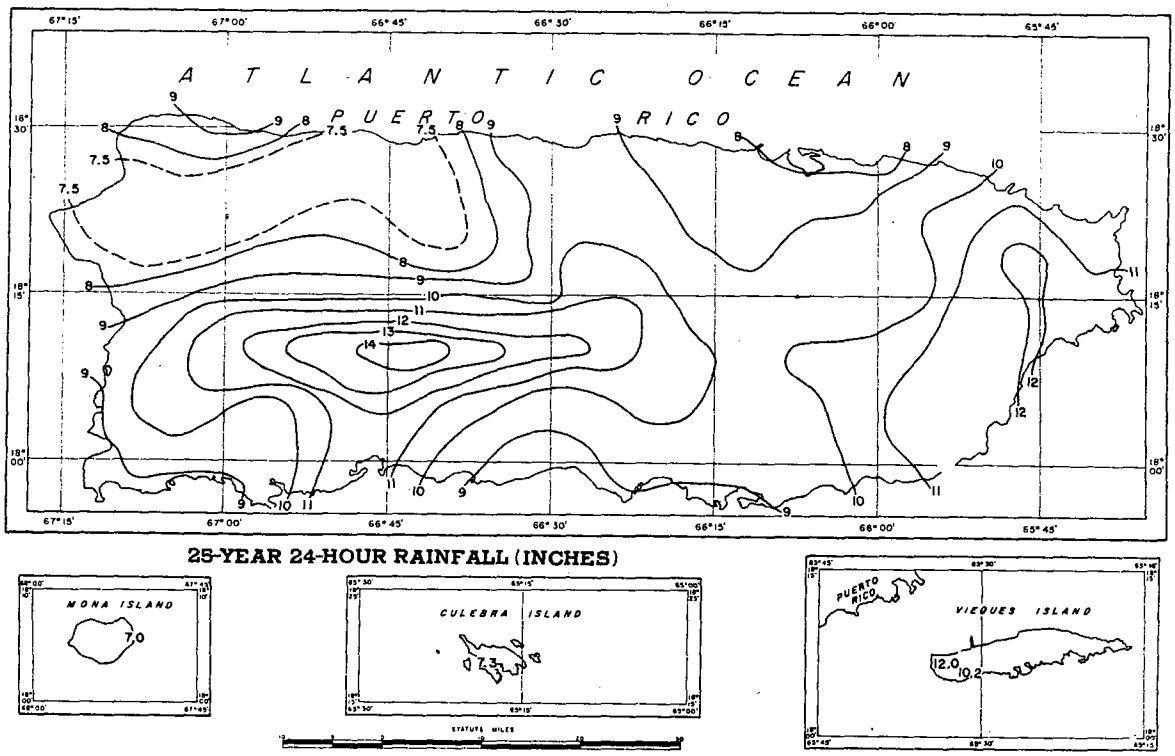

FIGURE 4–53.—25-yr. 24-hr. rainfall for Puerto Rico (in.).

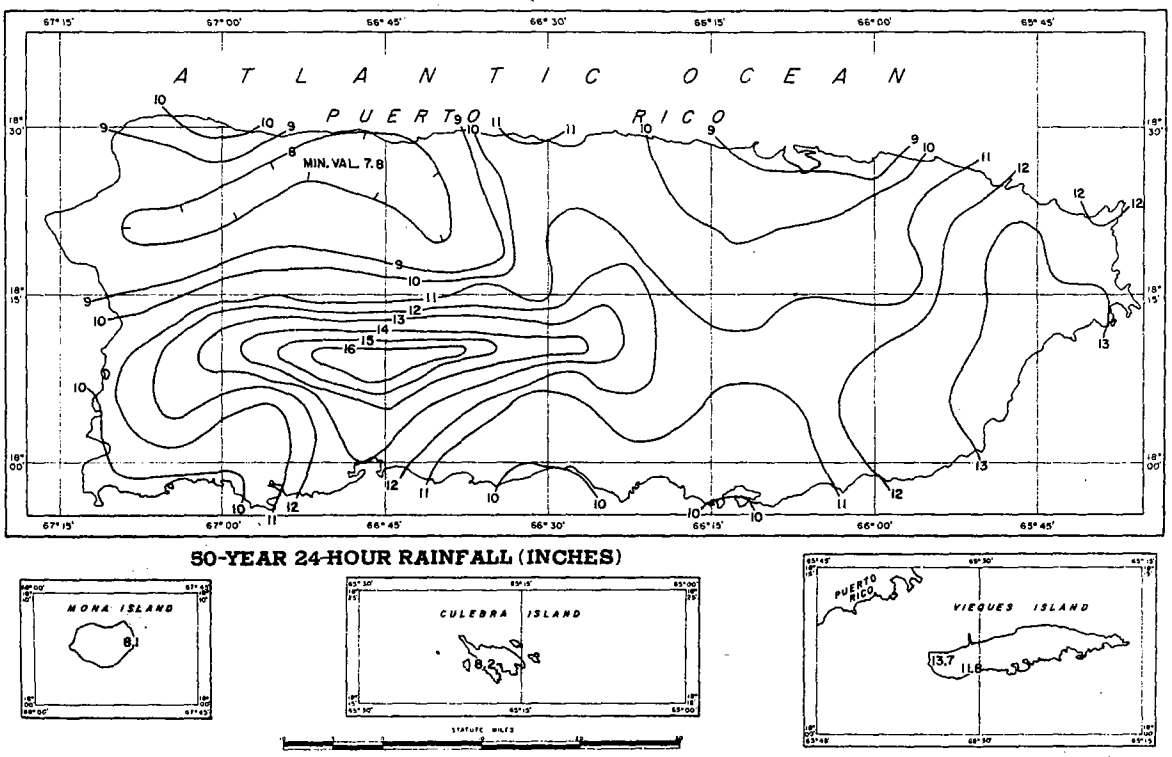

FIGURE 4–54.—50-yr. 24-hr. rainfall for Puerto Rico (in.).

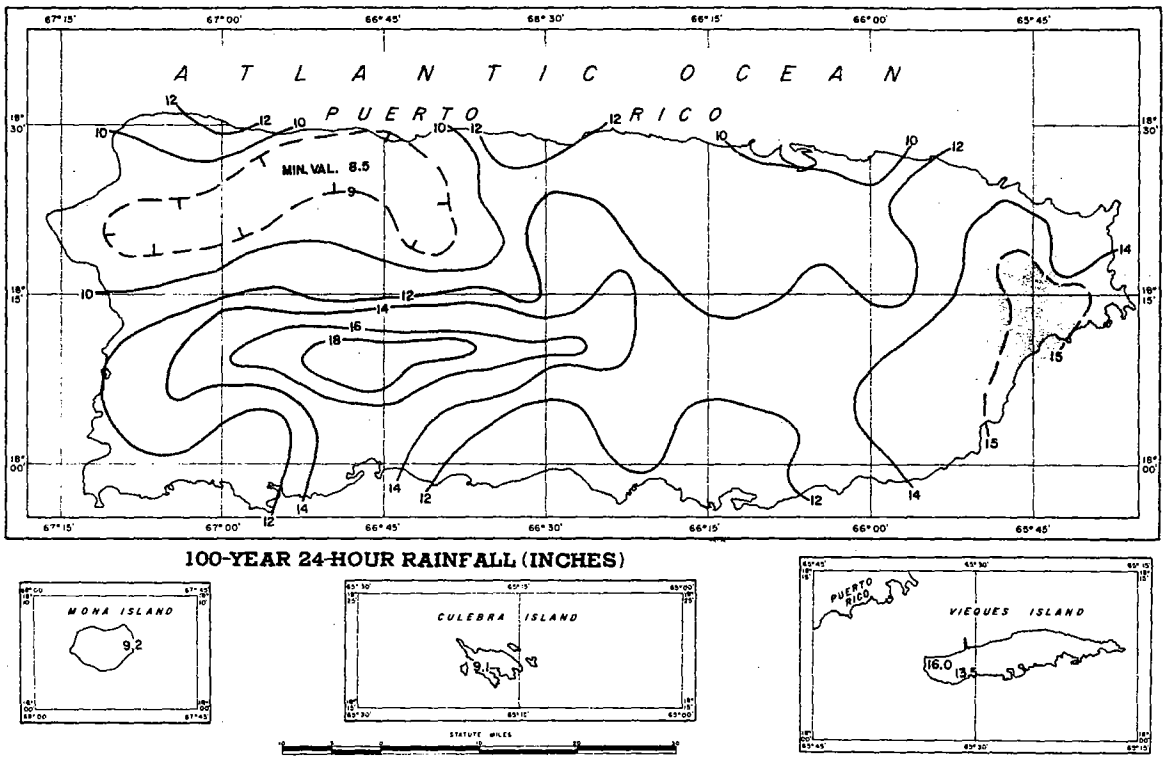

FIGURE 4-55.—100-yr. 24-hr. rainfall for Puerto Rico (in.)

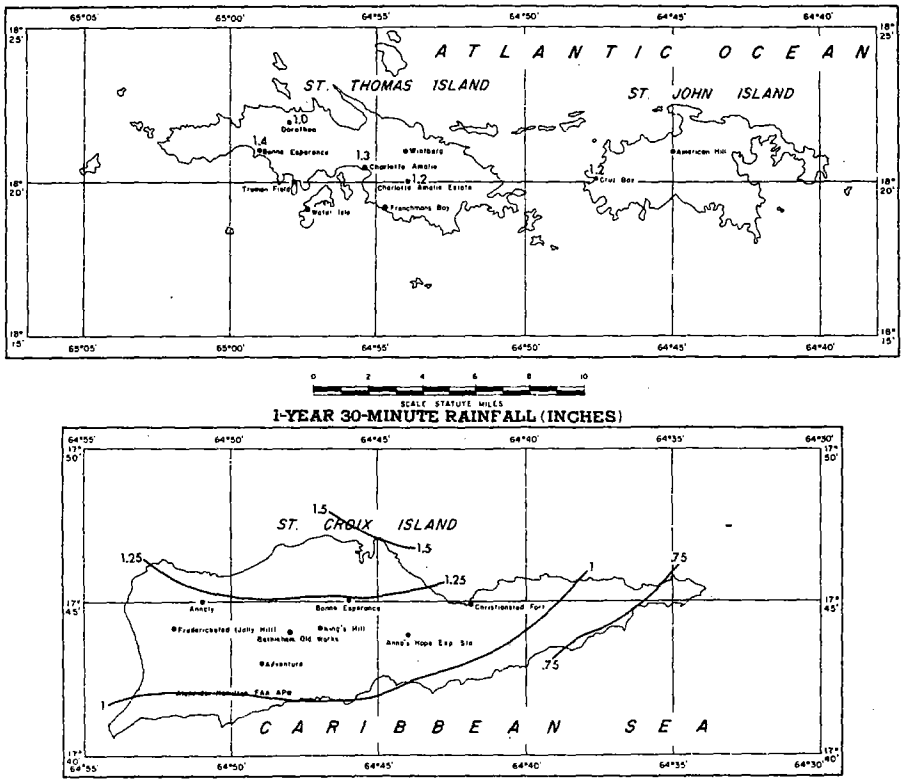

FIGURE 4-56.—1-yr. 30-min. rainfall for Virgin Islands (in.).

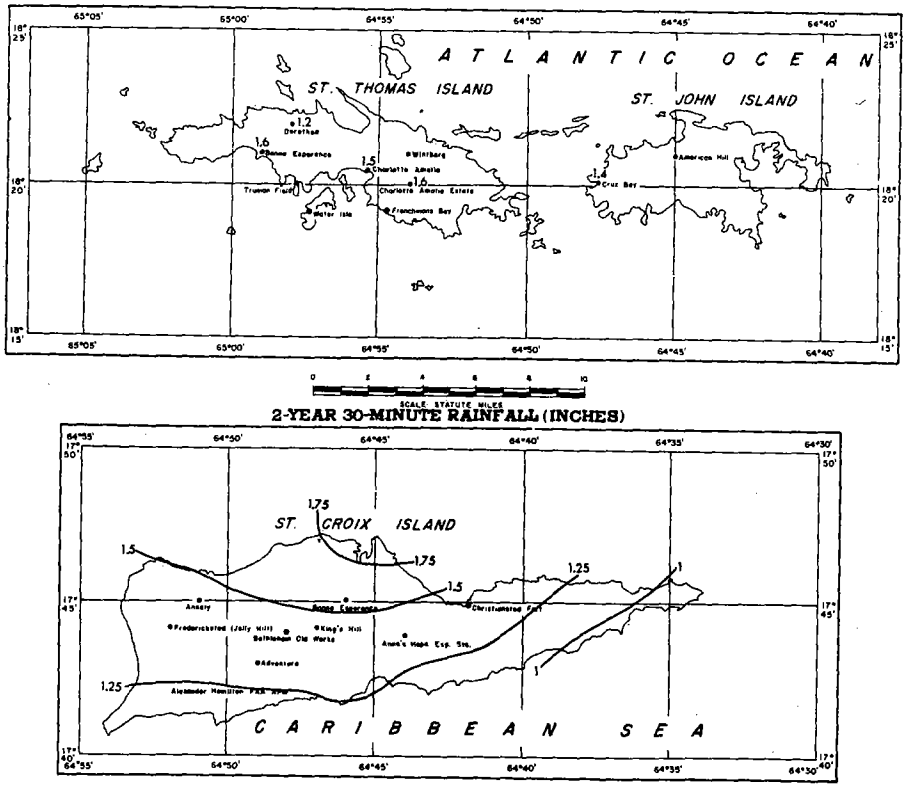

FIGURE 4–57.—2-yr. 30-min. rainfall for Virgin Islands (in.).

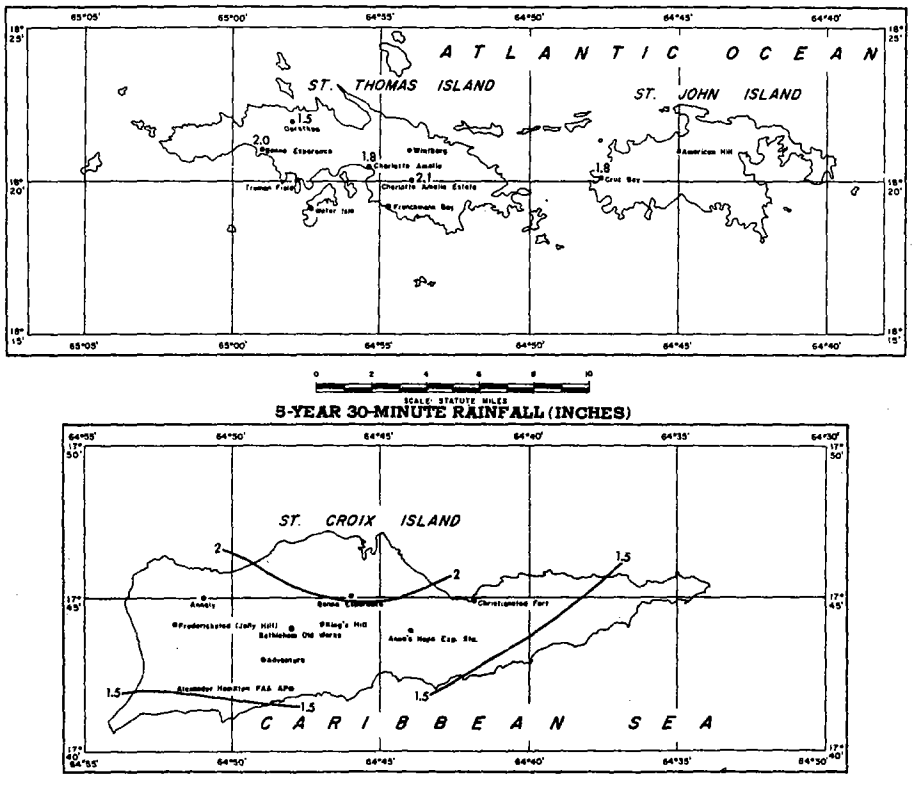

FIGURE 4–58.—5-yr. 30-min. rainfall for Virgin Islands (in.).

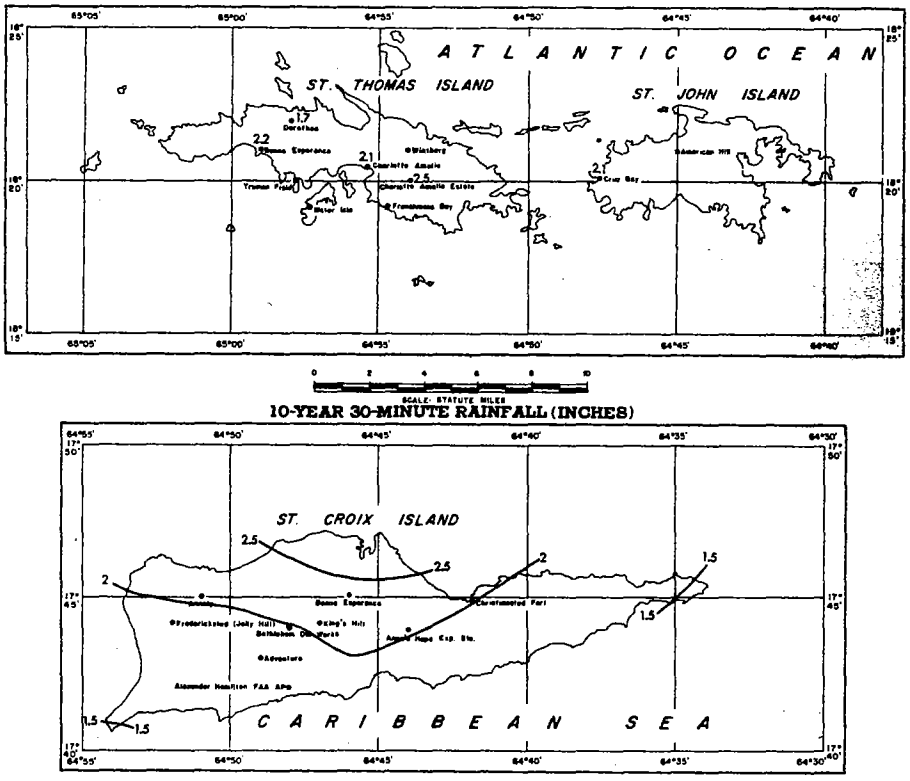

FIGURE 4–59.—10-yr. 30-min. rainfall for Virgin Islands (in.).

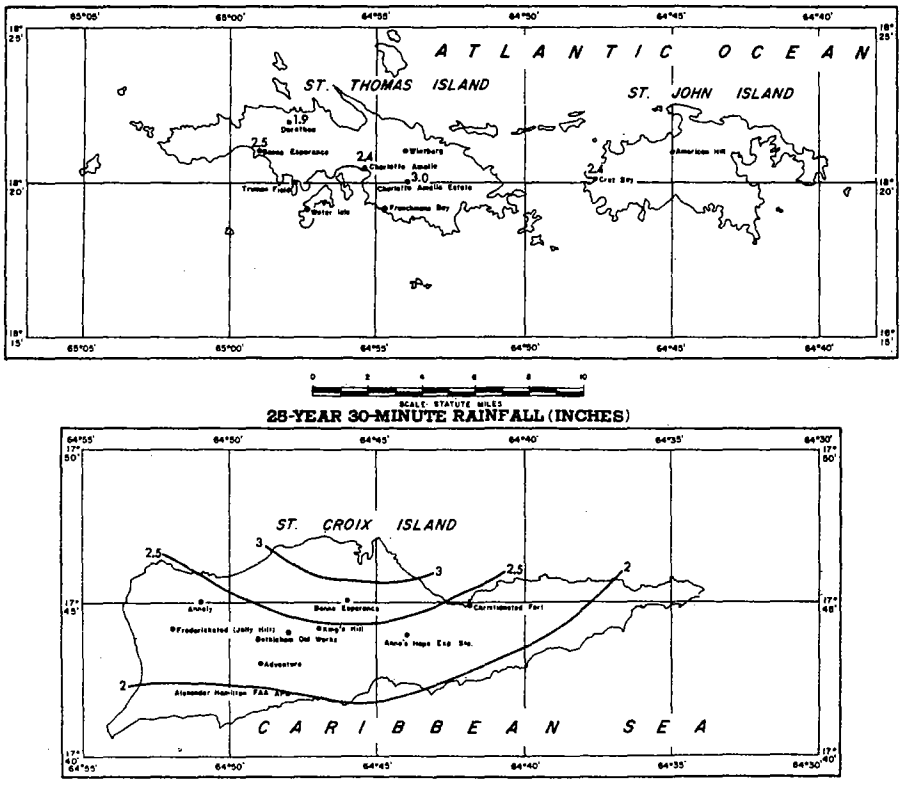

FIGURE 4–60.—25-yr. 30-min. rainfall for Virgin Islands (in.).

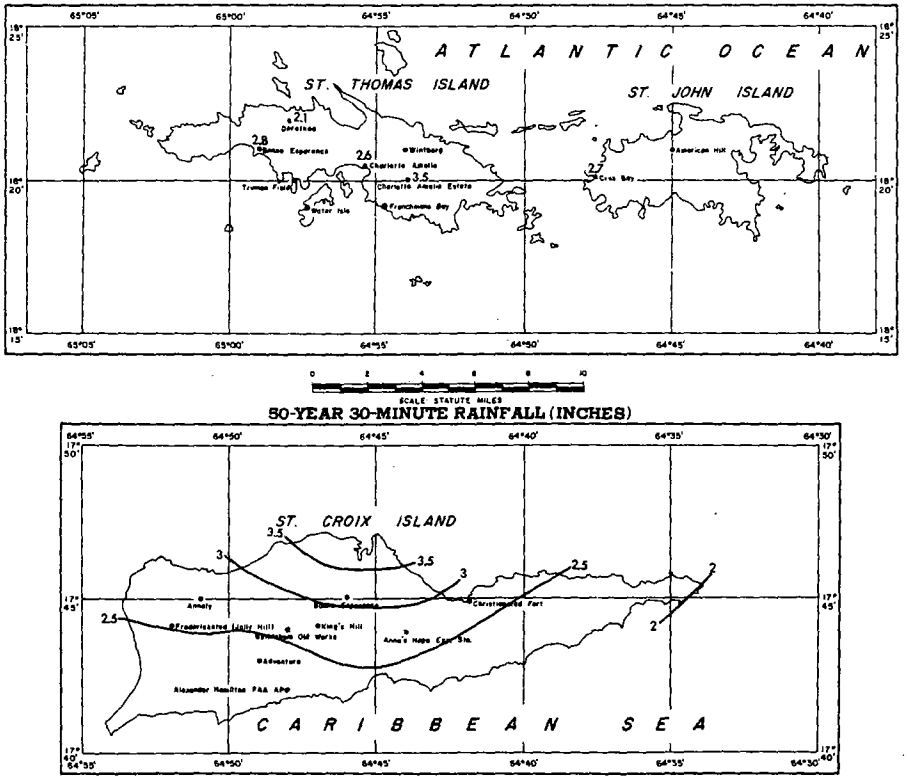

FIGURE 4–61.—50-yr. 30-min. rainfall for Virgin Islands (in.).

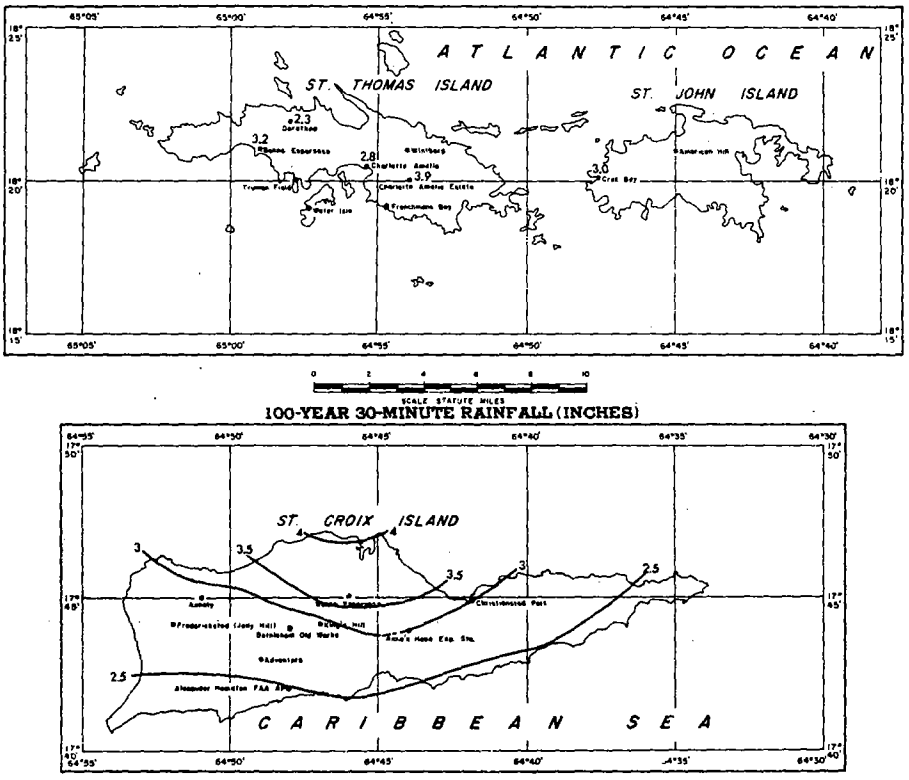

FIGURE 4–62.—100-yr. 30-min. rainfall for Virgin Islands (in.).

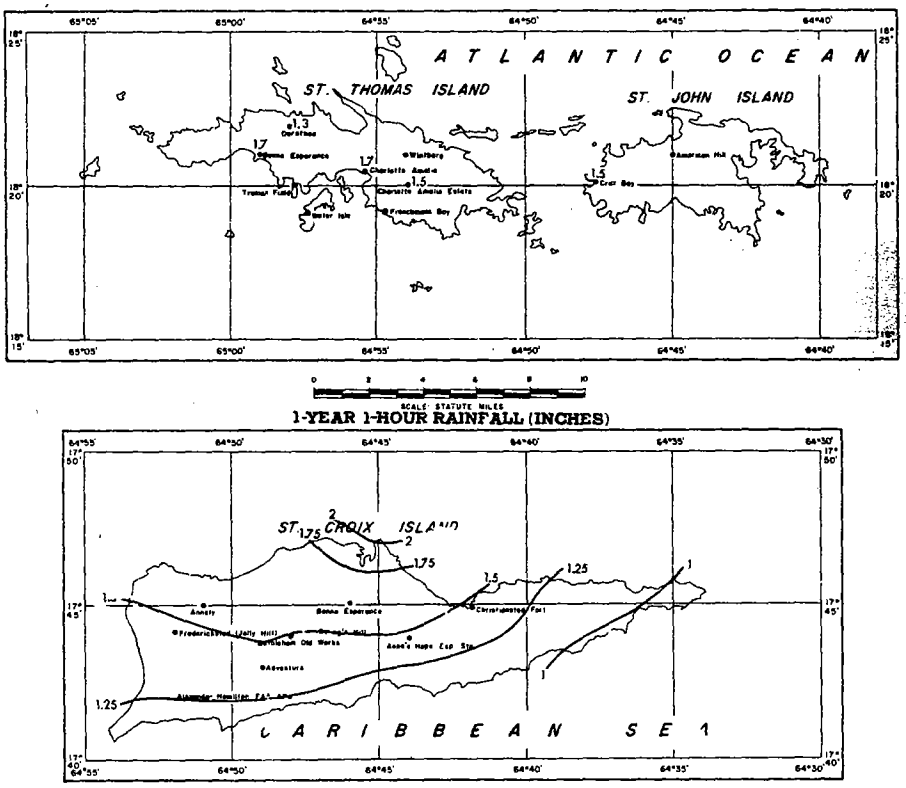

FIGURE 4–63.—1-yr. 1-hr. rainfall for Virgin Islands (in.).

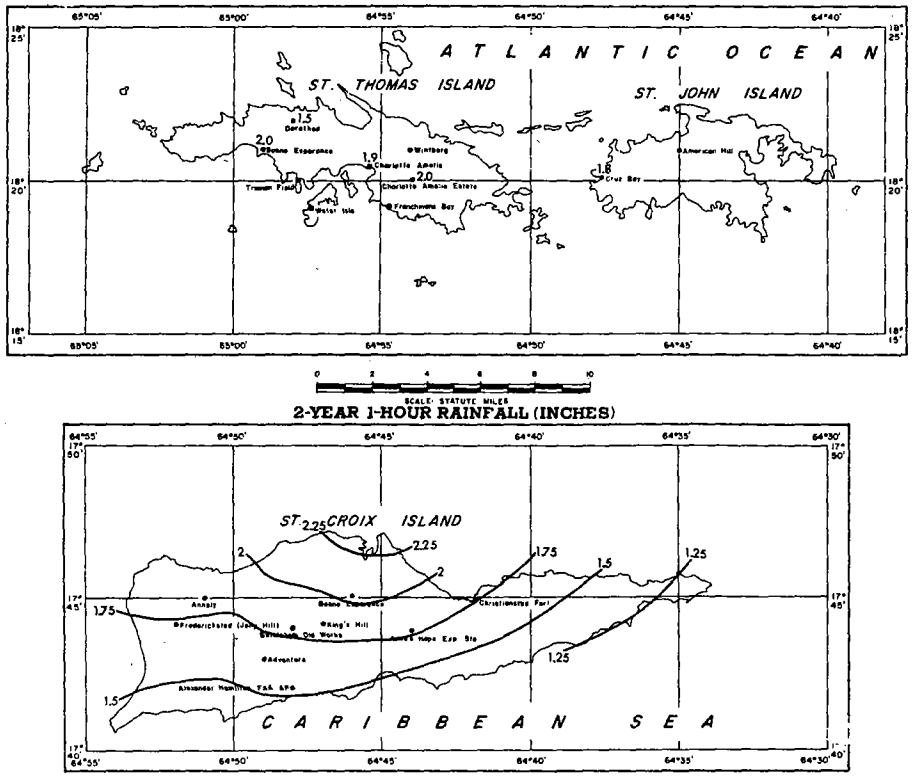

FIGURE 4–64.—2-yr. 1-hr. rainfall for Virgin Islands (in.).

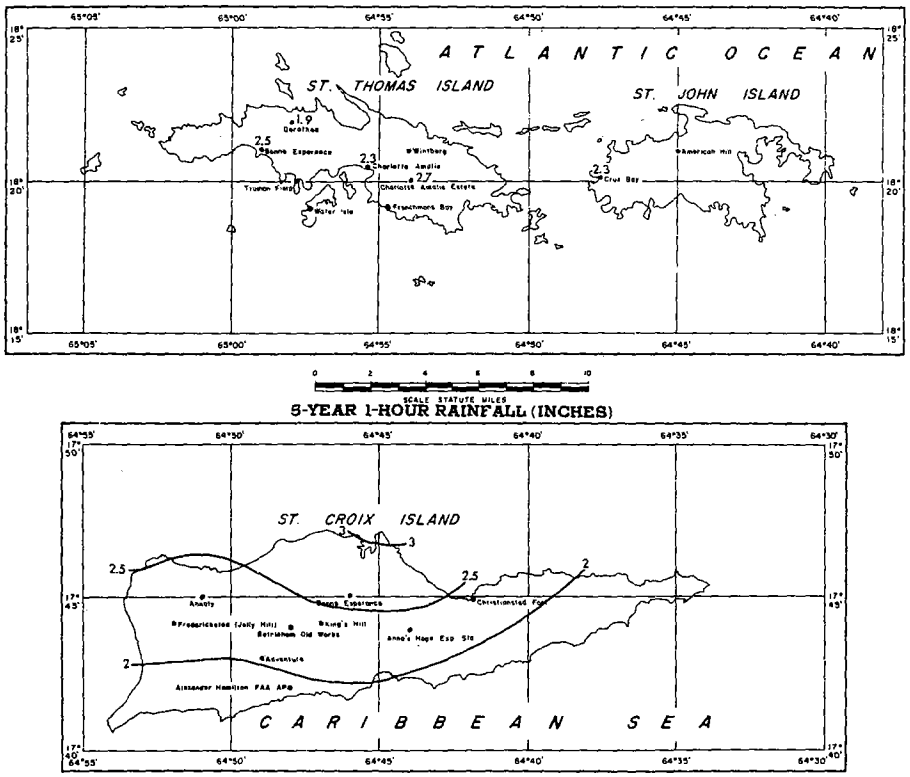

FIGURE 4–65.—5-yr. 1-hr. rainfall for Virgin Islands (in.).

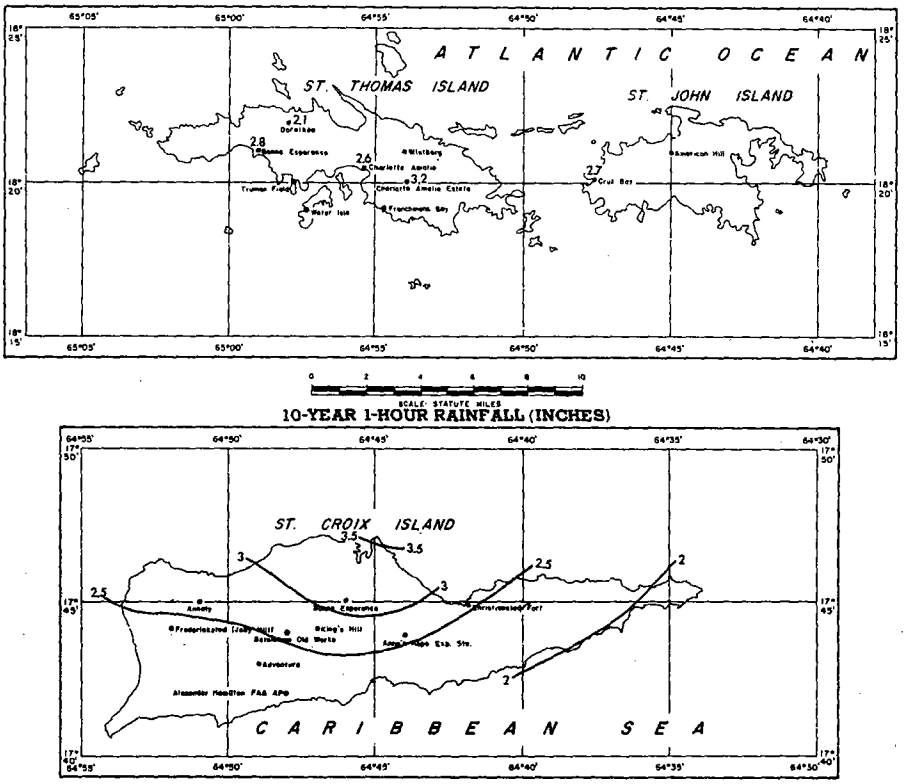

FIGURE 4–66.—10-yr. 1-hr. rainfall for Virgin Islands (in.).

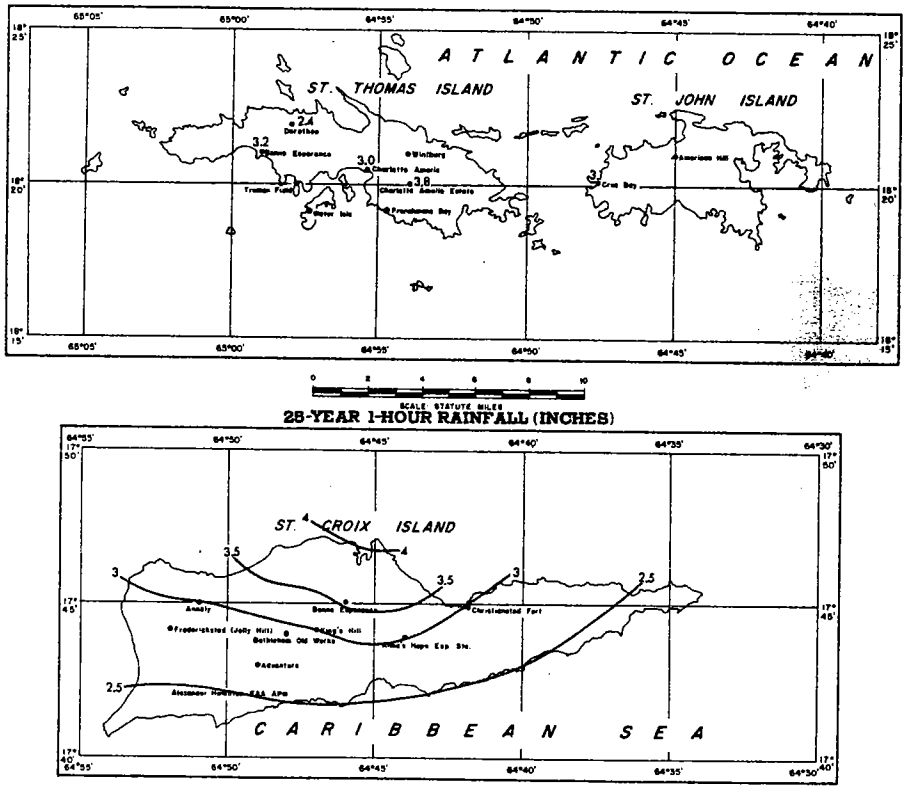

FIGURE 4–67.—25-yr. 1-hr. rainfall for Virgin Islands (in.).

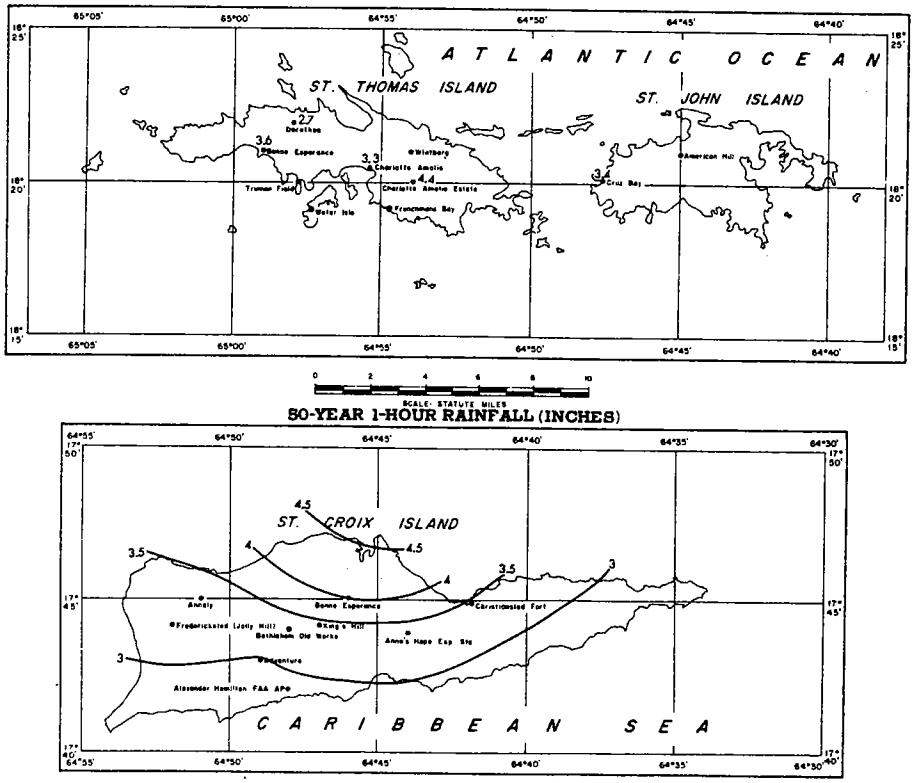

FIGURE 4–68.—50-yr. 1-hr. rainfall for Virgin Islands (in.).

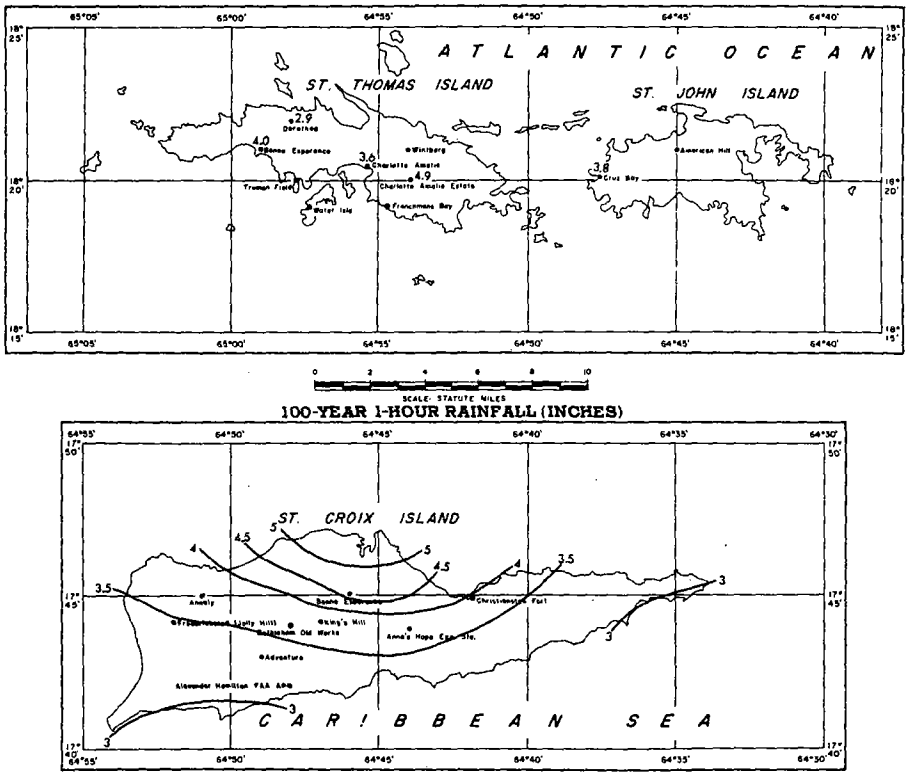

FIGURE 4–69.—100-yr. 1-hr. rainfall for Virgin Islands (in.).

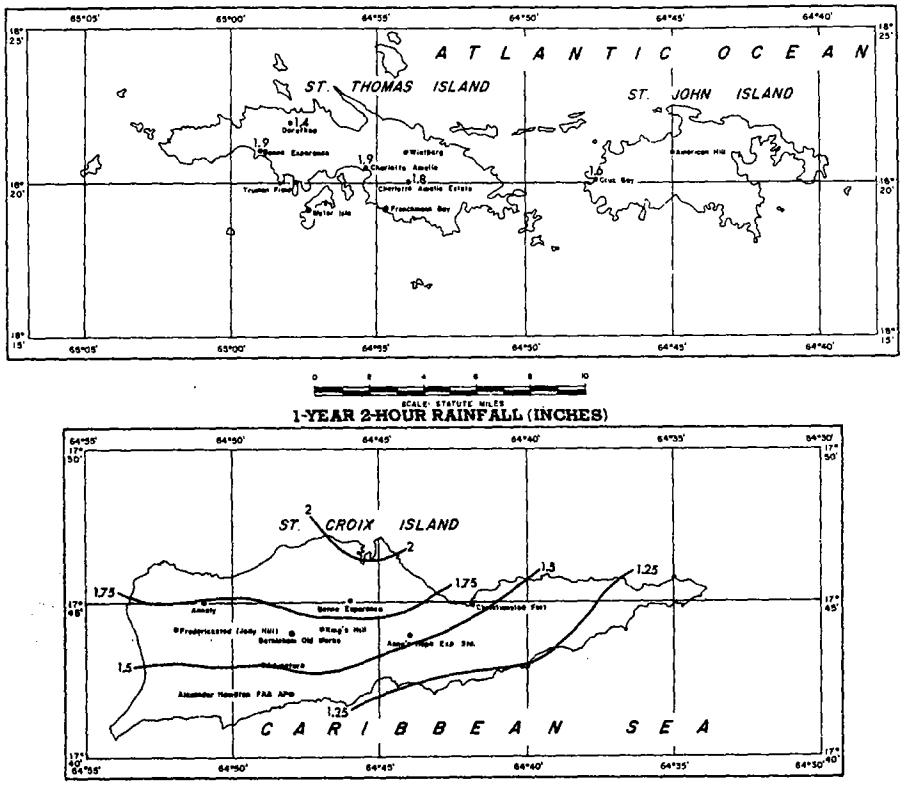

FIGURE 4–70.—1-yr 2-hr rainfall for Virgin Islands (in.).

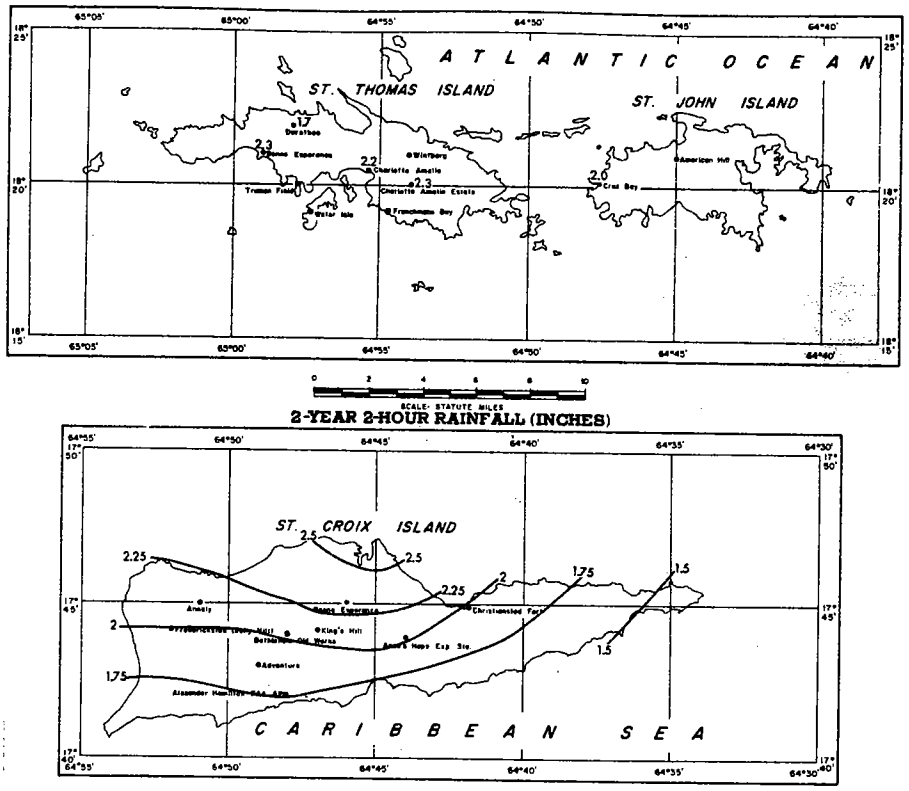

FIGURE 4–71.—2-yr. 2-hr. rainfall for Virgin Islands (in.).

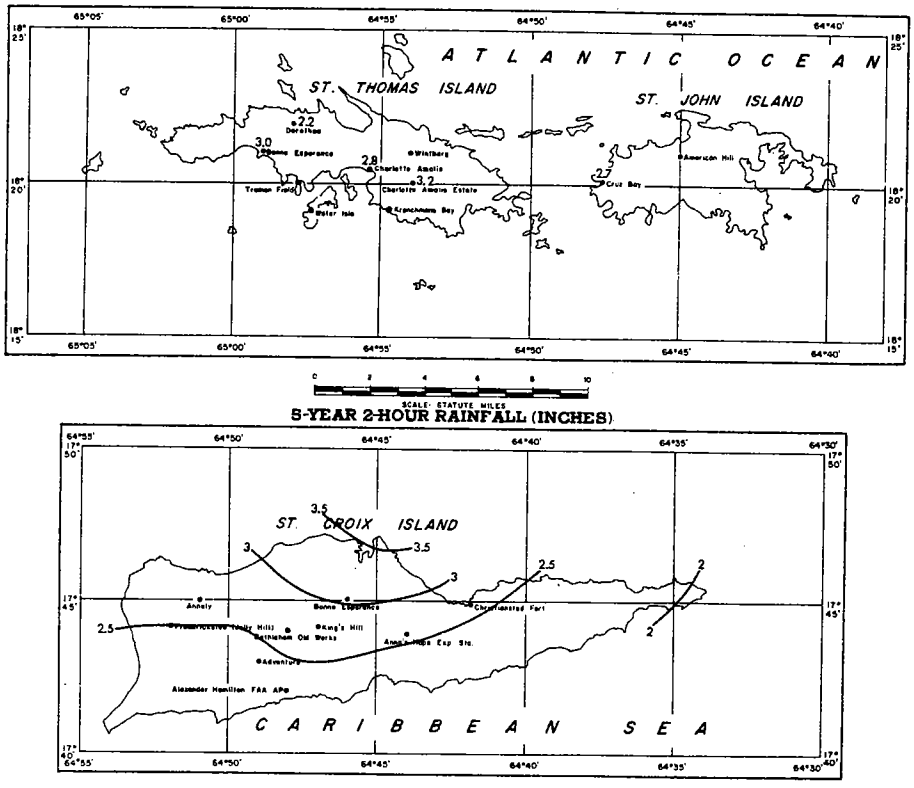

FIGURE 4–72.—5-yr. 2-hr. rainfall for Virgin Islands (in.).

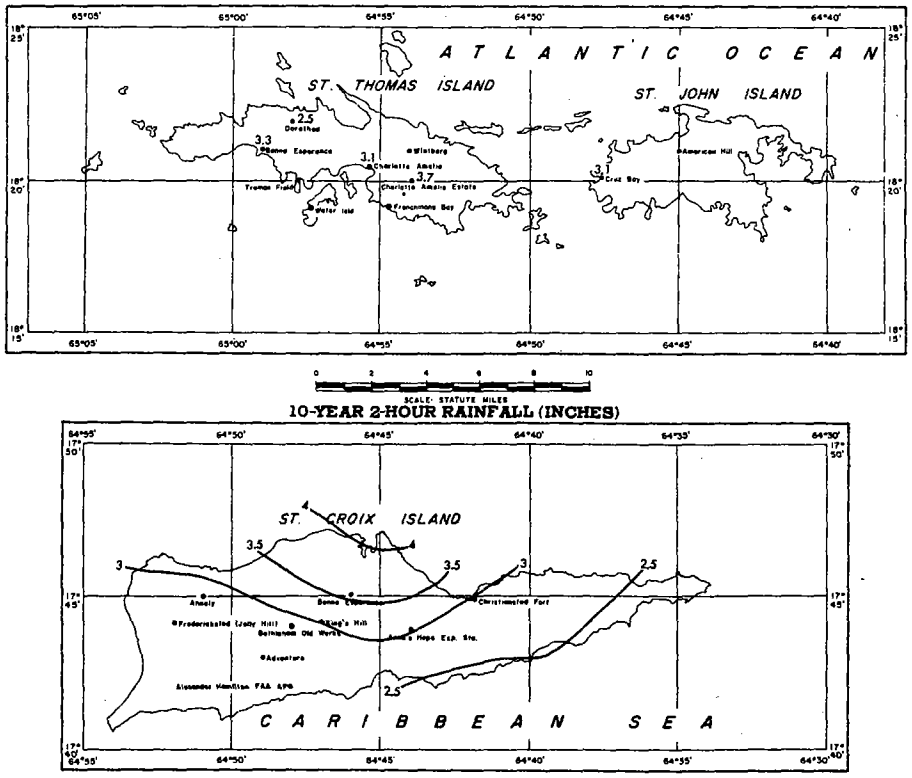

FIGURE 4–73.—10-yr. 2-hr. rainfall for Virgin Islands (in.).

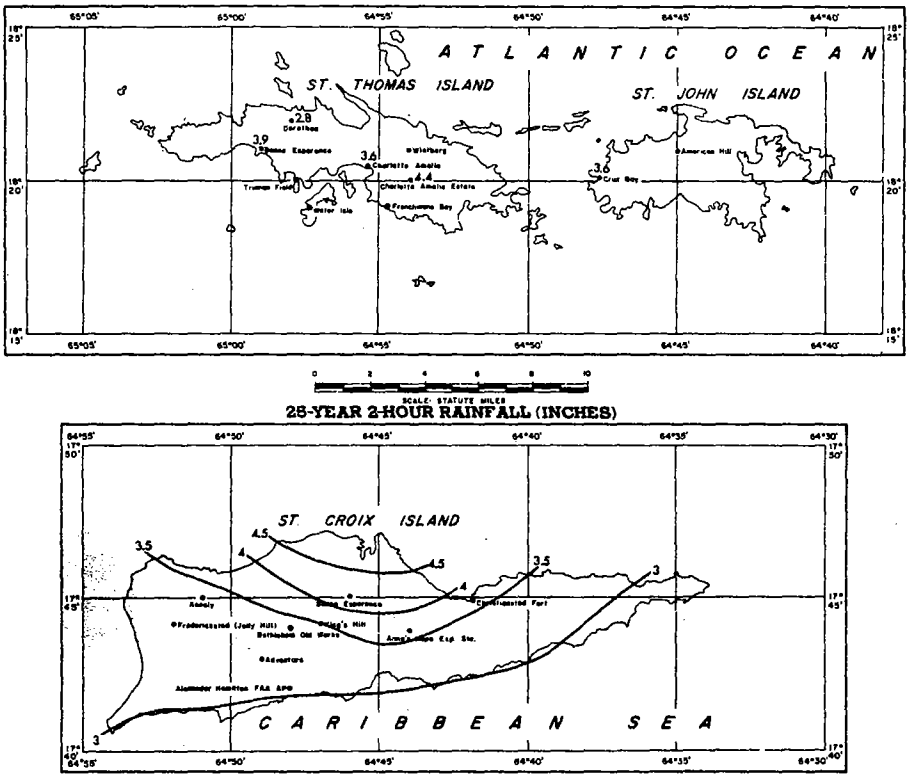

FIGURE 4–74.—25-yr. 2-hr. rainfall for Virgin Islands (in.).

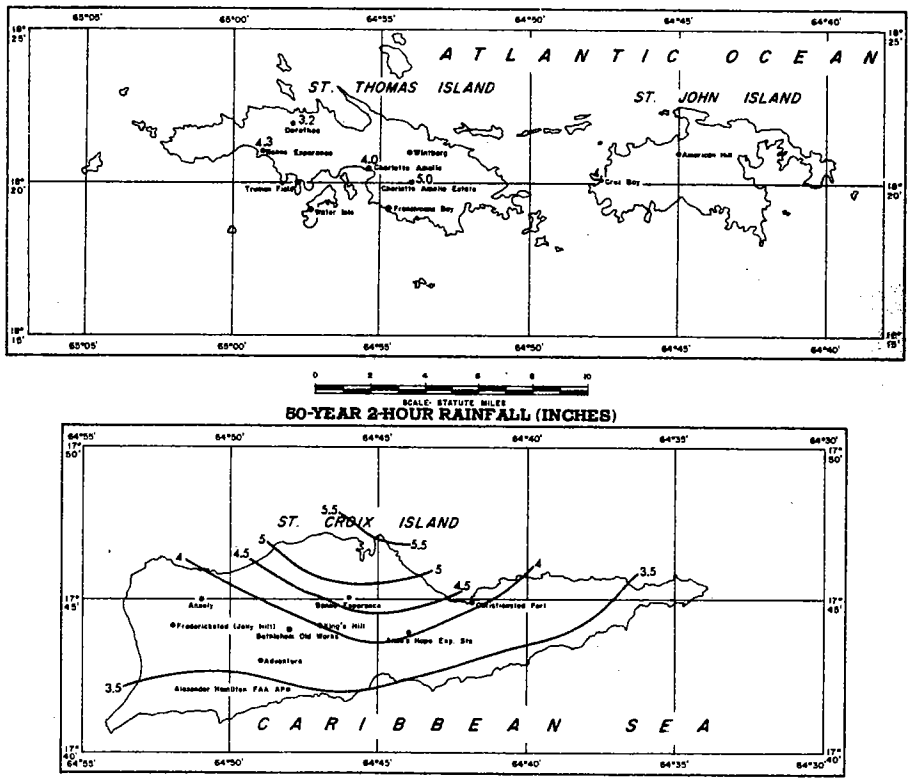

FIGURE 4–75.—50-yr. 2-hr. rainfall for Virgin Islands (in.).

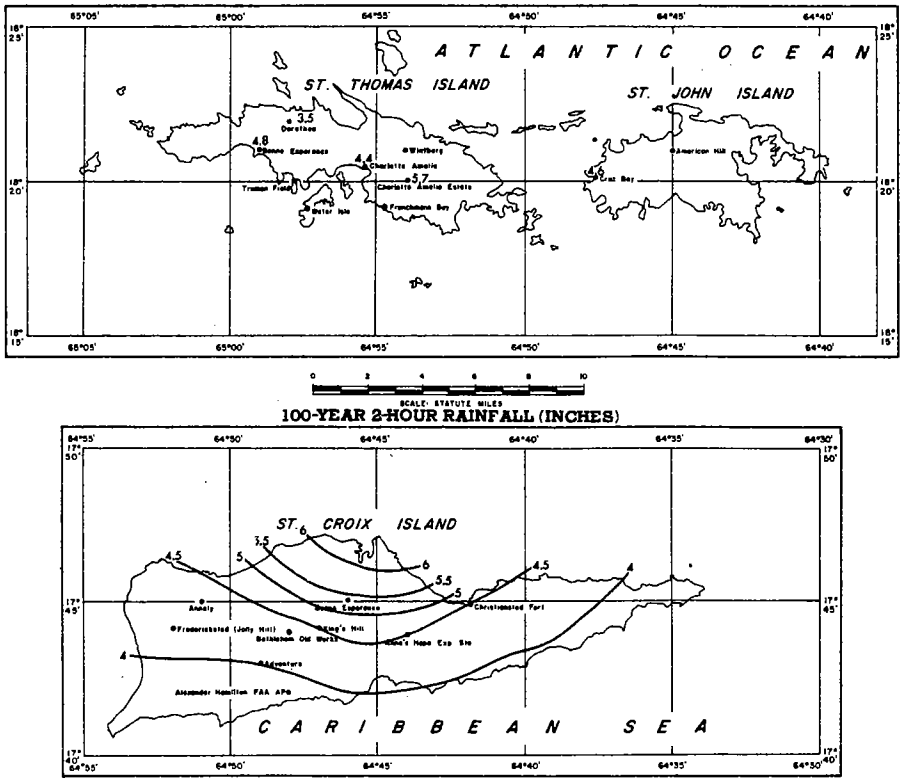

FIGURE 4–76.—100-yr. 2-hr. rainfall for Virgin Islands (in.).

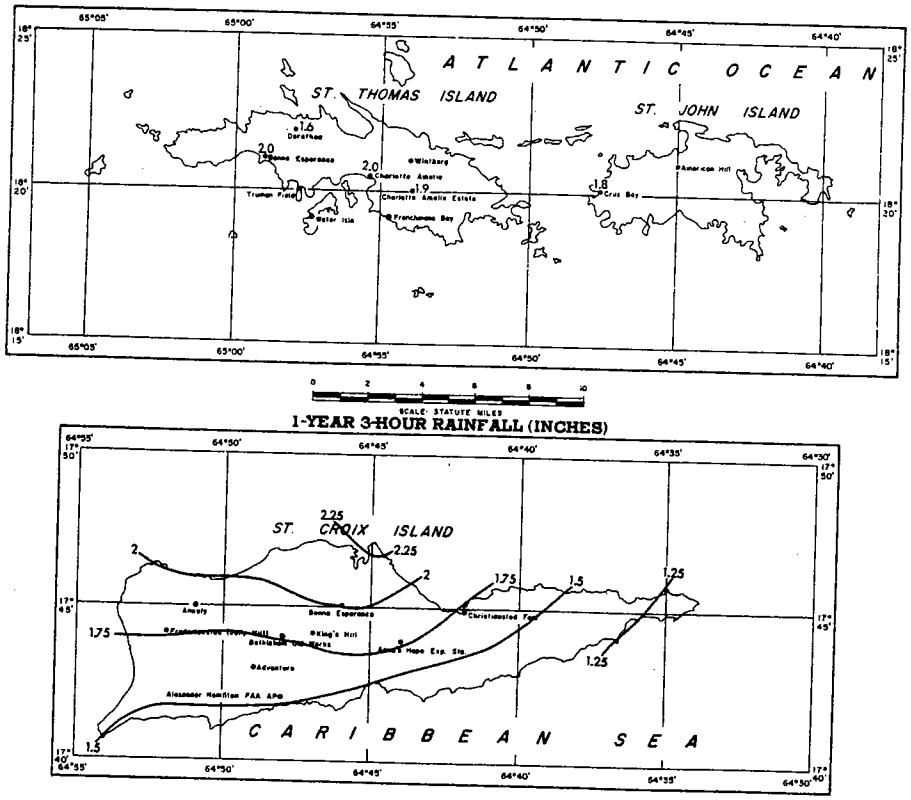

FIGURE 4–77.—1-yr. 3-hr. rainfall for Virgin Islands (in.).

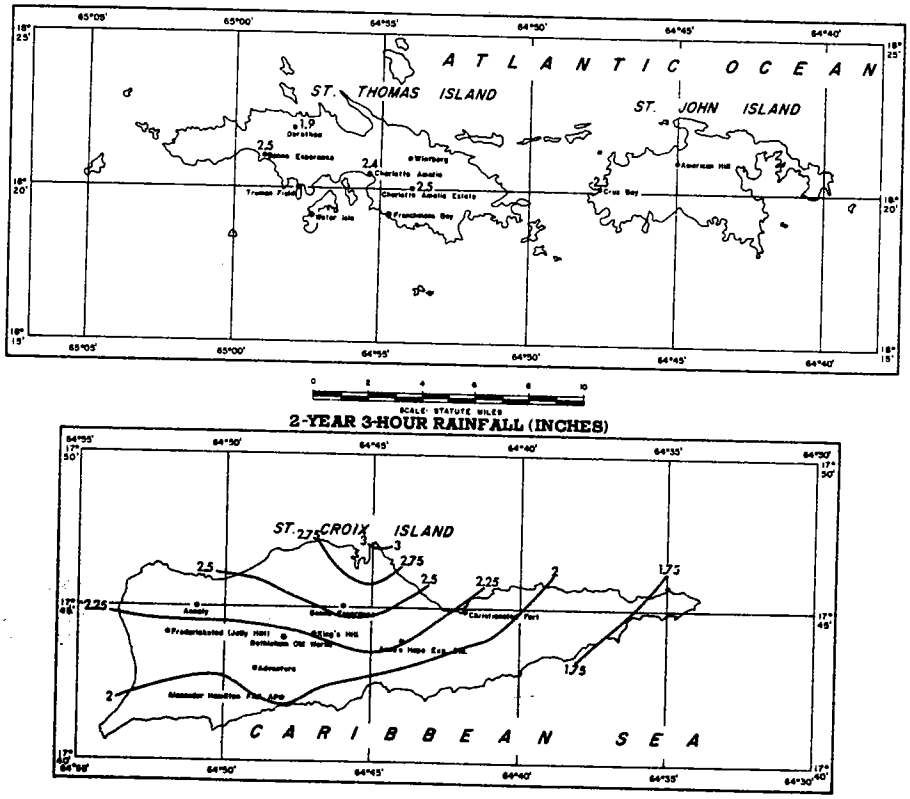

FIGURE 4–78.—2-yr. 3-hr. rainfall for Virgin Islands (in.).

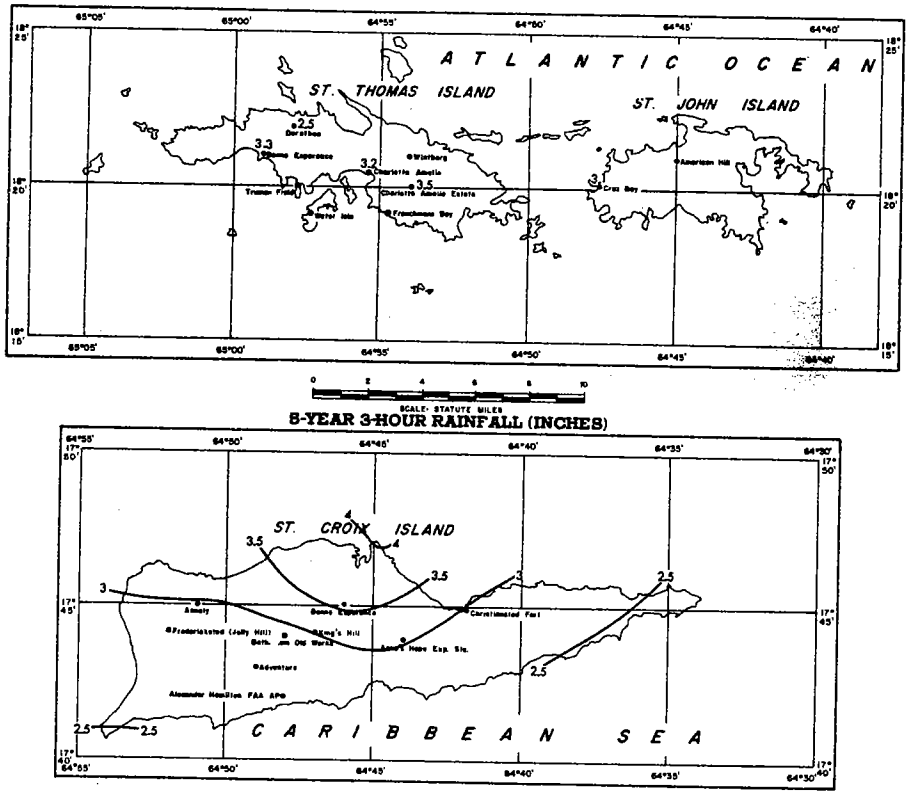

FIGURE 4–79.—5-yr. 3-hr. rainfall for Virgin Islands (in.).

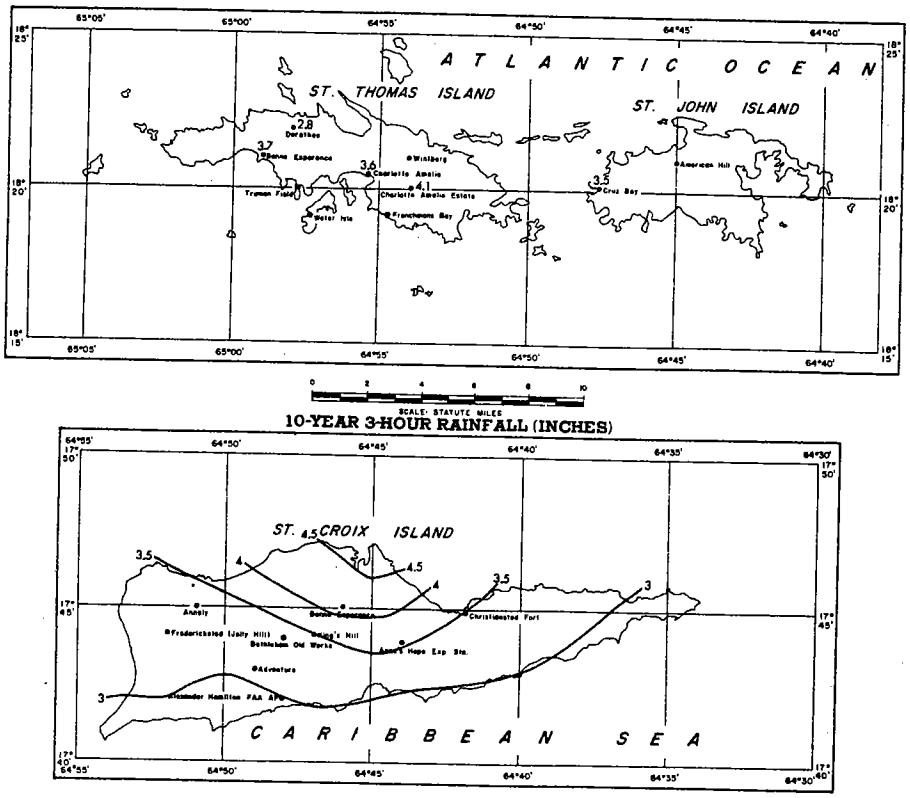

FIGURE 4–80.—10-yr. 3-hr. rainfall for Virgin Islands (in.).

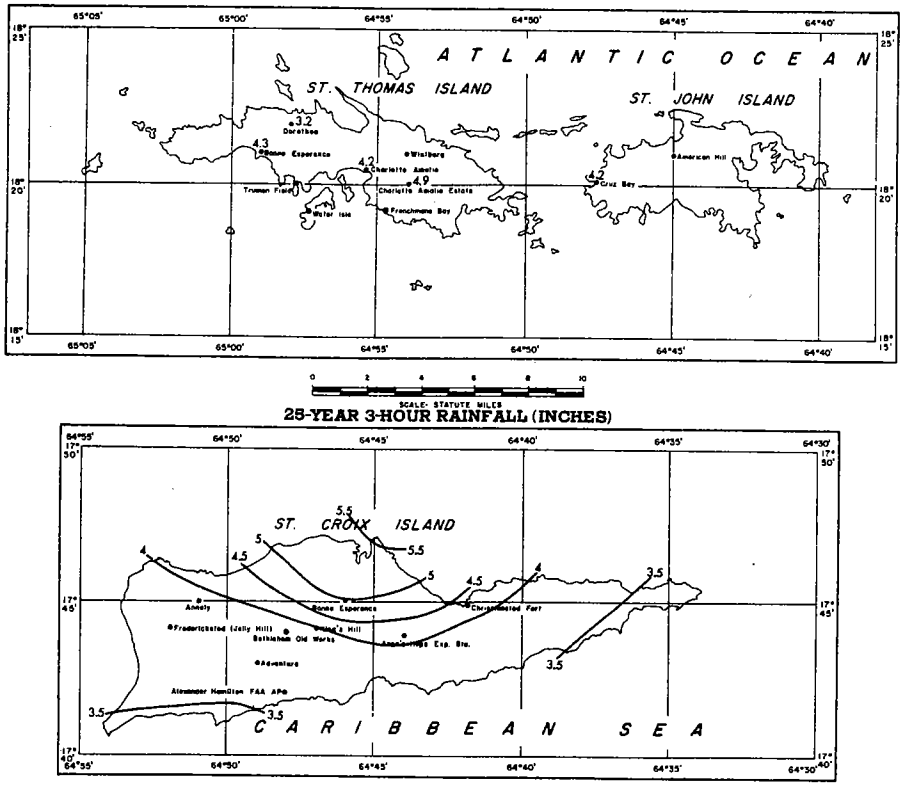

FIGURE 4–81.—25-yr. 3-hr. rainfall for Virgin Islands (in.).

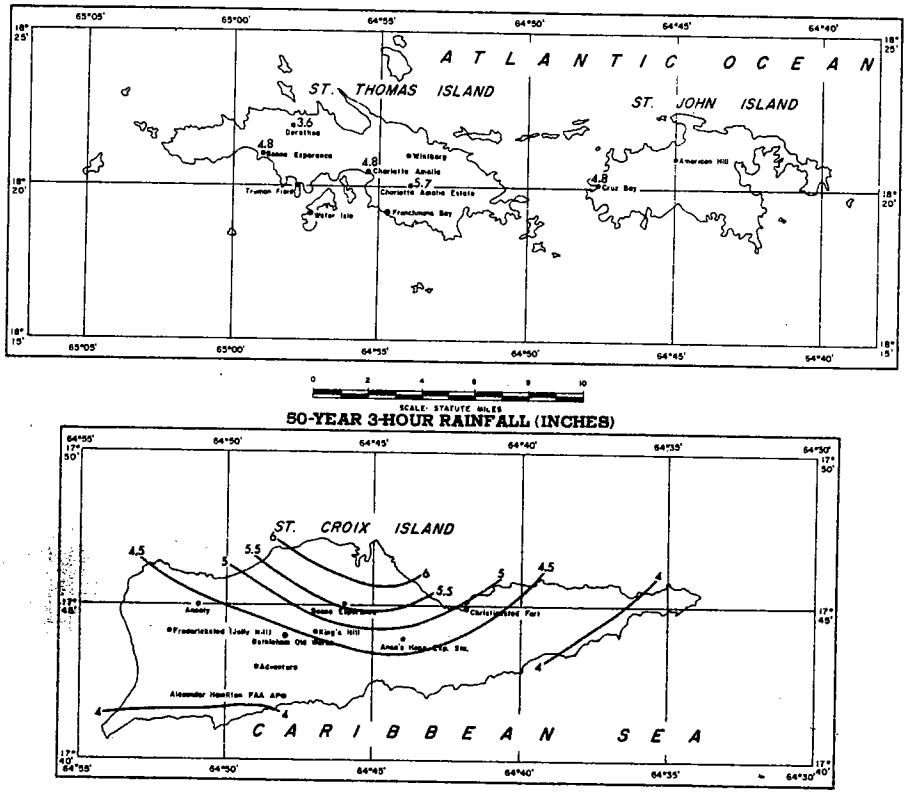

FIGURE 4–82.—50-yr. 3-hr. rainfall for Virgin Islands (in.).

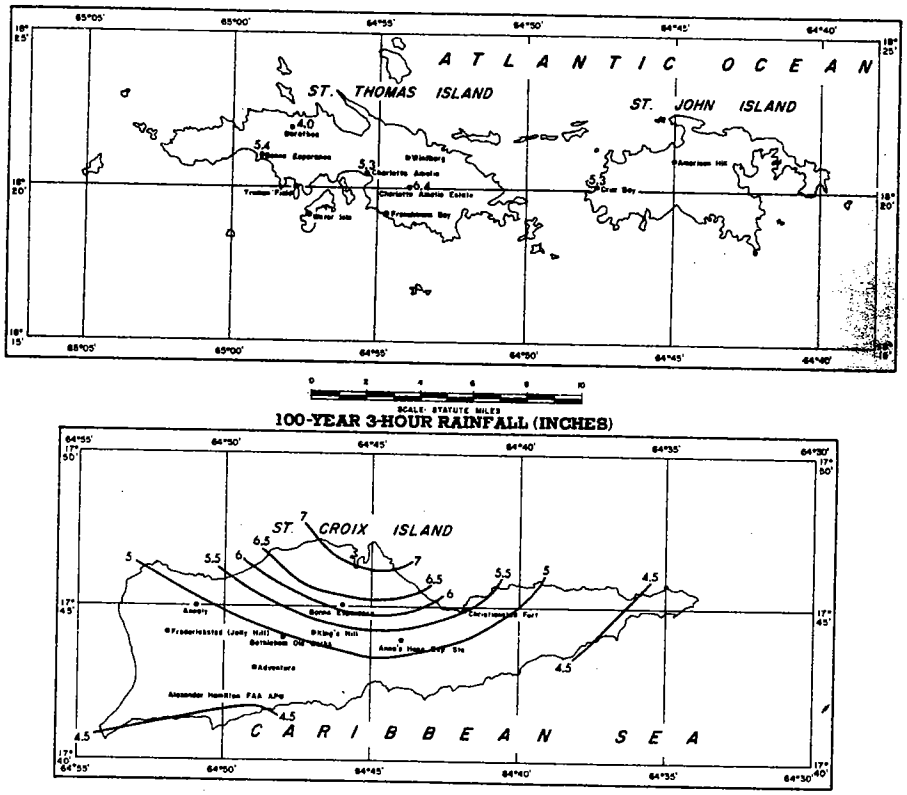

FIGURE 4–83.—100-yr. 3-hr. rainfall for Virgin Islands (in.).

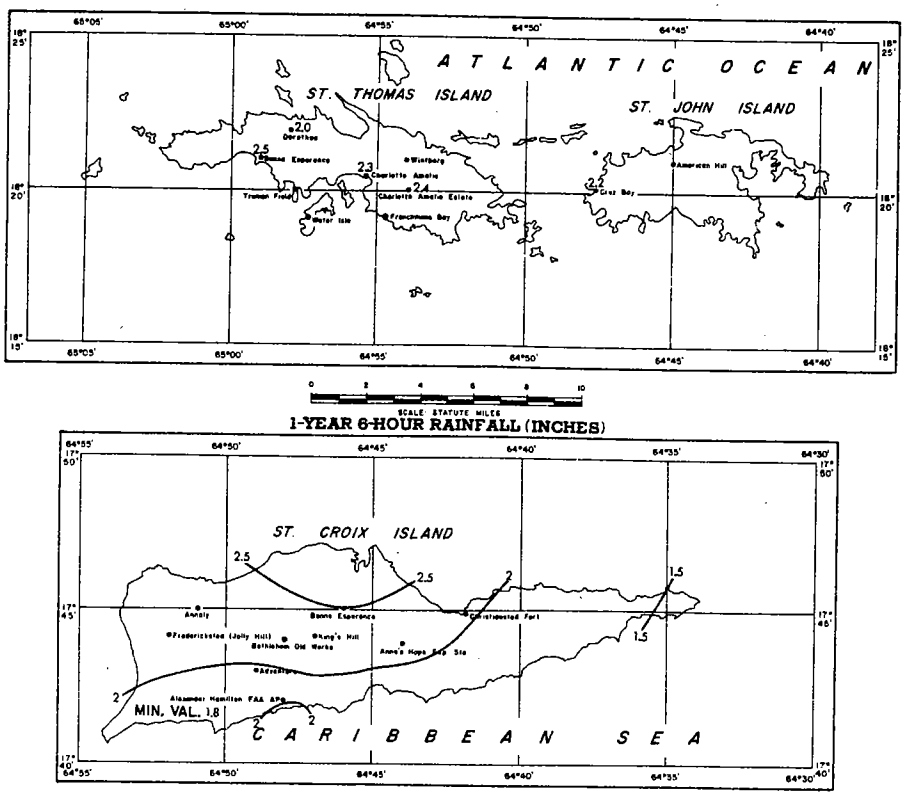

FIGURE 4–84.—1-yr. 6-hr. rainfall for Virgin Islands (in.).

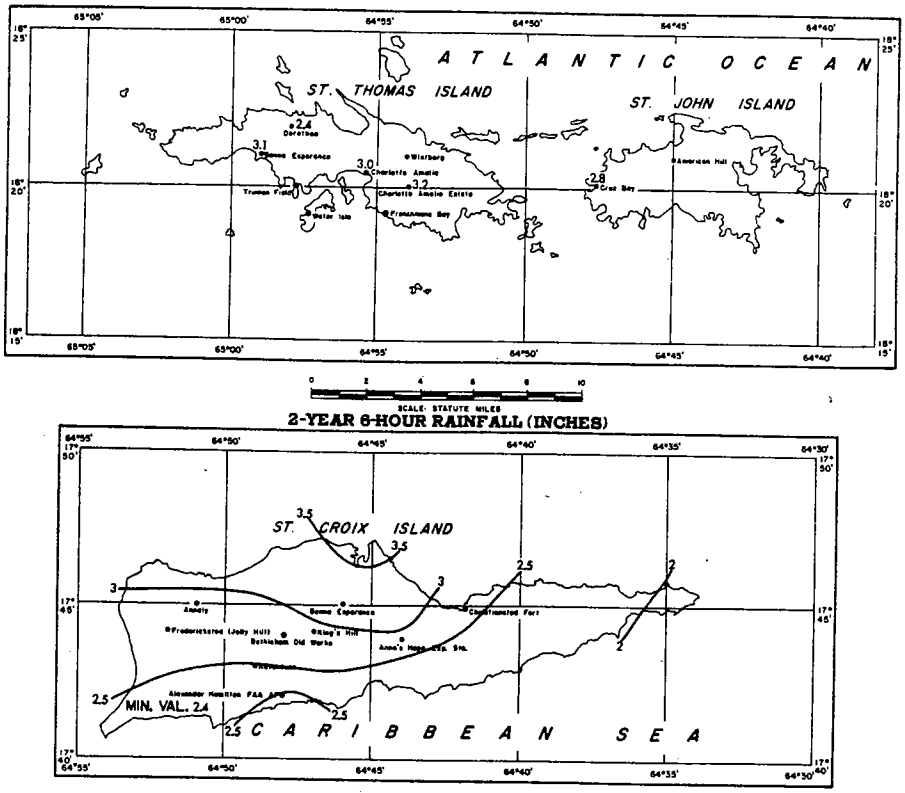

FIGURE 4–85.—2-yr. 6-hr. rainfall for Virgin Islands (in.).

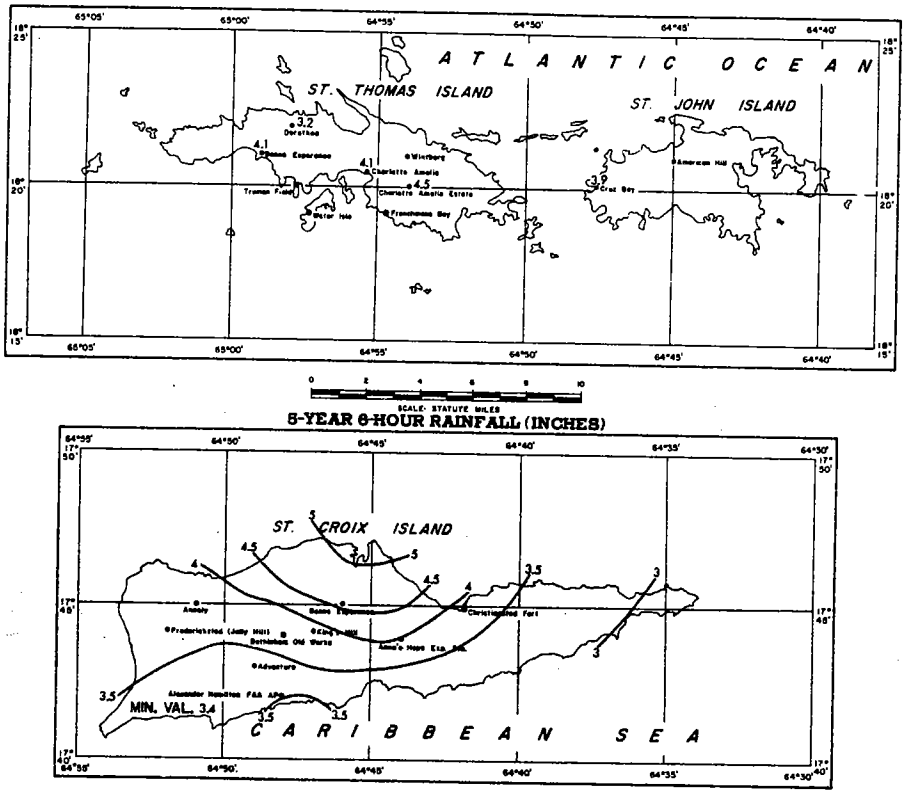

FIGURE 4–86.—5-yr. 6-hr. rainfall for Virgin Islands (in.).

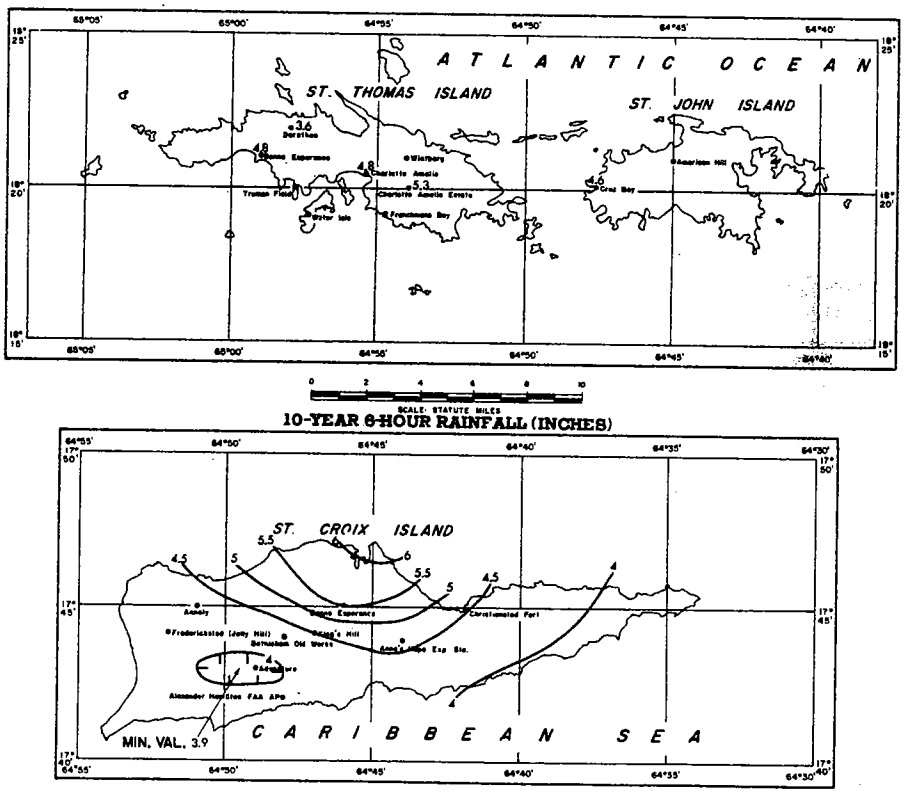

FIGURE 4–87.—10-yr. 6-hr. rainfall for Virgin Islands (in.).

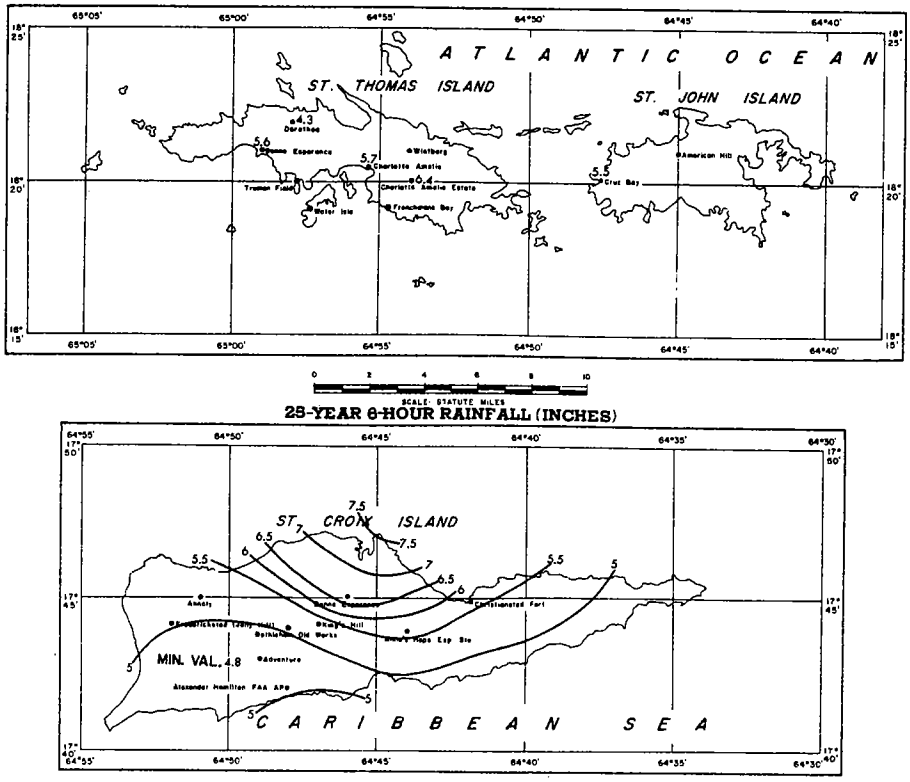

FIGURE 4–88.—25-yr. 6-hr. rainfall for Virgin Islands (in.)

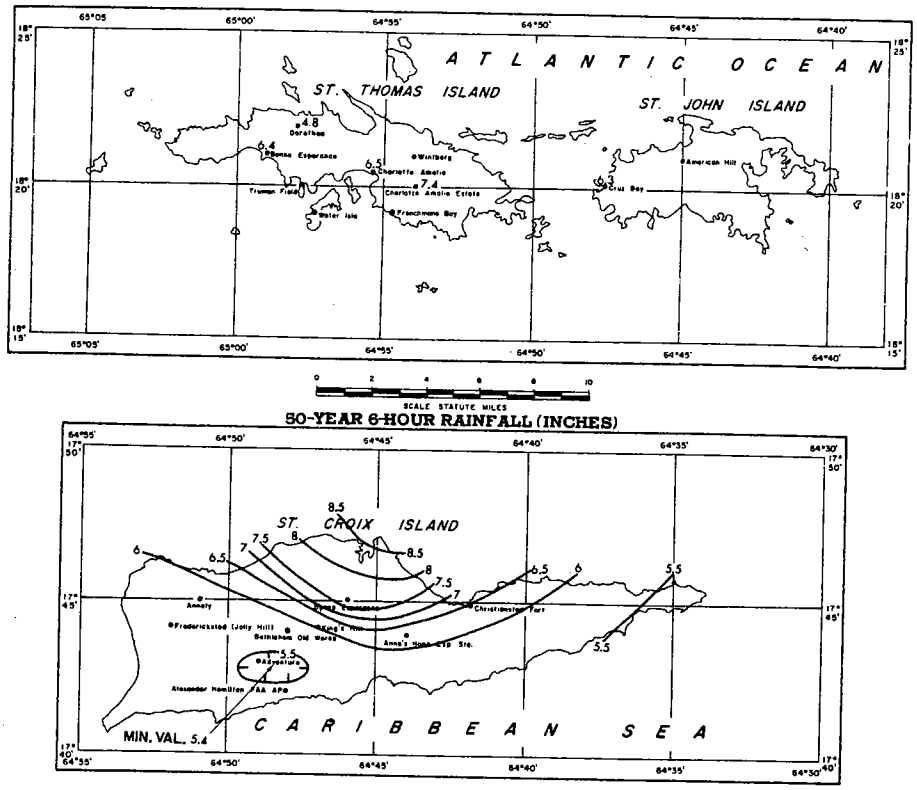

FIGURE 4–89.—50-yr. 6-hr. rainfall for Virgin Islands (in.).

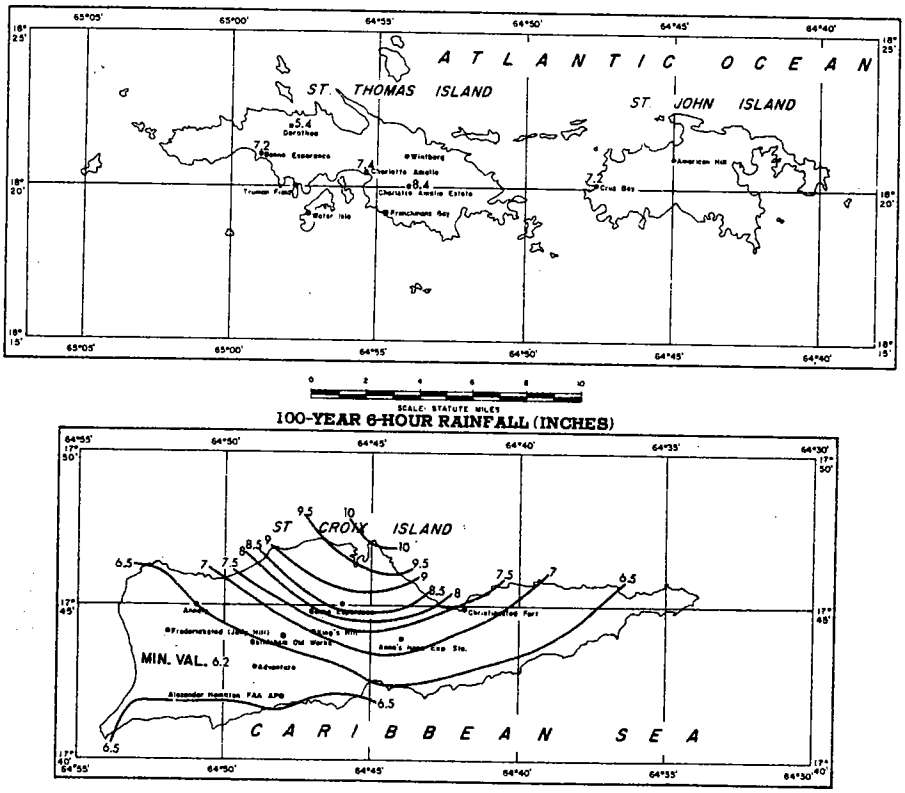

FIGURE 4–90.—100-yr. 6-hr. rainfall for Virgin Islands (in.).

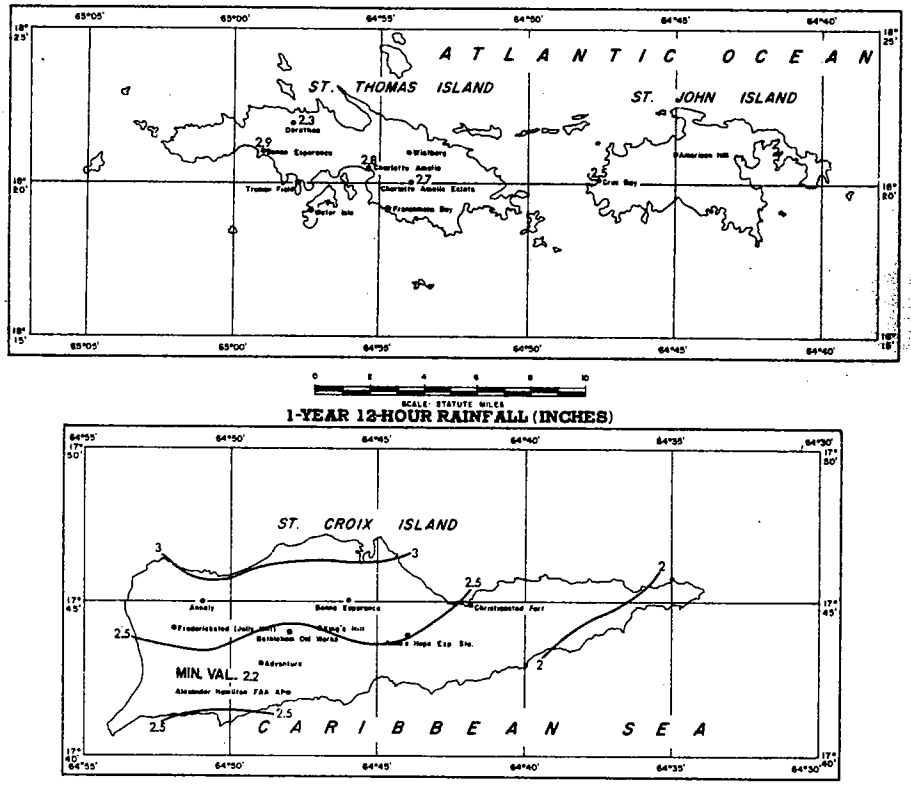

FIGURE 4–91.—1-yr. 12-hr. rainfall for Virgin Islands (in.).

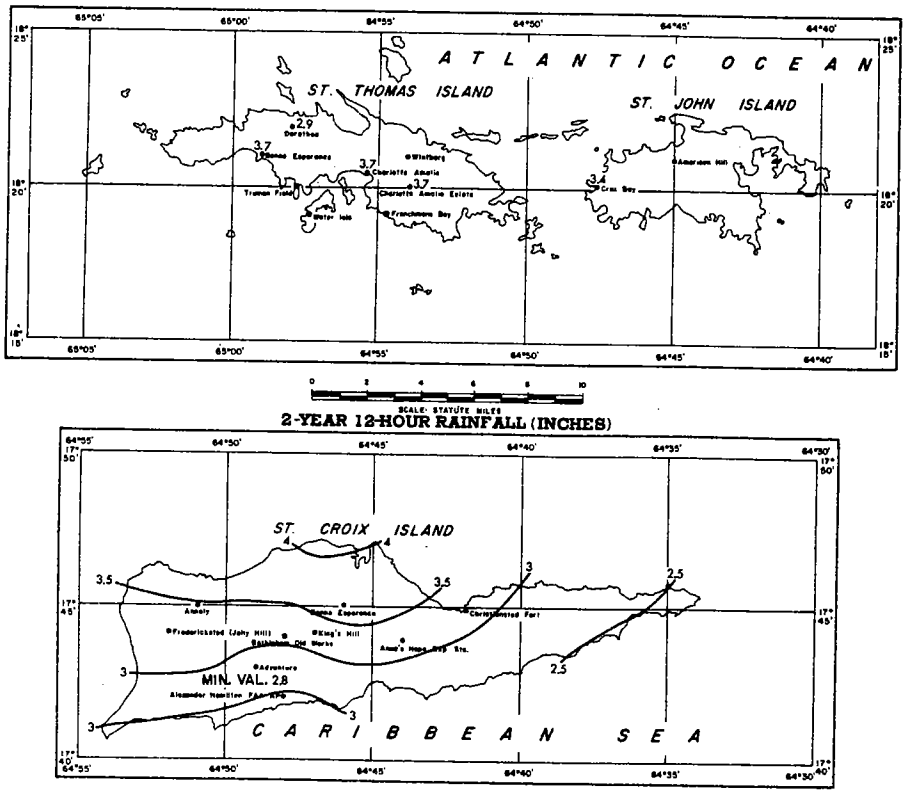

FIGURE 4–92.—2-yr. 12-hr. rainfall for Virgin Islands (in.).

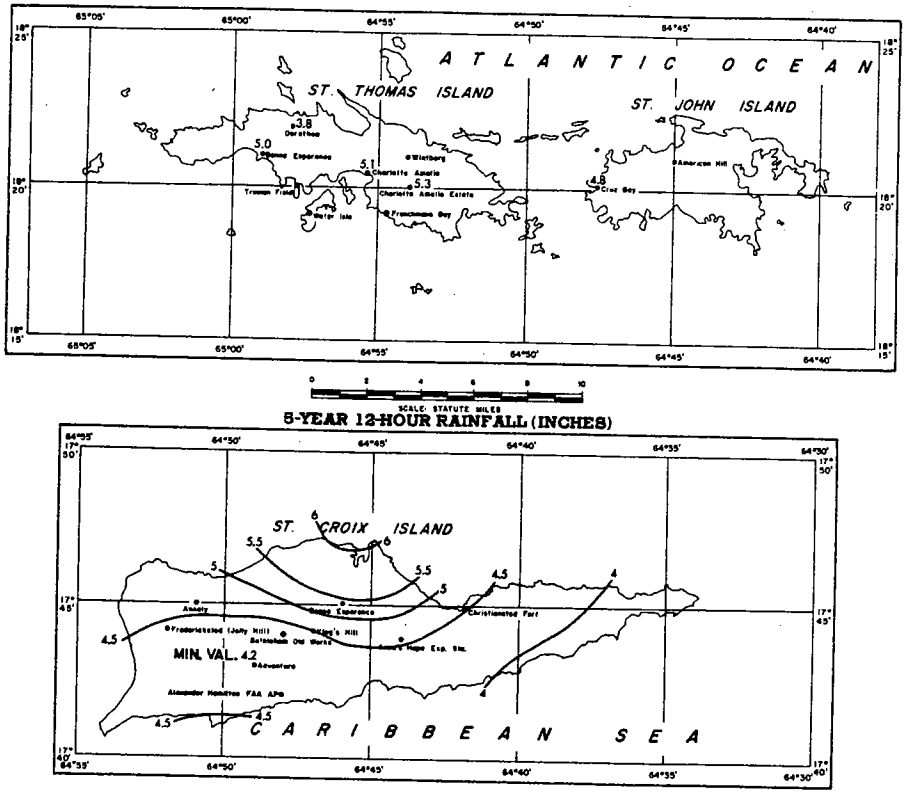

FIGURE 4–93.—5-yr. 12-hr. rainfall for Virgin Islands (in.).

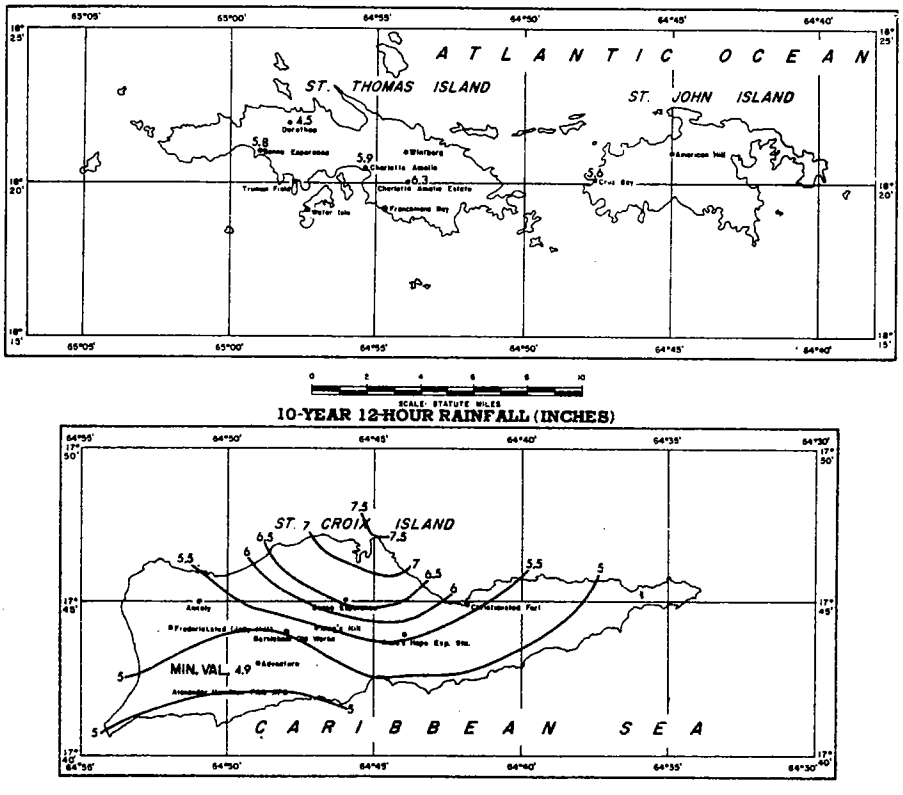

FIGURE 4–94.—10-yr. 12-hr. rainfall for Virgin Islands (in.).

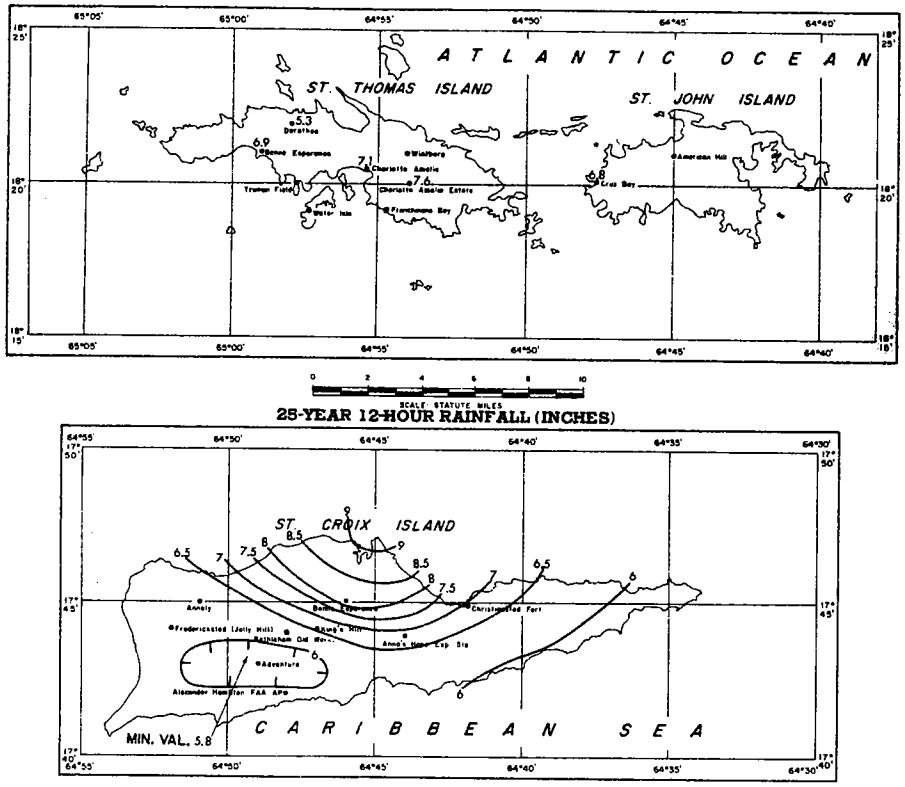

FIGURE 4–95.—25-yr. 12-hr. rainfall for Virgin Islands (in.).

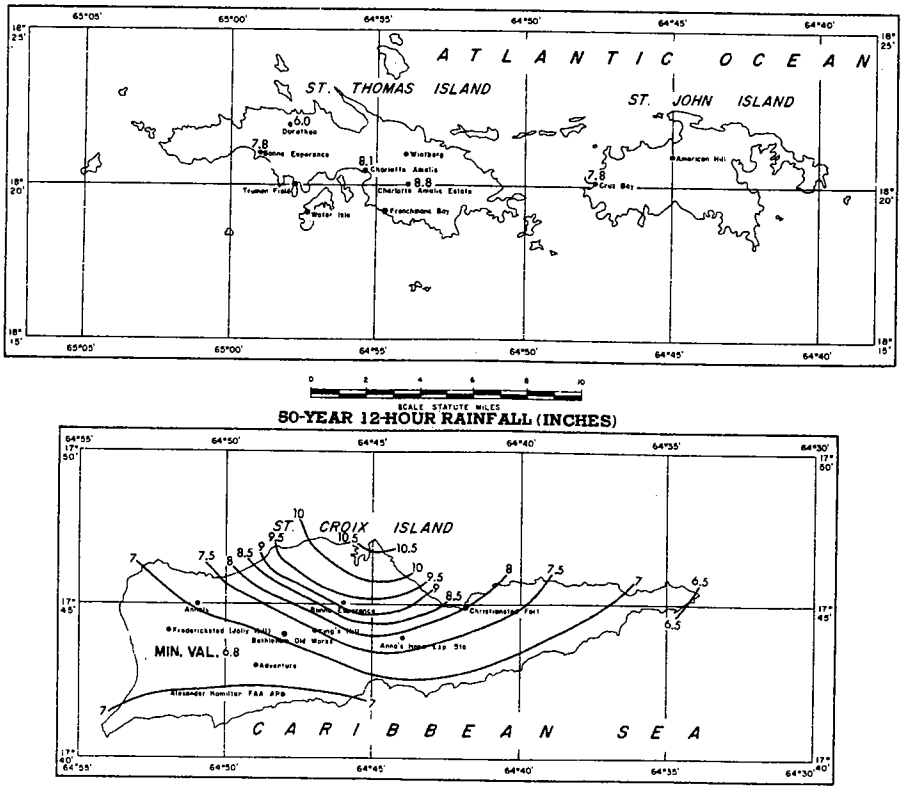

FIGURE 4–96.—50-yr. 12-hr. rainfall for Virgin Islands (in.).

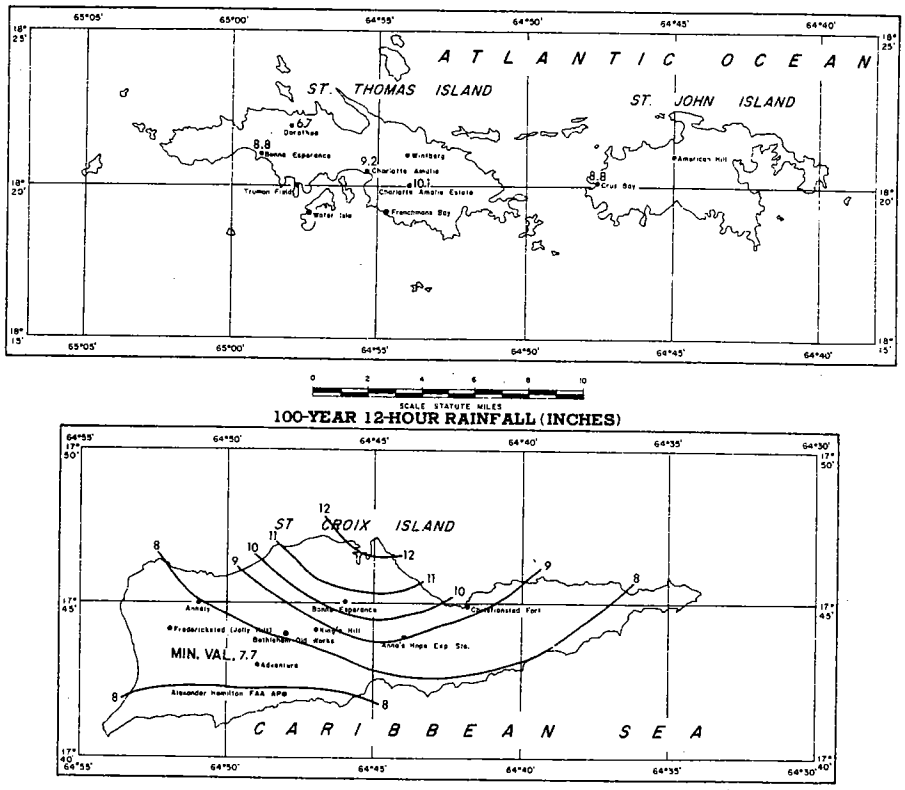

FIGURE 4–97.—100-yr. 12-hr. rainfall for Virgin Islands (in.).

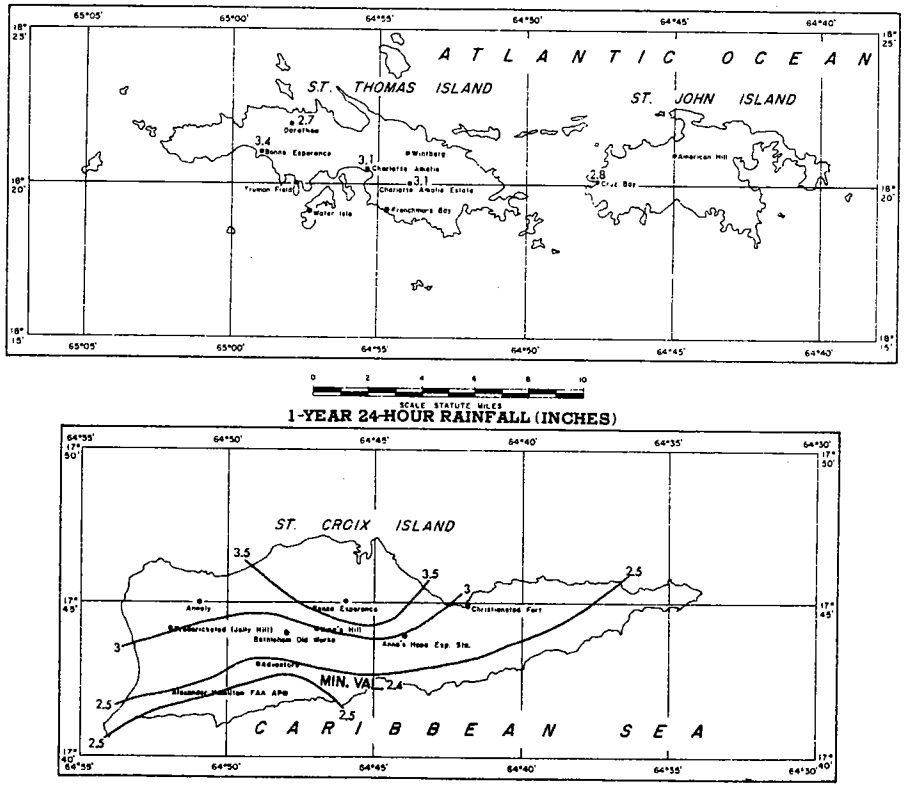

FIGURE 4–98.—1-yr. 24-hr. rainfall for Virgin Islands (in.).

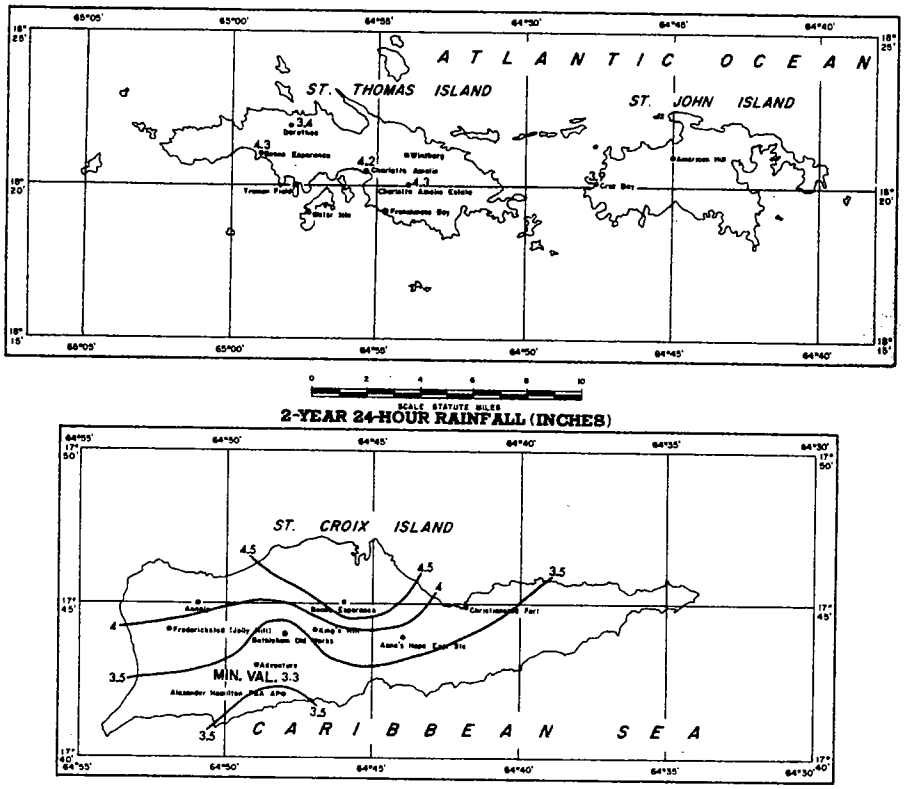

FIGURE 4–99.—2-yr. 24-hr. rainfall for Virgin Islands (in.).

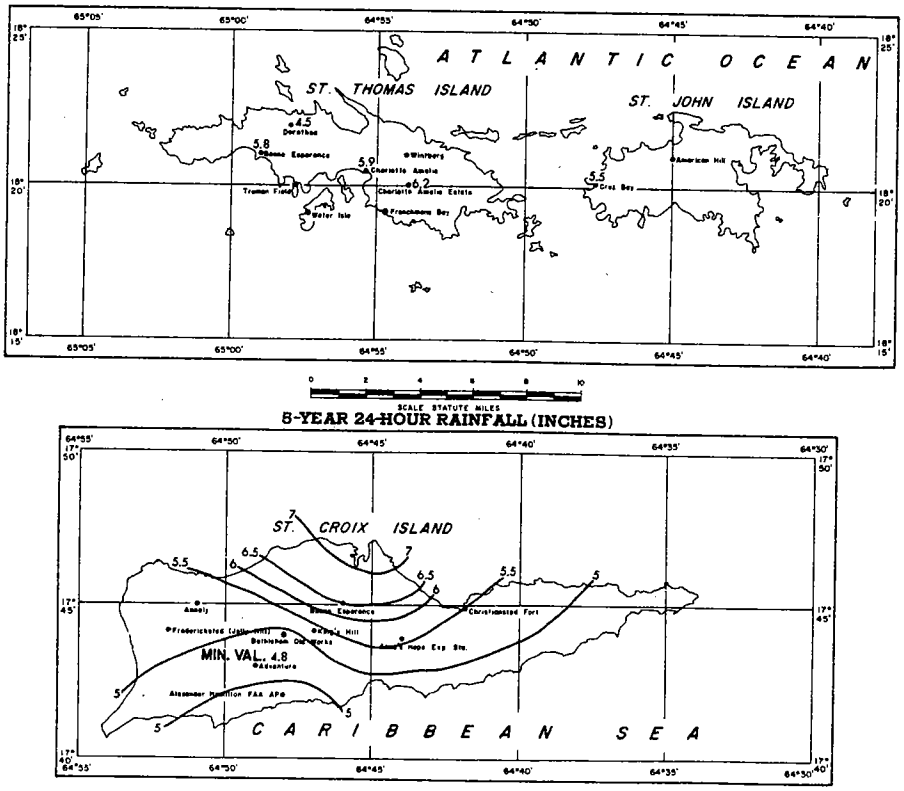

FIGURE 4–100.—5-yr. 24-hr. rainfall for Virgin Islands (in.).

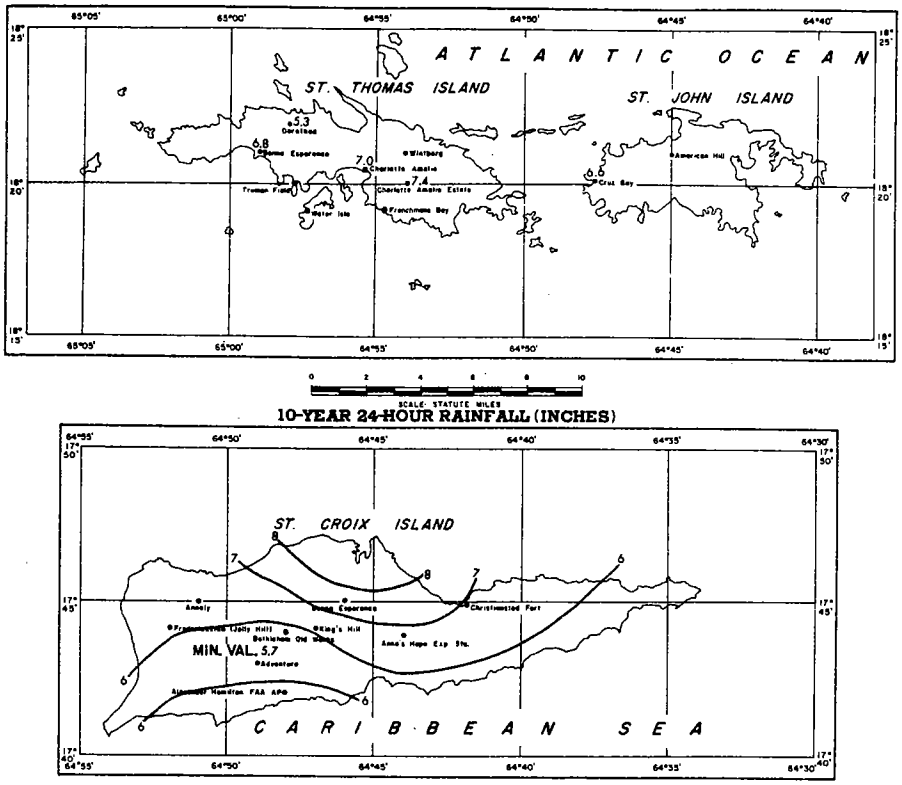

FIGURE 4–101.—10-yr. 24-hr. rainfall for Virgin Islands (in.).

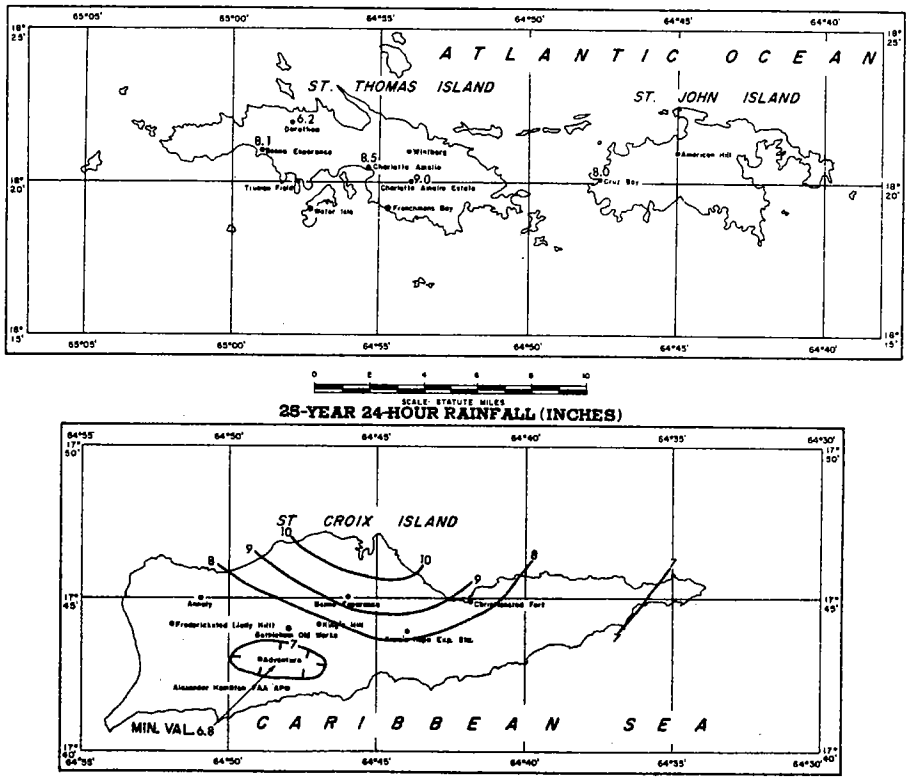

FIGURE 4–102.—25-yr. 24-hr. rainfall for Virgin Islands (in.).

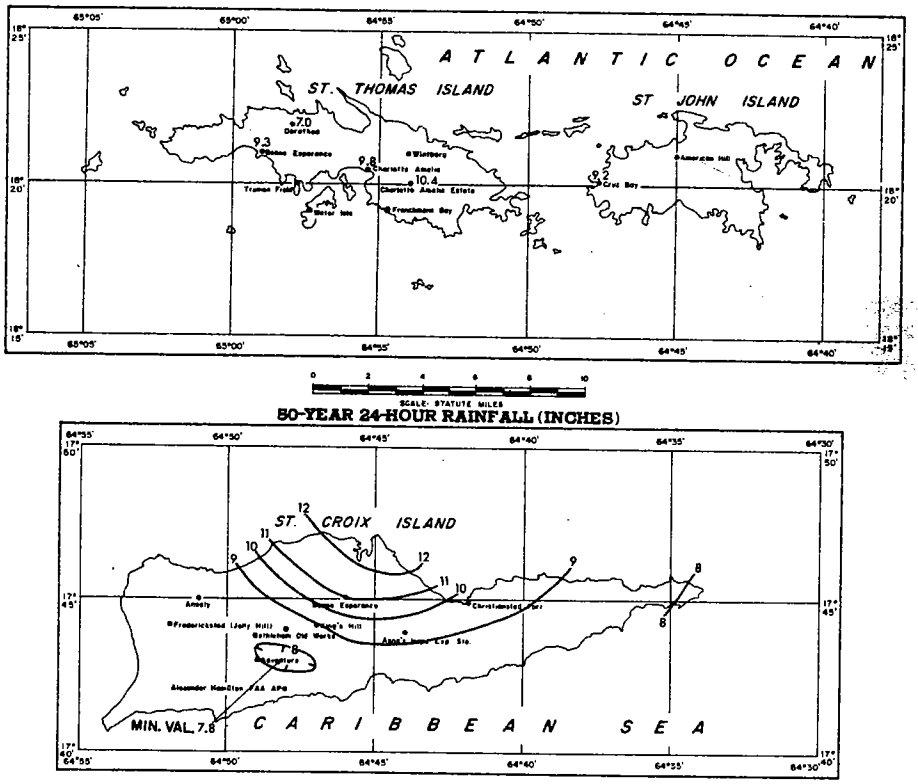

FIGURE 4–103.—50-yr. 24-hr. rainfall for Virgin Islands (in.).

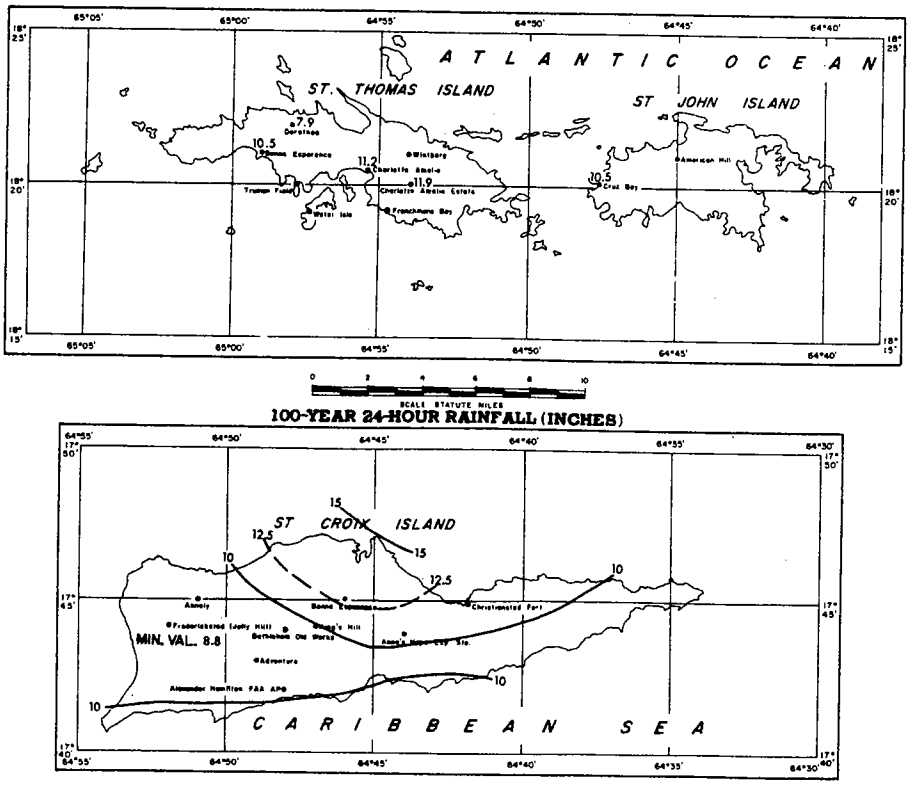

FIGURE 4–104.—100-yr. 24-hr. rainfall for Virgin Islands (in.).

REFERENCES

1. M. A. Quinones, "High Intensity Rainfall and Major Floods in Puerto Rico," *Proceedings American Society of Civil Engineers*, vol. 79, Sep. No. 364, Dec. 1953, 35 pp
2. L. L. Weiss and W. T. Wilson, "Precipitation Gage Shields," *Extrait des Comptes Rendus et Rapports—Assemblée Généralé de Toronto*, International Union of Geodesy and Geophysics, Gentbrugge, vol. 1, 1958, pp. 462–484.
3. C. L. Jordan and M. Shiroma, "A Record Rainfall at Okinawa," *Bulletin of the American Meteorological Society*, vol. 40, No. 12, Dec. 1959, pp. 609–612.
4. J. Coronas, S. J., "The Typhoon of July 11 to 19, 1911," *Meteorological Bulletin*, Phillipines Weather Bureau, July 1911, pp. 186–190.
5. I. R. Tannehill, *Hurricanes*, 9th ed., Princeton University Press, 1956, 308 pp.
6. W. Cry, W. H. Haggard, and H. S. White, "North Atlantic Tropical Cyclones," U.S. Weather Bureau, *Technical Paper No. 36*, 1959, 214 pp.
7. H. E. Graham and D. E. Nunn, "Meteorological Considerations Pertinent to Standard Project Hurricane, Atlantic and Gulf Coasts," *National Hurricane Research Project Report No. 33*, U.S. Weather Bureau, Nov. 1959, 76 pp.
8. H. Riehl, *Tropical Meteorology*, McGraw-Hill Book Co., Inc., New York, 1954, pp. 293–295.
9. B. I. Miller, "The Three-Dimensional Wind Structure Around a Tropical Cyclone." *National Hurricane Research Project Report No. 15*, U.S. Weather Bureau, Jan. 1958, pp. 12–21.
10. H. R. Byers, *General Meteorology*, McGraw-Hill Book Co. Inc., New York, 1944, pp. 431–436.
11. J. A. Colón, "Meteorological Conditions over Puerto Rico during Hurricane Betsy," *Monthly Weather Review*, vol. 87, No. 2, Feb. 1959, pp. 69–80.
12. O. L. Fassig, "San Felipe—The Hurricane of September 13, 1928, at San Juan, P.R.," *Monthly Weather Review*, vol. 56, No. 9, Sept, 1928, pp. 350–352.
13. V. A. Myers, "Characteristics of United States Hurricanes Pertinent to Levee Design for Lake Okeechobee, Florida," *Hydrometeorological Report No. 32*, U.S. Weather Bureau, Mar. 1954, pp. 2–17.
14. A. K. Showalter, "Rates of Precipitation from Pseudoadiabatically Ascending Air," *Monthly Weather Review*, vol. 72, No. 1, 1944, p. 1.
15. C. S. Gilman and L. L. Weiss, "A Numerical Solution for Irrotational Flow over a Mountain Barrier," *Transactions, American Geophysical Union*, vol. 31, No. 5, Oct. 1950, pp. 699–706.
16. P. Queney, "Theory of Perturbations in Stratified Currents with Applications to Air Flow over Mountain Barriers," *Miscellaneous Report No. 23*. Dept. of Meteorology, University of Chicago, 1947, 81 pp.
17. R. J. Grace, "Betsy's Roving Eye," *Monthly Weather Review*, vol. 84, No. 8, Aug. 1956, pp. 311–312.
18. G. Norton, "Hurricanes of the 1950 Season," *Monthly Weather Review*, vol. 79, No. 1, Jan. 1951, pp. 11–12.
19. D. M. Hershfield, "Estimating the Probable Maximum Precipitation," *Journal of the Hydraulics Division, Proceedings of the American Society of Civil Engineers*, vol. 87, No. HY 5, Sept. 1961, pp. 99–116.
20. U.S. Weather Bureau, "Rainfall Intensities for Local Drainage Design in Western United States," *Technical Paper No. 28*, Nov. 1956, 46 pp.
21. U.S. Weather Bureau, "Rainfall Intensity-Frequency Regime, Part 1—The Ohio Valley," *Technical Paper No. 29*, June 1957, 44 pp.
22. Corps of Engineers, U.S. Army, *Storm Rainfall in the United States*, Feb. 1954.
23. U.S. Weather Bureau, "Generalized Estimates of Probable Maximum Precipitation for the United States, West of the 105th Meridian," *Technical Paper No. 38*, 1959, 66 pp.
24. D. M. Hershfield, "Rainfall-Frequency Atlas of the United States," U.S. Weather Bureau, *Technical Paper No. 40*, May 1961, 115 pp.
25. E. J. Gumbel, *Statistics of Extremes*, Columbia University Press, New York, 1958, 375 pp.
26. D. M. Hershfield and M. A. Kohler, "An Empirical Appraisal of the Gumbel Extreme-Value Procedure," *Journal of Geophysical Research*, vol. 65, No. 6, June 1960, pp. 1737–1746.
27. D. M. Hershfield and W. T. Wilson, "A Comparison of Extreme Rainfall Depths from Tropical and Nontropical Storms," *Journal of Geophysical Research*, vol. 65, No. 3, Mar. 1960, pp. 959–982.

APPENDIX A

PROBABLE MAXIMUM PRECIPITATION FOR LOCAL CLOUDBURSTS

A.1 Introduction

A.1.1 It was pointed out in chapter 3 that the shorter-duration PMP for hurricanes could be exceeded by localized cloudbursts. Because of the very small likelihood that a cloudburst of PMP magnitude would occur on a particular small watershed, it was stated that cloudburst PMP could ordinarily be disregarded. It sometimes happens, however, that an engineer wishes to design for the most critical rainfall intensity regardless of the probability of its occurrence. For short durations and very small watersheds, the most critical rainfall intensity would almost always be associated with a local cloudburst. It is for these reasons that estimates of the upper limits of cloudburst rainfall are presented here.

A.2 Cloudburst PMP

A.2.1 It is generally admitted that little can be done to maximize cloudburst rainfall because of the localized nature of the storm. The present meteorological network is much too sparse to permit reliable evaluation of the temperature, humidity, and wind conditions in such a storm. Hence, the limiting values of such rainfall, or PMP, are assumed to be the envelope of the highest intensities observed. This is the basis of the PMP values computed by equation 1.1 and presented in table A–1. No relation between the magnitude of cludburst rainfall and land elevation has ever been found, so the values of table A–1 may be considered to be applicable to any point in the problem area without adjustment except for size of area.

TABLE A–1 —*Probable maximum cloudburst rainfall*

Duration (min)	Amt (in.)	Duration (hr)	Amt. (in)
5	4 6	1	15 3
10	6 4	2	21 4
15	7 8	3	26 1
20	9 0	4	30.0
30	10 9	5	33 5
45	13 3	6	36 6

A.3 Depth-area relations

A.3.1 The highly concentrated rainfall in cloudbursts of outstanding magnitude results in a much more rapid decrease of average depth with area than is found in general type storms and hurricanes. A survey of *Storm Rainfall in the United States* [22] yielded depth-area data for 17 intense local cloudbursts. The average depths for areas up to 500 sq. mi. for specific durations from 1 to 6 hr. were converted into terms of percentage of the maximum station, or point, precipitation. The percentages for a specific duration were then plotted against size of area. There was considerable scatter in these plots. For example, the percentages for 1-hr. rainfall for 500 sq. mi. ranged from 23 to 67. The Thrall, Tex., storm of September 9–10, 1921, yielded the highest percentages for all durations and for all sizes of area. Its percentage values considerably exceeded the next highest for the 1- to 3-hr. durations, suggesting that its depth-area characteristics are not typical of the local cloudburst. (This apparent departure from more typical areal distribution could well be the result of a too liberal isohyetal pattern). The Thrall, Tex., storm data was therefore eliminated in the depth-area relations.

A.3.2 In an attempt to develop cloudburst depth-area relations most typical of the world's record rainfall intensities, depth-area data for storms with intensities at least half of those given in table A–1 were separately identified. This reduced the number of basic storms (Thrall, Tex., storm excluded) from 16 to 9. The storms and their basic depth-area-duration data are listed in table A–2. An envelope of the highest percentage values of these data resulted in the set of curves of figure A–1. The results would have been just about the same if data for all 16 storms had been used.

A.3.3 An interesting feature of the depth-area curves of figure A–1 is that many of the controlling percentage values were associated with the Ewan, N.J., storm of September 1, 1940. That storm, while

TABLE A-2.—*Storm data used to determine depth-area relations for local cloudbursts (average depths in in.)*

Area (sq. mi.)	Duration (hr.) 1	2	3	4	5	6
Cheyenne, Okla., storm of Apr. 3–4, 1934						
Max. sta.						20.0
10						17.3
100						14.4
200						13.3
500						11.5
D'Hanis, Tex., storm of May 31, 1935						
Max. sta.		15.0		22.0		22.0
5		13.0		20.6		21.0
50		12.1		17.9		18.2
100		11.1		16.0		16.4
200		9.7		13.5		14.0
500		7.6		10.1		10.9
Cherry Creek, Colo., storm of May 30–31, 1935						
Max. sta.						24.0
5						22.1
10						20.6
20						18.8
50						16.0
100						13.7
200						11.2
300						9.7
400						8.6
500						7.8
Rodburn, Ky., storm of July 4, 1939						
10			18.6			20.0
100			13.2			14.4
200			10.4			11.9
500			7.5			9.4
Ewan, N.J., storm of Sept. 1, 1940						
Max. sta.	7.3	11.3	14.2	16.7	19.4	21.0
10	6.8	10.4	13.2	15.9	18.4	20.1
50	5.3	9.3	12.3	14.7	16.8	18.6
100	4.6	8.5	11.3	13.6	15.4	17.1
200	3.8	7.3	9.9	11.8	13.5	15.0
500	2.8	5.4	7.6	9.1	10.4	11.3
Plainville, Ill., storm of May 22, 1941						
Max. sta.	8.4	8.4	8.4			
10	6.4	6.5	6.5			
100	3.7	4.5	4.5			
200	2.9	3.7	3.7			
500	1.9	2.6	2.6			

TABLE A-2.—Continued.

Area (sq. mi.)	Duration (hr.) 1	2	3	4	5	6
Smethport, Pa., storm of July 17–18, 1942						
Max. sta.						30.7
1						29.3
5						26.4
10						24.7
20						22.8
50						19.7
100						16.4
200						13.1
300						11.2
400						10.0
500						9.1
Glenville, W. Va., storm of Aug. 4–5, 1943						
Max. sta.			14.6			
10			11.0			
20			10.2			
50			9.2			
100			8.2			
200			6.8			
500			5.2			
Holt, Mo., storm of June 22, 1947						
Max. sta.	10.7	11.8	12.0			
10	10.4	11.5	11.7			
100	6.5	8.5	8.8			
200	4.0	7.1	7.5			
500	3.1	5.2	5.8			

definitely a cloudburst, may not have been entirely independent of the hurricane which moved northward off the New Jersey coast on that date. The hurricane center was all of 150 mi. from the coast, and no rain was recorded in the coastal areas. There was a general rain area inland, however, and relatively heavy rainfalls were reported at various inland stations. The rainfall reported at Ewan nevertheless far surpassed the other amounts reported, indicating that localized influences in the circulation pattern must have been chiefly responsible for the unusual magnitude of that storm.

A.4 Chronological distribution

A.4.1 No one has ever satisfactorily determined a typical time distribution for cloudburst rainfall. It appears that the chances of the heaviest intensities

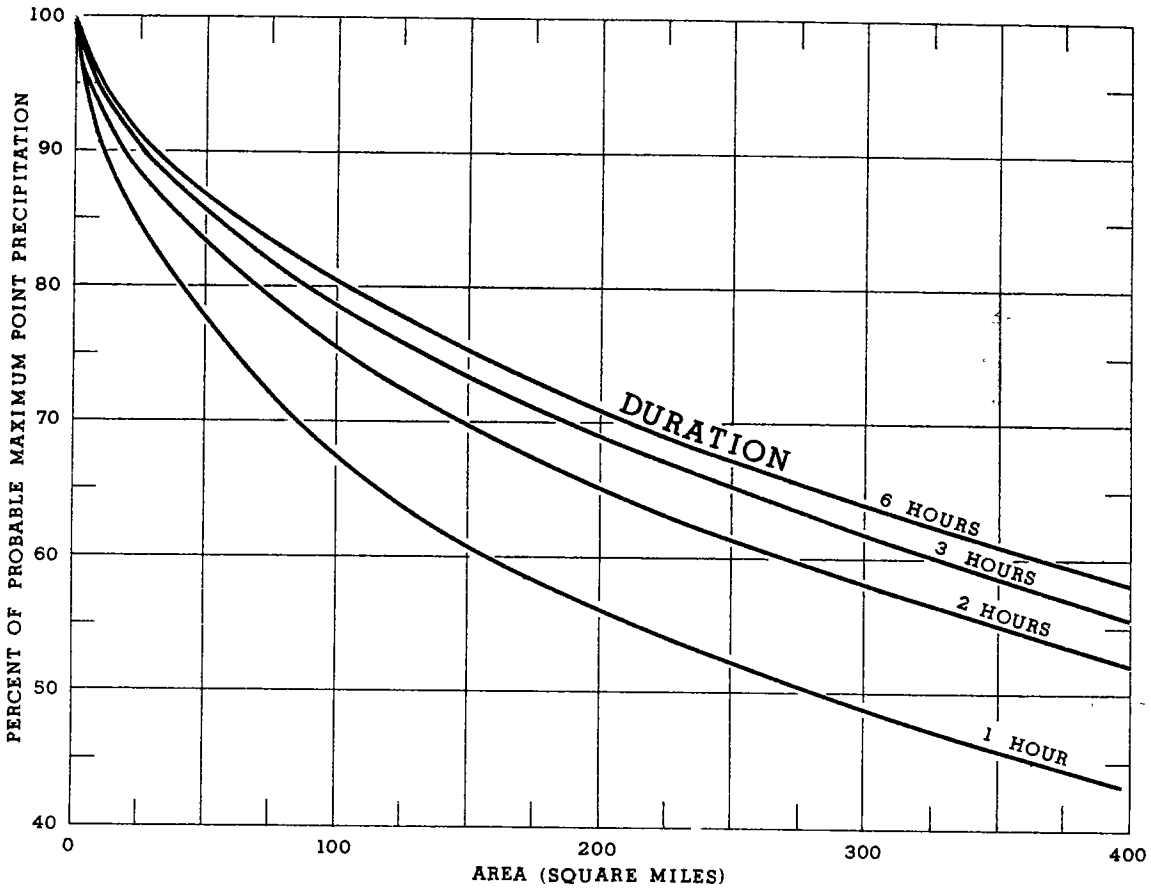

FIGURE A–1.—Depth-area curves for cloudburst PMP for use with table A–1.

occurring at the beginning, middle, or end of the storm are just about equal. It is suggested, therefore, that the increments of cloudburst rainfall be arranged in the most critical manner for determining the probable maximum flood.

A.5 Appraisal

A.5.1 The estimates of PMP from cloudbursts must be considered to be somewhat less realistic than those from hurricanes. First, there is some question as to whether cloudbursts of world record magnitude could occur in the problem area (pars. 1.3.4—1.3.5). Second, the chance that a localized storm could ever occur on a problem watershed is, practically speaking, infinitesimal. These two reasons suggest that the hurricane PMP values of figures 3–6 through 3–11, together with the depth–duration relations of figure 3–12 and the depth-area relation of figure 3–13, may yield more reasonable values of PMP regardless of watershed size.

Weather Bureau Technical Papers

*No. 1. Two-year normals of pressure, temperature, and hourly station pressures for the United States. Washington, D.C. 1945.

Supplement. Normal monthly pressure charts for the United States at the surface and synoptic hours. Washington, D.C. 1945.

*No. 2. Maximum recorded United States point rainfall for 5 min. to 24 hrs. Washington, D.C. 1947.

*No. 3. Extreme temperatures and freeze data for Washington, D.C. 1947.

*No. 4. Topographically adjusted normal rainfall for the Potomac and Appalachian basins. Washington, D.C. 1947.

*No. 5. Highest persisting dewpoints in the United States. Washington, D.C. 1947.

*No. 6. Upper air average values of temperature, pressure, and relative humidity over the United States and Alaska. Washington, D.C. 1948.

*No. 7. A report on thunderstorm conditions affecting flight operations. Washington, D.C. 1948.

*No. 8. The climatic handbook for Washington, D.C. Washington, D.C. 1949.

*No. 9. Temperature at selected stations in the United States, Alaska, Hawaii, and Puerto Rico. Washington, D.C. 1949.

No. 10. Mean precipitable water in the United States. Washington, D.C. 1949. .30

No. 11. Weekly mean values of daily total solar and sky radiation. Washington, D.C. 1949 .15. Supplement No. 1, 1955. 05.

*No. 12. Sunshine and cloudiness at selected stations in the United States, Alaska, Hawaii, and Puerto Rico. Washington, D.C. 1951.

No. 13. Mean monthly and annual evaporation data from free water surface for the United States, Alaska, Hawaii, and the West Indies. Washington, D.C. 1950 .15

*No. 14. Tables of precipitable water and other factors for a saturated pseudo-adiabatic atmosphere. Washington, D.C. 1951.

No. 15. Maximum station precipitation for 1, 2, 3, 6, 12, and 24 hours: Part I: Utah, Part II: Idaho, 1951, each .25; Part III: Florida, 1952, .45; Part IV: Maryland, Delaware, and District of Columbia; Part V: New Jersey, 1953, each .25; Part VI: New England, 1953, .60; Part VII: South Carolina, 1953, .25; Part VIII: Virginia, 1954, .50; Part IX: Georgia, 1954, .40; Part X: New York, 1954, .60; Part XI: North Carolina; Part XII: Oregon, 1955, each .55; Part XIII: Kentucky, 1955, .45; Part XIV: Louisiana; Part XV: Alabama, 1955, each .35; Part XVI: Pennsylvania, 1956, .65; Part XVII: Mississippi, 1956, .40; Part XVIII: West Virginia, 1956, .35; Part XIX: Tennessee, 1956, .45; Part XX: Indiana, 1956, .55; Part XXI: Illinois, 1958, .50; Part XXII: Ohio, 1958, .65; Part XXIII: California, 1959, $1.50; Part XXIV: Texas, 1959, $1.00; Part XXV: Arkansas, 1960, .50.

*No. 16. Maximum 24-hour precipitation in the United States. Washington, D.C. 1952.

No. 17. Kansas-Missouri floods of June–July 1951. Kansas City, Mo. 1952. .60

*No. 18. Measurements of diffuse solar radiation at Blue Hill Observatory. Washington, D.C. 1952.

No. 19. Mean number of thunderstorm days in the United States. Washington, D.C. 1952. .15

No. 20. Tornado occurrences in the United States. Washington, D.C. 1952. .35

*No. 21. Normal weather charts for the Northern Hemisphere. Washington, D.C. 1952.

*No. 22. Wind patterns over lower Lake Mead. Washington, D.C. 1953

No. 23. Floods of April 1952—Upper Mississippi, Missouri, Red River of the North. Washington, D.C. 1954. $1.00

(Continued on inside back cover)

* Out of print.

Weather Bureau Technical Papers

(Continued from inside front cover)

No. 24. Rainfall intensities for local drainage design in the United States. For durations of 5 to 240 minutes and 2-, 5-, and 10-year return periods. Part I: West of 115th meridian. Washington, D.C. 1953, .20; Part II: Between 105° W. and 115° W. Washington, D.C. 1954. .15

No. 25. Rainfall intensity-duration-frequency curves. For selected stations in the United States, Alaska, Hawaiian Islands, and Puerto Rico. Washington, D.C. 1955 .40

No. 26. Hurricane rains and floods of August 1955, Carolinas to New England. Washington, D.C. 1956. $1.00

*No. 27. The climate of the Matanuska Valley. Washington, D.C. 1956

*No. 28. Rainfall intensities for local drainage design in western United States. For durations of 20 minutes to 24 hours and 1- to 100-year return periods. Washington, D.C. 1956.

No. 29. Rainfall intensity-frequency regime. Part 1—The Ohio Valley, 1957, .30; Part 2—Southeastern United States, 1958, $1.25; Part 3—The Middle Atlantic Region, 1958, .30; Part 4—Northeastern United States, 1959, $1.25; Part 5—Great Lakes Region, 1960, $1.50.

No. 30. Tornado deaths in the United States. Washington, D.C. 1957. .50

No. 31. Monthly normal temperatures, precipitation, and degree days. Washington, D.C. 1956. .25

No. 32. Upper-air climatology of the United States. Part 1—Averages for isobaric surfaces, height, temperature, humidity, and density. 1957, $1.25. Part 2—Extremes and standard deviations of average heights and temperatures. 1958, .65; Part 3—Vector winds and shear. 1959. .50

No. 33. Rainfall and floods of April, May, and June 1957 in the South-Central States. Washington, D.C. 1958. $1.75

No. 34. Upper wind distribution statistical parameter estimates. Washington, D.C. 1958. .40

No. 35. Climatology and weather services of the St. Lawrence Seaway and Great Lakes. Washington, D.C. 1959. .45

No. 36. North Atlantic tropical cyclones. Washington, D.C. 1959. $1.00

No. 37. Evaporation maps for the United States. Washington, D.C. 1959 .65

No. 38. Generalized estimates of probable maximum precipitation of the United States west of the 105th meridian for areas to 400 square miles and durations to 24 hours. Washington, D.C. 1960 $1.00

No. 39. Verification of the Weather Bureau's 30-day outlooks. Washington, D.C. 1961. .40

No. 40. Rainfall frequency atlas of the United States for durations from 30 minutes to 24 hours and return periods from 1 to 100 years. 1961. $1.75

No. 41. Meridional cross sections, upper winds over the Northern Hemisphere. 1961. $1.25

Technical Papers for sale by Superintendent of Documents, U.S. Government Printing Office, Washington 25, D.C.

APPENDIX B

GLOSSARY

adiabatic—Applies to changes of air temperature resulting only from compression or expansion accompanying an increase or decrease of atmospheric pressure.

advection—The transport of an atmospheric property solely by the motion of the atmosphere.

annual series—A series of data composed of the annual maximum observations. For example, the annual maximum daily rainfall is the largest of the 365 observations of daily rainfall.

cloudburst—Any sudden heavy fall of rain, generally of the shower type.

coefficient of variation—A relative measure of dispersion which is obtained by dividing the standard deviation by the mean.

cold front—The leading edge of an advancing cold air mass.

condensation—The physical process by which a vapor becomes a liquid or solid.

convergence—A net horizontal inflow of air into a given space. The resulting accumulation of mass is limited by vertical motion. Hence, if there is convergent flow at the ground, there must be an upward vertical motion. If there is horizontal convergence in any upper layer, there must be upward and/or downward motion.

cyclone—A closed counterclockwise (in the Northern Hemisphere) atmospheric circulation.

dewpoint—The temperature to which air must be cooled at constant pressure and constant water-vapor content in order for saturation to occur.

divergence—A net horizontal outflow of air from a given space. The resulting deficit is compensated by a downward movement of air from aloft when the outflow is at the surface and by upward and/or downward movement when the outflow is at an upper level.

easterly wave—A migratory wave-like disturbance, or weak trough of low pressure, in the easterly winds of the Tropics.

entrainment—The mixing of environmental air into a pre-existing organized air current so that the environmental air becomes part of the current.

extratropical cyclone, Low, or storm—A low-pressure area of the middle and higher latitudes.

eye—The roughly circular area of comparatively light winds and fair weather found at the center of a severe tropical cyclone.

Gumbel method—Method developed by E. J. Gumbel for fitting extreme-value data to the Fisher-Tippett type I distribution.

Gumbel paper—Special probability paper constructed for the analysis of extreme values. If the data plot close to a straight line, the Gumbel theoretical solution is considered applicable.

hurricane—A severe tropical cyclone with winds exceeding 72 m.p.h. in the North Atlantic Ocean, Caribbean Sea, or Gulf of Mexico.

instability—A state in which the vertical distribution of temperature is such that a particle of air, if given either an upward or downward impulse, will tend to move away with increasing speed from its original level.

isopluvial—A line through points having the same precipitation value for a particular return period.

isovel—A line in a given surface connecting points with equal wind speed.

lapse rate—The rate of change of an atmospheric variable with height, the variable being temperature unless otherwise specified.

millibar—A subunit of pressure equal to a force of 1,000 dynes/cm.^{2}. The mean sea level pressure for the standard atmosphere is 1013 mb.

mixing ratio—In a system of moist air, the ratio of the mass of water vapor to the mass of dry air.

moisture charge (or moisture supply)—The water-vapor content of a column or layer of air.

orographic precipitation—Precipitation resulting when moist air is forced to rise by mountain ranges or other elevated land formations lying across the path of the wind.

partial-duration series—A series of data composed of observations above an arbitrary threshold, e.g., all daily rainfall amounts above 2.0 in.

probable maximum precipitation—The highest rainfall intensity meteorologically possible for a given duration over a specific area.

pseudoadiabatic lapse rate—The rate at which saturated air cools during adiabatic ascent if its moisture is precipitated immediately upon condensation.

reduced variate—A mathematical function of the return period, corrected for length of record.

return period—The average number of years within which the magnitude of a given event will be equaled or exceeded.

specific humidity—In a system of moist air, the ratio of the mass of water vapor to the total mass of the system.

spill-over—Precipitation formed over the windward side of a mountain range but falling to the ground on the lee side.

standard deviation—A measure of dispersion of data around their arithmetical mean. If the data follow the normal distribution, approximately two-thirds of the observations will be within plus and minus one standard deviation of the mean.

standard error—The standard deviation of the sampling distribution of the statistic.

tornado—A violently rotating column of air with a vortex, commonly several hundred yards in diameter, whirling usually counter-clockwise at speeds estimated at 100 to over 300 m.p.h.

tropical cyclone—The general term for a cyclone originating over the tropical oceans.

tropical storm—A tropical cyclone with winds stronger than 32 m.p.h. but less than 73 m.p.h.

Tropics—That portion of the earth's surface lying between 23°27′ N. and 23°27′ S.

trough—An elongated area of relatively low atmospheric pressure.

typhoon—A hurricane in the western Pacific Ocean.

waterspout—A tornado or lesser whirlwind occurring over water.

☆U. S. GOVERNMENT PRINTING OFFICE: 1962—605284